HYPOXIA-INDUCED CHROMATIN CHANGES AND ATM SIGNALLING

Mónica Olcina del Molino
Linacre College

Thesis submitted to the University of Oxford in accordance with the requirements for the degree of Doctor of Philosophy

Hilary Term, 2014
University of Oxford

Supervisor

Dr Ester M. Hammond

Assessment Committee

Dr David R. Mole

Dr Manuel Stucki



The study presented in this thesis was performed at the CR-UK & MRC Oxford Institute for Radiation Oncology, Department of Oncology, University of Oxford. This work was supported by a MRC studentship, a MRC Centenary Award and grants from Cancer Research UK.

Word count: 44357 (excluding references)

ABSTRACT

Hypoxia-Induced Chromatin Changes And ATM signalling

Submitted for the Degree of Doctor of Philosophy

Mónica Olcina del Molino, Linacre College, Hilary Term, 2014

The DNA damage response (DDR) is a complex signalling cascade triggered in response to stress, in an attempt to maintain genomic integrity. Components of this pathway, such as ATM-mediated signalling, have been proposed to act as a barrier in the early stages of tumourigenesis. Regions of low oxygen concentrations (hypoxia) occur in most solid tumours and are associated with a poor prognostic outcome. Here, we investigated the DDR induced following hypoxia-induced replication stress in an attempt to decipher the mechanism of ATM activation in response to physiological stresses that do not induce DNA damage. We hypothesized that hypoxia-mediated chromatin changes could impact on ATM signalling. We have characterised H3 methylation in response to hypoxia and found oxygen dependent changes in H3K9me3, including both global and replication fork associated increases in this histone modification. Importantly, we have found that decreases in H3K9me3 result in loss or attenuation of ATM activation. Notably, in a background of replication stress and increased H3K9me3, ATM inhibition or loss leads to accumulation of DNA damage and a significant decrease in replication rates in hypoxia. We propose that when replication stress occurs in the presence of hypoxia-induced chromatin changes, ATM activation is facilitated by the induction of H3K9me3. In this context, we propose a novel and stress specific role for ATM-mediated signalling in maintaining replication and preventing the generation of DNA breaks that may compromise genomic integrity. Moreover, the biological consequences of the hypoxia-induced chromatin context and in particular hypoxia-induced H3K9me3 include the repression of *APAK*, a negative regulator of p53. Activation of p53 is a key consequence of the hypoxia-induced DDR. Here we found that SETDB1, one of the H3 methyltransferases induced by hypoxia, mediates *APAK* repression. We propose that H3K9me3 plays a role in regulating APAK expression to allow optimal induction of p53 dependent apoptosis in hypoxic conditions suggesting a further role for H3K9me3 in facilitating DDR signalling in hypoxia. Together, these data suggest that the hypoxic chromatin context is critical for the role of the DDR as a barrier to tumourigenesis and predict that altering the chromatin landscape in combination with DNA damaging therapies would be efficacious in the treatment of hypoxic tumours.

To my wonderful parents

ACKNOWLEDGMENTS

I would like to start by thanking Ester - the amazing woman that I have had the pleasure to have as a supervisor. I will always be extremely grateful to her for all the trust and support. She gave me the confidence to develop and pursue my ideas; has always looked out for me and has offered me countless opportunities. Ester has certainly been instrumental in making me the scientist that I have become. I could not have asked for a better DPhil experience and she has been integral in making that happen. Ester, tell your father that we are still not making dinosaurs in a Petri dish, although sometimes it might feel like we are (see next page).

I would also like to say a huge thank you to everyone in the Hammond lab for making this a wonderful place to work in: Selva, Iosifina (GG), Cindy, Kasia (Bunia), Joana, Liam, as well as all past members and visitors. Visiting or MRes students such as Eve, Stephan, Agnieke, Nina and Eleanor contribute tremendously to creating the great team spirit that is characteristic of the lab. I am also very grateful to past lab members Zuzana and Isabel, who taught me so much when I started my DPhil and I knew nothing at all. Isabel, many thanks for your drawing skills too. You have all contributed immensely in your own special ways. In particular I would like to thank Selva - we both started our journey in the Hammond lab together and ever since he has been amazing. Special thanks to GG for understanding me so incredibly well and for all her help and support. Thanks to Cindy for being so encouraging and for talking me into running the marathon with her! Bunia will always be our lab Queenie - thanks for all those great chats and for your expert advice, Queenie. Thanks to sweet Joana too for being so willing to help and for all her kind support.

Many people in the Gray Institute have been extremely helpful over the years, I am sorry I cannot name everyone here. Special thanks to Emma, Mark, Stav, Simon, Nikola, Blaz, Sophie, Angelos, Aswin, Lydia, Enni, Sarah, Martin, Anika, Yanyan, Bruno, Paco, Garth, Jose, Rita and Maria. Dafni, “my replication expert” and dear friend - thank you so much for all your invaluable advice. A very special and warm thank you to the 20 Jeune street gang: Daniel, Selva (again), Giulia and Torben. Daniel, thank you particularly for all that support and motivation.

Many thanks to David Mole and Johannes Schödel for helping us set up the chromatin immunoprecipitation assay. I am also thankful to the members of my thesis committee: Matt Cockman and Colin Goding, and to Larry Turner, Sarah Norman, Katie Higgins, Eric O’Neill and Niki Sibson for their support.

I would like to extend special thanks to Andy Ryan for always taking the time to offer some insightful advice or a humorous comment that would make the day better.

Thank you to all my friends and family back in Spain and Manchester that have always had such faith in me. In particular I am very grateful to Adriana and Roger for all their support and for listening to my “hypoxia stories” and always paying such great attention.

I cannot thank David enough for all his incredible support and patience. I have learnt a lot from him and have no doubt I will continue to do so in the future. I very much look forward to our next challenge together. Thanks to Martin Hewings too for his comments on an earlier manuscript version of this work.

Finally, I would like to dedicate this thesis to my wonderful and inspirational parents. It goes without saying that words here are not enough to thank them both. I need to specially thank my father for his unconditional love and support, for his optimism and for always giving me that extra bit of courage if times were challenging or if I decided to take unconventional paths. Also, thank you for meticulously reading my thesis! To my mother, my inspiration, I owe the strength and determination to carry on, whatever the circumstances. I think of her and thank her every day of my life.

Many thanks! ¡Moltíssimes gràcies! ¡Muchísimas gracias!

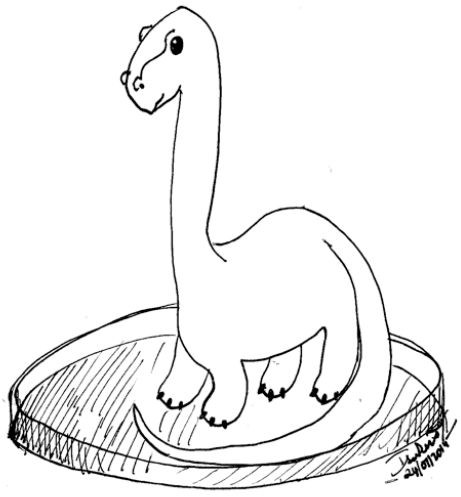


TABLE OF CONTENTS

ABSTRACT ..... **III**
ACKNOWLEDGMENTS ..... **V**
LIST OF TABLES ..... **XI**
LIST OF FIGURES ..... **XII**
LIST OF ABBREVIATIONS ..... **XV**

CHAPTER 1 INTRODUCTION **1**
1.1 Cancer **1**
1.2 Hypoxia and cancer **3**
1.3 The DNA Damage Response **9**
1.3.1 Types of DNA lesion 9
1.3.2 DNA Damage signalling 14
1.3.3 Initiation of DDR signalling in hypoxia 17
1.3.4 ATR-mediated DNA-damage response: The response to replication stress 18
1.3.5 Hypoxia-induced ATR-CHK1 signalling 20
1.3.6 ATM mediated DNA damage response: The response to DSBs 23
1.3.7 Hypoxia-induced ATM signalling in the absence of DSBs 28
1.3.8 Two pathways collide – HIF-1 and the DDR 30
1.3.9 Reoxygenation and the DNA damage response 33
1.3.10 Hypoxia-mediated repression of DNA repair 34
1.4 Chromatin **38**
1.4.1 Chromatin structure 38
1.4.1.1 Histone post-translational modification 39
1.4.1.2 DNA methylation 42
1.4.1.3 Nucleosome remodelling 44
1.4.2 Chromatin changes and the DDR 45
1.4.3 Crosstalk between chromatin changes and DNA replication 51
1.4.4 Chromatin dynamics and hypoxia 55
1.5 Chromatin remodelling, the DDR and cancer **59**
AIM **61**

CHAPTER 2 MATERIALS AND METHODS.....62

2.1 Materials 62

2.1.1 General laboratory and cell culture reagents 62

2.1.2 Antibodies.....65

2.1.3 Antibiotics 69

2.1.4 Primers.....69

2.2 Methods..... 72

2.2.1 Cell lines 72

2.2.2 Cryopreservation of cell lines.....73

2.2.3 Drug treatments 74

2.2.4 Hypoxia treatment 74

2.2.5 Exposure to γ-irradiation 75

2.2.6 RNA interference.....75

2.2.7 Retroviral transduction 76

2.2.8 Lentiviral tranduction 77

2.2.9 DNA transfection.....78

2.3 Protein analysis and biochemistry 79

2.3.1 Cell lysis and protein sample preparation.....79

2.3.2 SDS PAGE (SDS-Polyacrylamide Gel Electrophoresis) 79

2.3.3 Western blotting 81

2.3.4 Immunofluorescence microscopy.....81

2.3.5 Biochemical fractionation.....83

2.3.6 Isolation of proteins on nascent DNA (iPOND).....83

2.4 Molecular biology 86

2.4.1 Preparation of media and agar plates.....86

2.4.2 Transformation of bacteria 86

2.4.3 Growth of overnight cultures from colonies.....87

2.4.4 Agarose gel electrophoresis.....87

2.4.5 Large-scale preparation (Maxi-preparation) of plasmid DNA 87

2.4.6 Determination of DNA purity and concentration 88

2.4.7 RNA extraction and purification 88

2.4.8 Determination of RNA purity and concentration 89

2.5 Quantitative PCR (qPCR) 89

2.5.1 Reverse transcription 89

2.5.2 qPCR reactions 89

2.6 Chromatin immunoprecipitation..... 91

2.7 Single-molecule DNA fiber analysis 95
2.8 Alkaline comet assay 97
2.9 Phosphatase activity assay 97
2.10 Fluorescence-activated cell sorting 98
2.11 Apoptosis assay (by cell morphology) 99
2.12 Immunohistochemistry staining 99
2.13 Xenograft study 100
2.14 Analysis 100

CHAPTER 3 HYPOXIA-INDUCED ATM SIGNALLING 101
3.1 INTRODUCTION 101
3.2 RESULTS 103
3.2.1 Hypoxia-induced replication stress in the absence of damage 103
3.2.2 Hypoxia-induced ATM-mediated signalling 107
3.2.3 Replication stress in a hypoxic context leads to ATM activation 109
3.3 DISCUSSION 119

CHAPTER 4 MECHANISM OF ATM ACTIVATION IN HYPOXIA 122
4.1 INTRODUCTION 122
4.2 RESULTS 124
4.2.1 Characterisation of hypoxia-induced chromatin changes 124
4.2.2 H3K9me3 is required for ATM activation in hypoxia 132
4.3 DISCUSSION 141

CHAPTER 5 THE ROLE OF HYPOXIA-INDUCED ATM 145
5.1 INTRODUCTION 145
5.2 RESULTS 146
5.2.1 H3K9me3 is enriched at the replication fork following hypoxia-induced replication stress 146
5.2.2 Loss of ATM activity leads to accumulation of DNA damage in hypoxia 152
5.2.3 Increased H3K9me3 correlates with a requirement for ATM activity to resolve replication stress 159

5.3 DISCUSSION 163

CHAPTER 6 FURTHER BIOLOGICAL CONSEQUENCES OF HYPOXIA INDUCED H3K9Me3 166

6.1 INTRODUCTION 166

6.2 RESULTS 168

6.2.1 Choice of candidate genes 168

6.2.2 APAK is repressed in an oxygen dependent manner 173

6.2.3 SETDB1 is involved in mediating *APAK* repression in hypoxia 177

6.2.4 APAK and p53-mediated apoptosis 181

6.3 DISCUSSION 183

CHAPTER 7 GENERAL DISCUSSION 187

7.1 ATM and its role in replication in an H3K9me3-rich context 189

7.2 Hypoxia-induced chromatin changes and the absence of detectable DNA damage 193

7.3 Targeting the hypoxia-induced DDR and chromatin changes 195

7.4 Hypoxia-induced chromatin changes and ATM-mediated signalling – Break or accelerator of tumourigenesis? 196

APPENDICES 199

APPENDIX A 199

Published papers 199

APPENDIX B 255

B.1. Validation of ATM phosphorylation in MEFs 255

B.2. Details of primers used in Chapter 6 (Figure 6.1) 256

APPENDIX C 257

Statement of previous acceptance or concurrent submission of thesis for degree 257

REFERENCES 258

LIST OF TABLES

Table 1.1. Table summarising selected mechanism of hypoxia-induced repression of a number of DNA repair genes 36
Table 1.2. Table summarising chromatin-reading domains together with the sites they have been reported to bind 45
Table 1.3. Table summarising the role of selected chromatin regulators in DDR signalling or repair 50
Table 1.4. Table summarising the mechanism of hypoxia-induced epigenetic repression of a number of DNA repair genes 58
Table 2.1. Chemicals and cell cultures reagents 63
Table 2.2. Antibodies used for western blotting 65
Table 2.3. Antibodies used for immunofluorescence (IF) 67
Table 2.4. Antibodies used for chromatin immunoprecipitation (ChIP) 67
Table 2.5. Antibodies used for Single-Molecule DNA Fiber Analysis (DFA) 67
Table 2.6. Antibodies used for fluorescence-activated cell sorting (FACS) 67
Table 2.7. Antibodies used for immunohistochemistry (IHC) 68
Table 2.8. Secondary antibodies used 68
Table 2.9. Primers used for quantitative PCR (qPCR) 70
Table 2.10. Primers used for ChIP-qPCR 71
Table 2.11. Recipe for stacking gel 79
Table 2.12. Recipe for separating gel (6-20%) 80
Table 2.13. Components used to make up the reaction mix for qPCR 90
Table 2.14. Recipe for SDS cell lysis buffer 93
Table 2.15. Recipe for ChIP dilution buffer 93
Table 2.16. Recipe for low salt wash solution 94
Table 2.17. Recipe for high salt wash solution 94
Table 2.18. Recipe for LiCl wash buffer 94
Table 2.19. Recipe for TE buffer 94
Table 2.20. Recipe for elution buffer 94
Table 6.1. Table of candidate genes to be tested for hypoxia-induced H3K9me3 enrichment by ChIP-qPCR 171

LIST OF FIGURES

Figure 1.1. The hallmarks of cancer 2
Figure 1.2. Schematic representation of the different levels of oxygenation found in tumours 5
Figure 1.3. Schematic representation of the oxygen dependent regulation of the HIF family of transcription factors 8
Figure 1.4. Schematic representation of the DDR/DNA repair pathways activated following exposure to a variety of stresses 13
Figure 1.5. Schematic representation of the DDR 16
Figure 1.6. Schematic representation of the DDR induced in response to hypoxia and reoxygenation 22
Figure 1.7. Schematic representation of the principal domains in the ATM protein 24
Figure 1.8. Schematic representation of the crosstalk between DNA damage response/replication factors and HIF-1 32
Figure 1.9. Illustration of the three main ways to achieve chromatin remodelling 43
Figure 1.10. Schematic representation of the model for the role of KAP-1 in mediating chromatin remodelling 47
Figure 1.11. Schematic representation of the regulation of chromatin maturation during replication 54
Figure 1.12. Schematic representation of the dynamic hypoxia-induced regulation of the chromatin context 56
Figure 2.1. Overview of iPOND experiment 85
Figure 2.2. Schematic representation of the DNA fiber protocols 96
Figure 3.1. Oxygen dependence of the hypoxia-induced DDR. 103
Figure 3.2. Exposure to <0.1% but not 2% O_2 leads to replication stress 105
Figure 3.3. Exposure to hypoxia (<0.1% O_2) does not lead to the generation of significant detectable DNA damage 106
Figure 3.4. Hypoxia-induced ATM is active 107
Figure 3.5. KAP-1 phosphorylation is ATR independent 109
Figure 3.6. Hypoxia-induced ATM activity is absent from G_1 phase 110
Figure 3.7. Hypoxia-induced ATM activity is restricted to S-phase 111
Figure 3.8. Phosphorylated KAP-1-S824 does not form distinct foci in hypoxia 112

Figure 3.9. Hypoxia-induces replication stress and ATM activity 114
Figure 3.10. Hu leads to ATM activation in hypoxic conditions..... 116
Figure 3.11. Hu treatment in hypoxia leads to replication stress but no DNA damage 117
Figure 3.12. Oncogene-induced replication stress leads to ATM activation in hypoxic conditions 118
Figure 3.13. Proposed model for ATM activation in response to replication stress.. 120
Figure 4.1. Hypoxia-induces a number of chromatin changes 125
Figure 4.2. Hypoxia-induced H3K9me3 is cell-cycle independent 126
Figure 4.3. Hypoxia leads to the induction of HP1β levels 128
Figure 4.4 Histone methyltransferases are induced at the protein but not mRNA level by hypoxia..... 130
Figure 4.5. Hypoxic regulation of histone methyltransferases is HIF-1 independent 131
Figure 4.6. KAP-1 siRNA mediated knockdown leads to a moderate reduction in H3K9me3 and ATM phosphorylation in hypoxia 133
Figure 4.7. Loss of Suv39h1/2 abrogates hypoxia-induced ATM-S1981 134
Figure 4.8. Suv39h1/2 regulate the mRNA level of certain ATM phosphatases 136
Figure 4.9. Hypoxia-induced enrichment of H3K9me3 on *PP2A-C* 137
Figure 4.10. mRNA level of *PP2A-C* is downregulated in response to <0.1% O_2 but not 2% O_2 138
Figure 4.11. Phosphatase activity of PP2A-C is reduced in hypoxia 139
Figure 4.12 Hypoxia-induced H3K9me3 correlates with ATM activity *in vitro* and *in vivo* 140
Figure 4.13. Schematic representation of the proposed model for ATM activation in hypoxia..... 144
Figure 5.1. Optimisation of EdU exposure for iPOND experiments 147
Figure 5.2. H3K9me3 is associated with replication forks in hypoxia 148
Figure 5.3. H3K9me3 is not detected at the replication fork following thymidine chase experiment..... 149
Figure 5.4. Short Hu treatment does not affect the levels of H3K9me3 either globally or at the replication fork..... 151
Figure 5.5. Loss of ATM activity leads to DNA damage accumulation in hypoxia . 153
Figure 5.6. ATM inhibition or loss does not result in DNA damage accumulation in mild hypoxia (2% O_2) 154

Figure 5.7. 53BP1 foci following ATM inhibition accumulate in S-phase 156
Figure 5.8. KAP-1 knockdown does not lead to DNA damage accumulation in hypoxia 158
Figure 5.9 Loss of ATM activity does not lead to DNA damage accumulation in response to reoxygenation 159
Figure 5.10. ATM inhibition has no effect on replication restart but leads to an increase in origin firing following reoxygenation-induced replication restart 161
Figure 5.11 ATM controls replication speed in hypoxia 162
Figure 5.12. Schematic representation of our model for the activation and role of ATM in hypoxia 163
..... 172
Figure 6.1. ChIP-qPCR analysis for possible enrichment of H3K9me3 binding on DDR/DNA repair genes in hypoxia 172
Figure 6.2. Specific H3K9me3 enrichment on *APAK* in response to hypoxia 174
Figure 6.3. *APAK* is repressed in an oxygen dependent manner 176
Figure 6.4. *APAK* is repressed in HIF-1 independent manner 177
Figure 6.5. *APAK* is repressed in a SETDB1 dependent manner 178
Figure 6.6. *APAK* is repressed in G9a independent manner 179
Figure 6.7. *APAK* is repressed in a Suv39h1 independent manner 180
Figure 6.8. *APAK* overexpression leads to reduced apoptosis in hypoxia 182
Figure 7.1. Schematic representation of our model of ATM activation and function in hypoxia 188
Figure 7.2. Chromatin maturation regulation during replication in response to normoxia and hypoxia 191
Figure 7.3. Summary of possible downstream ATM targets to be investigated in future studies 194
Figure B.1. Validation of ATM phosphorylation in MEFs using a monoclonal antibody with reactivity towards mouse ATM 255

LIST OF ABBREVIATIONS

53BP1	p53-binding protein 1
9-1-1	RAD9-RAD1-HUS1 complex
aa	amino acid
c-ABL	c-ABL oncogene1, non-receptor tyrosine kinase
ADP	adenosine diphosphate
AMP	adenosine monophosphate
APAK	ATM and p53-associated KZNF Protein
ASF1	anti-silencing function 1
AT	ataxia telangiectasia
ATM	ataxia telangiectasia mutated
ATP	adenosine triphosphate
ATR	ataxia-telangiectasia and RAD3-related
ATRIP	ATR-interacting protein
BER	base excision repair
BRCA	breast cancer susceptibility gene
BRCT	breast cancer C-terminal
BRD4	bromodomain containing 4
BrdU	5-bromo-2'-deoxyuridine
BRG1	brahma-related gene 1/BRG1 associated factor 190A
BRM	Brahma
BSA	bovine serum albumin
°C	degrees centigrade
CAF-1	chromatin assembly factor 1
CBP	CREB binding protein
CDC	cell division control
CDK	cyclin dependent kinase
CDT1	chromatin licensing and DNA replication factor 1
CHD/Mi-2	chromodomain, helicase, DNA-binding protein
CHFR	checkpoint with forkhead and RING finger domains
ChIP	chromatin immunoprecipitation

CHK	checkpoint protein
CldU	5-chloro-2′-deoxyuridine
CK2	casein kinase 2
CODDD	carboxy-terminal oxygen dependent degradation domain
CREB	cyclic AMP-responsive element-binding
CT	threshold cycle
CtIP	CtBP interacting protein
DAPI	4',6-diamidino-2-phenylindole
DDR	DNA damage response
DFA	DNA fiber analysis
DMEM	Dulbecco's modified Eagle medium
DMOG	dimethyloxaloylglycine
DMSO	dimethylsulphoxide
DNA	deoxyribonucleic acid
DNA-PK	DNA-dependent protein kinase
DNA-PKcs	DNA-dependent protein kinase catalytic subunit
DOT1L	DOT1-like histone H3K79 methyltransferase
DOX	doxorubicin
DSB	double-strand break
ssDNA	single-stranded DNA
E2F	E2F transcription factor
EdU	5-ethynyl-2'-deoxyuridine
EDTA	ethylenediaminetetraacetic acid
EXO1	exonuclease 1
EYA1	eyes absent homologue 1
EYA3	eyes absent homologue 3
EZH2	enhancer of zeste homolog 2
FACS	fluorescence activity sorting assay
FAT	FRAP-ATM-TRRAP
FATC	FAT-C terminal
FBS	foetal bovine serum
FEN1	flap endonuclease 1
FUCCI	fluorescent ubiquitination-based cell cycle indicator

g	gravity
G9a	euchromatic histone-lysine N-methyltransferase 2
GFP	green fluorescent protein
GINS	SLD5, PSF1, PSF2 and PSF3 complex
Gy	Gray
HAT	histone acetyltransferase
H3	histone H3
HEPES	4-(2-hydroxyethyl)-1-piperazineethanesulfonic acid
HERV	human endogenous retrovirus
HDAC	histone deacetylase
HDM	histone demethylase
HIF-1	hypoxia-inducible factor -1
HMGN1	high mobility group nucleosome-binding domain-containing protein 1
HMM	hidden markov model
HMT	histone methyltransferase
HP1	heterochromatin protein 1
HR	homologous recombination
HRE	hypoxia responsive element
Hu	hydroxyurea
IdU	5-Iodo-2′-deoxyuridine
IF	immunofluorescence
INO80	inositol requiring 80
iPOND	isolation of proteins on nascent DNA
IR	ionising radiation
ISWI	imitation switch
JMJD1A	Jumonji domain-containing protein 1A
JMJD2B	Jumonji domain-containing protein 2B
K	lysine
KAP-1	krüppel-associated box domain associated protein 1
kDa	kilo Dalton
KZNF	krüppel-type zinc finger
KRAB	krüppel-associated box
LOH	loss of heterozygosity

MBT	malignant brain tumour
MCM	minichromosome maintenance
MDC1	mediator of DNA damage checkpoint protein 1
Me	methylation
MMR	mismatch repair
MMS	methyl methanesulfonate
MMSET	multiple-myeloma-related WHSC1
MOF/KAT8	males absent on the first/lysine acetyltransferase 8
MRE11	meiotic recombination 11 homolog A
MRG15	mortality factor 4-like protein 1
MRN	MRE11/RAD50/NBS1
MTA1	metastasis associated 1
c-MYC	myc proto oncogene
NCS	neocarzinostatin
NBS1	Nijmegen breakage syndrome protein 1/nibrin
NER	nucleotide excision repair
NHEJ	non-homologous end-joining
NODDD	amino-terminal oxygen dependent degradation domain
dNTP	deoxyribonucleotide triphosphates
NuRD	nucleosome remodelling and histone deacetylation
OIS	oncogene induced senescence
PARP1	poly (ADP-ribose) polymerase 1
PCAF	p300/CBP-associated factor
PCNA	proliferating cell nuclear antigen
PCR	polymerase chain reaction
PBS	phosphate buffered saline
PHD	plant homeodomain
PI3K	phosphatidylinositol-3-kinase
PI3KK	phosphatidylinositol-3-kinase like kinase
PI4K	phosphatidylinositol-4-kinase
PI	propidium iodide
PP2A	serine/threonine protein phosphatase 2A
PP2A-C	protein phosphatase 2, catalytic subunit, alpha isozyme

PP4	serine/threonine protein phosphatase 4
PSF1	DNA replication complex GINS protein PSF1
PSF2	DNA replication complex GINS protein PSF2
PSF3	DNA replication complex GINS protein PSF3
qPCR	quantitative real-time PCR
Q	glutamine
R	arginine
RB	retinoblastoma
RBCC	RING finger-B box 1 and 2 coiled-coil region
RBX1	ring box 1, E3 ubiquitin protein ligase
RDS	radio-resistant DNA synthesis
RING	really interesting new gene
RNA	ribonucleic acid
RNF	ring finger protein
RNR	ribonucleotide reductase
ROS	reactive oxygen species
RPA	replication protein A
RPC	replisome progression complex
RPM	revolutions per minute
RT	room temperature
RUVBL1	ruvB-like 1
RUVBL2	ruvB-like 1
SAM	s-adenosyl methionine
SD	standard deviation
SE	standard error of the mean
S	serine
SET	suppressor of variation 3-9, enhancer of zeste, trithorax
SET8	SET domain containing 8
SETDB1	SET domain, bifurcated 1
SK2	E3 ubiquitin ligase S-phase associated protein 2
SMARCAD1	SWI/SNF related matrix associated actin dependent regulator of chromatin subfamily A containing DEAD/H box 1
SMC1	structural maintenance of chromosomes 1

SLD5	GINS complex subunit 4
SP-A	surfactant protein A
SSB	single-strand break
SUMO	small ubiquitin-like modifier
Suv39h1/2	suppressor of variegation 3-9 homologue 1/2
SWI/ SNF	switch/sucrose non-fermentable
T	threonine
TIP60	tat-interactive protein 60
TIPIN	TIMELESS-interacting protein
TLK1	tousled-like kinase
TOPBP1	DNA topoisomerase 2-binding protein 1
TSA	trichostatin A
UBC9	ubiquitin carrier protein 9
URHF1	ubiquitin-like PHD and RING finger domain-containing protein
dUTP	deoxyuridine triphosphate
UV	ultraviolet
VHL	von-Hippel-Lindau
WB	western blotting
WD40	WD40 repeat domain
WDHD1	WD repeat and HMG-Box DNA binding protein 1
WSTF	William syndrome transcription factor
XRCC	X-ray cross-complementation group
Y	tyrosine

CHAPTER 1

INTRODUCTION

1.1 Cancer

Cancer can be described as a group of diseases in which cells have the ability to undergo aberrant or uncontrolled growth and can invade other tissues. In the year 2000 Hanahan and Weinberg published a seminal article describing six acquired characteristics that, if adopted by a cell, lead to increased survival, proliferative capacity and invasion potential (Hanahan and Weinberg, 2000). In 2011 the same authors updated the six hallmarks to include two further emerging hallmarks and two enabling characteristics. Deregulated cellular metabolism and the ability of cancer cells to evade immune system detection and destruction were the two newly characterised emerging hallmarks. These are summarised in Figure 1.1. Of note, genomic instability, a feature central to the study presented here, was described by the authors as arguably the most prominent enabling characteristic (Hanahan and Weinberg, 2011).

Moreover, the increased proliferative capacity of a tumour gives rise to two other important features in cancer development and progression. Firstly, the increased replication rates necessary to maintain proliferation in tumours may increase the number of replication errors, further contributing to genomic instability. Secondly, the

increased growth experienced by cancers frequently leads to a situation where the available oxygen is not enough to support the rapidly dividing cancer cell population. This leads to the generation of regions of hypoxia (low oxygen levels). Both DNA replication stress as well as severe levels of hypoxia are events that will induce the activation of a complex signalling cascade designed to limit genomic instability. The detailed understanding of how this occurs, as well as its consequences, are questions pivotal to this study.

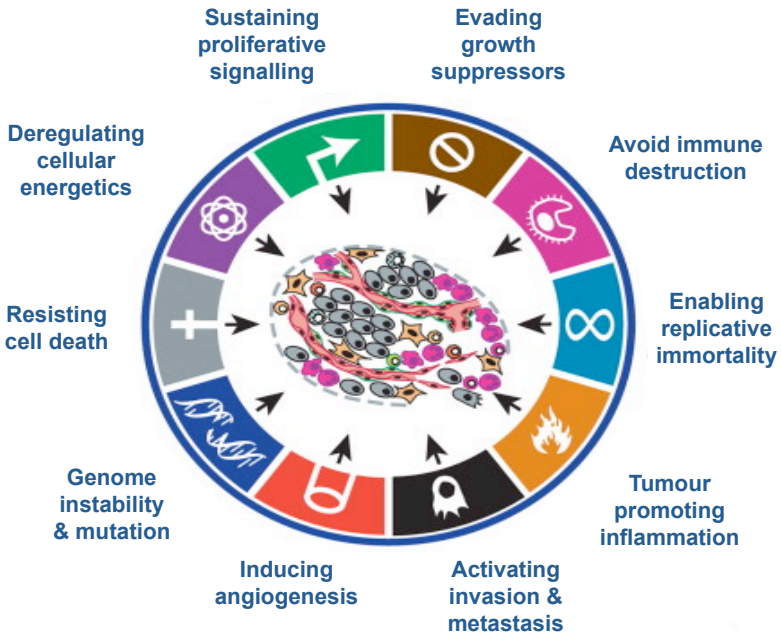


Figure 1.1. The hallmarks of cancer
The diagram illustrates the hallmark capabilities as described originally in 2000 together with the updated emerging hallmarks and enabling capabilities. Adapted and reprinted from Cell, vol 144, issue 5, 4 March 2011, Hanahan, D. and Weinberg, R.A., Hallmarks of Cancer: The Next Generation, 646-674, Copyright (2011), with permission from Elsevier.

1.2 Hypoxia and cancer

The majority of solid tumours develop in an environment of sub-optimal oxygen (O_2) concentration. Hypoxia, at least in part, is a result of the tumour vasculature, which is generally chaotic and disorganised in comparison to normal vasculature. The lack of lymphatic drainage together with the frequent blockages and shunts that exist in tumours can result in high interstitial pressure, leading to transient or permanent collapse of blood vessels. This results in a situation where the rapidly proliferating tumour, despite inducing angiogenesis to form new blood vessels, is unable to maintain appropriate oxygen supply to the whole tissue. Regions of the tumour between 70-200 μm away from a functional blood vessel will ultimately become hypoxic (Figure 1.2). The variability in this distance range probably reflects the different levels of tolerance to hypoxia displayed by different cells as well as the variable oxygen consumption requirements. In *in vivo* settings hypoxia, therefore, occurs as a gradient of oxygen tensions ranging from "physiologically normal" levels of oxygenation (which vary between different tissues but will typically range from 3-7%) to mild hypoxia (0.5-3%) and anoxia (0%) (Vaupel et al., 1989). Some examples of "physiologically normal" oxygen levels for different tissues are 4.6% for brain, 5.6% for lung or 1.05-4.61% oxygen in skin (Dings et al., 1998; Le et al., 2006; Wang et al., 2003). While it is informative to think about hypoxia in terms of % of oxygen, it is important to remember that a tissue is considered to be hypoxic only when the oxygen levels available are below what is considered necessary for that particular tissue, irrespective of the actual % oxygen value. Furthermore, oxygen gradients found in tumours typically fluctuate giving rise to reoxygenation, which can occur following the reopening of a temporarily occluded vessel (Dewhirst et al., 2008). The presence of varying levels of hypoxia in tumours has been demonstrated to be

significant for a number of reasons. These include a number of hypoxia-induced biological changes undertaken in an attempt to adapt and thrive under these conditions. Typically, the main mediators of the hypoxic response are the HIF (hypoxia-inducible factor) transcription factors, which are composed of an oxygen-labile α subunit (HIF-1α, HIF-2α, HIF-3α) and a shared constitutively expressed protein (HIF-1β/ARNT) (Brahimi-Horn and Pouyssegur, 2009). The HIF proteins are responsive to a wide range of oxygen tensions. HIF-1α and HIF-2α possess structurally similar domains and their stability is regulated through two oxygen-dependent degradation domains (NODDD and CODDD). These allow proteolytic degradation of the α subunit in the presence of oxygen, 2-oxoglutarate (α-ketoglutarate) and iron (II) by members of the PHD (prolyl-hydroxylase domain protein) family of enzymes (Schofield and Ratcliffe, 2004). PHD2 hydroxylates HIF-1α at proline 402 and/or 564 facilitating the interaction between HIF-1α and VHL (von-Hippel-Lindau protein), which acts as the recognition component of an E3 ligase complex (Bruick and McKnight, 2001; Cockman et al., 2000; Maxwell et al., 1999). Hydroxylation events are followed by the recruitment of HIF-1α to the ubiquitin-ligase complex containing Elongin C, Elongin B, Cullin 2 and RBX1 (ring box 1), which will result in HIF-1α ubiquitylation and subsequently proteasomal degradation (Cockman et al., 2000; Kaelin and Ratcliffe, 2008; Lisztwan et al., 1999). In the absence of oxygen, however, HIF-1α accumulates and is able to combine with HIF-1β to form a complex that enters the nucleus and binds to the HRE (hypoxia responsive element) sequences (5'-RCGTG-3' (R=purine, A or G)) of specific genes (Fine and Norman, 2002). HIF-1 then acts as a transcriptional regulator for genes involved in angiogenesis, glycolysis, glucose transport, and increased oxygen delivery, amongst others (Vaupel and Harrison, 2004) (Figure 1.3).

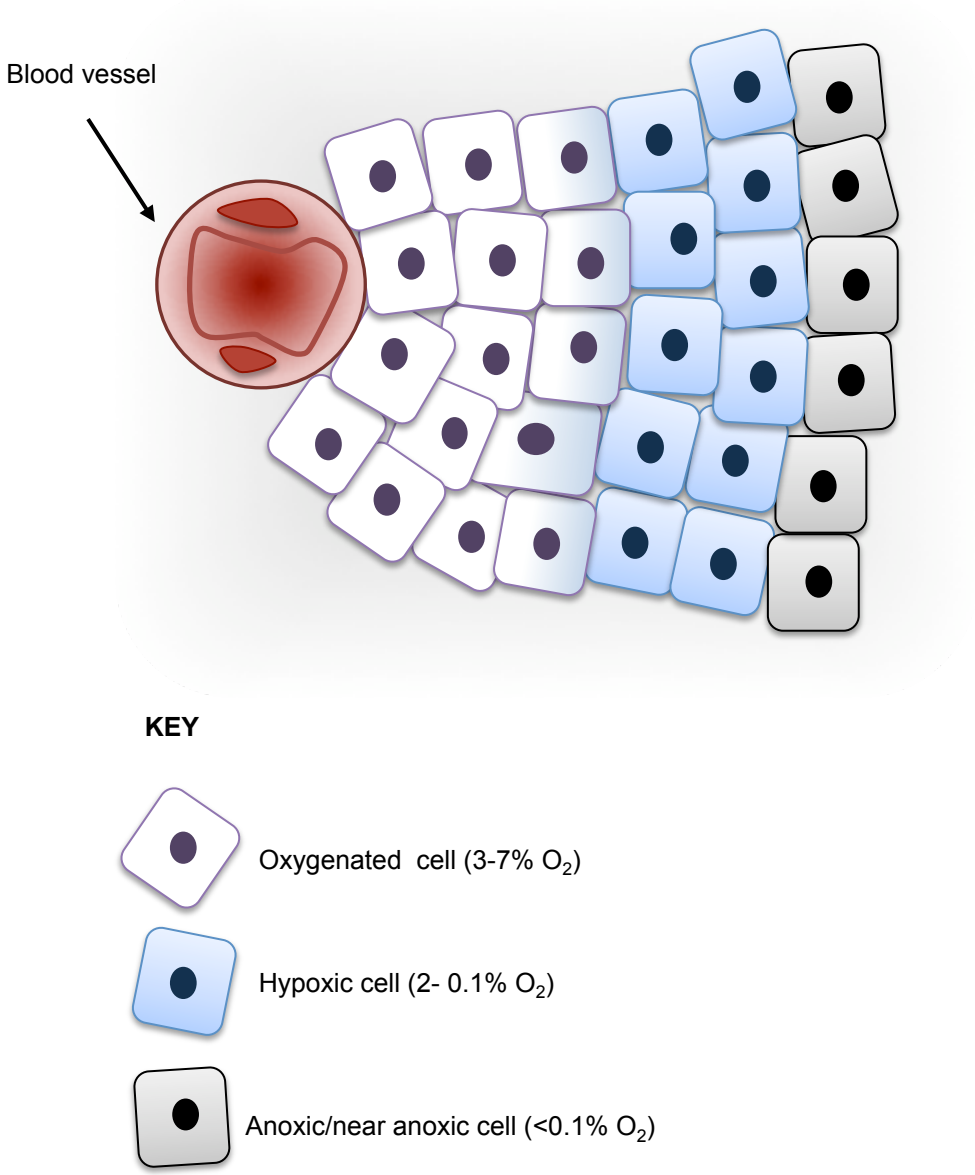


Figure 1.2. Schematic representation of the different levels of oxygenation found in tumours
Cells found next to a functional blood vessel have access to sufficient oxygen. Note that these levels of oxygenation are not comparable to air (20-21% O_2). As the distance between tumour cells and the blood vessel increases, the available oxygen starts to become limiting, gradually giving rise to hypoxic and finally anoxic cells. In this study, normoxic conditions refer to conditions where the oxygen concentration is comparable to that of air and for convenience are referred to as 21% O_2. Adapted from (Denko, 2008; Horsman et al., 2012).

Transcriptional activation by HIF-1 also requires the recruitment of co-activators such as p300 and CBP (CREB binding protein). FIH-1 (factor inhibiting HIF-1) hydroxylates asparagine 803 in an oxygen and 2-oxoglutarate dependent manner and in doing so prevents the binding of HIF-1α and p300/CBP (Lando et al., 2002). Interestingly, expression of HIF-1α and HIF-2α has been shown to differ between hypoxic tissues indicating they have different roles (Maxwell, 2005). For example, HIF-1α has been shown to be involved in causing cell cycle arrest following moderate hypoxia by inhibition of c-MYC, while HIF-2α may enhance cell cycle progression by promoting the activation of c-MYC and some of its target genes (Gordan et al., 2007). Interestingly, HIF-3α is a HIF-1 transcriptional target that is involved in HIF-1 inhibition (Makino et al., 2007). The increasing number of pathways and mechanisms employed by cancer cells to promote HIF-1 stabilisation and transcriptional activity reflects the survival advantage conferred by HIF-1 activation in tumours. These include oncogene gain of function as well as tumour suppressor loss of function, such as the loss of VHL (Semenza, 2010).

HIF-dependent transcriptional activation of many genes in response to hypoxia has been shown by use of expression array analysis coupled to HIF-knockdown (Elvidge et al., 2006; Hu et al., 2003). Combining gene expression profiling with chromatin immunoprecipitation (ChIP) followed by DNA hybridisation to tiled arrays (ChIP-ChIP), or more recently ChIP followed by "next-generation" sequencing of recovered DNA (ChIP-seq) as well as the use of RNA-seq have also proved invaluable in furthering the understanding of HIF transcriptional regulation and binding (Mimura et al., 2012; Schodel et al., 2012; Schodel et al., 2011; Xia et al., 2009). HIF-1 dependent gene repression has also been demonstrated and likely occurs through an indirect mechanism, since direct interaction of HIF-1 with repressed genes

has not been observed (Mole et al., 2009). It is important to note that as oxygen levels become progressively limiting, a state of general transcriptional repression develops. In these situations, repression can reach 75% at 24 hours in <0.01% oxygen and is typically considered to be HIF-1 independent (Johnson and Barton, 2007).

Clinically, tumour hypoxia is associated with a poor prognostic and predictive outcome, irrespective of treatment type (Brown and Wilson, 2004; Toustrup et al., 2012; Vaupel and Hockel, 2001). With regards to chemotherapy, resistance can be mediated by a number of different mechanisms including hypoxia-induced inhibition of proliferation, selection for cells resistant to apoptosis in hypoxia, as well as an increase in acidosis that may reduce the uptake of weakly basic drugs (Graeber et al., 1996; Hickman et al., 1994; Hockel and Vaupel, 2001). The abnormal tumour vasculature leading to the development of hypoxia also compromises drug delivery (Hockel and Vaupel, 2001). Interestingly, since the biological response to hypoxia includes increased invasion and metastatic potential, hypoxia also correlates with poor treatment outcome when tumours are surgically excised (Brown and Wilson, 2004). In addition, radiosensitivity starts decreasing as tumour oxygen partial pressures reach 3.29-3.95% oxygen (25-30 mmHg), with the dose required to achieve the same biological effect being 2-3 times greater in the complete absence of oxygen. This phenomenon is known as the “Oxygen Enhancement Ratio”. The dependence on oxygen availability for the appropriate induction of DNA damage following irradiation, has been attributed to the formation of reactive oxygen species (ROS) following the interaction of radiation with water, as well as the “fixation” of the induced damage in the presence of oxygen. Therefore, this phenomenon is typically associated with

severe levels of hypoxia (<0.1% O_2) (Brown and Giaccia, 1998; Gray et al., 1953; Hockel et al., 1996a; Hockel et al., 1996b).

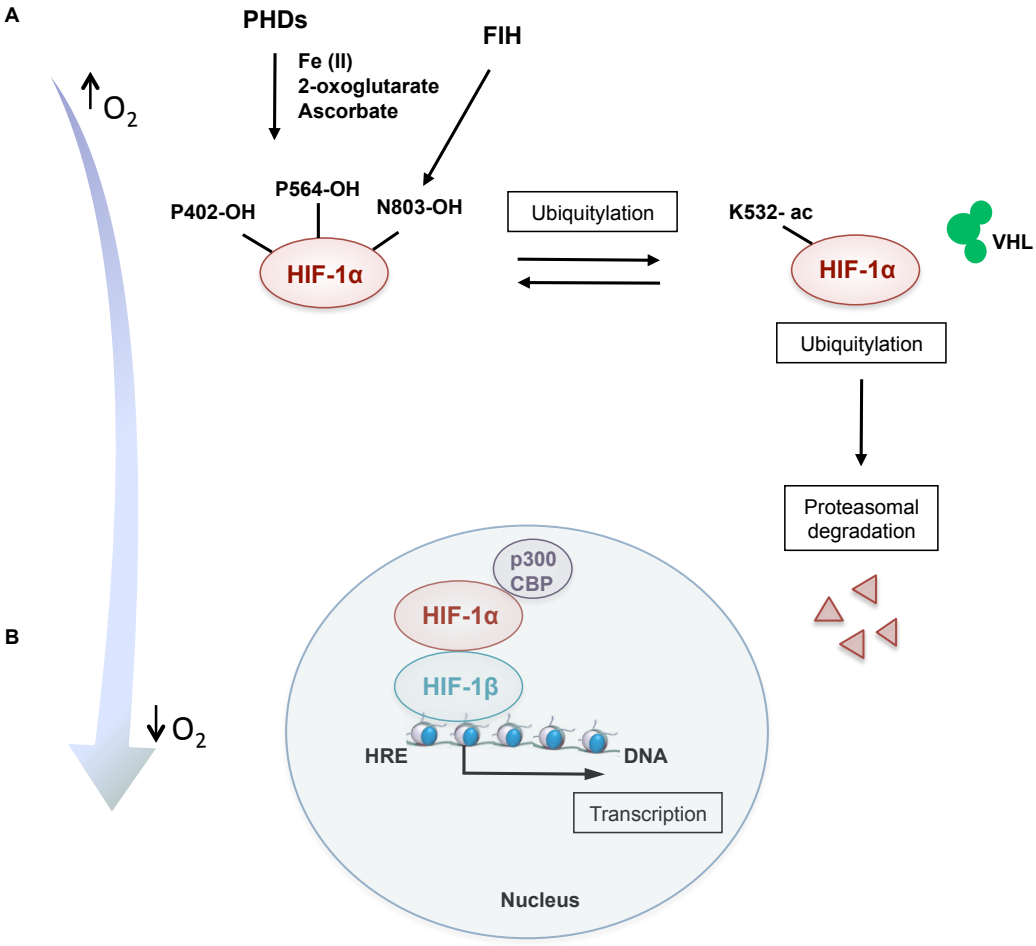


Figure 1.3. Schematic representation of the oxygen dependent regulation of the HIF family of transcription factors
(A) In the presence of oxygen, iron (Fe (II)), 2-oxoglutarate and ascorbate HIF-1α is hydroxylated by PHDs at the indicated residues. FIH can also direct asparagine hydroxylation. These modifications as well as acetylation on lysine 532 facilitate HIF-1α ubiquitylation and proteasomal degradation. **(B)** In the absence of oxygen, HIF-1α forms a heterodimer with HIF-1β (and co-activators such as p300/CBP) which binds to the HRE of target genes. This drives transcriptional activation of such genes in hypoxia. Adapted from (Giaccia et al., 2003; Schofield and Ratcliffe, 2004).

Moreover, these extremely low oxygen tensions are also associated with two other important phenomena. Firstly, hypoxia leads to the induction of the UPR (unfolded protein response) in a HIF-1 independent manner (Rouschop et al., 2010). Secondly, severe hypoxia results in the activation of the DDR (DNA damage response), despite the absence of any detectable damage being induced under these conditions. The activation of the DDR also occurs primarily in a HIF-1α independent manner (Bencokova et al., 2009; Hammond et al., 2004). The initiating signals for the activation of the DDR as well as its role will be described in detail below.

1.3 The DNA Damage Response

1.3.1 Types of DNA lesion

The integrity of the genetic material encoded in DNA is constantly being threatened by exogenous as well as endogenous environmental factors (summarised in the top blue box in Figure 1.4) (Lindahl and Barnes, 2000). Spontaneous base changes such as depurination, deamination and oxidation, for example, can be relatively common in a mammalian cell, with up to 10^4 events/cell having the potential to lead to hydrolysis of DNA glycosyl bonds and subsequent base loss (Lindahl and Nyberg, 1972). All types of challenge to the integrity of DNA must be sensed and recognised efficiently if genomic stability is to be maintained (Rouse and Jackson, 2002). Different lesions are repaired by pathways that have evolved to neutralise specific insults (see Figure 1.4, where the different DNA lesions shown in the red box lead to the activation of specific repair pathways shown in the green box) (Ciccia and Elledge, 2010; de Laat et al., 1999; Jackson and Bartek, 2009; Kuzminov, 1995; Li, 2008). Interestingly, despite the variety in repair pathways that have evolved to

neutralise DNA lesions, the various forms of stress ultimately trigger similar signal transduction pathways, typically referred to as the DDR. Challenges that can occur during the course of DNA replication are one of the main triggers of this complex system developed to maintain genomic stability. During DNA replication (which in following sections will be frequently referred to as simply "replication"), the unwinding of double-stranded DNA must be temporally coordinated with DNA synthesis in the 5′ to 3′ direction (Johnson and O'Donnell, 2005). Replication starts by loading the set of enzymes and proteins that collectively undertake DNA replication (the replisome) onto origins of replication (Benkovic et al., 2001). Following the binding of the origin recognition complex, MCM2-7 (minichromosome maintenance complex 2-7) double hexamers are loaded by CDC6 (cell division control protein 6) and CDT1 (chromatin licensing and DNA replication factor 1) on both dormant as well as active origins (Bochman and Schwacha, 2009). S-phase cyclin dependent kinases (CDKs) and CDC7 then promote the binding of CDC45 and GINS to MCM and this serves to activate both MCM and licensed origins (Costa et al., 2011; Remus and Diffley, 2009). Following DNA unwinding into daughter (leading and lagging) strands by the replicative helicases, areas of single-stranded DNA (ssDNA) form and become coated by RPA (replication protein A). RPA creates a binding site for the RPC (replisome progression complex), containing claspin, TIMELESS, TIPIN and WDHD1/AND-1 (Gambus et al., 2006). Leading strand DNA synthesis will be undertaken by polymerase (Pol) ε while lagging strand synthesis requires the stepwise synthesis, flap removal and ligation of Okazaki fragments. To this end, the primase-Pol α complex synthesises a RNA primer with a short DNA fragment that can then be extended by Pol δ. Once two Okazaki fragments are ligated by flap endonuclease FEN1 and DNA ligase 1 the primer and short DNA are removed

(Beattie and Bell, 2011; Johnson and O'Donnell, 2005). The binding of Pol ε and Pol δ with their template is facilitated by the sliding clamp PCNA (proliferating cell nuclear antigen) (Johnson and O'Donnell, 2005). Replication factor C acts as the clamp loader and regulates the timely synthesis of leading and lagging strands (Errico and Costanzo, 2010). The coordination of this sequence of events can be disrupted during replication stress if the replisome runs into DNA lesions, or fork barriers, such as a DNA repetitive elements or transcription complexes. Replication stress results in slowing down of the replication machinery until the stress can be resolved and has thus recently been defined as a decrease in the rate of replication fork progression, leading to stalling and decreased DNA synthesis (Brewer and Fangman, 1988; Cha and Kleckner, 2002; Puddu et al., 2011; Zeman and Cimprich, 2013). It is important to note that replication forks may eventually collapse following prolonged replication stress leading to the generation of a DNA break at these sites. Until recently, this was thought to happen most commonly at regions known as common fragile sites. These are A-T rich regions of the genome that usually contain large genes typically undergoing late replication, and where active origins are scarce. However, a recent report demonstrated that replication stress results in DNA damage generation primarily in another subset of fragile sites, named early replicating fragile sites. These newly characterised fragile sites occur in actively transcribed genes found near replication origins, containing high G-C content and undergoing early replication (Barlow et al., 2013). Moreover, replication stress can also arise following treatment with ribonucleotide reductase (RNR) inhibitors such as hydroxyurea (Hu), or DNA polymerase inhibitors such as aphidicolin. Aberrant oncogene activation, such as cyclin E overexpression, has also been found to induce replication stress and this is thought to occur due to increased origin firing and nucleotide pool depletion (Bester

et al., 2011). In these cases, disruption of DNA replication can also eventually lead to DNA breaks following replication fork stalling and collapse. Furthermore, treatment with Hu or c-MYC oncogene overexpression can exacerbate the fragility of early replicating fragile sites (Barlow et al., 2013). DSB (double-strand break) formation can occur at sites of replication fork collapse, either by passive breakage (not necessarily through endonucleolytic cleavage) or due to the action of endonucleases that may be activated in an attempt to process aberrant structures such as persistent ssDNA or reversed forks (Sogo et al., 2002; Zeman and Cimprich, 2013).

Interestingly, severe hypoxia (<0.1% O_2) leads to replication stress without the concomitant generation of detectable DNA damage (Bencokova et al., 2009). Strikingly, even prolonged exposure to hypoxia-induced replication stress does not lead to detectable SSB (single-strand break) or DSB formation (Figure 1.4). Damage is detected under these conditions only following depletion/inhibition of certain DDR components (Olcina et al., 2010; Pires et al., 2012).

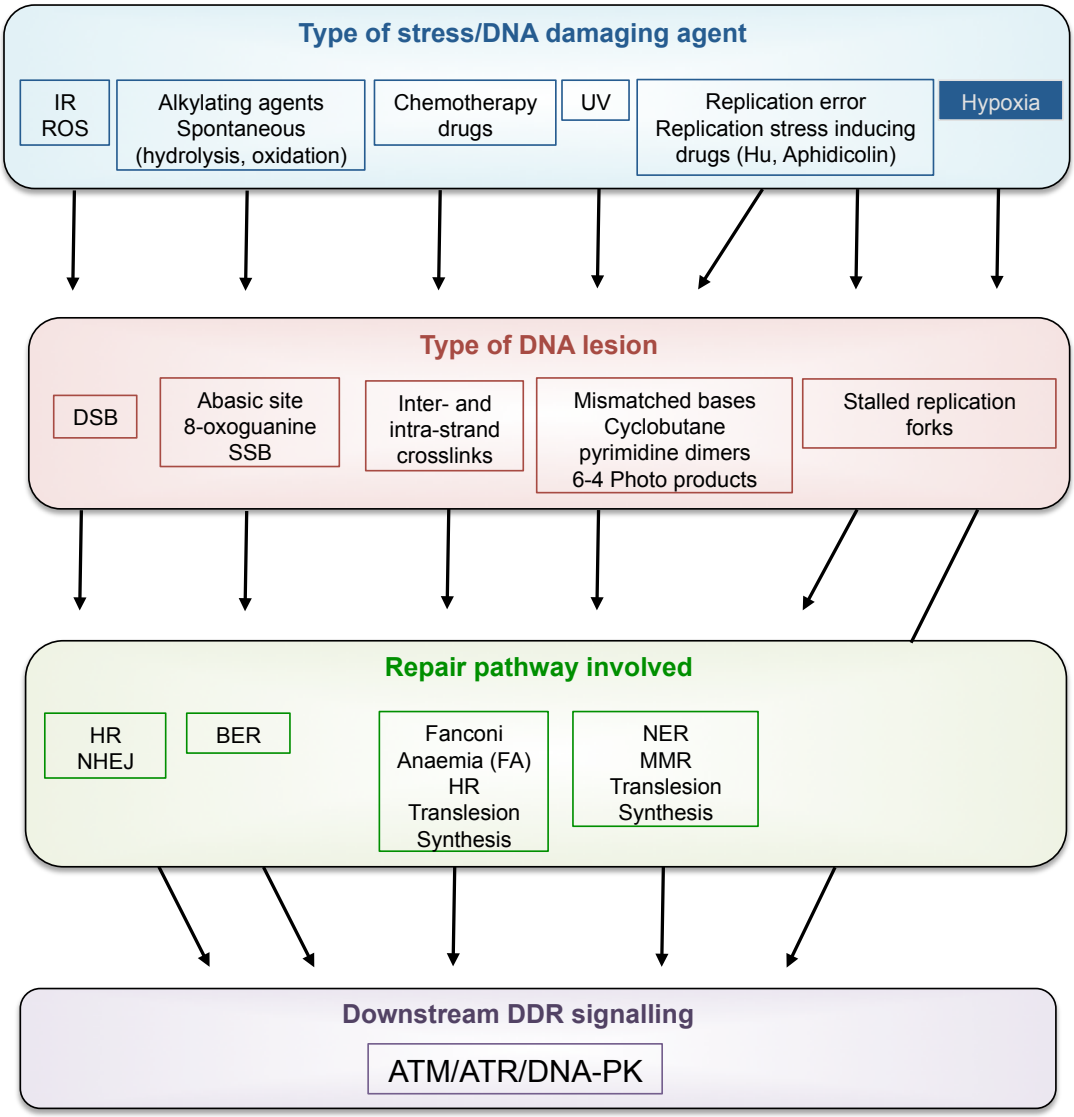


Figure 1.4. Schematic representation of the DDR/DNA repair pathways activated following exposure to a variety of stresses
A cell may encounter a number of endogenous and exogenous stresses that can generate a variety of lesions. These lesions are repaired by specific pathways. Ultimately, most lesions trigger DDR signalling, which is typically initiated by one or several of the three main apical kinases, ATM/ATR/DNA-PK. Notably, hypoxia, while leading to an increase in replication stress and replication fork stalling does not induce detectable DNA damage. While DNA repair is generally repressed in hypoxia, a particular DDR is induced following hypoxia-induced replication stress. Adapted from (Ghosal and Chen, 2013; Rouse and Jackson, 2002).

1.3.2 DNA Damage signalling

The "classical" response to DNA damage leads to the activation of a complicated kinase signalling cascade that includes sensing and responding to the insult, as well as coordinating a number of downstream events generally resulting in cell cycle arrest, DNA repair, senescence or apoptosis (shown in Figure 1.5 and reviewed in (Ciccia and Elledge, 2010)). This cascade can be envisioned as having three principal kinases although there is considerable crosstalk between them. Put simply, if the stress activating the DDR leads to the generation of ssDNA, the ATR (ataxia-telangiectasia and RAD3-related) PI3K (phosphatidylinositol-3-kinase) like kinase (PIKK) will be activated (Cimprich and Cortez, 2008). Alternatively, if the insult leads to the generation of a DSB two other members of the PIKK family, ATM (ataxia-telangiectasia mutated) and DNA-PK (DNA-dependent protein kinase), become activated (Jackson and Bartek, 2009). ATM is generally regarded as the main upstream kinase of the signalling pathway activated in response to DSBs, while DNA-PK is mainly involved in the repair of DSBs in the NHEJ pathway (Collis et al., 2005).

One of the key effectors of the DDR is the tumour suppressor protein, p53, which can induce both cell cycle arrest and apoptosis (Green and Kroemer, 2009; Harper and Elledge, 2007; Riley et al., 2008; Vousden and Lane, 2007; Yee and Vousden, 2005). Initial studies characterising the hypoxia-induced DDR were undertaken following from the observation that hypoxia induces p53 activation, and indeed this event is likely a principal consequence of the hypoxia-induced DDR (Graeber et al., 1994; Hammond et al., 2002). In response to hypoxia, p53 is phosphorylated at a number of residues including serine 15, which has been proposed to be important in mediating nuclear accumulation of p53 (Hammond et al., 2002). The initial stabilisation of p53

in hypoxia is also facilitated by phosphorylation on residues 6, 9, 20, 37 and 46 (Hammond and Giaccia, 2005). Interestingly, hypoxic conditions, which lead to the activation of p53, tend to induce apoptosis as opposed to a cell cycle arrest in G_1. p53 activation is, in fact, critical for hypoxia-induced apoptosis and loss of p53 decreases this apoptotic response (Graeber et al., 1996). Regions of hypoxia have been elegantly shown to correlate with high apoptosis in tumours with wild-type p53, whereas low apoptosis levels are observed in hypoxic tumour regions that have lost p53 (Graeber et al., 1996).

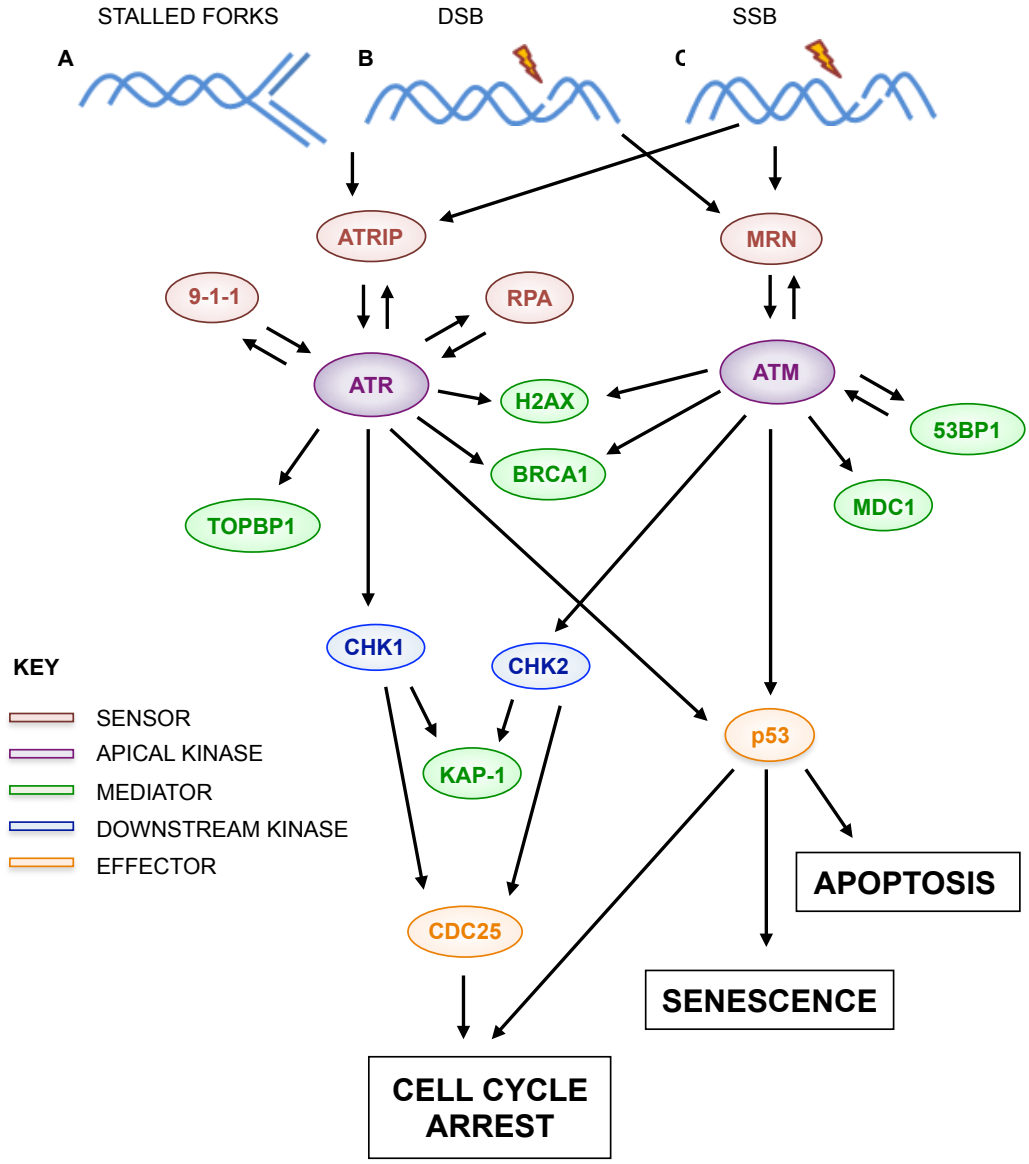


Figure 1.5. Schematic representation of the DDR
(A) Stalled replication forks, **(B)** SSBs**,** and/or **(C)** DSBs, can lead to the activation of the DDR. While (A), (B) and (C) can all lead to the activation of ATR-mediated signalling, ATM-mediated signalling is typically thought to be induced mainly following DNA breaks (B and C). Two important consequences of the activation of these signalling pathways are cell cycle arrest and apoptosis. The colour coding for each protein involved in the cascade is given in a key on the left. For simplicity, only certain aspects of the ATR- and ATM-signalling pathways have been included in this diagram. Adapted from (Olcina and Hammond, 2014; Sulli et al., 2012).

1.3.3 Initiation of DDR signalling in hypoxia

As mentioned above, hypoxia-induced replication stress leads to the activation of the DDR in the absence of detectable DNA damage (Hammond et al., 2002). Analysis of DNA damage formation by the use of comet assays or staining for the presence of 53BP1 (p53-binding protein 1) foci has demonstrated that hypoxia, in the absence of reoxygenation, does not induce detectable DNA damage. Interestingly, the histone variant H2AX is robustly phosphorylated on serine 139 (γH2AX) in response to hypoxia (<0.1% O_2) (Bencokova et al., 2009). However, the γH2AX signal observed in hypoxic conditions is diffuse and pan-nuclear as opposed to forming the discreet nuclear foci seen in response to treatment with DNA damaging agents such as IR (ionising radiation). This pattern of γH2AX staining is reminiscent of the response to replication stress as initiated, for example, by treatment with Hu or aphidicolin (Toledo et al., 2011). These data suggest that hypoxia induces a DDR characterised by the robust induction of γH2AX, but that this is more likely to occur as a result of replication stress rather than DSBs (Hammond et al., 2002). More recently, nucleotide levels have been measured *in vitro* with dATP showing the greatest decrease in response to severe hypoxia in parallel with the replication stress. Importantly, nucleotide levels remain stable in mild hypoxia (for example 2% O_2) where no replication stress is observed (Pires et al., 2010b). This has been hypothesized to be the result of decreased RNR activity in these conditions since RNR catalyses the conversion of ribonucleotides to deoxyribonucleotides using oxygen to regenerate a free radical at its active site (Pires et al., 2010b; Probst et al., 1989; Reichard and Ehrenberg, 1983). DNA fiber technology has been used to image individual ongoing or stalled forks, as well as to measure the rate of ongoing replication fork speeds. This demonstrated a decrease in origin firing and fork speeds, as well as an increase in

stalling of replication forks in response to severe hypoxia but not under mild hypoxic conditions. The occurrence of these aberrant replication structures correlates with the formation of RPA foci, suggesting the presence of ssDNA (Pires et al., 2010b). Together, these data support the hypothesis that, in response to severe hypoxia, increased stalled replication leads to the accumulation of regions of ssDNA and a DDR (Olcina and Hammond, 2014).

1.3.4 ATR-mediated DNA-damage response: The response to replication stress

As described above, following replication stress induced by Hu, UV radiation, inter-strand crosslinks, bulky adduct formation as well as severe hypoxia; replication forks slow down and in some instances stall. Despite the decrease in replication fork progression, the MCM helicase continues unwinding DNA leading to the formation of ssDNA regions. Resected DSBs can also result in ssDNA generation. These ssDNA regions become coated by RPA in order to prevent processes such as DNA reannealing (Chen et al., 2013; Cortez et al., 2001; Fanning et al., 2006; Zou and Elledge, 2003). ATRIP (ATR-interacting protein) binds to RPA thereby recruiting ATR to the sites of RPA-coated ssDNA. RAD17 is then directed to these sites where it loads the 9-1-1 complex (composed of RAD9-RAD1-HUS1). The activity of ATR is enhanced by the phosphorylation of RAD17, 9-1-1 and the ATR activator, TOPBP1 (DNA topoisomerase 2-binding protein 1). ATR plays a critical role in the maintenance of fork integrity and checkpoint response, and many studies have shown that if ATR function is lost, DNA repair and viability are severely compromised (Cliby et al., 1998; Hurley et al., 2007). Activation of ATR at a stalled replication fork serves two major functions: inhibition of origin firing and induction of cell cycle

arrest. Furthermore, a function for ATR in preventing the depletion of RPA pools by halting unscheduled origin firing has recently been demonstrated (Toledo et al., 2013). ATR also attempts to maintain fork integrity by stabilising the fork, facilitating fork restart and inhibiting recombination. These functions are undertaken to allow fork restart once the stress or lesion has been resolved. In situations where the stress cannot be removed, dormant origin firing can be triggered to allow replication to resume (McIntosh and Blow, 2012). Lesions can also be bypassed by repriming the replication machinery followed by filling of the generated ssDNA gap with translesion synthesis polymerases or by undertaking template switching (Zeman and Cimprich, 2013).

One of the best characterised ATR substrates is CHK1 (checkpoint kinase 1), which is phosphorylated at serine 317 and 345. Phosphorylation of these sites also requires the activities of three other proteins: TOPBP1, Claspin and TIPIN. Phosphorylated and active CHK1 can direct cell cycle regulation by mediating a checkpoint response (Dai and Grant, 2010; Liu et al., 2000; Sanchez et al., 1997). If the cell senses an insult, checkpoints halt the cycle to allow sufficient time for any damage incurred by the cell to be repaired. This prevents key cellular events, such as chromosome segregation or DNA replication, being carried out in damaged or repairing cells. Much of the cell cycle regulation is carried out by the CDC25 phosphatases that in turn regulate cyclin/CDK complexes by de-phosphorylating and thereby activating CDKs. CHK1 dependent phosphorylation of the CDC25A phosphatase, for example, leads to its inactivation and a G_1/S phase arrest (Cortez et al., 2001). The maintenance of the G_1/S checkpoint is also achieved via p53 and the activation of cyclin dependent kinase inhibitor 1A (p21). p21 interacts with CDK2

and CDK4 hindering the interaction between CDK2/cyclin E and CDK4/cyclin D (Sancar et al., 2004).

1.3.5 Hypoxia-induced ATR-CHK1 signalling

ATR has been found to phosphorylate a number of downstream targets in hypoxia including CHK1 (Hammond et al., 2002; Hammond et al., 2003a, 2004) (Figure 1.6). If ATR or CHK1 are depleted/inhibited, damage accumulates in hypoxia pointing to a role for ATR/CHK1 in stabilising replication forks under these conditions (Hammond et al., 2004). If hypoxic cells are allowed to undergo reoxygenation following acute hypoxia, stalled replication forks can restart. In this context, an unscheduled increase in the number of new origins being fired occurs as a result of CHK1 inhibition. CHK1, therefore, probably maintains genomic integrity following replication restart by delaying origin firing after reoxygenation-induced DNA damage, possibly to allow repair before replication can resume (Pires et al., 2010b). Hypoxia-induced CHK1 phosphorylates downstream targets including TLK1 (tousled-like kinase 1) (Pires et al., 2010a). TLK1 is a serine/threonine kinase that is usually inactivated once phosphorylated by CHK1 following DNA damage, and is thought to facilitate a number of processes including DNA replication and chromatin remodelling (Groth et al., 2003). The role of TLK1 in hypoxia has not been fully investigated.

ATR/CHK1 inhibition or knockdown sensitises cells to hypoxia/reoxygenation as assayed by colony formation assay (Hammond et al., 2004). This has been shown using several methodologies including gene silencing or the use of knockout or kinase dead cell lines (Hammond et al., 2004; Hammond and Giaccia, 2004). More recently, the use of specific ATR and CHK1 inhibitors has also been shown to have promising sensitising effects (Cazares-Korner et al., 2013; Pires et al., 2012). Two specific ATR inhibitors, VE-821 and VE-822, were shown recently to reduce viability of a variety

of tumour cell lines to a range of oxygen concentrations (Fokas et al., 2012; Pires et al., 2012; Prevo et al., 2012). Moreover, VE-821 was shown to enhance radiation-induced loss of viability of cells exposed to both normoxic as well as hypoxic conditions, showing the potential that these types of compounds could have in combination therapies (Pires et al., 2012). Importantly, the use of VE-821 either as a single agent or in combination with genotoxic agents led to a reversible growth arrest in normal cells (Charrier et al., 2011; Reaper et al., 2011b). Interestingly, the increased sensitivity to hypoxia/reoxygenation observed upon CHK1 loss is thought to be predominantly dependent upon CHK1 loss during reoxygenation, since abrogation of CHK1 activity during both reoxygenation and hypoxia does not lead to additional sensitisation. The promising effects seen with CHK1 inhibitors in tumours with high levels of endogenous or exogenous replication stress suggest they should also be effective for the targeting of severely hypoxic tumour cells (Gilad et al., 2010; Schoppy et al., 2012). The use of hypoxia-activated CHK1 inhibitors has indeed recently been reported to specifically kill cancer cells when used under hypoxic conditions (Cazares-Korner et al., 2013).

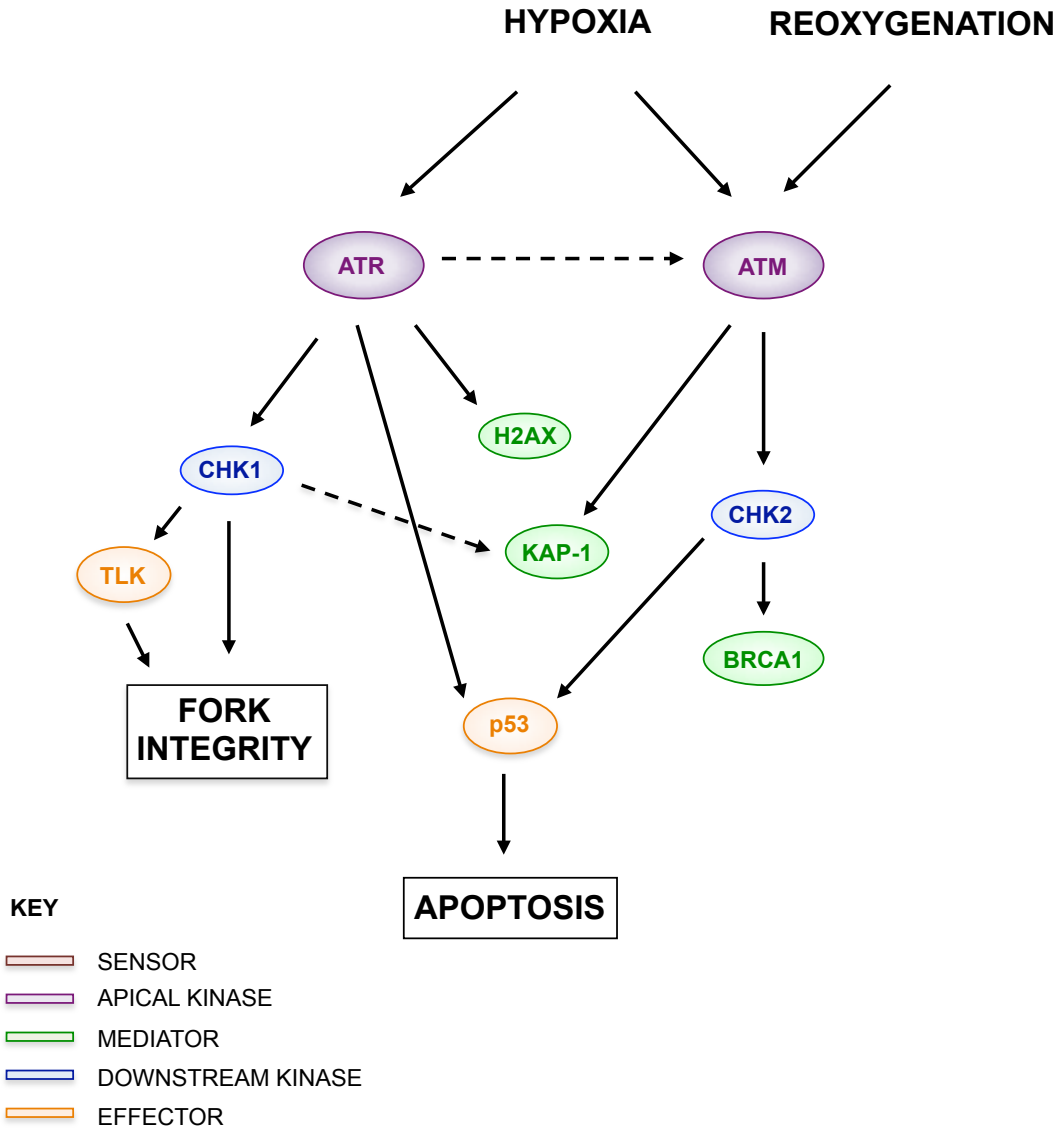


Figure 1.6. Schematic representation of the DDR induced in response to hypoxia and reoxygenation
Severe hypoxia induces a DDR. ATR- as well as ATM-mediated signalling arms of the hypoxia-induced DDR are illustrated in this diagram. Reoxygenation following periods of hypoxia leads to the generation of ROS, which can cause DNA breaks. These breaks in turn also activate the DDR. The colour coding for each protein involved in the cascade is given in a key on the left. Adapted from (Olcina and Hammond, 2014).

1.3.6 ATM mediated DNA damage response: The response to DSBs

A single DSB can be lethal for a cell so it is particularly important to sense and repair it appropriately (Jeggo and Lobrich, 2007; Shiloh, 2003). ATM is the apical kinase involved in responding to this type of damage. ATM is a 350 kDa protein that shares PI3K-like domains, FAT (FRAP-ATM-TRRAP) and FATC (FAT-C terminal) domains with other PIKKs (Figure 1.7). Like ATR and DNA-PKcs, ATM preferentially phosphorylates peptides with serine or threonine residues followed by glutamine (S/T-Q motif). ATM is recruited to sites of damage via its interaction with the MRN complex. This complex is comprised of MRE11 (mitotic recombination 11), RAD50 and NBS1 (Nijmegen breakage syndrome 1). When the MRN complex binds to DNA, it does so in such a manner that facilitates the interaction between the coiled coil domains of MRN complexes on different broken DNA strands, allowing the physical proximity of these broken ends (Moreno-Herrero et al., 2005). ATM is recruited to the DNA break via the ATM binding site in NBS1 (Falck et al., 2005). Binding to the broken DNA ends stimulates ATM activation by the formation of active monomers from inactive ATM dimers, a process aided by autophosphorylation at several serine residues such as 367, 1983, 1981 and 2996 (Bakkenist and Kastan, 2003; Kozlov et al., 2011; Kozlov et al., 2006). However, while ATM autophosphorylation is important for its retention at the break it is not essential for initial tethering of ATM to the DSB site (So et al., 2009).

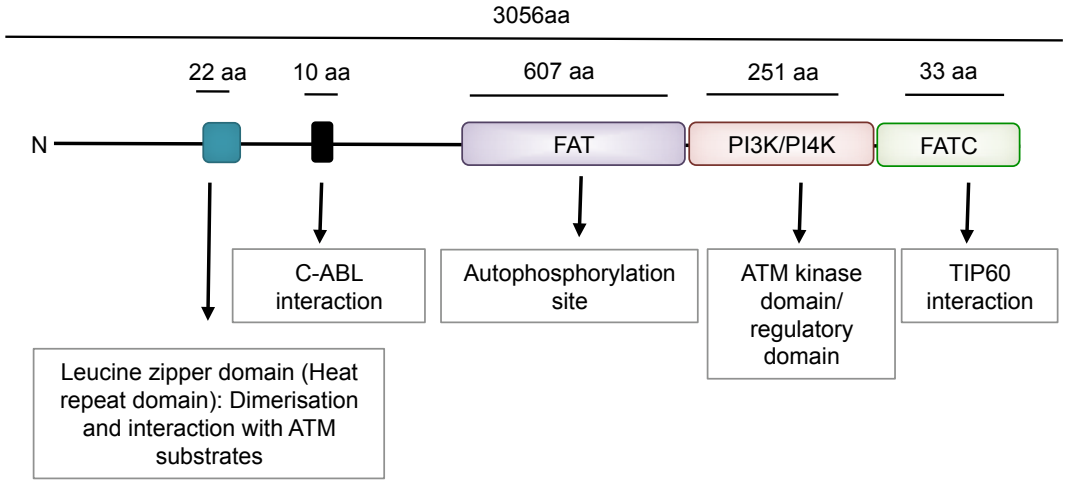


Figure 1.7. Schematic representation of the principal domains in the ATM protein
A brief description of the proposed function of each domain is given in the white boxes. The number of amino acids (aa) for each domain as well as for the whole protein is indicated above the domains/full length protein (Stracker et al., 2013).

Disruption to DNA following a break occurs in the context of the chromatin structure around which DNA is wrapped. Chromatin structure consequently is now thought to impact on the initial sensing of damage, as well as the subsequent repair capabilities of a cell (this will be discussed in further detail in section 1.4.2) (Soria et al., 2012). Phosphorylation of the histone variant H2AX on serine 139, for instance, is an early and extremely important event occurring in response to DSBs. Of note, H2AX knockout mice are sensitive to IR, display chromosomal instability and have defects in DNA repair, as well as in the recruitment of DNA repair factors such as NBS1 (Celeste et al., 2002). ATM, DNA-PKcs and ATR can all direct the phosphorylation of H2AX (Rogakou et al., 1998). This modification is important for the recruitment of MDC1 (mediator of DNA damage checkpoint 1), a protein that

further enhances γH2AX. MDC1 interacts with the C-terminal tail of γH2AX through its BRCT (BRCA1 C-terminal) domain (Stucki et al., 2005). The interaction between γH2AX and MDC1 initiates a feedback loop that encourages further MRN recruitment and ATM activation (Goldberg et al., 2003; Lou et al., 2006; Lukas et al., 2004; Stucki and Jackson, 2006). Furthermore, the RAD50 and NBS1 components of the MRN complex are ATM targets, establishing a further feedback loop for signal amplification, at least in response to IR (Gatei et al., 2011; Gatei et al., 2000; Lim et al., 2000; Wu et al., 2000).

MDC1 itself is also a target of ATM and its phosphorylation is important for the binding of RNF8 (Goldberg et al., 2003; Huen et al., 2007; Kolas et al., 2007; Mailand et al., 2007). RNF8 directs a number of ubiquitylation signalling events that result in the polyubiquitylation of H2A and H2AX next to the break by the formation of lysine-63 (K63)-linked polyubiquitin chains (Huen et al., 2007; Kolas et al., 2007; Mailand et al., 2007; Wang and Elledge, 2007). Another E3 ubiquitin ligase, RNF168, binds to these modified histones leading to further K63 polyubiquitylation. These events allow the accessibility of checkpoint and repair factors such as 53BP1 and BRCA1 (breast cancer 1, early onset 1) and their accumulation at the break (Huen et al., 2007; Kolas et al., 2007; Mailand et al., 2007; Stewart et al., 2009). 53BP1 foci formation also requires MDC1 and its interaction with γH2AX (Stewart et al., 2003; Stucki et al., 2005). BRCA1 and 53BP1 can facilitate binding of ATM with the MRN complex, as does the ubiquitylation of NBS1 (on K63) by E3 ubiquitin ligase, SKP2 (Lee et al., 2010a; Wu et al., 2012a). Furthermore, ATM dependent phosphorylation of BRCA1 is critical for the response to IR-induced DSB. In this respect, BRCA1 interacts with BRCA2 enabling the targeting of recombination repair protein RAD51

to the DSB to be repaired. BRCA1 can also promote DNA resection by interacting with CtIP (CtBP interacting protein) and the MRN complex (Chen et al., 2008).

In most cell lines, however, only 10-15% of DSBs have been proposed to depend on ATM activity for appropriate repair following γ-ray induced DSBs (Riballo et al., 2004). This percentage has been suggested to correspond to the fraction of DSBs generated in heterochromatin areas (since these areas correspond to 10-15% of the genome). ATM dependent KAP-1, (Krüppel-associated box (KRAB) domain-associated protein 1), phosphorylation following DSB generation has been shown to be particularly important for facilitating repair, in these heterochromatin rich regions (Cann and Dellaire, 2011; Goodarzi et al., 2008). KAP-1 is a 97 kDa nuclear protein known to be phosphorylated at serine 824 in an ATM dependent manner following a variety of genotoxic stresses, including IR (White et al., 2006). The involvement of KAP-1 in chromatin remodelling during DSB repair will be discussed in further detail in section 1.4.2. Of note, in regions of heterochromatin, 53BP1 and BRCA1 foci formation at DSBs are dependent on ATM mediated KAP-1 phosphorylation at serine 824 (Noon et al., 2010). Phosphorylation of KAP-1 at serine 473 has recently also been noted. This site was shown to be phosphorylated in a CHK1 or CHK2 dependent manner in response to IR. CHK1, however, is the most prominent kinase mediating phosphorylation at residue 473 in response to insults leading to replication stress such as aphidicolin treatment (Blasius et al., 2011). ATM also phosphorylates RNF20-RNF40 allowing ubiquitylation of H2B and further facilitating chromatin relaxation. The formation of 53BP1 and γH2AX foci are also tightly regulated by recruitment of the RNF20-RNF40 heterodimer to the break (Moyal et al., 2011). A member of the nucleosome remodelling and histone deacetylation (NuRD) complex, CHD4, (chromodomain, helicase, DNA binding 4), has been proposed to be phosphorylated

by ATM on serine 1349 following IR, with repair defects being observed upon mutation of this phosphorylation site (Urquhart et al., 2011).

Besides its critical role in orchestrating the repair of DSBs, ATM is important for eliciting appropriate checkpoint responses following DNA damage, with defects in G_1, S and G_2 checkpoints arising in the absence of ATM. Cells from ataxia-telangiectasia (A-T) patients (harbouring mutations in the *ATM* gene) or from $ATM^{-/-}$ mice, exhibit radio-resistant DNA synthesis (RDS) following IR since they cannot prevent S-phase entry (Jeggo et al., 1998; Savitsky et al., 1995). Interestingly, patients with ataxia-telangiectasia like disorder (A-TLD) and Nijmegen breakage syndrome (NBS), caused by MRE11 and NBS mutations respectively, also display the RDS phenotype (Carney et al., 1998; Stewart et al., 1999). ATM dependent phosphorylation of a number of downstream targets including, p53, CHK1 and CHK2, are required for checkpoint activation (Jeggo et al., 1998; Kastan, 2004). In the context of the S-phase checkpoint, ATM has been shown to inhibit DNA replication in the presence of DSBs mainly by phosphorylating CHK1 and CHK2, which in turn phosphorylate CDC25A. Degradation of CDC25A following CHK1/CHK2 dependent phosphorylation maintains CDK2 in its inactive phosphorylated state, thereby precluding CDC45 loading on DNA replication origins (Costanzo et al., 2000; Falck et al., 2002; Sorensen et al., 2003). Interestingly, a second branch to this checkpoint response occurs through ATM dependent phosphorylation of NBS1, which is required for the phosphorylation of SMC1 (structural maintenance of chromosomes 1) (at serines 957 and 966). SMC1 phosphorylation at these two sites has been proposed to be important for checkpoint activation independently of CHK2/CDC25A/CDK2 since NBS and A-TLD cells

show comparable CHK2 activation, downregulation of CDC25A and decreased CDK2 activity to control cells (Falck et al., 2002; Yazdi et al., 2002).

1.3.7 Hypoxia-induced ATM signalling in the absence of DSBs

Importantly, the hypoxia-induced DDR also leads to the activation of ATM (Bencokova et al., 2009). This is somewhat paradoxical since, as discussed above severe hypoxia does not lead to the generation of detectable DSBs or SSBs. However, heat, hypotonic stress (which can cause replicative stress) and agents which modify chromatin have all been associated with an increase in ATM activity in the absence of DNA damage (Bakkenist and Kastan, 2003). More recently, oxidative stress generated following treatment with H_2O_2 has also been demonstrated to induce ATM activity independently of the MRN complex, once again in the absence of DNA damage (Guo et al., 2010). The only physiological stress known to activate ATM in the absence of DNA damage to date, however, is hypoxia (Bencokova et al., 2009).

Following hypoxia-induced replication stress, ATM is phosphorylated at serine 1981 and has been shown to phosphorylate downstream targets including KAP-1, CHK2 and DNA-PKcs (Bencokova et al., 2009). The phosphorylation of KAP-1 is somewhat surprising as it has previously been described to be entirely dependent on the presence of DSBs (Goodarzi et al., 2009). Furthermore, once phosphorylated by ATM, CHK2 can phosphorylate p53 at serine 20 and BRCA1 at serine 988 (Gibson et al., 2006). In contrast to ATM activation following DNA damage, hypoxia-induced ATM activity is independent of the MRN complex. As the principal role of the MRN complex is in the initial detection of DSBs, this is supportive of DSBs not being the signal that induces the DDR in hypoxia. Similarly to what happens in response to

DNA damage, the mediator protein MDC1 does amplify hypoxia-induced ATM activity and is required for maximal phosphorylation of ATM targets, for example KAP-1. However, again in contrast to the response to *bona fide* DNA damage, BRCA1, 53BP1 and RNF8 are not subsequently recruited to form nuclear foci by MDC1 in hypoxic conditions (Bencokova et al., 2009). ATM is a predominantly nuclear protein although some reports indicate it is also active in the cytoplasm (Ambrose et al., 2007; Watters et al., 1997). During hypoxia, phosphorylated ATM is found in the nucleus but does not appear to be tightly associated with chromatin. This is once more consistent with the fact that ATM is not activated in response to or recruited to sites of DNA breaks (Bencokova et al., 2009). The role of ATM in severe hypoxia is unclear, although ATM knockdown has been shown to cause sensitisation to hypoxia/reoxygenation (Freiberg et al., 2006b).

The induction of ATM by chromatin modifying agents suggests the possibility that ATM responds directly to the stalled replication forks in hypoxia, as these forks would presumably present altered chromatin modifications (Bakkenist and Kastan, 2003; Bencokova et al., 2009). Interestingly, the autophosphorylation (on serine 2056) and recruitment of DNA-PKcs in response to hypoxia (0.1-1% O_2) has been associated with hypoxia-mediated changes in histone 3 (H3) acetylation. In these studies the authors proposed that DSBs were not the signal for DNA-PKcs activation since recruitment of the XRCC4-DNA-ligase IV complex, that would presumably be recruited to the DNA break, did not accompany such activation (Bouquet et al., 2011).

The mechanism of ATM activation in response to severe hypoxia, however, is still not fully understood. It is possible that hypoxia-induced ATR may contribute to ATM phosphorylation and activation. This possibility is supported by the finding that in response to UV or Hu, ATR phosphorylates ATM (Stiff et al., 2006). Further

investigation of this hypothesis in hypoxia is technically challenging since ATM is activated in response to pharmacological inhibition or genetic knockdown of ATR. As previously mentioned, this is believed to be due to the collapse of hypoxia-induced stalled replication forks (Toledo et al., 2011). In support of this model, we recently demonstrated that a potent ATR inhibitor (VE-821) induces DNA damage detected by the presence of 53BP1 foci in hypoxic cells (Pires et al., 2012).

1.3.8 Two pathways collide – HIF-1 and the DDR

Recently, it has been demonstrated that ATM is active in milder hypoxic conditions (0.2-1% O_2) (Cam et al., 2010). In these conditions, ATM has been shown to increase HIF-1α stability through phosphorylation at serine 696. ATM dependent phosphorylation of HIF-1α leads to the upregulation of a negative regulator of mTORC1 (mammalian target of rapamycin complex 1), REDD1 (regulated in development and DNA damage responses 1), and a subsequent reduction in mTORC1 signalling in hypoxia (Cam et al., 2010).

Given that ATM shares substrates with other PIKK family members, it is perhaps not surprising that ATR and DNA-PKcs have also been shown to affect HIF-1α levels, pointing to a further link between these two signalling pathways (Bouquet et al., 2011; Fallone et al., 2012; Matsuoka et al., 2007; Pires et al., 2012). Cells grown as spheroids treated with the ATR inhibitor VE-821 were found to have lower levels of the HIF-1α target GLUT1 compared to untreated spheroids. This observation was expanded to show that in the presence of VE-821, HIF-1α stabilisation was delayed in hypoxic conditions and that this correlated with delayed induction of HIF-1α target genes. The effect of ATR inhibition on HIF-1α stability and activity appeared

transient. It is likely that this is due to the concomitant induction of ATM, which can also stabilise HIF-1α as described previously. Despite this, the role of ATR in stabilising HIF-1α is of significant interest. An increasing number of human tumours have been shown to harbour ATM mutations suggesting ATR inhibition may have prolonged effects on HIF-1α activity in certain cases. Interestingly, ATR inhibition was shown to slow down hypoxia-induced cell motility in a HIF-1α dependent manner suggesting that agents of this type might have an unexpected impact on tumour spread. In addition, Economopoulou *et al.,* have shown that in response to mild hypoxia (1% O_2), where no replication stress is observed, H2AX is phosphorylated at serine 139 in an ATR dependent manner in proliferating endothelial cells. The low levels of DNA damage arising during normal replication were thought to serve as the activating signal for DDR activation and H2AX phosphorylation in this case. These studies showed that γH2AX was required for pathological neovascularisation in hypoxia. Notably, loss of γH2AX had no effect on developmental angiogenesis (Economopoulou et al., 2009; Olcina and Hammond, 2014; Rankin et al., 2009).

In addition, further links between replication and HIF-1 have recently been described. Semenza and colleagues demonstrated that MCM3 can suppress the activity of the transactivation domain of HIF-1α while MCM7 enhances HIF-1α ubiquitylation and degradation (Hubbi et al., 2011). The same group has also proposed that the HIF-1α subunit can act independently of HIF-1β and its transcriptional role to inhibit DNA replication by interacting with CDC6. This interaction promoted CDC6 and MCM binding but hindered phosphorylation and activation of MCM by CDC7. Together these interactions were proposed to lead to a reduction in DNA replication at 1% O_2 (Hubbi et al., 2013).

PARP1 (Poly (ADP-ribose) polymerase 1) has also been demonstrated to be important for HIF-1α activation in a number of models. This observation was first reported in a murine model of skin carcinogenesis, where PARP1 inhibition resulted in reduced HIF-1α activation (Martin-Oliva et al., 2006). Similar findings were subsequently reported in chronic myeloid leukaemia cells following small interfering RNA (siRNA)-mediated knockdown of PARP1, as well as in PARP1 knockout MEFs. PARP1 was found to bind to HIF-1α and its activity was required for HIF-1α activation (Elser et al., 2008).

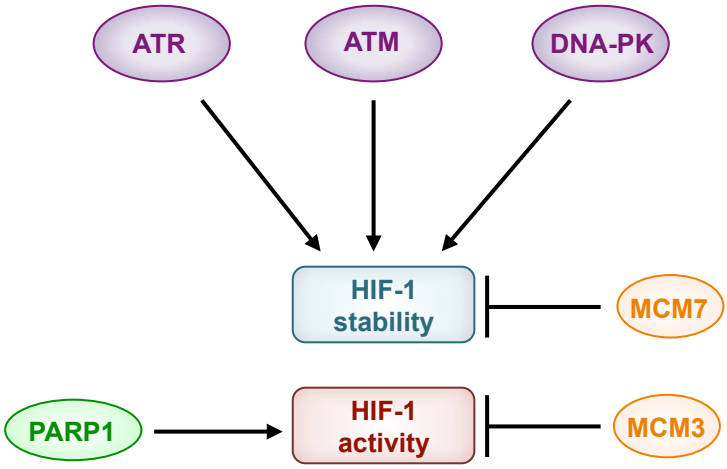


Figure 1.8. Schematic representation of the crosstalk between DNA damage response/replication factors and HIF-1
ATM regulates HIF-1α stability by phosphorylation at serine 696. ATR and DNA-PK can also increase HIF-1α stability and activity but whether they directly phosphorylate HIF-1 is not known to date. The activity of PARP1 can also increase HIF-1α activity. MCM3-7 can inhibit HIF-1 activity or stability (Bouquet et al., 2011; Cam et al., 2010; Elser et al., 2008; Hubbi et al., 2013; Hubbi et al., 2011; Martin-Oliva et al., 2006; Pires et al., 2012).

1.3.9 Reoxygenation and the DNA damage response

As previously mentioned, reoxygenation following periods of hypoxia leads to the induction of DNA damage. Reoxygenation-induced damage signalling can be inhibited with the use of ROS scavengers, suggesting that ROS induces DNA damage and the subsequent DDR after reoxygenation (Hammond et al., 2003a). In response to reoxygenation, ATM has been shown to phosphorylate downstream targets including p53 and CHK2, with ATM dependent CHK2 phosphorylation leading to G_2 arrest (Gibson et al., 2005). In the absence of CHK2, cells undergo elevated levels of apoptosis and the G_2 arrest is abrogated (Freiberg et al., 2006a; Freiberg et al., 2006b; Hammond and Giaccia, 2004). If cells are exposed to acute periods of severe hypoxia (under 12 hours) and are then allowed to undergo reoxygenation they can undergo replication restart (Pires et al., 2010b). It is important to note that these cells restart following the induction of ROS-induced DNA damage and in a context of reduced DNA repair (described in section 1.3.10), potentially leading to increased genomic instability. Importantly, human tumour cells, with intact p53 function will undergo p53 dependent apoptosis if exposed to periods of acute hypoxia followed by reoxygenation. In contrast, when cells are exposed to longer periods of hypoxia (for example, over 12 hours) replication does not restart in response to reoxygenation. Expression analysis determined that numerous key replication factors are repressed in hypoxic conditions, including members of the MCM family. In addition, several members of this complex such as, MCM3, MCM4, MCM5 and MCM6 have been shown to become unbound from chromatin in cells exposed to over 12 hours of severe hypoxia. Replication and DNA synthesis restart cannot occur in these cases, even if reoxygenation occurs and nucleotide levels are restored (Pires et al., 2010b).

In addition, after reoxygenation, ATM has been shown to be important in regulating pathological angiogenesis by limiting excessive ROS. Loss of ATM results in increased ROS, activation of the mitogen activated kinase p38α and subsequent apoptosis in endothelial cells. This supports a distinct role for ATM in hypoxia/reoxygenation independent of its role in the DDR (Okuno et al., 2012).

1.3.10 Hypoxia-mediated repression of DNA repair

The hypoxia-induced DDR has been proposed to act as a barrier to tumourigenesis and could potentially act as a protection mechanism against genomic instability (Negrini et al., 2010; Pires et al., 2010b; Squatrito et al., 2010). Hypoxia, however, can also contribute to this cancer hallmark in a number of ways. For instance, aberrant DNA replication, gene amplification and repression of a number of important DNA repair pathways have all been linked to the hypoxic microenvironment (Bindra and Glazer, 2005; Bristow and Hill, 2008; Klein and Glazer, 2010; Rice et al., 1986; Young et al., 1988; Yuan et al., 2000). Importantly, repression of DNA repair in hypoxia can have detrimental consequences on genome integrity following exposure to DNA damaging agents under hypoxic conditions. Indeed, increased residual DSBs and chromosomal aberrations have been noted following irradiation of cells in G_0-G_1 phase under chronic hypoxia or anoxia, and this was proposed to be the result of reduced repair capabilities under hypoxic conditions (Kumareswaran et al., 2012). A summary of selected repair pathways known to be repressed in hypoxia as well as the mechanism of repression is shown in Table 1.1.

It is worth noting that repression of DNA repair pathways occurs in both mild as well as severe hypoxia suggesting that a large proportion of the hypoxic tumour may

experience compromised repair. Moreover, the hypoxia-induced DDR is also repressed following prolonged exposures to severe hypoxia. The rapid hypoxia-induced phosphorylation of many of the members of the DDR occurring following replication stress has been shown to diminish following exposure to chronic hypoxia. This is most notable in the case of CHK1 phosphorylation, where the rapid and robust induction declines after prolonged hypoxia (Pires et al., 2010a; Pires et al., 2010b).

It is also important to note that many of the DNA repair factors described above are also important facilitators of DNA damage sensing and signalling. For instance, BRCA1 forms a complex with MSH2 and MSH6, which is important for appropriate genomic stability maintenance following DNA damage (Wang et al., 2000). The appropriate activation of the S-phase checkpoint following IR, also relies on the interaction between ATM and MLH1 as well as CHK2 and MSH2 (Brown et al., 2003). The involvement of many of these proteins in DNA damage signalling and not just repair further highlights the impact of their repression in contributing to genomic instability.

Table 1.1. Table summarising selected mechanisms of hypoxia-induced repression of a number of DNA repair genes

Gene	Mechanism of repression	Repair pathway	Reference
BRCA1	Promoter binding by E2F4/p130	HR	(Bindra et al., 2007; Bindra et al., 2005a)
RAD51	Promoter binding by E2F4/p130	HR	(Bindra et al., 2007; Bindra et al., 2005a)
RAD51	Impairment of mRNA translation	HR	(Chan et al., 2008)
RAD52	Repression by miR-210 in hypoxia	HR	(Crosby et al., 2009)
RAD23B	miR-373-mediated repression in hypoxia	NER	(Crosby et al., 2009)
MLH1	HIF-1α independent transcriptional repression of MYC	MMR	(Bindra and Glazer, 2007)
MLH1	HIF-1α dependent regulation of transcription factors DEC1 and DEC2 (negative regulators of *MLH1*)	MMR	(Nakamura et al., 2008)
MSH2	HIF-1α dependent displacement of MYC binding leading to HIF-1α and p53 dependent transcriptional repression	MMR	(Koshiji et al., 2005).
MSH2	HIF-1α independent transcriptional repression of MYC	MMR	(Bindra and Glazer, 2007)
MSH6	HIF-1α dependent displacement of MYC binding leading to HIF-1α and p53 dependent transcriptional repression	MMR	(Koshiji et al., 2005).

The hypoxia-induced repression of DNA repair can be exploited for therapeutic benefit through a concept similar to synthetic lethality. Synthetic lethality describes a situation where a combination of mutations or inhibition of two genes or proteins leads to lethality whereas the loss of either alone results in viability (Kaelin, 2005). This concept is becoming increasingly exploited as a potential means of therapeutically targeting the DDR. The most common example of synthetic lethality, aside from in yeast, is the use of PARP inhibitors in tumours with mutations in BRCA1/2. In these situations, the loss of BRCA1, for instance, and the pharmacological inhibition of PARP lead to a reduced repair capability by the tumour and an increased cell kill. This likely results from the fact that the tumour cells have become somewhat addicted to the DDR components being targeted due to the loss of the tumour suppressor (Bryant et al., 2005; Farmer et al., 2005). Synthetic lethality between ATR and PARP inhibition has also been demonstrated (Peasland et al., 2011). Since hypoxia leads to the repression of a number of DNA repair pathways, the concept of synthetic lethality can be applied to any tumour where repair pathways are compromised. This is known as "context synthetic lethality" and has again been exemplified with the use of PARP inhibitors. In hypoxic cells where members of the HR pathway, such as RAD51 or BRCA1, are repressed, the use of a PARP inhibitor, ABT-888, sensitised cells to hypoxia/reoxygenation and was also shown to radiosensitise hypoxic tumour cells (Chan et al., 2010; Liu et al., 2008). Context synthetic lethality may, therefore, open up the possibility of using synthetically lethal interactions in a range of solid tumours where hypoxia can provide the context deregulation of particular pathways. It could be envisioned that the use of inhibitors to other parts of the DDR that work in synergy with DNA repair pathways, would also render hypoxic tumour cells more sensitive to these kinds of agents while causing

minimal effects to normal tissues (not present in hypoxic regions). Furthermore, the recently established requirement of members of the DDR, such as ATM, ATR or PARP, for full HIF-1 signalling underpins how promising strategies aimed at targeting the DDR or DNA repair may be.

1.4 Chromatin

1.4.1 Chromatin structure

Within the nucleus DNA is packed compactly into chromatin. Chromatin is composed of nucleosomes consisting of 146 bp of DNA, which are wrapped twice around an octamer of histones, two H2A-H2B dimers and an H3-H4 tetramer (shown in Figure 1.9) (Luger et al., 1997). These histones are organised with their globular domains forming the core and their flexible tails extending outside of the nucleosome. Nucleosomes are connected by linker histones H1 or H5 which are associated with pieces of linker DNA of 10-80 bp. Chromatin acquires its condensed form by folding these complexes into higher order structures, which can change very dynamically in response to different stimuli or between cell types (Kenneth and Rocha, 2008). The regulation of chromatin structure is essential for a number of processes including transcription, replication, repair, suppression of transposable elements, cellular differentiation and X-chromosome inactivation (Portela and Esteller, 2010).

Changes to chromatin structure mainly occur at three main levels: histone post-translational modification, DNA methylation and nucleosome remodelling (Portela and Esteller, 2010). It is important to bear in mind that a high degree of co-operation and crosstalk exists between these three levels of chromatin regulation. Importantly,

incorporation and modification of histone variants can also have a profound impact on the chromatin landscape (Kouzarides, 2007; Portela and Esteller, 2010).

1.4.1.1 Histone post-translational modification

Modifications on histones mainly occur on their protruding histone tails and include phosphorylation of serine and threonine residues, lysine acetylation and ubiquitylation, and methylation of lysine and arginine. These modifications may have signalling roles and/or can affect higher-order chromatin structure (Kouzarides, 2007; Strahl and Allis, 2000). Genomic regions harbouring different histone modifications are often broadly classified into two categories, euchromatin and heterochromatin. Euchromatin refers to areas of the genome, which are thought to be more transcriptionally "accessible" and are characterised by high histone acetylation, as well as H3K4, H3K36 and H3K79 trimethylation. Regions of heterochromatin correspond to areas that have high levels of H3K9, H3K27 and H4K20 methylation, high nucleosomal density and are typically less transcriptionally active (Li et al., 2007). Different chromatin states have been proposed to have different biological outcomes, the ultimate effect depending on the combination of histone modifications occurring in a nucleosome or region. Interestingly, the classification of the genome into up to 51 distinct chromatin states (based on the binding of diverse histone modifications in different regions) was recently proposed, suggesting that systematic genome annotation according to combinatorial histone modifications patterns may be possible (Ernst and Kellis, 2010).

Acetylation on lysine residues on the N-terminal tail of histones neutralises the positive charge on histone tails disturbing the interaction between histones and

negatively charged DNA. This modification is, therefore, regarded as one that results in a more "open" chromatin conformation and therefore generally leads to transcriptional activation (Kouzarides, 2007; Vidali et al., 1978). Histone methylation can result in both transcriptional activation or repression depending on the residue and histone being targeted. This modification does not act by altering the charge on DNA but rather it likely serves as a binding site for other chromatin modifying or transcription factors thereby altering the transcriptional outcome. Histone phosphorylation also serves as a signal for the recruitment or activation of other factors, as is the case of γH2AX following DNA damage (Rogakou et al., 1998; Stucki et al., 2005). It is interesting to note that antagonising modifications have been shown to localise within the same nucleosome, with both repressing and activating marks occurring on different H3 proteins of the same nucleosome (Voigt et al., 2012).

Modifications to the histone tails are undertaken by a plethora of enzymes, including HMTs (histone methyltransferases), HDMs (histone demethylases), HATs (histone acetyltransferases) and HDACs (histone deacetylases) (Black et al., 2012). Notably, many HMTs, HDMs, HATs and HDACs also have non-histone targets, for example, G9a and HDAC1 both direct post-translational modifications on p53 (Huang et al., 2010; Huang et al., 2007; Luo et al., 2000).

Since histone methylation, and in particular H3 methylation, will receive the greatest attention in subsequent chapters, the mechanisms regulating this histone modification will be discussed in further detail below. Histone methylation was traditionally regarded as a far more stable modification than acetylation. However, its maintenance has also recently been demonstrated to lie in tight balance between HMTs and HDMs (Greer and Shi, 2012). There are two main families of lysine histone methyltransferases (KMTs): the SET (suppressor of variation 3-9, enhancer of

zeste, trithorax)-containing family and the non-SET-containing family (Figure 1.9) (Dillon et al., 2005; Feng et al., 2002). Both of these classes of KMTs methylate their targets by transferring a methyl group from SAM (S-adenosyl methionine). The substrate binding sites of SET-containing methyltransferases are positioned on opposite sides of the SET domain allowing these enzymes to catalyse several rounds of methylation. This means that histones and SAM are located either side of the domain but are connected by a deep highly specific channel that can accommodate the histone lysine chain. The substrate cannot escape the SET domain in this conformation until full methylation has occurred (Black et al., 2012). During heterochromatin replication the methyltransferase SETDB1 and CAF-1 (chromatin assembly factor 1) mediate H3K9me1 deposition. This mark is then thought to act as a building block for further H3K9 di- and trimethylation by KMTs, Suv39h1/2. CAF-1 also recruits HP1 (heterochromatin protein 1), which recognises H3K9me3 through its chromodomain and facilitates further Suv39h1/2 recruitment (domains present in different histone modifying enzymes are shown in Table 1.2) (Taverna et al., 2007). Suv39h1 recognises H3K9me3 through its chromodomain and interaction between the enzyme and the chromatin mark will create a positive feedback loop for further methylation (Loyola et al., 2009; Towbin et al., 2012). In addition, KAP-1 can also mediate the spreading of heterochromatin by forming complexes with SETDB1 and CHD3/Mi-2α (part of the NuRD complex). In this context, SUMOylated KAP-1 recruits SETDB1 and stimulates its HMT activity (Ivanov et al., 2007). Furthermore, HMTs PRDM3 and PRDM16 have recently been shown to monomethylate H3K9 on cytoplasmic histones, thereby facilitating heterochromatin formation by allowing modified histone incorporation onto heterochromatic regions (Pinheiro et al., 2012).

Like the KMTs, the demethylases are divided into two main classes. The first class to be discovered contains LDS1 and LSD2, which both have FAD (flavin-adenine dinucleotide) dependent amine oxidase domains (Karytinos et al., 2009; Shi et al., 2004). The second class of demethylases are the JmjC (Jumonji C) containing family which catalyses oxidation of methyl groups by using oxygen, iron (II) and 2-oxoglutarate as cofactors (Klose et al., 2006; Tsukada et al., 2006).

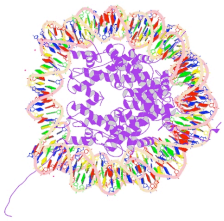
1.4.1.2 DNA methylation

DNA methylation is catalysed by DNA (cytosine-5) methyltransferases (DNMTs) and almost always occurs on CpG dinucleotides. CpG dinucleotides cluster in CpG islands, regions of more than 200 bases with a G+C content of at least 50% and where CpG frequencies are higher than just statistically expected (with a ratio of observed to statistically expected frequencies of 0.6). Regions of lower CpG content lying proximal to CpG islands can also undergo methylation and are known as CpG island shores. General loss of DNA methylation is characteristic of cancer cells, however, high methylation of CpG shores and certain CpG islands has also been reported. CpG methylation is associated with transcriptional inactivation, especially when it occurs on promoter regions. There are three known catalytically active DNMTs: DNMT1, DNMT3A and DNMT3B, which methylate cytosine by using SAM to transfer the methyl group (Portela and Esteller, 2010). DNMT1 is recruited to DNA by URHF1 (ubiquitin-like containing PHD and RING finger domains 1) or PCNA and mediates maintenance DNA methylation by recognising hemimethylated DNA (Avvakumov et al., 2008; Chuang et al., 1997; Sharif et al., 2007). DNMT3A and DNMT3B mediate *de novo* methylation by recruitment through histone methyltransferases EZH2 or G9a.

DNMTL is not catalytically active but it has been proposed to promote methylation by *de novo* methyltransferases (Portela and Esteller, 2010) (Figure 1.9).

A

Histone modifications

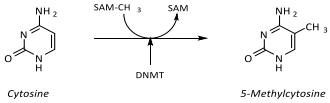


Name	Site
Suv39h1/2	H3K9me3
G9a/GLP	H3K9me1/2
SETDB1	H3K9me1/3
PRDM2/RIZ1	H3K9me1/2/3
MLL	H3K4me3
EZH2	H3K27me3
Suv420h1/2	H4K20me2/3
DOT1L1	H3K79me1/2/3

Name	Site
TIP60	H2A/H3/H4
MOZ	H2A/H3/H4
MORZ	H2A/H3/H4
MOF	H2A/H3/H4
p300/CBP	H2A/H2B/H3/H4
GCN5	H3/H4
PCAF	H3/H4

B

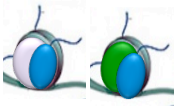
DNA methylation



Name	Proposed function
DNMT1	Maintenance DNA methylation
DNMT3A	De novo DNA methylation
DNMT3B	De novo DNA methylation

C

Nucleosome remodelling



Name	ATPase domain
SWI/SNF	BRM/BRG1
ISWI	SNF2H/SNF2L
INO80	INO80 or related SWRI-like factors (eg p400)
MI-2/CHD	CHD1-9

Figure 1.9. Illustration of the three main ways to achieve chromatin remodelling

(A) Histone modifications are undertaken by a variety of enzymes. Shown are some of the main methyltransferases and acetyltransferases. For simplicity, only histone methylation and acetylation have been included in this figure. A nucleosome with protruding histone tails is also shown (PDB ID code: 1AOI). **(B)** A schematic representation of a cytosine methylation reaction is shown. DNA methylation is usually undertaken by one of the three enzymes shown. **(C)** Nucleosome remodelling can be carried out by ATPase enzymes within chromatin remodelling complexes. The

four principal families of chromatin remodellers and their ATPase domains are shown. Adapted from (Portela and Esteller, 2010).

1.4.1.3 Nucleosome remodelling

Nucleosome remodelling can be undertaken by a number of ATP dependent chromatin remodellers (Figure 1.9). Many of these are part of conserved complexes composed of other chromatin remodelling as well as non-chromatin associated proteins. All remodellers contain an ATPase domain (from the superfamily 2 (SF2) of translocases) as well as domains that regulate the ATPase activity. Remodellers are classified according to the different regulatory domains present within the four subfamilies, SWI/SNF, ISWI, CHD and INO80. Through interaction with multiple factors, these complexes can affect nucleosome position as well as histone variant changes. SWI/SNF, ISWI and CHD remodeller ATPase activities are typically associated with nucleosome positioning while INO80 is preferentially involved in histone variant exchange (Stanley et al., 2013). Nucleosomes can be repositioned by remodellers via movement of the whole histone octamer along DNA. It is important to note that these complexes can cooperate; SWI/SNF and ISWI, for instance, can work together to create a nucleosome-free region at promoters to allow accessibility of transcription factors (Clapier and Cairns, 2009).

Table 1.2. Table summarising chromatin-reading domains together with the sites they have been reported to bind
Adapted from (Taverna et al., 2007).

Name	Site
Chromodomain	H3K9me2/3, H3K27me2/3
Double Chromodomain	H3K4me1/2/3
Chromo Barrel	H3K36me2/3
Tudor	Rme1/2
Tandem Tudor	H3K4me3, H4K20me1/2/3
MBT	H3K4me1, H4K20me1/2, H1K26me1
PHD	H3K4, H3K4me3, H3K9me3, H3K36me3
Bromodomain	Various Kac
WD40	H3R2, H3K4me2
14-3-3	H3S10
BRCT	H2AXS139
ADD	H3K4

1.4.2 Chromatin changes and the DDR

It is now becoming apparent that chromatin changes can have a profound impact on the DDR. This can either be by physically protecting DNA from damage, affecting the spread of DDR signalling, or by regulating the mechanism of response to DNA damage within specific chromatin environments (Sulli et al., 2012). A select list of factors known to impact chromatin structure and the DDR is shown in Table 1.3. However, a more detailed description of chromatin modifying factors known to impact on ATM activation and signalling will be described in the text.

Evidence suggests that following IR, DNA that is lacking histones or other chromatin components, sustains a greater degree of damage than DNA associated with a high chromatin compaction (Costes et al., 2007; Elia and Bradley, 1992). As mentioned above, H2AX phosphorylation is one of the first signalling events to occur following DNA damage. γH2AX mainly occurs in regions of euchromatin or in the

periphery of heterochromatic regions suggesting that heterochromatin is refractory to the spreading of this histone mark. In regions of heterochromatin, ATM-mediated signalling has been demonstrated to be particularly important for efficient repair of DSB (Goodarzi et al., 2008). In this respect, ATM dependent phosphorylation of transcriptional co-repressor KAP-1 appears to be particularly important to relieve KAP-1 mediated heterochromatinisation, thereby facilitating repair (Figure 1.10) (Goodarzi et al., 2008; Groner et al., 2010; Ziv et al., 2006). SUMOylation of KAP-1 at lysines 554, 779 and 804 by UBC9 (ubiquitin carrier protein 9) is thought to allow the interaction between KAP-1 and chromatin remodeller CHD3.1 promoting heterochromatin formation (Goodarzi et al., 2011; Ivanov et al., 2007; Zeng et al., 2008). However, following the generation of a DSB, ATM dependent KAP-1 phosphorylation at serine 824 disrupts the KAP-1-CHD3 complex thereby promoting chromatin relaxation, as evidenced by micrococcal nuclease assay (Goodarzi et al., 2010; Goodarzi et al., 2008). This process can be reversed by dephosphorylation of KAP-1 by protein phosphatase PP4, allowing restoration of the CHD3.1-SUMO-KAP-1 complex (Lee et al., 2012). The involvement of KAP-1 in heterochromatin DSB repair further supports the idea that the chromatin context in which a break is induced is important for the subsequent mounting of an appropriate response.

Significantly, features characteristic of heterochromatin may also serve to facilitate ATM activation (Sun et al., 2009). When ATM is tethered to the DSB, it is acetylated at its regulatory domain by the TIP60 (Tat-interactive protein 60) acetyltransferase, which is thought to be recruited to the DSB in a complex with ATM

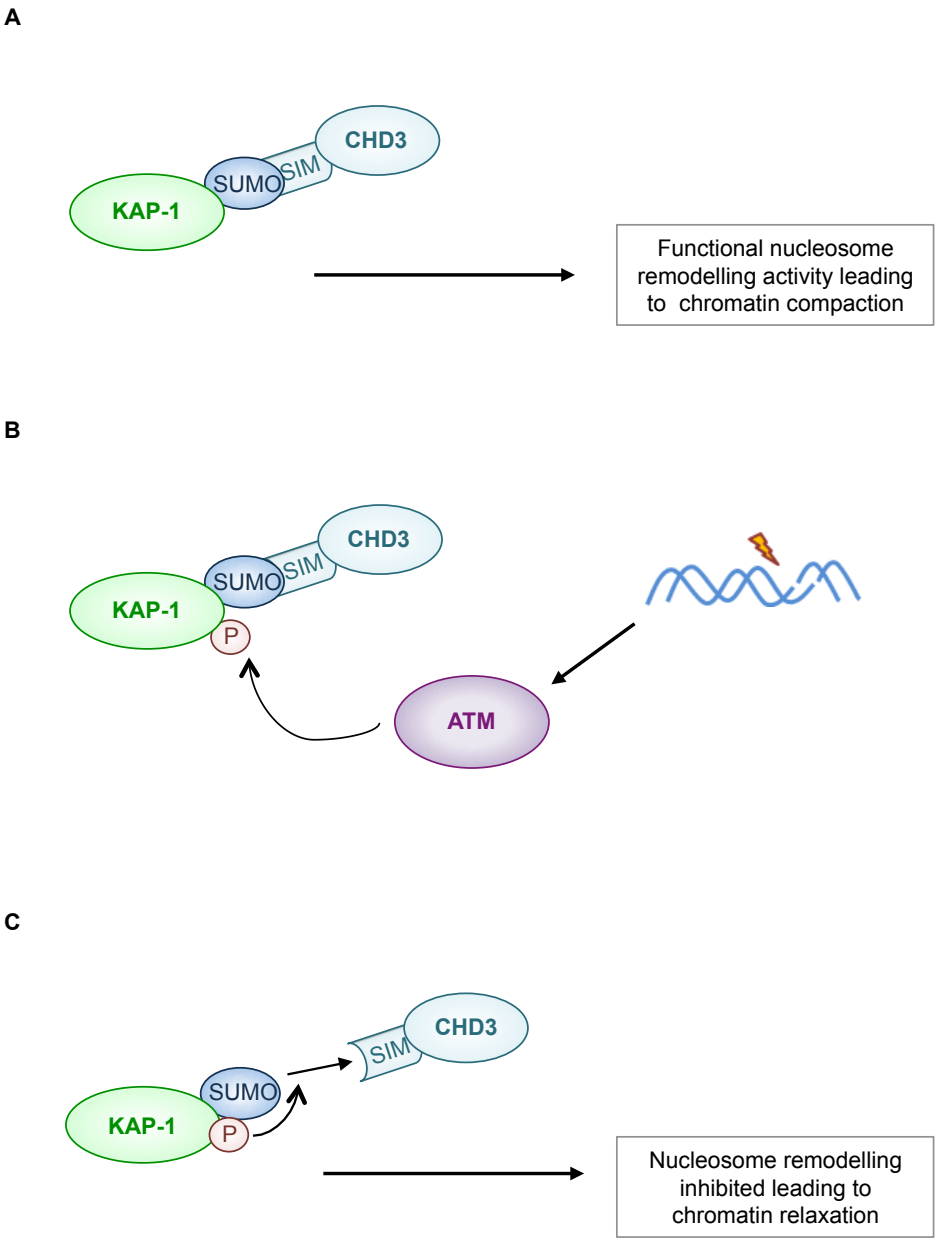


Figure 1.10. Schematic representation of the model for the role of KAP-1 in mediating chromatin remodelling
(A) Under conditions of no stress, interactions between SUMO-KAP-1 and the SIM domain in CHD3.1 promote nucleosome remodelling activities leading to chromatin compaction in heterochromatin areas. **(B)** Following DNA damage, ATM dependent phosphorylation of KAP-1 at serine 824 displaces the SUMO-CHD3.1 interaction, releasing CHD3.1 from KAP-1 enriched heterochromatin, subsequently leading to chromatin relaxation. Adapted from (Goodarzi et al., 2011).

(Sun et al., 2005). Acetylation of ATM by TIP60 is important for stimulating ATM kinase activity and requires a permissive chromatin environment. An accessible area of H3K9me3 around the damaged site is particularly important for the initial activation of TIP60. Displacement of HP1β from H3K9me3, via the phosphorylation of HP1β on threonine 51 by CK2 (casein kinase 2), is a requirement for the recruitment of TIP60 to the DSB. Furthermore, c-ABL dependent TIP60 phosphorylation on tyrosine (Y) 44 has recently been shown to enhance TIP60 binding to H3K9me3 following DNA damage (Kaidi and Jackson, 2013; Sun et al., 2005; Sun et al., 2009). Nevertheless, certain controversy exists regarding the precise role of the HP1 proteins in response to DSBs. HP1 proteins exist as three isoforms, HP1α, β and γ, all of which have been demonstrated to localise at damage sites. HP1α recruitment appears important for induction of 53BP1 and RAD51 foci at these sites independently of H3K9me3 and the chromodomain but dependent on CAF-1 and the chromoshadow domain (a chromo-like domain) (Baldeyron et al., 2011). The tethering of HP1 proteins to the sites of DSB somewhat conflicts with the previously described displacement of HP1β from chromatin to allow ATM signalling (Sun et al., 2009).

Moreover, it is important to note that several other factors that regulate chromatin structure (and are not necessarily associated with heterochromatin) have been found to coordinate appropriate ATM activation and phosphorylation of its downstream targets following IR, including histone acetyltransferase MOF/KAT8. Depletion of MOF results in a decrease in IR-induced H4K16 acetylation and ATM autophosphorylation (Gupta et al., 2005). Optimal ATM activation has also been shown to depend on nucleosome-binding protein, HMGN1, which modulates the interaction of ATM with chromatin. Following IR, HMGN1-mediated H3K14

acetylation appears important in this mechanism since treatment with an HDAC inhibitor bypasses the requirement for HMGN1 for optimal ATM activation (Kim et al., 2009). Moreover, E3 ubiquitin ligases, RNF8 and CHFR work together to regulate histone ubiquitylation which in turn has an effect on H4K16 acetylation by the MRG15 dependent acetyltransferase complex in response to IR (Wu et al., 2011).

Table 1.3. Table summarising the role of selected chromatin regulators in DDR signalling or repair

Name	Type	Specificity	Role in repair/DDR	Reference
WSTF	Tyrosine kinase	H2AXY142	Promotes apoptosis initiation if damage is too severe	(Xiao et al., 2009)
EYA1/3	Phosphatase	H2AXY142	Facilitates γH2AX expansion through MDC1 recruitment	(Cook et al., 2009; Stucki, 2009)
DOT1L	HMT	H3K79me2	Exposure of H3K79me2 following DNA damage may provide a binding site for 53BP1	(Huyen et al., 2004)
SET8	HMT	H4K20me1	H4K20me1 levels increase at DSB facilitating 53BP1 recruitment	(Botuyan et al., 2006; Oda et al., 2010).
MMSET	HMT	H4K20me2/3	H4K20me2/3 increase at DSB site facilitating 53BP1 recruitment	(Pei et al., 2011)
CHD4	ATPase chromatin remodeller	Various	Promotes DSB repair particularly during S/G_2	(Chou et al., 2010; Larsen et al., 2010)
JMJD2B	JmjC HDM	H3K9me2/3	Increased JMJD2B leads to less IR-induced γH2AX and increased cell survival	(Young et al., 2013)
BRD4	Transcriptional regulator	Various acetylation sites	BRD4 isoform B maintains compaction around DSB preventing γH2AX signalling	(Floyd et al., 2013).
HDAC	-	Various	Facilitate HR, NHEJ and ATM signalling	(Miller et al., 2010)
CBP p300	HAT	H3K56ac	Checkpoint and chromatin assembly recovery	(Vempati et al., 2010)

1.4.3 Crosstalk between chromatin changes and DNA replication

Appropriate coupling of DNA replication to maintenance of chromatin organisation during genome duplication is important in order to preserve genetic and epigenetic integrity. This involves the transfer of parental histones and their post-translational modifications onto nascent DNA, as well as the incorporation of new histones in order to preserve nucleosome density (Figure 1.11). This process is achieved in several steps. The first stage involves chromatin decondensation and nucleosome disruption. This is followed by histone recycling, where parental $(H3\text{-}H4)_2$ tetramers are positioned randomly onto daughter strands to form nucleosomes with either new or old H2A-H2B dimers (Annunziato, 2012; Groth, 2009). Interestingly, the majority of H3-H4 tetramers are positioned close to their original locus (Jackson and Chalkley, 1981a, b; Radman-Livaja et al., 2011). The exact mechanism allowing such transfer is still not clearly understood, however, it is likely that MCM2-7 and ASF1 play a role. ASF1 can be found in complex with MCM2-7 and a fraction of ASF1 has been found to be chromatin bound and co-localising with MCM2. Binding of ASF1 and the MCM helicase is maintained by an H3-H4 dimer, suggesting that MCM2-7 can bind non-nucleosomal histones (Groth et al., 2007). Moreover, H3 can interact with the amino-terminal domain of MCM2 and histone modifications associated with new histones are found in ASF1-H3-H4 complexes (Jasencakova et al., 2010). ASF1 may therefore bind and subsequently incorporate parental H3-H4 dimers at replication forks. It is possible, however, that other factors or passive histone transfer might also play a role in this process (English et al., 2006; Natsume et al., 2007).

Incorporation of parental histones must be followed by synthesis and incorporation of new histones. Histone supply is tightly regulated to ensure increased

assembly of canonical histones, H3.1, H3.2, H4, H2A, H2B and H1 during S phase. This includes increases in mRNA stability as well as transcriptional and translational control of histones (Marzluff et al., 2008). Newly synthesised H3.1 and H4 form dimers that are received in the nucleus by the heterotrimeric histone deposition complex CAF-1. ASF1 binds to the p60 subunit of CAF-1 and in doing so transfers the new histones (Mello et al., 2002). The specificity of CAF-1 for histone H3.1 probably results in the select transfer of H3.1 onto the nascent DNA strands, H3.3 being incorporated by alternative means (Ahmad and Henikoff, 2002; Ray-Gallet et al., 2011). Soluble histone H3.1-H4 dimers have a variety of pre-deposition marks with 70% of these being diacetylation on H4K5 and K12 (Sobel et al., 1995). H3 is also acetylated on K14 and K18 (Das et al., 2009; Jasencakova et al., 2010; Loyola et al., 2009). Importantly, 30% of soluble H3.1 also undergoes K9 monomethylation, probably by SETDB1 (Campos et al., 2010). Establishment of this mark, however, is thought to be prevented by H3K14 and K18 acetylation (Alvarez et al., 2011).

New histone marks are mainly associated with a state of chromatin relaxation. This can be useful as it provides the DNA accessibility necessary for DNA repair or transcriptional activation (Annunziato and Seale, 1983; Perry and Annunziato, 1989). These marks, however, must be removed once DNA replication is complete and the DNA accessibility is no longer required. Chromatin maturation, therefore, needs to take place for faithful maintenance of full epigenetic states during replication. It is estimated that this process takes place about 40 kb or 200 nucleosomes behind the replication fork in mammalian cells. It is important to bear in mind, however, that not all epigenetic states are restored immediately through this process. Notably, appropriate removal of acetylation marks may also be necessary for fork stability

since HDAC inhibitor treatment or HDAC3 knockdown in human cells have been shown to decrease replication fork speed (Bhaskara et al., 2010; Conti et al., 2010).

PCNA is key to the recruitment of several chromatin remodellers important for chromatin assembly and maturation. Two of these are SNF2 remodelling complexes, WSTF (William syndrome transcription factor) and SMARCAD1 (SWI/SNF related matrix associated actin dependent regulator of chromatin subfamily A containing DEAD/H box 1). WSTF is recruited to replication sites throughout S phase to prevent unnecessary heterochromatin formation (Poot et al., 2004). In contrast, SMARCAD1 is a SWI/SNF-like remodeller that forms a repressive complex with HDAC1/2, G9a and KAP-1 that mediates histone deacetylation and H3K9me3, thereby facilitating heterochromatin formation following replication (Rowbotham et al., 2011).

During replication stress, co-ordination between the DNA replication machinery, histone recycling and maturation may be disturbed. For example, ASF-1 is found in complex with soluble histones bearing parental marks following replication stress. This may prevent appropriate transfer of histone marks onto nascent DNA, thereby, leading to loss of epigenetic information (Jasencakova et al., 2010). The histone marks or DNA may also be altered following such stress. Furthermore, if the fork collapses following prolonged replication stress, this is likely to lead to further changes in chromatin dynamics. Indeed, oncogene-induced replication stress and damage following such stress in primary cells can lead to an increase in heterochromatin marks such as H3K9me3 (Di Micco et al., 2011).

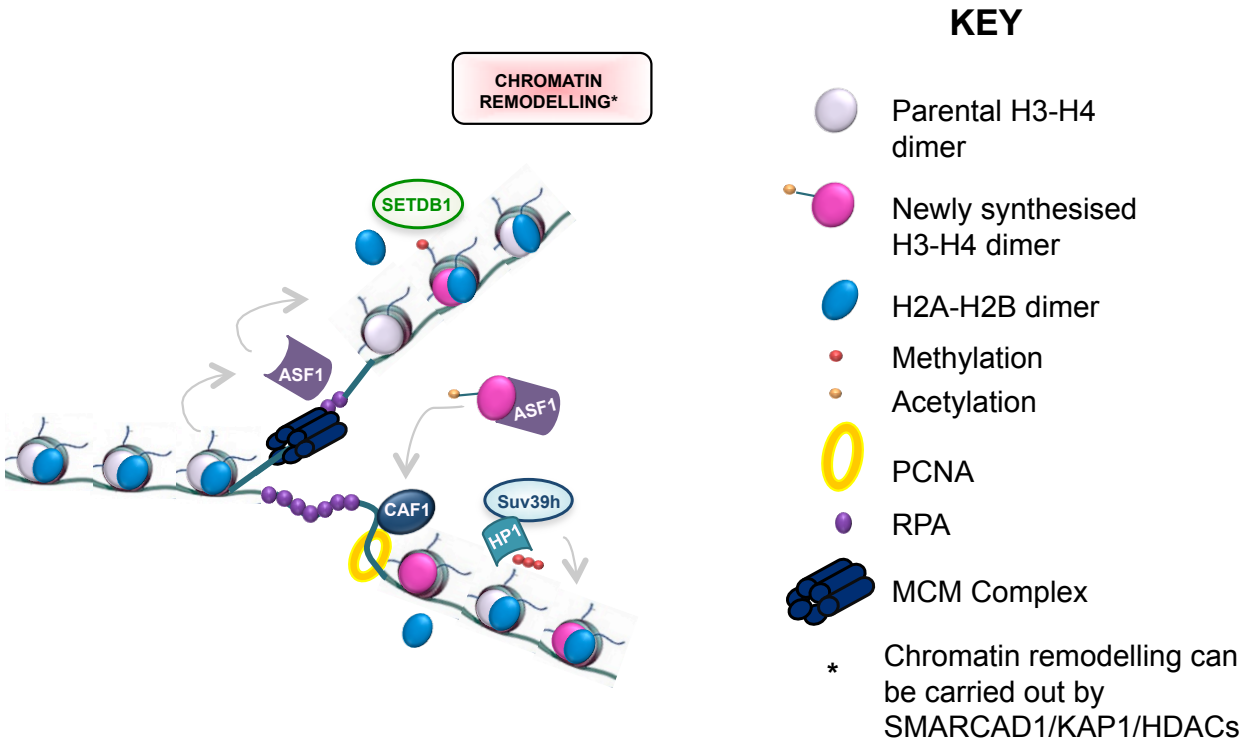


Figure 1.11. Schematic representation of the regulation of chromatin maturation during replication

During normal replication recycled parental histones and newly synthesised histones are assembled into nucleosomes. This process is tightly regulated and likely requires the coordinated action of factors such as the MCM complex, PCNA, ASF1 and CAF1. Newly formed chromatin is typically relaxed and must be remodelled into a more compact state by a variety of chromatin maturation factors such as SMARCAD1 or HDACs. Different chromatin remodellers may be required to replicate different chromatin regions. For example, heterochromatin replication may specifically require SETDB1, HP1 and Suv39h1/2. Adapted from (Alabert and Groth, 2012).

1.4.4 Chromatin dynamics and hypoxia

A number of chromatin changes occur in response to hypoxia in both a HIF-1 dependent and independent manner, with important consequences for gene expression (Johnson et al., 2008; Melvin and Rocha, 2012). In terms of chromatin remodellers, components of the SWI/SNF ATP dependent chromatin remodelling complex have been shown to bind to HIF-1α, thereby regulating hypoxia-inducible gene expression (Kenneth et al., 2009; Wang et al., 2004). Recent studies have suggested that HIF-1α and HIF-2α recruit BRG1 complexes to the promoters of HIF target genes to regulate their expression via nucleosome remodelling in a BRG1 ATPase dependent manner (Sena et al., 2013). MTA1, a component of the NuRD complex, also interacts with HIF-1α and can induce its deacetylation, with MTA1 expression correlating with enhanced HIF-1α stability and increased transcription of certain HIF-1α targets, such as *VEGF* (Moon et al., 2006; Yoo et al., 2006).

The interplay between HIF-1α and enzymes that directly catalyse the methylation or demethylation of target histone residues has been described in the literature. For example, HIF-1α acts as an enhancer of *SLC2A3*, the gene encoding GLUT3, by interacting with histone demethylase JMJD1A. In this case, HIF-1α dependent recruitment of this demethylase to the *SLC2A3* locus results in H3K9me2 demethylation and increased gene expression (Mimura et al., 2012). Many of the JmjC family of demethylases have also been shown to be HIF-1α targets (Pollard et al., 2008; Yang et al., 2009).

Suv39h1 and Suv39h2 have been shown to be activated under hypoxic conditions (2% O_2) in foetal lung epithelial cells. Suv39h1/2 repress SP-A (surfactant protein A) and such regulation is linked to developmental stage of these cells (Benlhabib and

Mendelson, 2011). Suv39h1 has been shown to be regulated in a HIF-1α dependent manner in response to DMOG (dimethyloxaloylglycine). This regulation was proposed to be linked to the radioprotection conferred by DMOG, suggesting important links between DDR, hypoxia and chromatin remodelling (Ayrapetov et al., 2011).

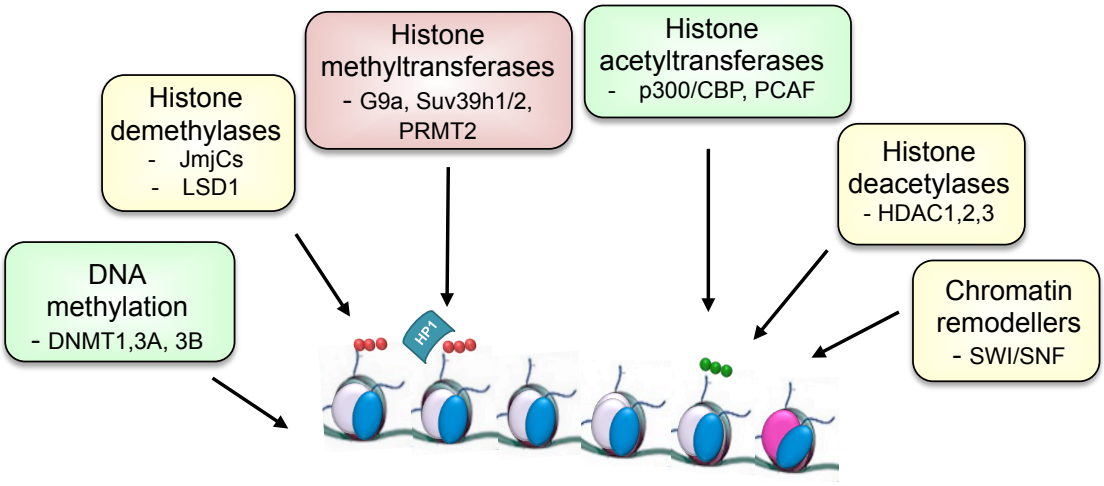


Figure 1.12. Schematic representation of the dynamic hypoxia-induced regulation of the chromatin context
Hypoxia regulates many of the enzymes involved in histone methylation and acetylation resulting in a number of hypoxia-specific chromatin changes. Chromatin remodellers from the SWI/SNF family as well as histone acetyltransferases play important roles in facilitating HIF-1α transcription. Boxes coloured yellow represent chromatin changes leading towards transcriptional activation or repression. A red coloured box represents chromatin changes leading to transcriptional repression whereas green boxes indicate transcriptional activation. Adapted from (Melvin and Rocha, 2012).

Hypoxic regulation of chromatin remodellers in a HIF-1α independent manner has also been reported in the literature. In some cases, regulation of chromatin modifying enzymes has been shown to be HIF-1α independent despite the fact that

these enzymes can frequently co-operate with HIF-1α to regulate transcriptional changes. This is the case of G9a, another histone methyltransferase that is induced at the protein but not transcriptional level in response to hypoxia (1% O_2) in a HIF-1α independent manner. G9a, however, can methylate non-histone targets under hypoxic conditions such as Reptin/RUVBL2 and Pontin/RUVBL1, both of which have ATPase and DNA helicase activity and are subunits of the TIP60 complex. G9a methylation of Pontin facilitates the expression of a subset of HIF-1α target genes by promoting p300 recruitment to target promoters (Lee et al., 2011). Similarly, G9a-mediated methylation of Reptin on lysine 67 facilitates HIF-1α-mediated transcription of another subset of genes. In this case, however, methylation prevents the negative regulation of Reptin on genes such as *VEGF* by preventing HDAC1 recruitment to gene promoters by Reptin (Lee et al., 2010b).

Given the widespread hypoxic regulation of histone modifying enzymes it is perhaps not surprising that many hypoxia-induced histone modifications have also been reported, including changes in histone acetylation, methylation and phosphorylation. Hypoxic-induction of G9a, for instance, leads to an increase in H3K9me2 (Chen et al., 2006). *MLH1* repression has been found to correlate with an increase in the activity of histone methyltransferase G9a and the subsequent enrichment of H3K9me2 at its promoter region, in a HIF-1α independent manner (Chen et al., 2006). In a separate study, hypoxia-induced HDACs were found to be important for the repression of *MLH1* since the use of TSA, an HDAC inhibitor, prevented *MLH1* repression (Mihaylova et al., 2003).

H3K4me3 is another hypoxia-induced posttranslational modification usually associated with active transcription. Increases in H3K9me3 and subsequent decreases

in H3K9ac have been reported in a number cancer cells exposed to hypoxia with the subsequent repression of a number of different genes, including some involved in DNA repair such as *RAD51* and *BRCA1* (Johnson and Barton, 2007; Lu et al., 2011). A summary of the mechanism of epigenetic changes leading to DNA repair gene repression is given in Table 1.4.

Table 1.4. Table summarising the mechanisms of hypoxia-induced epigenetic repression of a number of DNA repair genes

Gene	Mechanism of repression	Repair pathway	Reference
BRCA1	Decreased promoter H3K4 methylation and H3K9 acetylation and increased H3K9 methylation in hypoxia	HR	(Lu et al., 2011)
RAD51	Decreased promoter H3K4 methylation and H3K9 acetylation and increased H3K9 methylation in hypoxia	HR	(Lu et al., 2011)
MLH1	Hypoxia-induced histone deacetylases	MMR	(Mihaylova et al., 2003)
MLH1	G9a-mediated enrichment of H3K9me2 in hypoxia in a HIF-1α independent manner	MMR	(Chen et al., 2006)

1.5 Chromatin remodelling, the DDR and cancer

The DDR has been proposed to act as a critical barrier to tumourigenesis, a fact that may help explain the strong selection pressure to mutate DDR genes in cancer (Bartkova et al., 2005; Bartkova et al., 2006; Gorgoulis et al., 2005; Halazonetis et al., 2008; Kastan and Bartek, 2004). Loss of DDR activation has been reported to lead to loss of oncogene-induced senescence (OIS) and an increase in cellular transformation, with OIS occurring at least in part in an ATR dependent manner (Di Micco et al., 2006). Furthermore, ATR haplo-insufficiency together with endogenous levels of K-RAS in p53 heterozygous mice result in enhanced incidence of lung adenocarcinoma, spindle cell sarcoma and thymic lymphoma (Gilad et al., 2010).

Given that DDR signalling occurs within a particular chromatin context, it is important to consider chromatin remodelling when appreciating the role of the DDR as a barrier to tumourigenesis. γH2AX, for instance, is known to be expressed in early-stage tumours, and unlike other DDR markers is not lost during neoplastic progression (Bartkova et al., 2005; Gorgoulis et al., 2005; Nuciforo et al., 2007). However, in a variety of tumours the region encoding the H2AX gene is frequently mutated or deleted (Bonner et al., 2008). Links between altered expression of chromatin associated factors and tumour progression also exist. SETDB1, for instance is found in a region in chromosome 1 frequently amplified in melanoma with SETDB1 overexpression correlating with increased tumour invasiveness in a zebrafish melanoma model (Ceol et al., 2011). This histone methyltransferase has also been found to be amplified in non-small and small cell lung cancer cells (Rodriguez-Paredes et al., 2013). In contrast, while complete loss of the chromatin remodeller CHD5 is embryonic lethal, single allele loss results in increased proliferation and cancer incidence. Loss of CHD5 by 1p36 deletion or promoter hypermethylation is

associated with tumour development and progression in a variety of tumour types, including ovarian, breast and colorectal carcinoma (Wong et al., 2011; Wu et al., 2012b). Furthermore, in an Eμ-*myc* mouse model, *TIP60* haplo-insufficiency resulted in increased MYC-driven lymphomagenesis due to failure to mount a full MYC-driven DDR. This is consistent with a role for TIP60 as a tumour suppressor in the pre/early neoplastic stages. Interestingly, *TIP60* was found to frequently undergo mono-allelic loss in mammary, head and neck cancers as well as lymphomas, with a subsequent reduction in *TIP60* mRNA expression in these tumours (Gorrini et al., 2007). The selection pressure to mutate/inactive chromatin remodelling factors with functions in the DDR underscores the cooperation that exists between the DDR, chromatin and cancer progression. Gaining a better understanding of the mechanisms underlying such cooperation as well as its consequences should, hopefully, further our knowledge of tumour initiation and progression.

AIM

The interplay between chromatin changes and the response to DNA damage, replication stress or hypoxia has recently gained much attention (Alabert and Groth, 2012; Melvin and Rocha, 2012; Sulli et al., 2012). Our hypothesis was that the hypoxia-induced chromatin changes could impact on ATM signalling. In this study we focused on H3K9me3, given that this histone modification had previously been linked to the DDR and ATM activation (Goodarzi et al., 2008; Kaidi and Jackson, 2013; Sun et al., 2009). Further characterisation of the details of the replication stress and histone methylation changes induced by hypoxia was undertaken in order to address the hypothesis. In doing so, we furthered our understanding of the oxygen dependent regulation of some of the enzymes that catalyse this histone modification as well as the biological consequences of hypoxia-induced H3K9me3 with respect to gene expression regulation.

CHAPTER 2

MATERIALS AND METHODS

2.1 Materials

2.1.1 General laboratory and cell culture reagents

Cell culture media was supplied by Sigma-Aldrich UK and cell culture plasticware was obtained from Costar. In addition the following reagents described in Table 2.1 were used.

Table 2.1. Chemicals and cell cultures reagents

Name	Producer/UK distributor
Acetic acid	Sigma-Aldrich UK
Acrylamide/Bis Solution, 30%, 29:1	BioRad
Agarose	Sigma-Aldrich UK
APS (ammonium persulfate)	Fisher Scientific
Biotin-azide	Invitrogen/Life technologies
β-mercaptoethanol	Fisher Scientific
Blocking buffer LiCor	LiCor
BSA (bovine serum albumin)	Fisher Scientific
Bromophenol blue	Fisher Scientific
Calcium chloride	Fisher Scientific
CldU (5-chloro-2′-deoxyuridine)	Sigma-Aldrich UK
Chloroform	Fisher Scientific
DMEM (Dulbecco's modified Eagle's medium)	Sigma-Aldrich UK
DharmaFECT 1	Fisher Scientific
EDTA (ethylenediaminetetraacetic acid)	Sigma-Aldrich UK
DEPC (diethyl pyrocarbonatecarbonate)	Fisher Scientific
DMSO (dimethylsulphoxide)	Fisher Scientific
EdU (5-ethynyl-2'-deoxyuridine)	Invitrogen/Life technologies
Ethanol	Fisher Scientific
Ethidium bromide	Sigma-Aldrich UK
FBS (foetal bovine serum)	Autogen Bioscience
Formaldehyde	Sigma-Aldrich UK
Glycine	Sigma-Aldrich UK
Glycogen	Sigma-Aldrich UK
HEPES (4-(2-hydroxyethyl)-1-piperazineethanesulfonic acid)	Fisher Scientific
HCl (hydrochloric acid)	Sigma-Aldrich UK
H_2O_2 (hydrogen peroxide)	Fisher Scientific
IdU (5-iodo-2′-deoxyuridine)	Sigma-Aldrich UK

Igepal® CA-630	Sigma-Aldrich UK
LB (Luria broth)	Sigma-Aldrich UK
Lithium chloride	Fisher Scientific
Lipofectamine LTX	Invitrogen/Life technologies
Methanol	Fisher Scientific
NEM (N-ethylmaleimide)	Sigma-Aldrich UK
Nonidet^{TM} P-40	Sigma-Aldrich UK
Paraformaldehyde	Fisher Scientific
PBS (phosphate buffered saline)	Fisher Scientific
Phenol:chloroform:isoamyl-alcohol	Sigma-Aldrich UK
PMSF (phenylmethylsulfonyl fluoride)	Sigma-Aldrich UK
Polybrene	Sigma-Aldrich UK
ProLong® Gold	Invitrogen/Life technologies
Propidium iodide (PI)	Sigma-Aldrich UK
RNAse A (ribonuclease A)	Sigma-Aldrich UK
Sodium bicarbonate	Sigma-Aldrich UK
Sodium deoxycholate	Sigma-Aldrich UK
Sodium dodecyl sulphate (SDS)	Fisher Scientific
Super optimal catabolite (SOC)	Sigma-Aldrich UK
SYBR® Green	Applied Biosystems
SYBR® Gold	Invitrogen/Life technologies
TEMED (tetramethylethylenediamine)	Fisher Scientific
Thymidine	Sigma-Aldrich UK
Trypsin 0.05% EDTA	Sigma-Aldrich UK
Tris-Glycine	Fisher Scientific
Tris-HCl (tris(hydroxymethyl)aminomethane hydrochloride)	Fisher Scientific
Triton-X-100	Fisher Scientific
TRIzol®	Invitrogen/Life technologies
Tween 20	Fisher Scientific
Urea	Fisher Scientific

2.1.2 Antibodies

Table 2.2. Antibodies used for western blotting

Name	Species	Dilution	Clone ID	Producer/Cat number
53BP1	Rabbit	1:500	-	Novus Biologicals, NB100-904
Phospho-53BP1 (S25)	Rabbit	1:1000	-	Bethyl/Universal Biologicals Cambridge, # A300-652A
β-Actin	Mouse	1:100000	AC-15	Santa Cruz Biotechnology, sc-69879
APAK	Rabbit	1:500	-	Sigma-Aldrich UK Prestige Antibodies, HPA053022
Phospho-ATM (S1981)	Rabbit	1:10000	EP1890Y	Epitomics, # 2152-1
Phospho-ATM (S1981)	Rabbit	1:1000	10H11.E12	Rockland antibodies & assays,200-301-400S
ATM	Mouse	1:1000	MAT3-4G10/8	Sigma-Aldrich UK, A1106
Phospho-CHK1 (S345)	Rabbit	1:1000	-	Cell Signaling/New England, Biolabs, # 2341
Phospho-CHK2 (T68)	Rabbit	1:1000	-	Cell Signaling/New England Biolabs, # 2661
CHK2	Mouse	1:1000	Clone 7	Upstate/Millipore, # 05-649
GAPDH (6C5)	Mouse	1:4000	6C5	Novus Biologicals, NB600-502
Phospho-H2AX (S139)	Mouse	1:500	JBW301	Upstate/Millipore, 05-636
Histone 3	Rabbit	1:5000	-	Abcam, ab1791
Histone 3	Mouse	1:5000	-	Cell Signaling/New England Biolabs, # 3638S
H3K9me2	Rabbit	1:1000	-	Cell Signaling/New England Biolabs, # 9753
H3K9me3	Rabbit	1:2000	-	Upstate/Millipore, # 07-442
H3K27me3	Rabbit	1:1000	C36B11	Cell Signaling/New England Biolabs, # 9733
H3K36me3	Rabbit	1:1000	-	Cell Signaling/New England Biolabs, # 9763

H3K79me3	Rabbit	1:1000	-	Cell Signaling/New England Biolabs, # 9756
Phospho-H3S10	Rabbit	1:1000	-	Cell Signaling/New England Biolabs, # 9701
HIF1-α	Mouse	1:500	54/HIF-1α	Becton Dickinson Biosciences, # 610959
HP1β	Rabbit	1:500		Abcam, ab10478
KAP-1	Rabbit	1:10000	-	Bethyl/Universal Biologicals Cambridge, # A300-274A
PARP1	Rabbit	1:1000	-	Cell Signaling/New England Biolabs, #9542
Phospho-KAP-1 (S473)	Rabbit	1:1000	Poly6446	Biolegend, # 644602
Phospho-KAP-1 (S824)	Rabbit	1:1000	-	Bethyl/Universal Biologicals Cambridge, # A300-767A
PCNA	Rabbit	1:200	FL-261	Santa Cruz Biotechnology, # sc-7907
Phospho-p53 (S15)	Rabbit	1:500	-	Cell Signaling/New England Biolabs, # 9284
RPA p32	Rat	1:2000	4E4	Cell Signaling/New England Biolabs, # 2208
SETDB1	Rabbit	1:500	-	Upstate/Millipore, # 07-1568
Suv39h1	Rabbit	1:500	-	Abcam, ab33056
Suv39h2	Rabbit	1:100	-	Abcam, ab71683
β-Tubulin	Rabbit	1:1000	-	Abcam, ab6046

Table 2.3. Antibodies used for immunofluorescence (IF)

Name	Species	Dilution	Clone ID	Producer/Cat number
53BP1	Rabbit	1:500	-	Novus Biologicals, NB100-904
Phospho-ATM (S1981)	Mouse	1:100	-	Chemicon International, MAB3806
Phospho-H2AX (S139) (γH2AX)	Mouse	1:800	JBW301	Upstate/Millipore, 05-636
H3K9me3	Rabbit	1:2000	-	Upstate/Millipore, #07-442
Phospho-KAP-1 (S824)	Rabbit	1:1000 1:200	-	Bethyl/Universal Biologicals Cambridge, # A300-767A
RPA32	Rat	1:200	4E4	Cell Signaling/New England Biolabs, # 2208

Table 2.4. Antibodies used for chromatin immunoprecipitation (ChIP)

Name	Species	Dilution	Clone ID	Producer/Cat number
Histone 3	Rabbit	3 µg/IP	-	Abcam, ab1791
H3K9me3	Rabbit	6 µg/IP	-	Abcam, ab8898

Table 2.5. Antibodies used for Single-Molecule DNA Fiber Analysis (DFA)

Name	Species	Dilution	Clone ID	Producer/Cat number
Rat anti-BrdU	Rat	1:500	BU1/75 (ICR1)	Oxford Biotechnology, OBT0030
Mouse anti-BrdU	Mouse	1:500	B44	Becton Dickinson Biosciences, 347580 (7580)

Table 2.6. Antibodies used for fluorescence-activated cell sorting (FACS)

Name	Species	Dilution	Clone ID	Producer/Cat number
Phospho-KAP-1 (S824)	Rabbit	1:1000	-	Bethyl/Universal Biologicals Cambridge, # A300-767A
H3K9me3	Rabbit	1:2000	-	Upstate/Millipore, #07-442

Table 2.7. Antibodies used for immunohistochemistry (IHC)

Name	Species	Dilution	Clone ID	Producer/Cat number
Phospho-ATM (S1981)	Rabbit	1:1000	EP1890Y	Epitomics, # 2152-1
CAIX	Mouse	1:100	-	Prof. Adrian Harris, Oxford, UK
H3K9me3	Rabbit	1:5000	-	Abcam, ab8898

Table 2.8. Secondary antibodies used

Name	Dilution	Application	Producer/Cat number
Alexa Fluor 680 goat anti-mouse IgG (H+L)	1:10000	WB	Invitrogen, #A21057
Alexa Fluor 680 goat anti-rabbit IgG (H+L)	1:10000	WB	Invitrogen, #A21076
Alexa Fluor 680 goat anti-rat IgG (H+L)	1:10000	WB	Invitrogen, #A21096
IRDye 800CW donkey anti-mouse IgG	1:5000	WB	LI-COR, #926-32212
IRDye 800CW donkey anti-rabbit IgG	1:5000	WB	LI-COR, #926-32213
Alexa Fluor 488-conjugated goat anti-rabbit IgG	1:250	IF/FACS	Invitrogen, A11070
Alexa Fluor 594-conjugated goat anti-rat IgG	1:250	IF	Invitrogen, A11007
Alexa Fluor 555-conjugated goat anti-rat IgG	1:500	DFA	Invitrogen, A21434
Alexa Fluor 488-conjugated goat anti-mouse F(ab')2 fragment	1:500	DFA	Invitrogen, A11017

2.1.3 Antibiotics

Ampicillin and kanamycin (Fisher Scientific) were made up as a stock solution of 50 mg/ml. The final concentrations of ampicillin and kanamycin were 50 μg/ml. Puromycin (Fisher Scientific) was made as a stock solution of 2 mg/ml and used as indicated in each application. All antibiotics were made up in sterile distilled water, aliquoted and stored in -20^{o}C.

2.1.4 Primers

The primers used in this study are listed in Table 2.9 and Table 2.10. For ChIP-qPCR analysis, regions of H3K9me3 binding for each target gene were chosen by using the UCSC genome browser (http://genome.ucsc.edu/) (Assembly used: GRCh37/hg19). Once the loci were chosen, primers were designed using Primer 3 software (Steve Rozen, Helen J. Skaletsky (1998). Primer3. Code available at: (http://www-genome.wi.mit.edu/genome_software/other/primer3.htm.). Primers were designed so that amplification products would not exceed 200 base pairs (bp) in length. Primers designated as "control" indicate those primers that were designed to target regions where minimal H3K9me3 binding was predicted from the UCSC genome browser (assembly as above). Full details (including UCSC genome browser tracks) of the primers used in Chapter 6, Figure 6.1 are included in Appendix B.

Table 2.9. Primers used for quantitative PCR (qPCR)
h=human, *m*=mouse primers. Where *h* or *m* are not specified the primers=human.

Oligonucleotide Name	Sequence
***18S* Forward**	TAGAGGGACAAGTGGCGTTC
***18S* Reverse**	CGGACATCTAAGGGCATCAC
***APAK* Forward**	CAAAGGCAAGATGGAGAAGC
***APAK* Reverse**	TAGGTGTGAGGCTCGTCTGA
***GLUT-1* Forward**	ATACTCATGACCATCGCGCTAG
***GLUT-1* Reverse**	AAAGAAGGCCACAAAGCCAAAG
***HIF-1α* Forward**	TTCACCTGAGCCTAATAGTCC
***HIF-1α* Reverse**	CAAGTCTAAATCTGTGTCCTG
***HIF-1β* Forward**	GACTACTGCCAACCCCGAAA
***HIF-1β* Reverse**	CTCTGGACAATGGCTCCTCC
***hPP2A-C* Forward**	GTCTGTGGAGATGTGCATGG
***hPP2A-C* Reverse**	GCTCTCATGATTCCCTCGAA
***mPP2A-C* Forward**	TACTCCGAGGGAATCACGAG
***mPP2A-C* Reverse**	CGGATGTGATCCAGTGTGTC
***SETDB1* Forward**	ACATCCTCAGCCTCTGCACT
***SETDB1* Reverse**	TTCCAGTACCGGTCAGATCC
***SUV39H1* Forward**	ATCCGCGAACAGGAATATTACC
***SUV39H1* Reverse**	GAGGATACGCACACACTTGAGATT
***SUV39H2* Forward**	CTGATGAGTTCACAGTGGATGCA
***SUV39H2* Reverse**	TTTGGGTCACAACTATGATTCACA
***mWIP1* Forward**	CGGCAGTGTGATGAACAAGT
***mWIP1* Reverse**	TGTGGACACTGGTGTCTGGT

Table 2.10. Primers used for ChIP-qPCR

Oligonucleotide Name	Sequence
***53BP1* Forward**	TTGCAACGCTCTTCTGAATG
***53BP1* Reverse**	TGCTCAGCCGAGAACAATAG
***APAK* Forward 1**	GTGTGGCAAGGCCTTTAGTC
***APAK* Reverse 1**	GGGCTTCTCACCAGTATGGA
***APAK* Forward 2**	TGGGAAAGCCTTTATTCGTG
***APAK* Reverse 2**	CTCCAGTGTGAATTCGCTGA
***APAK* Forward (control)**	GCTACAGCCTGCCTGGTATT
***APAK* Reverse (control)**	ACACAAAACCACAGCCACAC
***ATM* Forward**	GCTGTCTTTCTGCCATGTGA
***ATM* Reverse**	ATTGTGGGTTTCTGGTGAGG
***EXO1* Forward**	GGAGAAACCCTGATTGGACA
***EXO1* Reverse**	CCAAGAACCCACCAATTCTG
***HP1α* Forward**	GAGGGCATCTTCTGATTGTTG
***HP1α* Reverse**	CATGCATTGCAGGATGCTTA
***PP1P5K1* Forward**	CATGGAACACCCTTCAAACC
***PP1P5K1* Reverse**	TGGGGTATATCTGGCAGGAG
***PP2A-C* Forward**	GATGGGGTTTTACCGTGTTG
***PP2A-C* Reverse**	CCAAAGCAGGTGGATGACTT
***PP2A-C* Forward (control)**	ATCTCAGCCCCATGTTGTTC
***PP2A-C* Reverse (control)**	GCTCTTGTGCAGTCACATCG

2.2 Methods

2.2.1 Cell lines

RKO human colorectal cancer cells, Calu-6 human non-small cell lung cancer cells (Dr Anderson Ryan), W9 suv39h1/2$^{+/+}$, D15 suv39h1/2$^{-/-}$ MEFs (Prof. Thomas Jenuwein, Freiburg, Germany) (Peters et al., 2001), NIH 3T3, p53$^{-/-}$MEFs, (Prof. Xin Lu, Oxford, UK), HEK 293T and H1299 cells (expressing Fucci (Fluorescent ubiquitination-based cell cycle indicator) plasmids: pRetroX-SG2M-Cyan and pRetroX-G1-Red) (Dr Anderson Ryan), were used in this study. pRetroX-SG2M-Cyan allows expression of hGEMININ (with amino acid residues 1-110) fusion tagged with fluorescent protein AmCyan1. The fusion protein is nuclear and present in S, G_2 and M cell-cycle phases. Following M phase, GEMININ is degraded by proteasomal degradation. AmCyan has excitation and emission maxima of 458 nm and 489 mm respectively. pRetroX-G1-Red allows the expression of hCDT1 (with amino acid residues 30-120) tagged with red fluorescent protein mCherry. The fusion protein is present at high levels in the G_1 of the cell-cycle, at the end of which it is ubiquitylated and degraded by the proteasome. mCherry is a mutant fluorescent protein with excitation and emission maxima of 587 nm and 610 nm respectively (Sakaue-Sawano et al., 2008).

All cells were cultured in DMEM supplemented with 10% FBS, in a standard humidified incubator at 37^{o}C and 5% CO_2. The pair of W9 suv39h1/2$^{+/+}$ and D15 suv39h1/2$^{-/-}$ MEFs was cultured in DMEM media containing 0.1 mM β-mercaptoethanol. Cells were passaged three times a week. Routine tissue culture involved the preparation of a cell suspension by removal of the medium, washing with PBS and trypsinising cells for 1 minute with Trypsin-EDTA. Trypsin was then

inactivated by adding fresh media. Cell density was determined by adding 10 µl of cell suspension to a Neuenbauer haemocytometer chamber, and standard cell counting. The desired cell numbers were seeded in fresh media prior to all experiments.

Cells were routinely mycoplasma tested using the PlasmoTest™ kit (InvivoGen). In brief, cells were grown in antibiotic free media and harvested when 90-100% confluent. Cells were then heated for 15 minutes at 100°C. 50 µl of the above suspension was added to 200 µl of HEK-Blue cells (1-3.5 x 10^5 cells/ml) in HEK-Blue™ detection medium (InvivoGen). Cells were plated in duplicate in a 96-well plate, together with positive and negative controls provided by the manufacturer and incubated for 24 hours under normal tissue culture conditions. Appearance of a blue colour following incubation indicated the presence of lipoprotein expressed by all types of bacteria and mycoplasma. A pink colour indicated a negative result, suggesting absence of mycoplasma.

2.2.2 Cryopreservation of cell lines

Cells at 70% confluence were trypsinised, resuspended in 5 ml of fresh media and centrifuged at 400 x g for 5 minutes at RT (room temperature). The supernatant was then gently removed. The remaining cells were resuspended in 1 ml of medium containing 10% FBS, 80% medium and 10% DMSO and placed in a 1.5 ml cryovial (Thermo Scientific Nunc, 363401). The vial was placed in -80^{o}C for 24 hours in a Mr Frosty (Nalgene, #CRY-OFF-700C) containing 2-propanol before being stored in liquid nitrogen for long-term storage.

When recovering cells from liquid nitrogen, these were thawed quickly in a 37°C water bath. Thawed cells were then transferred to 5 ml of pre-warmed medium. Cells were centrifuged at 600 x g for 5 minutes at RT. The supernatant was carefully removed and discarded and the pelleted cells were resuspended in fresh medium and placed in a 75 cm^2 flask.

2.2.3 Drug treatments

The ATM inhibitor, KU-55933, (2-morpholin-4-yl-6-thianthren-1-yl-pyran-4-one) (ATP-competitive inhibitor of ATM Kinase) (Calbiochem, #118500) was used at a concentration of 10 μM for the indicated time periods. Doxorubicin (Sigma-Aldrich UK) was used at a concentration of 2 μM for 4 or 18 hours as indicated in each experiment. Okadaic acid (OA) (Sigma-Aldrich UK) was used at a concentration of 0.5 μM for 2 hours. G9a inhibitor, UNC0642 (Structural Genomics Consortium, Toronto), was used at the concentrations indicated for 96 hours before starting the indicated timepoints for each experiment (Vedadi et al., 2011). EdU and thymidine were used at a concentration of 10 μM. Stock solutions of compounds were prepared in DMSO, aliquoted and kept at -20°C. In addition, Hu (Sigma-Aldrich UK) was prepared in distilled sterile water and was used at a concentration of 1 mM for the indicated time periods. Stock solutions of Hu were also kept at -20°C.

2.2.4 Hypoxia treatment

Hypoxia treatment was carried out using a Bactron II anaerobic chamber (Shell Labs). No oxygen is supplied to this chamber, however, a complete absence of oxygen cannot be guaranteed at all times due to potential leaks. The oxygen

concentration at any one time is estimated to be no higher than 0.1%. Therefore, the oxygen tension for experiments carried out in this chamber will be referred to as <0.1% O_2 throughout the text. For all experiments to be carried out in the anaerobic chamber, cells were plated on glass dishes to minimise the amount of potential oxygen being introduced into the chamber (since plastic absorbs and retains oxygen). An *in vivo* 400 Ruskinn hypoxic chamber was used for oxygen concentrations of 2%-0.2%. The oxygen tension in the chambers was routinely tested by the use of an OxyLite probe (Oxford Optronix). Unless the experiments involved periods of reoxygenation, cells were harvested inside the chambers with equilibrated solutions.

2.2.5 Exposure to γ-irradiation

All irradiations were carried out using a Gamma Service® GSR D1 irradiator containing a Cs^{137} source. The dose rates of the system, as determined by the supplier, were 1.938 Gy/minutes and 1.233 Gy/minutes depending on the distance from the source. Samples were positioned on shelf 1 and the exposure times were calculated in order to expose cells to the required dose.

2.2.6 RNA interference

KAP-1 siRNA (sequence: GGCCCUAUUCUGUCACGAAtt) (Applied Biosystems), ATM siRNA (sequence: GCGCAGUGUAGCUACUUCUUCUAUU) (Invitrogen), HIF-1β siRNA (UGUUUGUCAACCAACAGAGUdtdt) (Thermo Scientific), SETDB1 siRNA sequence (AAGAUGGGCUUUCAUGUUA) (Thermo Scientific), G9a siRNA sequence (GGACCUUCAUCUGCGAGUA) (Thermo Scientific) or Stealth RNAi negative control (Invitrogen) were transfected into cells

using DharmaFECT 1 at a final concentration of 50 nM. 2 x 10^5 cells were seeded in a 3.5 mm plate or equivalent on the day before carrying out the transfection. The following day, a 1 mM siRNA solution was prepared. Two tubes were then prepared per transfection as follows:

Tube 1: 100 µl 2 µM siRNA, plus 100 µl serum-free media per well

Tube 2: 4 µl DharmaFECT 1, plus 196 µl serum-free media per well

The contents of each tube were then mixed. After 5 minutes the contents of both tubes were mixed and the mixture left to incubate for 20 minutes. The media on the cells to be transfected was then removed and the new transfection medium plus 1600 µl of antibiotic-free complete media was added to the cells. Cells were then left to incubate for 24-72 hours at 37^{o}C. Observation of the transfected cell was carried out after 24 hours in order to check for the presence of dead cells, which would indicate toxicity. If toxicity was observed, the transfection medium was replaced with fresh complete antibiotic-free media. Cells were harvested 72 hours post-transfection.

2.2.7 Retroviral transduction

MEFs were transduced with pBABE-Puro GFP, or pBABE-Puro K-RAS-V12 (Addgene plasmid 9052) (gift from Dr Eric O'Neill, Oxford, UK) as previously described (Palmero and Serrano, 2001). HEK 293T packaging cells at a concentration of 2 x 10^6 cells per dish were seeded prior to transfection. At least 7 hours post-seeding, 293T cells were transfected. To do so a mixture of 100 µl 2.5 M $CaCl_2$, 10 µg pCL-Eco (as the packaging plasmid), 10 µg of retroviral genome plasmid of interest and sterile water to 1 ml was mixed. While bubbling, 1 ml of 2 x HBSS (Hank's Buffered Salt Solution) buffer pH 7.12 (16.4 g NaCl, 11.9 g HEPES, 0.21 g Na_2HPO_4

and Milli-Q H_2O to 1 litre) was added to this mixture. This final mixture was left to stand for less than a minute before drop wise addition to the 293T plate. After 16-24 hours the media on the 293T cells was replaced. The recipient early passage non-transformed $p53^{-/-}$ MEFs to be infected were also plated at this time at a density of 8 x 10^5 cells per 10 cm dish. Following a further 24 hours the transfection efficiency was checked (by calculating the number of cells integrating the GFP plasmid). The retrovirus-containing media from the 293T cells was collected and replaced by fresh growth media. The retrovirus containing media was centrifuged at 700 x g at RT for 10 minutes to remove any remaining 293T cells. The supernatant was transferred to a clean tube and diluted in media at a ratio of 1:2. Polybrene (Sigma-Aldrich UK) was added to a final concentration of 1:1000 (8 mg/ml stock solution). Media from the recipient cells was removed and replaced with 10 ml of diluted viral supernatant. The infection was then repeated twice more (at least 7 hours apart). Following the third infection, media in the recipient cells was removed and replaced with media containing the relevant selection agent. The experiment was performed following the appropriate selection time. When using puromycin (1-2 μg/ml), selection time was 2-3 days.

2.2.8 Lentiviral tranduction

shRNAs targeting Suv39h1 (pSMP-Suv39h1 5′-GAGCTCACCTTTGATTACA-3′) (Addgene plasmid 36342), Suv39h2 (pSMP-Suv39h2 5′-CCCGTTACTGCTTCAGCAA-3′) (Addgene plasmid 36344) and a Luciferase control shRNA (pSMP-Luc 5′- CCCGCCTGAAGTCTCTGATTAA -3′) (Addgene plasmid 36394) were used (we thank Dr George Daley, Boston, USA, for depositing these plasmids in Addgene). RKO cells were transduced with shRNA lentiviruses as

previously described (Onder et al., 2012). Twenty-four hours after the last infection, cells were washed extensively (at least 10 washes with PBS) and grown in medium containing 1 μg/ml puromycin. It is important to note that since human cells were being lentivirally transduced all of the above steps were carried out in a designated "Lentiviral-work only" tissue culture hood. Extreme care was taken to avoid any contamination of the external surrounding environment with the virus or the lentivirally transduced cells until all traces of the virus had been cleared. Following at least 3 days of selection and once the cells were passaged at least 3 times, cells were returned to standard tissue culture conditions/passaging.

2.2.9 DNA transfection

Cells were transfected according to the manufacturer's instructions using Lipofectamine LTX (Invitrogen/Life technologies) at a final concentration of 5 μg of DNA, with MYC-tagged APAK (kindly provided by Chunyan Tian, Beijing, China) or MYC-empty (OriGene) plasmids (Tian et al., 2009). In brief, cells were seeded in a 6 cm plate or equivalent on the day before carrying out the transfection. DNA and Reagent Plus were added in a 1:1 ratio in serum-free DMEM media. Following a 5 minute incubation, 15 μl of Lipofectamine LTX was added to each transfection tube. After a further 20-30 minutes incubation period the media on the cells to be transfected was removed and the new transfection medium plus 4 ml of antibiotic-free complete media was added to the cells. Transfected cells were placed at 37^{o}C overnight before replating into glass dishes at a concentration that would allow the cells to be at 80% confluency at the time of the experiment (typically performed 8 hours after replating).

2.3 Protein analysis and biochemistry

2.3.1 Cell lysis and protein sample preparation

Cells were used at approximately 60-70% confluency and exposed to different treatments (as described for each experiment). Cells were scraped and pelleted into 1 ml of PBS and lysed in 50-100 µl of UTB (9 M urea, 75 mM Tris HCl, pH 7.5, 0.1 M ß-mercaptoethanol). These samples were then sonicated for 20 seconds before being centrifuged for a further 15 minutes at 16.2 x g at 4^{o}C to remove insoluble debris. The supernatant was then transferred to a new Eppendorf and 2 µl of such supernatant was used for protein quantification using a Nanodrop meter. Absorbance of the protein sample was read at 280 nm. UTB was used as blank when calibrating the meter. Two measurements were made each time and the average of both measurements was taken as the final protein concentration.

2.3.2 SDS PAGE (SDS-Polyacrylamide Gel Electrophoresis)

SDS-Polyacrylamide gels (6, 7.5, 10, 15 or 20%) were prepared following the recipe shown in Tables 2.11 and 2.12 (Sambrook and Russell, 2001).

Table 2.11. Recipe for stacking gel

Reagent	Volume
H_2O	6.1 ml
0.5 M Tris-HCl pH 6.8	2.5 ml
Acrylamide	1.3 ml
10% SDS	100 µl
10% APS	100 µl
TEMED	20 µl

Table 2.12. Recipe for separating gel (6-20%)

Reagent	Volume in accordance with gel %				
	6	7.5	10	15	20
H_2O	8.13 ml	7.4 ml	6.07 ml	3.75 ml	1.1 ml
1.5 M Tris-HCl pH 8.8	3.75 ml	3.75 ml	3.75 ml	3.75 ml	3.75 ml
Acrylamide	2.92 ml	3.65 ml	4.95 ml	7.25 ml	10 ml
10% SDS	150 µl	150 µl	150 µl	150 µl	150 µl
10% APS	75 µl	75 µl	75 µl	75 µl	75 µl
TEMED	18 µl	18 µl	18 µl	18 µl	18 µl

The appropriate volume of sample (typically corresponding to 50 µg of protein except when preparing samples to assess changes in histone modifications where 10-20 µg of protein were used), was added to 5 µl of sample buffer (3.3% SDS, 6 M urea, 17 mM Tris-HCl (pH 7.5), 0.07 M β-mercaptoethanol, 0.01% Bromophenol blue), and heated at 100^{o}C for 5 minutes. Protein ladder (Precision plus protein standards, BioRad) (5 µl) was loaded to one of the lanes in order to allow analysis of the molecular weight of the bands. Gels were electrophoresed at 100 V for 60 to 90 minutes in Tris-glycine running buffer (25 mM Tris base, 192 mM glycine, 0.1% (w/v) SDS). Where Mini-PROTEAN TGX^{TM} pre-cast gels were used (BioRad) these were electrophoresed at 200 V for 30-40 minutes in Tris-glycine running buffer.

2.3.3 Western blotting

Proteins in the electrophoresed gels were electro-transferred onto nitrocellulose membranes (BioRad) at 100 V for 1 hour in transfer buffer (25 mM Tris base, 150 mM glycine, 20% (v/v) methanol). The membranes were then washed in PBS and placed in LiCor buffer diluted 1:2 in Tris-Buffered Saline (TBS) (50 mM Tris-HCl, pH 7.6, 150 mM NaCl) for 1 hour for blocking. Membranes were probed with primary antibody (diluted in 1:2 LiCor buffer:TBS-Tween) overnight at 4^{o}C while shaking. A list of all primary antibodies used for western blotting is given in Table 2.2. The following morning the membranes were washed 3 times in TBS-Tween for 10 minutes each time and probed with Alexa Fluor 680/ IRDye 800 anti-mouse and/or anti-rabbit secondary antibody (diluted to 1:10000 or 1:5000 in 1:2 LiCor buffer:TBS-Tween) for 1-2 hours at RT with shaking. Full details all secondary antibodies used for western blotting is given in Table 2.8. The membranes were then washed again twice in PBS-Tween before a final wash in PBS. Membranes were developed using the Odyssey infrared imaging system. Unless otherwise stated, experiments were performed in triplicate.

2.3.4 Immunofluorescence microscopy

Immunofluorescence was carried out in 4 well chamber slides. 36000 cells were plated per well. Treated cells were washed in PBS before being fixed in 4% fixation buffer (4% (w/v) paraformaldehyde, 2% (w/v) sucrose, 1 X PBS) for 15 minutes at RT. Following this fixation period cells were washed once in PBS in order to remove any traces of paraformaldehyde and were then incubated in 500 µl/well 1% PBS-Triton X-100 (PBS-T) for 10 minutes. Blocking was then carried out for 1 hour in 0.5-1 ml 2% (w/v) BSA in 0.1% PBS-T. Each well was then washed once in ice-cold

0.25% PBS-T before being treated with 150 µl/well of the appropriate primary antibody (diluted in 2% (w/v) BSA-PBS-T 0.1%) for 60 to 90 minutes at 37^{o}C in a humidified chamber. A list of all primary antibodies used for immunofluorescence is shown in Table 2.3 Following 3 washes (each of 5 minutes duration) in ice cold 0.25% PBS-T and a final wash in PBS, the slides were treated with 150 µl/well of secondary antibody Alexa Fluor 488 green and/or Alexa Fluor 594 red diluted 1:250 in 2% (w/v) BSA-PBS-T 0.1%, either for 60 minutes at 37^{o}C in a humidified chamber or for 20 minutes at RT and in the dark. Full details all secondary antibodies used for immunofluorescence is given in Table 2.8. Two further washes in ice cold 0.25% PBS-T and final wash in PBS were carried out before mounting the slides using ProLong® Gold mounting medium with DAPI (Invitrogen/Life technologies). The slides were then left for 24 hours in the dark before being sealed with nail varnish. All slides were analysed using a Bio-radiance confocal microscope, Nikon 90i microscope or LSM780 (Carl Zeiss Microscopy Ltd) confocal microscope.

Mitotic cells were collected by mitotic shake-off, replated and treated while in G_1 phase as previously described (Hammond et al., 2002; Schorl and Sedivy, 2007). The success of the mitotic shake was assessed by verifying that the majority of cells were present in doublets.

EdU labelling and co-staining were carried out using a Click-iT® EdU Alexa Fluor® 555 Imaging Kit, according to the manufacturer's instructions (Invitrogen/Life technologies). EdU labelling times used for each condition are stated in each figure legend.

2.3.5 Biochemical fractionation

Fractionation was carried out as described (Andegeko et al., 2001). Fractionation was carried out in four consecutive steps with the supernatant being collected at each stage. The first and second fractions (fractions I and II respectively) were fractionated in Nonidet P-40 buffer (containing 50 mM HEPES, pH 7.5, 150 mM NaCl, 1 mM EDTA, 0.2% Nonidet P-40). 0.5% Nonidet P-40 buffer was used to fractionate fraction III. Protease (complete EDTA free; Roche) and phosphatase (Phospho-Stop; Roche) inhibitors were added to all buffers. For the last fraction (fraction IV), harvested cells were lysed in 1X SDS-PAGE sample buffer. Equal aliquots of each fraction corresponding to 1/5th of the total sample volume were separated on 7.5 or 12% SDS-Polyacrylamide gels, and western blotting was carried out.

2.3.6 Isolation of proteins on nascent DNA (iPOND)

This procedure was carried out as previously described with some modifications (Sirbu et al., 2012). An overview of the experimental scheme is shown in Figure 2.1. In brief, 6-7 x 10^8 cells were used per condition. For cells exposed to hypoxia, EdU (10 μM) was added immediately before placing the cells in the chamber. Those cells allowed to reoxygenate before crosslinking and harvesting were treated with EdU as soon as they were taken out of the chamber and for the whole duration of the reoxygenation period (2 hours). For cells exposed to normoxia, EdU was added for 1 hour before crosslinking and harvesting. These EdU labelling times were optimised to ensure comparable amounts of EdU labelling were achieved for each condition. To this end, immunofluorescence analysis was carried out to assess the efficiency of the click reaction (and EdU incorporation) in parallel to each of iPOND experiment. Quantification of the relative amounts of EdU incorporated for each condition was

carried out using LSM780 (Carl Zeiss Microscopy Ltd) software, and expressed as an average of the mean intensity for all of the cells where EdU incorporation was analysed per condition. At least 3 different fields of view were counted per condition for each experiment. Unless otherwise stated experiments were performed in triplicate.

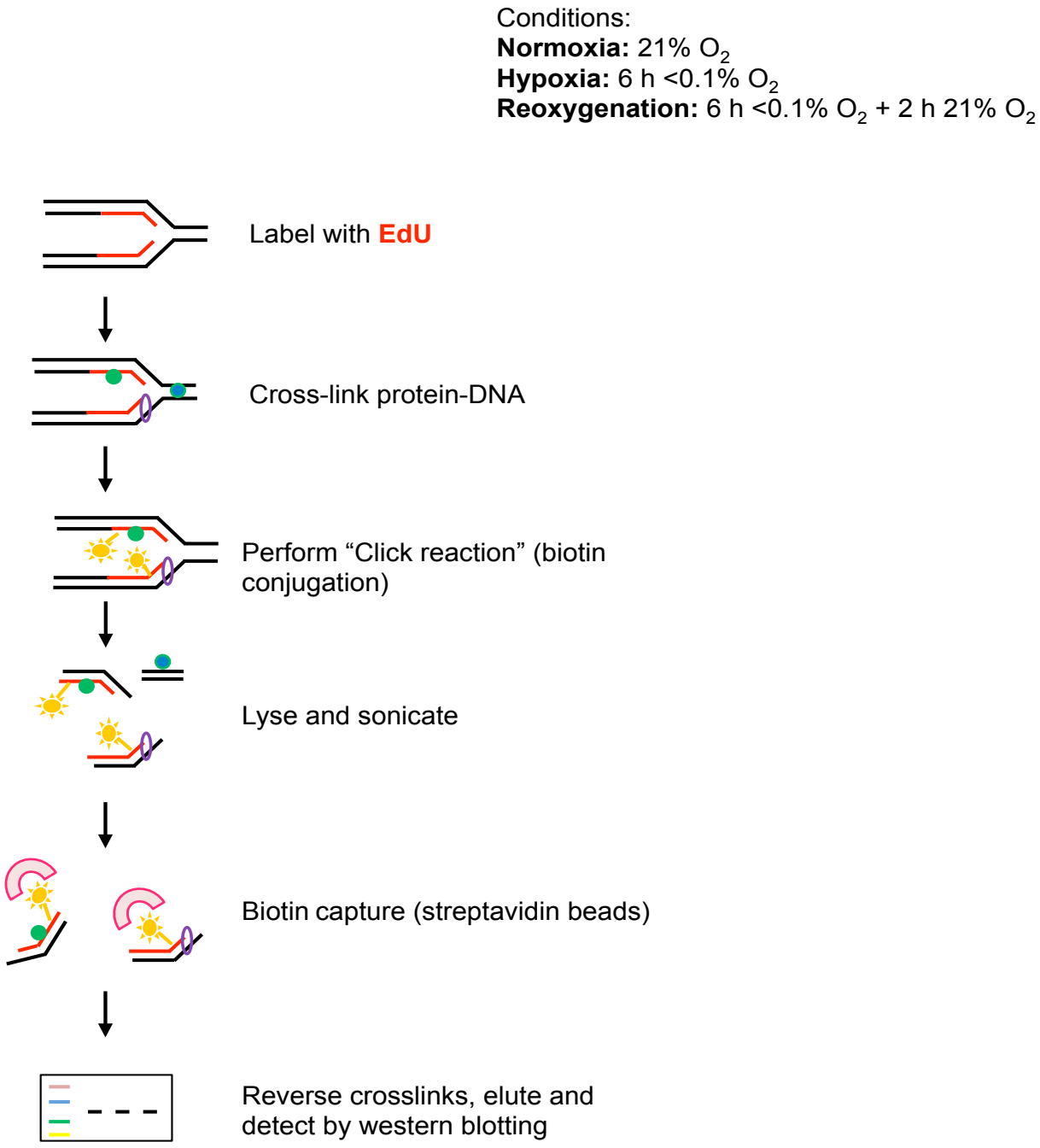


Figure 2.1. Overview of iPOND experiment
A schematic representation of the iPOND experiment performed with the three experimental conditions tested is shown. Adapted from (Olcina et al., 2013; Sirbu et al., 2012).

2.4 Molecular biology

2.4.1 Preparation of media and agar plates

Bacterial cultures were grown in LB. This was prepared by dissolving 25 g of LB in 1 litre of distilled water and sterilised by autoclaving at 121^{o}C, 15 psi for 30 minutes.

LB-agar was prepared by dissolving 35 g of LB-agar in 1 litre of deionised water and sterilised by autoclaving. Following boiling the LB-agar was allowed to cool to approximately 50^{o}C before being supplemented with antibiotics. 25 ml of liquid LB-agar was added to each sterile 9 cm diameter Petri dish around a Bunsen Burner flame. Plates were then allowed to set at RT and stored at 4^{o}C until needed for bacterial transformations.

2.4.2 Transformation of bacteria

Bacterial transformations for plasmid production were carried out in competent *Escherichia coli* DH5α cells (Invitrogen/Life technologies). 30 µg of competent cells were thawed on ice prior to addition of 5 µg DNA for each transformation. A 20 minute incubation of the cells on ice was then followed by heat shock at 42^{o}C for 30 seconds. A further 2 minute incubation of the cells in ice was then followed by addition of 500 µl of preheated (42^{o}C) SOC medium (Sigma-Aldrich UK). Transformation reactions were placed in an incubator at 37^{o}C for 1 hour with shaking at 225 rpm (Innova44 Inkubator). Transformation reactions were spread onto LB-agar plates and incubated overnight at 37^{o}C.

2.4.3 Growth of overnight cultures from colonies

A sterile tip was used to pick a single bacterial colony. These were grown in 150 µl of LB medium in a round-bottomed 14 ml tube at 37°C for 1 hour. This culture was then expanded in a 2 litre culture flask in 300 ml of LB (with the appropriate antibiotic) at 37°C overnight. Plates were parafilm sealed and kept in the fridge until required.

2.4.4 Agarose gel electrophoresis

Agarose gels for DNA analysis were prepared by dissolving agarose in 1X TBE buffer (89 mM Tris, 89 mM Boric acid, 2 mM EDTA) to a final concentration of 1-2 % (w/v) by heating the mixture to boiling point followed by cooling under running water before the addition of 1 µl of ethidium bromide per 100 µl of agarose mixture. The samples were diluted with 6X loading buffer (0.25% Bromophenol blue, 30% glycerol in a 10 mM Tris, 1 mM EDTA, pH 8.0 solution) before being loaded onto the gel. A DNA molecular weight marker (SmartLadder, Eurogentech) was run alongside the samples to assess DNA fragment size. Gel electrophoresis was carried out in 1X TBE at 120 V for 1 hour. DNA was visualised using an UV-transilluminator.

2.4.5 Large-scale preparation (Maxi-preparation) of plasmid DNA

Maxi-preparation of DNA was performed using a Qiagen kit according to the manufacturer's instructions.

2.4.6 Determination of DNA purity and concentration

DNA concentration was determined by measuring optical density (OD) at A_{260nm} with 1 A_{260nm} representing an equivalent of 50 µg of DNA in 1 ml distilled water. A ratio of absorbance of ≥1.8 at 260 nm and 280 nm indicated that DNA was pure and free from protein contamination.

2.4.7 RNA extraction and purification

RNA was extracted using 1 ml of TRIzol® per 5 cm dish. Following addition of TRIzol®, samples were incubated at RT for 5 minutes before addition of 200 µl of chloroform per 1 ml of TRIzol®. Samples were then shaken vigorously for 15 seconds before incubation at RT for 2-3 minutes. Centrifugation at 12000 x g at 4^{o}C for 15 minutes was then carried out. Centrifugation resulted in two phases with an upper colourless aqueous phase containing RNA. This aqueous phase was transferred carefully to a freshly labelled tube, always trying to avoid the interphase. 500 µl of isopropyl alcohol was then added per 1 ml TRIzol® before incubation of samples at RT for 10 minutes. A further centrifugation was then carried out at 12000 x g at 4^{o}C for 15 minutes in order to allow a gel-like pellet to form. The supernatant was removed and the pellet was washed with 1 ml 75 % ethanol. The samples were then vortexed shortly before centrifugation at 7500 x g 4^{o}C for 5 minutes. The pellet was then allowed to air-dry before re-suspension in 50-100 µl of DEPC-treated water. Prior to RNA quantification samples were placed in a 55^{o}C water bath for 10 minutes.

2.4.8 Determination of RNA purity and concentration

RNA purity and concentration was determined by using the Nanodrop spectrophotometer. Measuring the absorbance at OD_{260nm} calculated against 1 OD_{260nm} unit equivalent to 40 µg of RNA in 1 ml was used to quantify RNA concentration. An A_{260}/A_{280nm} ratio of 1.9-2.1 indicated that RNA was pure and protein-free (a reading below 1.6 indicated protein contamination).

2.5 Quantitative PCR (qPCR)

2.5.1 Reverse transcription

Verso (Thermo Scientific) or SuperScript® VILO™ (Invitrogen/Life Technologies) cDNA (complementary DNA) synthesis kits were used to reverse transcribe cDNA from total RNA according to manufacturer's instructions. cDNA to be used in qPCR experiments was diluted in DEPC-treated water to 1:50. Diluted cDNA was either used immediately or stored at -20°C.

2.5.2 qPCR reactions

Quantitative real time PCR was performed as previously (Pires et al., 2010b). For each qPCR experiment a reaction mix consisting of SYBR® Green PCR Master Mix, primers and DEPC-treated water was prepared as shown in Table 2.13. SYBR® Green PCR Master Mix is supplied in 2X concentration and contains SYBR® Green 1 dye, AmpliTaq Gold® DNA polymerase, dNTPs (deoxyribonucleotide triphosphates) with dUTP (deoxyuridine triphosphate); passive reference dye and optimised buffer components. 20 µl of reaction mix plus 5 µl of diluted cDNA were

loaded into each well of a 96-well plate. All primers were used at stock concentrations of 3.3 μM, except for *18S* that was used at 5 μM. Reactions were carried out in a 7500 Fast real time PCR detection system (Applied Biosystems) with the following conditions: 20 seconds at 50°C, 15 minutes at 95°C then 40 cycles of 15 seconds at 95°C, 30 seconds at 60°C, 30 seconds at 72°C, and finally a melt curve stage of 15 seconds at 95°C, 1 minute at 60°C, 30 seconds at 95°C and 15 seconds at 60°C.

For mRNA expression analysis, mRNA fold change levels were normalised to *18S* ribosomal RNA and calculated using a $2^{-\Delta\Delta Ct}$ method. Error bars indicate the error between three technical replicates ± RQ_{max} and RQ_{min} from one experiment.

For ChIP analysis, immunoprecipitation samples were diluted 1:6 in DEPC-treated water prior to performing standard qPCR reaction for the genes of interest (using the reaction mix shown in Table 2.13). The input samples were generally diluted 1:100 (except for the ChIP screen described in Figure 6.1, where the input was diluted 1:6). Fold enrichment was calculated relative to total H3 and as a % of input.

Table 2.13. Components used to make up the reaction mix for qPCR

Reagent	Volume/well
SYBR® Green PCR Master Mix	12.5 μl
Forward Primer	2.5 μl
Reverse Primer	2.5 μl
DEPC-treated H_2O	2.5 μl

2.6 Chromatin immunoprecipitation

Cells were seeded in two 15 cm plates per condition and were used at 60-70% confluency. At the end of the timecourse cells were cross-linked with 1% formaldehyde in DMEM for 10 minutes at RT while on a rocker. Crosslinking was then quenched with 1 M glycine in PBS for 5 minutes at RT. Cells were then washed 3 times with PBS and scraped into 5 ml PBS supplemented with protease inhibitor cocktail (Roche). Cells were then centrifuged 233 x g for 5 minutes at 4^{o}C. Pellets were resuspended in SDS cell lysis buffer (Table 2.14) and incubated on ice for 10 minutes. Following this incubation period cells were sonicated for 15 minutes at 4^{o}C (10 seconds pulse on, 50 seconds pulse off) using a Diagenode Bioruptor plus sonicator. In order to check that the sonication had proceeded successfully a 50 µl aliquot of chromatin was taken before and after sonication for each sample (as a shearing control). Chromatin was then diluted 1:10 using ChIP dilution buffer (Table 2.15). Protein A agarose beads (Millipore) were washed 3 times in ChIP dilution buffer and resuspended at 50% ChIP dilution buffer volume. 100 µl of 50% bead slurry were added to each sample to pre-clear the chromatin prior to immunoprecipitation. The mixture of diluted chromatin and beads was placed at 4^{o}C, rotating end-over-end for 1 hour. Following the pre-clearing period beads were centrifuged at 233 x g for 5 minutes at 4^{o}C and the pre-cleared chromatin was divided into 2 ml aliquots. Samples were divided into: antibodies of interest (shown in Table 2.4), pre-immune serum (Thermo Scientific) (referred to as IgG in figures throughout the text) or no antibody control and placed at 4^{o}C, rotating end-over-end overnight. 60 µl bead slurry was added to each sample following this period for 1 hour end-over-end at 4^{o}C. Beads were then collected by centrifugation at 233 x g at 4^{o}C for 5 minutes. At this point 500 µl of chromatin from the no antibody control was also

collected as pre-cleared input. Beads were then washed with 1 ml low salt wash solution (Table 2.16) transferred to a 1.5 ml Eppendorf and rotated end-over-end for 5 minutes at 4°C. Beads were collected by centrifugation at 400 x g for 3 minutes at 4°C and resuspended in 1 ml high salt wash solution (Table 2.17). Samples were placed rotating end-over-end for 5 minutes at 4°C before being centrifuged again at 400 x g for 3 minutes at 4°C. Samples were washed in 1 ml LiCl wash (Table 2.18) and again allowed to rotate end-over-end at 4°C, before centrifugation as before. Finally, samples were washed twice in 1 ml TE buffer (Table 2.19) before elution in freshly made 250 µl elution buffer (Table 2.20). Beads were eluted for 15 minutes end-over-end at RT. Following this time, beads were collected by centrifugation at 400 x g for 5 minutes at 4°C, before the elution process was repeated once again with a further 250 µl elution buffer. At this point, 400 µl elution buffer was added to 100 µl of input sample. 20 µl 5 M NaCl was added to each 500 µl volume of sample. Samples were inverted and centrifuged briefly before incubation at 65°C for 4 hours or overnight. If 50 µl sonication control samples were taken these were then processed at this time by addition of 5 µl 5 M NaCl and incubation at 65°C for 4 hours or overnight. Following this incubation period 10 µl 0.5 M EDTA, 20 µl 1 M Tris pH 6.5 and 2 µl 20 mg/ml proteinase K mix were added to each sample prior to incubation at 45°C for 1 hour. DNA was then extracted by phenol-chloroform purification by addition of 500 µl phenol:chloroform:isoamyl-alcohol to each sample (50 µl to the shearing controls). Samples were vortexed to emulsion and then centrifuged at 16.2 x g 4°C for 10 minutes. The aqueous layer was then transferred to a new 1.5 ml Eppendorf. 50 µl of 3 M NaOAc was added to each sample followed by a short vortex and addition of 1 µl of 20 µg/µl glycogen and 1 ml 100% ice cold ethanol. Samples were then placed at -20°C overnight. Samples were centrifuged the following day at 16200 x g 4°C for 45

minutes. The supernatant was removed and pellets were washed with 70% ethanol before further centrifugation at 16200 x g at 4^{o}C for 30 minutes. The supernatant was then removed and the remaining pellet was air-dried before re-suspension in 25 µl DEPC-treated water.

Table 2.14. Recipe for SDS cell lysis buffer

Final	Stock	Volume/50 ml
1% SDS	20%	2.5 ml
10 mM EDTA	0.5 M	1 ml
50 mM Tris pH 8.1	1 M	2.5 ml
25x Complete protease inhibitor	25X	2 ml
Milli-Q H_2O	-	43 ml

Table 2.15. Recipe for ChIP dilution buffer

Final	Stock	Volume/50 ml
0.01% SDS	20%	25 µl
1.1% Triton X-100	100%	550 µl
1.2 mM EDTA	0.5 M	120 µl
16.7 mM Tris pH 8.1	1 M	835 µl
167 mM NaCl	5 M	1.67ml
25x Complete protease inhibitor	25X	2 ml
Milli-Q H_2O	-	Up to 50 ml

Table 2.16. Recipe for low salt wash solution

Final	Stock	Volume/50 ml
0.1% SDS	20%	250 µl
1% Triton X-100	100%	500 µl
2 mM EDTA	0.5 M	200 µl
20 mM Tris pH 8.1	1 M	1 ml
150 mM NaCl	5 M	1.5 ml
Milli-Q H_2O	--	Up 50 ml

Table 2.17. Recipe for high salt wash solution

Final	Stock	Volume/50 ml
0.1% SDS	20%	250 µl
1% Triton X-100	100%	500 µl
2 mM EDTA	0.5 M	200 µl
20 mM Tris pH 8.1	1 M	1 ml
500 mM NaCl	5 M	5 ml
Milli-Q H_2O	-	Up 50 ml

Table 2.18. Recipe for LiCl wash buffer

Final	Stock	Volume/50 ml
0.25 M LiCl	8 M	1.6 ml
Igepal® 1%	100%	500 µl
1% Na deoxycholate	-	500 mg
1 mM EDTA	0.5 M	100 µl
10 mM Tris pH 8.1	1 M	500 µl
Milli-Q H_2O	-	Up to 50 ml

Table 2.19. Recipe for TE buffer

Final	Stock	Volume/50 ml
10 mM Tris pH 8.1	1 M	500 µl
1 mM EDTA	0.5 M	100 µl
Milli-Q H_2O	-	49.4 µl

Table 2.20. Recipe for elution buffer

Final	Stock	Volume/20 ml
0.1 M $NaHCO_3$	-	168.2 mg
1% SDS	20%	1ml
Milli-Q H_2O	-	Up to 20 ml

2.7 Single-molecule DNA fiber analysis

DNA fibers were produced as previously described with a few modifications (Pires et al, 2010). In brief, subconfluent cells were sequentially pulse labelled with 25 mM CldU and 250 mM IdU for 20 minutes and left at 21% O_2 in a 37^{o}C incubator (for normoxic samples). For the reoxygenation treated samples, cells were treated with 25 mM CldU and immediately placed in the hypoxic chamber (< 0.1% O_2). Following 5 hours of hypoxic treatment, cells were washed once with fresh warm media and then 250 mM IdU was added before placing cells at 21% O_2 for 1 hour. For hypoxic samples, cells were placed in the hypoxic chamber (<0.1% O_2) for 3 hours. Following this 3 hour period, 25 mM CldU was added for 2 hours while the cells were still kept at <0.1% O_2. Following this time period, cells were washed once with fresh warm media before addition of 250 mM IdU. A schematic representation of the protocol used is shown in Figure 2.2. Labelled cells were harvested and DNA fibers were spread and fixed with methanol/acetic acid (3:1 ratio). For staining, fibers were treated with 2.5 M HCl and incubated with rat anti-BrdU monoclonal antibody (for detection of CldU labelled tracts) and mouse anti-BrdU monoclonal antibody (for detection of IdU labelled tracts) for 1 hour at RT (details of the antibodies used are shown in Table 2.5). Slides were then fixed with 4% paraformaldehyde and incubated with Alexa Fluor 555-conjugated goat anti-rat IgG and Alexa Fluor 488-conjugated goat anti-mouse for 1 hour in a humidified chamber at 37^{o}C (Table 2.8). Fibers were imaged using a Bio-Rad Radiance or LSM780 (Carl Zeiss Microscopy Ltd) confocal microscope and analysed using ImageJ software (NIH). At least 200 replication structures were counted and at least 50-100 replication tracks were measured per experiment unless otherwise stated. Experiments were carried out in triplicate unless otherwise stated.

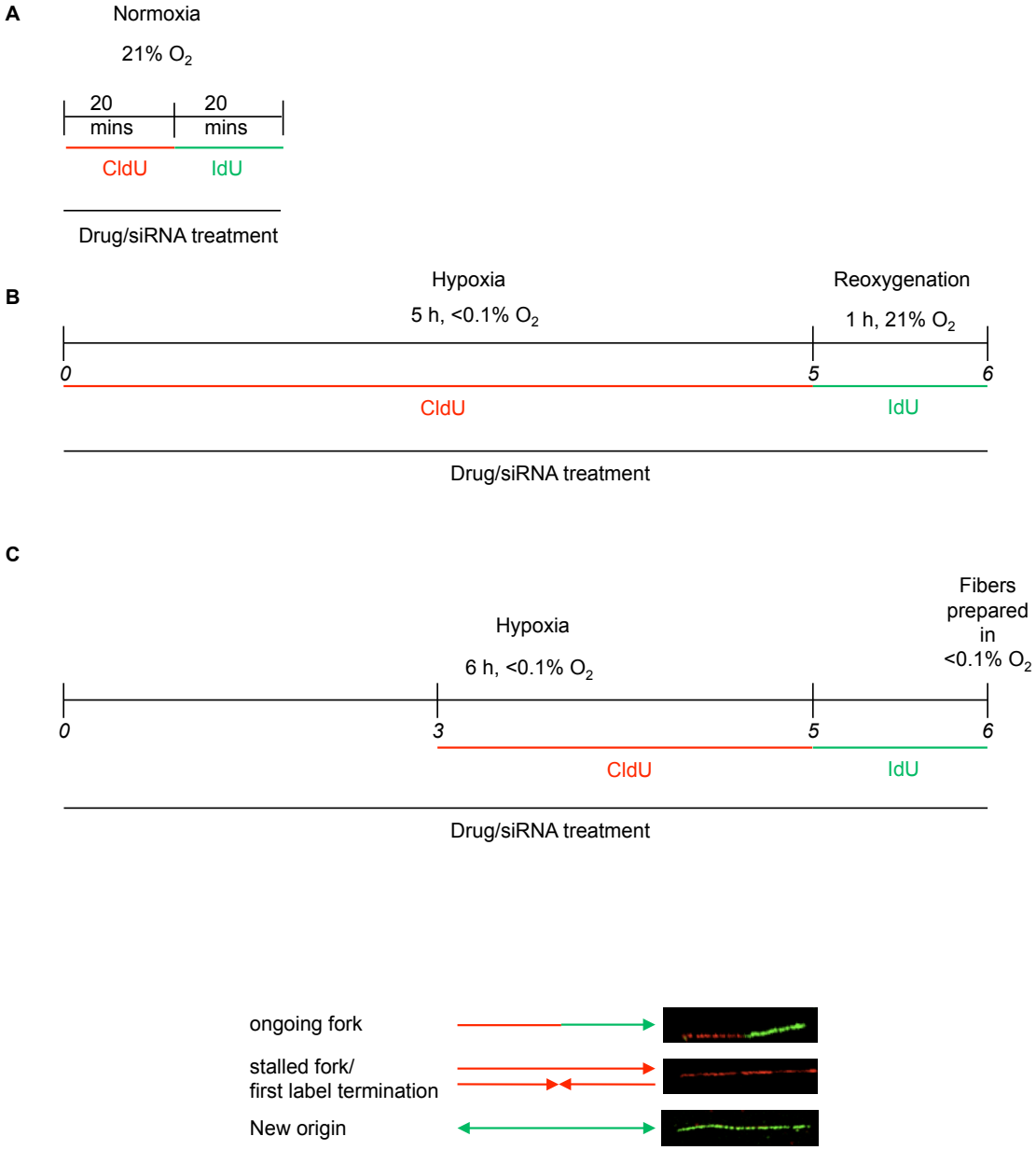


Figure 2.2. Schematic representation of the DNA fiber protocols (**A**) in Normoxia, (**B**) after Reoxygenation and (**C**) in Hypoxia (<0.1% O_2). Examples of the types of structures that can be scored following DNA fiber spreading and staining are also shown. Adapted from (Olcina et al., 2013).

2.8 Alkaline comet assay

Comet assays were performed as previously with modifications to allow hypoxic treatments (Parsons et al., 2012). All solutions used for hypoxic treatment were equilibrated at the indicated oxygen tensions. 6.5 x 10^4 cells were seeded and allowed to adhere for 12 hours, before exposing them to the indicated treatments. Treated cells were trypsinised and 250 µl of cell suspension was embedded in 1ml 1% low-melting agarose by quickly adding the cell suspension onto a coated slide and covering it with a coverslip before placing the slide on an ice tray for 5 minutes. Coverslips were then removed and Lysis buffer (2.5 M NaCl, 100 mM EDTA disodium salt, 10 mM Tris base, pH 10.5) was then added for an hour at RT in the dark in a Coplin jar. For hypoxic samples lysis was carried out under hypoxic conditions. Slides were removed and washed, followed by incubation in cold electrophoresis buffer (300 mM NaOH, 1 mM EDTA and 1% DMSO, pH >13) for 30 minutes. Electrophoresis was carried out at 25 V, 300 mA for 25 minutes. Slides were stained with SYBR® Gold after neutralisation with 0.5 M Tris-HCl (pH 8.0). Comets were analysed using Komet 5.5 image analysis software (Andor Technology). 50 cells were counted per slide. Two slides were counted per condition for each experiment.

2.9 Phosphatase activity assay

This assay was carried out according to the manufacturer's instructions (Millipore) with a few modifications. In brief, extracts were prepared in such a way as to ensure minimal phosphate content of the extracts (Tanaka et al., 1992). Cell extracts were resuspended in one packed-cell volume of buffer I, containing 10 mM Tris-HCl (pH 7.8), 200 mM KCl, 1 mg/ml of protease inhibitor cocktail, 1 mM PMSF

and 1 mM NEM. Cells were then resuspended in two packed-cell volumes of Buffer II containing 10 mM Tris-HCl (pH 7.8), 600 mM KCl, 40% glycerol, 0.1 mM EDTA and 0.2% Nonidet P-40. The cell lysate was then centrifuged at 9800 x g at 4^{o}C for 20 minutes and the supernatant was harvested and stored at 80^{o}C for at least 30 minutes prior to immunoprecipitation with PP2A-C antibody (Upstate/Millipore). Phosphatase activity was assessed by absorbance measurement at 650 nm on a POLARstar Omega plate reader (BMG Labtech).

2.10 Fluorescence-activated cell sorting

2 x 10^6 cells were seeded overnight and allowed to adhere. Cells were then placed in normoxia (21% O_2), hypoxia (<0.1% O_2 for 6 h) or irradiated with 5 Gy. Following treatment, cells were fixed with 4% paraformaldehyde for 15 minutes and then centrifuged at 300 x g for 5 minutes. Cells were then washed twice with PBS and permeabilised with 0.5% Triton-X for 20 minutes. Cells were then incubated with the primary antibody diluted 1:100 in 1% BSA in 1X PBS for 1 hour followed by the secondary antibody diluted 1:200 in 1% BSA in 1X PBS for 1 hour (details of primary and secondary antibodies used are shown in Table 2.6 and 2.8 respectively). Finally, the pellets were resuspended in PBS containing PI (10 μg/ml) and RNAse A (100 μg/ml) mixture and incubated at 37°C for 30 minutes. Analysis was carried out for 10000 cells per experimental condition using Becton Dickinson FACSort. Samples were later analysed using CellQuest Pro and ModFit LT software.

2.11 Apoptosis assay (by cell morphology)

To assess apoptosis by nuclear morphology both adherent and floating cells were collected and fixed in 4% paraformaldehyde (for 15 minutes) at the end of each timecourse. Nuclei were stained with ProLong® Gold mounting medium with DAPI. Apoptosis was plotted as the percentage of cells with fragmented DNA per field of view, with ten fields of view quantified per experiment. Each apoptosis experiment was performed at least 3 times.

2.12 Immunohistochemistry staining

IHC analysis was performed on 4 μm sections of paraffin-embedded Calu-6 xenografts sections as described with a few modifications (Bottini et al., 2000). Antigen retrieval was carried out for 1 minute and 30 seconds at 125°C with citrate buffer in 0.05% PBS-tween (pH 8.0). Endogenous peroxidase activity was blocked using 3% H_2O_2 for 30 minutes at RT. Non-specific antibody binding was avoided by treating samples with protein blocking solution (Abcam) for 15 minutes before adding the diluted primary antibody overnight at 4^oC. H3K9me3, CAIX and phospho-ATM-S1981 primary antibodies were used as described in Table 2.7. Slides were then incubated for 30 minutes with secondary EnVision System HRP-labelled polymer (Dako). Following this incubation, slides were stained with diaminobenzidene (DAB) solution (DAB+, Dako) for 1 minute for H3K9me3 staining or 2 minutes for CAIX and ATM-S1981 staining. Samples were counterstained with hematoxylin for 30 seconds and mounted with DPX mounting media (Surgipath). Slides were imaged using the Aperio system at 20X magnification and quantified using Scanscope

software. An intensity score of 2 or above represents high H3K9me3 or ATM-S1981 staining. Intensity scores of 1 or above represent CAIX positive regions.

2.13 Xenograft study

Calu-6 cells (0.1 ml, 1 x 10^6) were injected subcutaneously into female BALB/C nude mice (6-8 weeks old) at a single dorsal site. Growing tumours (100-400 mm^3) were formalin fixed and paraffin embedded. Animal study protocols were approved by the Institutional Ethics Committee and the Home Office (30/2834) and designed in accordance with the Scientific Procedures Act (1986) and the 2010 Guidelines for the welfare and use of animals in cancer research (Workman et al., 2010).

2.14 Analysis

Statistical analysis was carried out using Microsoft Excel. The formulas used to calculate the standard error (SE) and confidence intervals were as follows:

SE = standard deviation (SD)/√number of samples (n)

Confidence intervals (CI) = mean ± 1.96 x SE.

Protein bands were quantified using the LiCor Odyssey software. Images obtained following immunofluorescence were analysed using ImageJ software unless otherwise stated.

CHAPTER 3

HYPOXIA-INDUCED ATM SIGNALLING

3.1 INTRODUCTION

Conditions of hypoxia below 0.1% O_2 induce replication stress and activate the DDR; including both ATR- and ATM-mediated signalling (Bristow and Hill, 2008; Hammond et al., 2003a; Squatrito et al., 2010). There is a significant oxygen dependency to the hypoxia-induced DDR. Mild levels of hypoxia (2% O_2, for example) do not lead to replication stress and do not induce the activation of ATR or ATM (Bencokova et al., 2009; Hammond et al., 2002; Hammond et al., 2007). The reduction in nucleotide pools, known to occur specifically under severe hypoxic conditions (<0.1% O_2), has been proposed as a possible explanation for hypoxia-induced replication stress (Pires et al., 2010b). Interestingly, reductions in nucleotide pools following oncogenic activation of the Rb-E2F pathway have also been shown to result in disturbed replication fork progression and ultimately collapse of replication forks and DSB generation (Bester et al., 2011). Hu treatment leads to RNR inhibition and also induces replication stress due to nucleotide pool depletion (Anglana et al., 2003). Hypoxia and Hu-induced replication stresses have been previously mechanistically compared. This study revealed that both, a short exposure to Hu and severe hypoxia (<0.1% O_2), induce the formation of areas of ssDNA and the subsequent activation of ATR signalling (Hammond et al., 2003b). Upon prolonged

induction of replication stress following treatment with Hu, replication forks are thought to collapse and this leads to DSB formation, similarly to the situation following prolonged oncogene-induced replication stress (Bester et al., 2011; Hammond et al., 2003b). Notably, even prolonged exposures to <0.1% O_2 do not lead to the generation of DSB, suggesting that while replication stress occurs in response to hypoxia this does not lead to a complete disruption of DNA replication (Hammond et al., 2003b).

ATM activation following hypoxia-induced replication stress in the absence of detectable DNA breaks is extremely surprising. The sensing of aberrant replication structures by ATM in response to hypoxia has been proposed as a reason for ATM activation under these conditions (Bencokova et al., 2009). Hypoxia-induced replication stress may, therefore, serve as a trigger for ATM activation. However, it is unlikely that replication stress alone is sufficient to induce ATM activity since ATM signalling does not respond to replication stress unless DNA damage is also evident. For example previous reports have demonstrated that ATM dependent KAP-1 phosphorylation does not occur in response to doses of Hu or UV that induce replication stress in the absence of damage (Goodarzi et al., 2009; Ziv et al., 2006). However, it is important to note that hypoxia was not considered in these studies.

Intrigued by the activation of ATM in hypoxia in the absence of any detectable DNA damage we investigated the relationship between hypoxia-induced replication stress and ATM signalling to gain further insight into the mechanism of hypoxia-induced ATM activation.

3.2 RESULTS

3.2.1 Hypoxia-induced replication stress in the absence of damage

In order to investigate the oxygen dependency of the hypoxia-induced DDR in detail we used two hypoxic conditions (2% and <0.1% O_2). As expected, following exposure of colorectal RKO cancer cells to both of these oxygen tensions for the indicated times we observed HIF-1α stabilisation. However, we only observed evidence of both ATR- as well as ATM-mediated signalling at <0.1% O_2. This signalling included p53 phosphorylation at serine 15 (p53-S15) as well as ATM-S1981 phosphorylation and activation of downstream ATM targets such as KAP-1-S824 (Figure 3.1). Furthermore, only exposure to <0.1% O_2 resulted in RPA phosphorylation, as seen by a band shift following immunoblotting for total RPA32, which is indicative of replication stress.

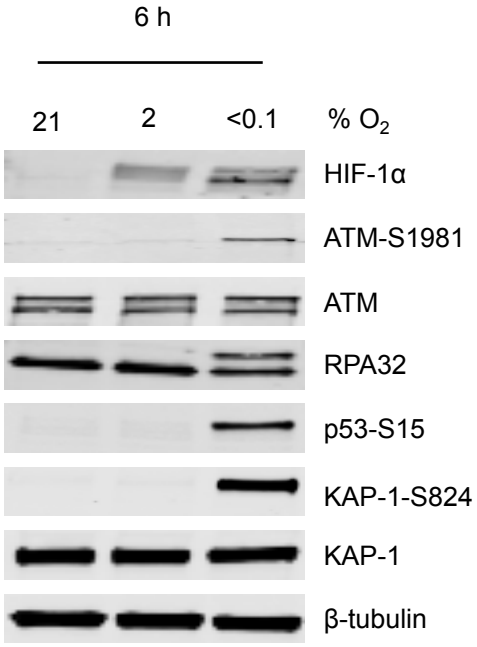


Figure 3.1. Oxygen dependence of the hypoxia-induced DDR.
RKO cells were exposed to 21%, 2% or <0.1% O_2 for 6 hours (h). Western blotting was carried out with the antibodies indicated; β-tubulin was used as a loading control.

Before proceeding further, we decided to investigate the induction of hypoxia-induced replication stress in the absence of detectable DNA damage in greater detail. To achieve this, DNA fibers were generated following the exposure of RKO cells to 21%, 2% and <0.1% O_2, and DNA replication rates as well as the types of replication structures were quantified. As shown in Figure 3.2A exposure of cells to 2% O_2 did not significantly change the types of replication structures with comparison to 21% O_2. In contrast, when cells were exposed to <0.1% O_2, there was a significant increase in the number of stalled replication forks and a decrease in the number of new origins being fired. In addition, upon exposure of cells to 2% O_2 there was no significant change in replication rates when compared to 21% O_2 (Figure 3.2B).

We next took two complementary approaches to confirm that the observed effects on DNA replication and DDR signalling were occurring in the absence of DNA damage. Firstly, the presence of two common DNA damage markers, γH2AX and 53BP1, were assessed by immunofluorescence following exposure to normoxia, hypoxia or neocarzinostatin (NCS) (as a control DNA damaging-inducing agent) (Figure 3.3A). As a control for the induction of replication stress the ability of cells to form RPA32 foci was also determined. As expected hypoxia (<0.1% O_2) resulted in the formation of RPA32 foci. Interestingly, this occurred in the presence of a strong pan-nuclear γH2AX signal, reminiscent of previously described signals correlating with replication stress (Toledo et al., 2011). This γH2AX signal contrasted with the distinct nuclear foci observed in response to NCS. Moreover, while no 53BP1 foci were observed in response in hypoxia, clear 53BP1 foci were detected in response to NCS. Secondly, the absence of DNA breaks was confirmed by alkaline comet assay. Once again, exposure of cells to hypoxia (<0.1% O_2) did not lead to the detection of

any significant DNA damage (as assessed by % of tail DNA) whereas treatment with IR resulted in a significant induction in the % tail DNA measured (Figure 3.3B).

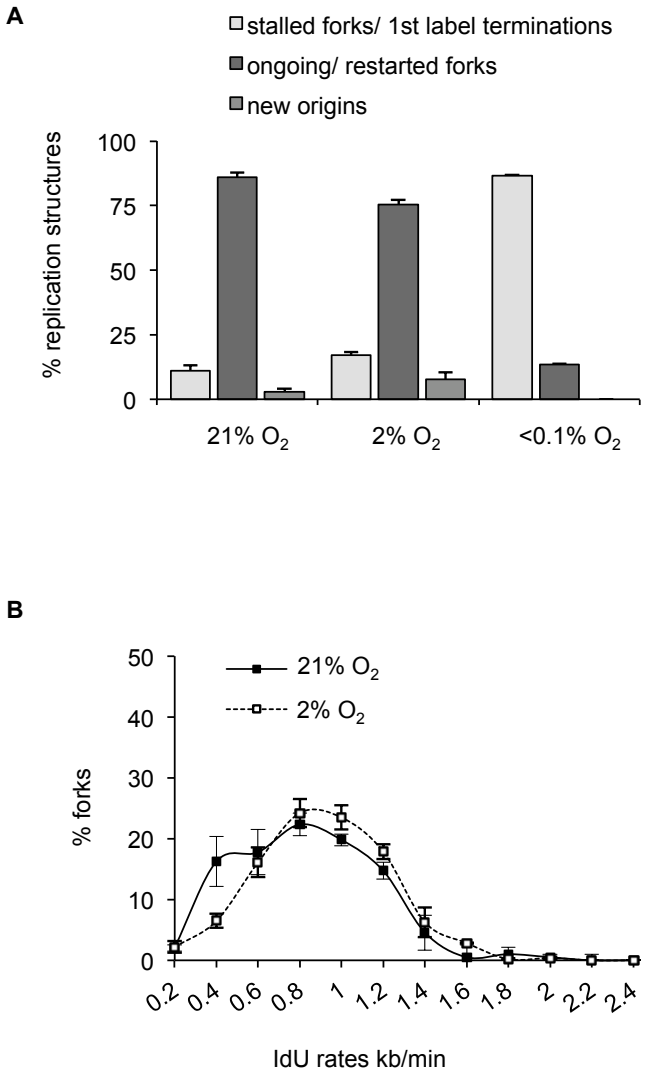


Figure 3.2. Exposure to <0.1% but not 2% O_2 leads to replication stress **(A)** RKO cells were exposed to 21, 2 or <0.1% O_2 for 6 hours and DNA fibers were spread, stained and scored. A graph of the replication structures scored following exposure to the three different oxygen tensions is shown, n=3. **(B)** The graph indicates the distribution of fork rates for the second label for the forks scored in (A) for cells exposed to 21% or 2 % O_2 for 6 hours (Pires et al., 2010b).

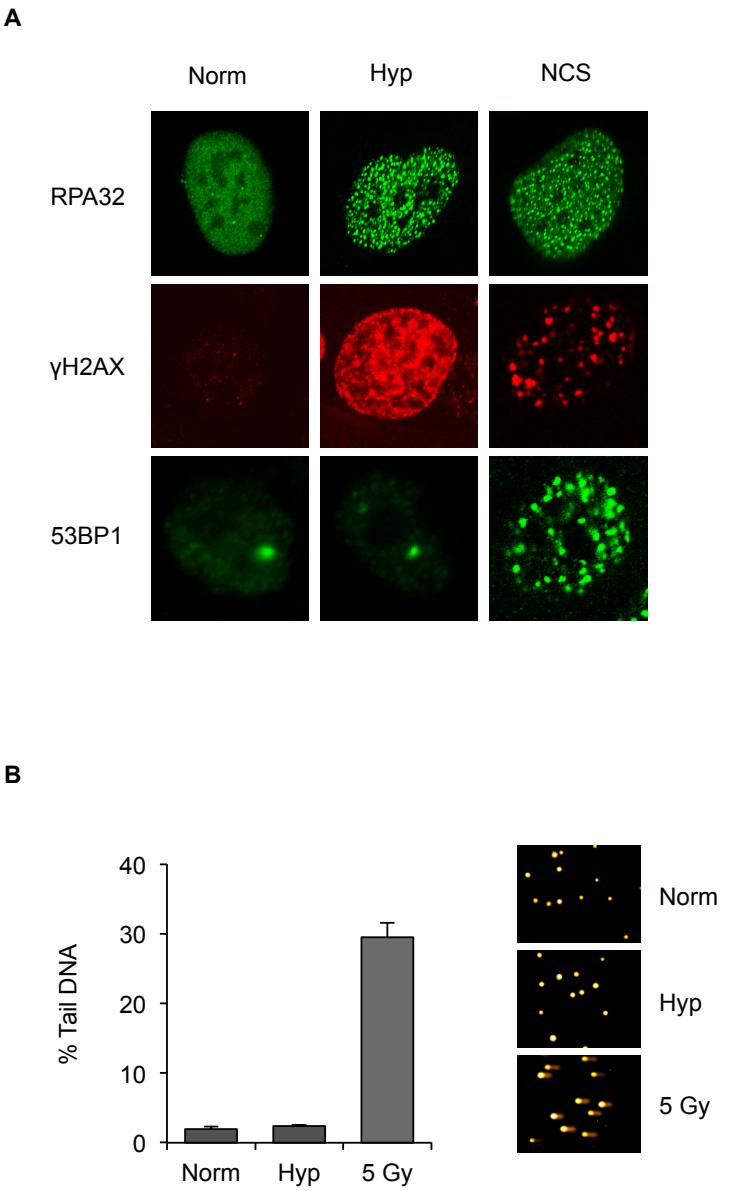


Figure 3.3. Exposure to hypoxia (<0.1% O_2) does not lead to the generation of significant detectable DNA damage
(A) RKO cells were exposed to Norm (21% O_2), Hyp (6 h, <0.1% O_2) or NCS (6 h, 200 ng/ml). Cells were then fixed and stained as indicated. The hypoxic cells were fixed in hypoxic conditions with equilibrated solutions to avoid reoxygenation. Images generated by Dr Zuzana Bencokova. (**B**) Quantification of the % comet tail DNA for each condition. Norm (21% O_2), Hyp (6 h, <0.1% O_2), IR (5 Gy, cells harvested immediately post-IR). Representative images of RKO cells treated as indicated and processed for alkaline comet assay are also shown next to the graph, n=3. Comet assays were performed by Selvakumar Anbalagan.

3.2.2 Hypoxia-induced ATM-mediated signalling

We next investigated ATM-mediated signalling in further detail by treating RKO cells with the ATM inhibitor, KU-55933, in response to hypoxia as well as following periods of reoxygenation. As expected, KAP-1-S824 and CHK2-T68 were rapidly phosphorylated in the DMSO treated cells in response to both hypoxia (<0.1% O_2) as well as reoxygenation. In the presence of the ATM inhibitor, however, phosphorylation of KAP-1-S824 and CHK2-T68, was markedly attenuated both in hypoxia as well as after reoxygenation (Figure 3.4).

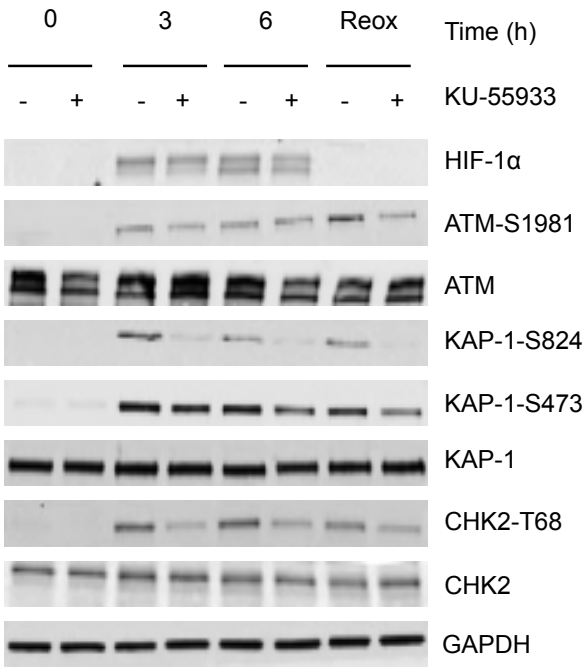


Figure 3.4. Hypoxia-induced ATM is active
RKO cells were exposed to <0.1% O_2 for the times indicated in the presence of DMSO or 10 μM ATM inhibitor (KU-55933). Reox=6 h, <0.1% O_2 followed by 1 h of 21% O_2. Western blotting was carried out with the antibodies indicated; GAPDH was used as a loading control.

These data suggest that ATM is active and phosphorylates downstream targets in hypoxia (Figure 3.2). An increase in phosphorylation of KAP-1 at residue 473 was also observed in response to hypoxia. Following ATM inhibition, however, KAP-1 phosphorylation at this residue was not reduced as markedly as KAP-1-S824 phosphorylation, consistent with reports indicating it is dependent on CHK1 activity in response to replication stress (Blasius et al., 2011) (Figure 3.4).

Given that ATM and ATR share a number of substrates and that the ATR-mediated response to hypoxia-induced replication stress has been described in detail, (Hammond et al., 2002; Matsuoka et al., 2007; Pires et al., 2010a; Pires et al., 2012) we decided to investigate the possible involvement of ATR in also mediating KAP-1 phosphorylation. RKO cells were treated with 25 nM of a recently described ATR inhibitor (VE-821) (Reaper et al., 2011a), and exposed to different periods of hypoxia (<0.1% O_2). As shown in Figure 3.5, ATR inhibition resulted in a reduction in the phosphorylation of classical ATR targets, such as CHK1-S345, demonstrating that the compound was an effective ATR inhibitor. KAP-1 phosphorylation at S824, however, was not diminished following treatment with this inhibitor. KAP-1 phosphorylation, in fact, appeared to be increased following ATR inhibition. We hypothesize that the increase in KAP-1-S824 occurs as a result of the induction of DNA damage following ATR inhibition in hypoxia, probably occurring due to replication fork collapse (Pires et al., 2012). Indeed, γH2AX, was also induced following ATR inhibition in hypoxia. Together, these results suggest that KAP-1 is phosphorylated in hypoxia, in an ATR independent but ATM dependent manner.

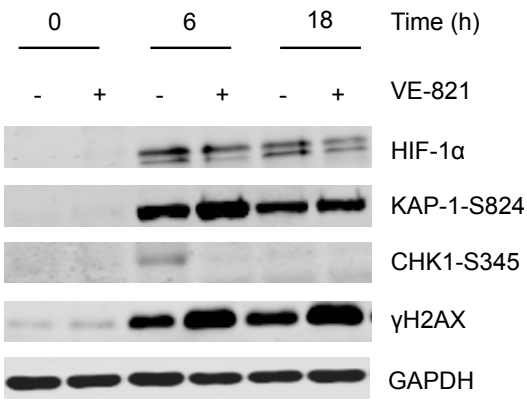


Figure 3.5. KAP-1 phosphorylation is ATR independent
RKO cells were treated with 25 nM of ATR inhibitor VE-821 or DMSO at <0.1% O_2 for the times indicated. A western blot indicating the different ATR and ATM targets blotted for is shown. GAPDH was used as a loading control.

3.2.3 Replication stress in a hypoxic context leads to ATM activation

We hypothesized that hypoxia-induced replication stress could signal to ATM. This hypothesis would imply that ATM dependent phosphorylation of downstream targets such as KAP-1-S824 should only occur in S-phase. We determined that KAP-1 was phosphorylated at serine 824 in approximately 50% of RKO cells exposed to <0.1% O_2 (Figure 3.6A). This number correlated with the proportion of the population known to be in S-phase following exposure to hypoxia (Bencokova et al., 2009). In contrast, KAP-1 was phosphorylated in approximately 100% of the cells in response to IR, used here as the positive DNA damage control. To confirm this, we generated an enriched population of RKO cells in the G_1 phase of the cell cycle using the mitotic shake-off technique and determined the levels of phosphorylated KAP-1-S824 and ATM-S1981 in these cells in response to normoxia, hypoxia or Dox (used as a DNA damage positive control) (Figure 3.6B). Hypoxic G_1 cells showed little or no

induction of KAP-1 or ATM phosphorylation whereas these two proteins were phosphorylated in most of the G_1 cells exposed to Dox.

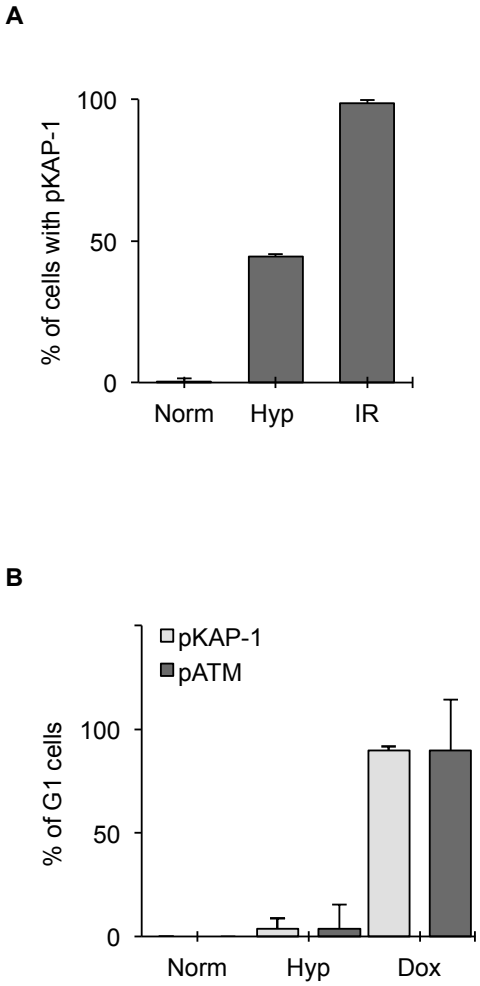


Figure 3.6. Hypoxia-induced ATM activity is absent from G_1 phase
(A) RKO cells were stained and scored for KAP-1 phosphorylation. Norm (21% O_2), Hyp (6 h, <0.1% O_2), or IR (1 Gy, cells fixed 30 minutes post IR). The quantification of the % of cells with pKAP-1 staining is shown, n=3. **(B)** A G_1 enriched population of RKO cells was generated using the mitotic shake-off technique. Cells were then fixed and stained with the antibodies indicated. Norm (21% O_2), Hyp (6 h, <0.1% O_2), Doxorubicin (Dox) (4 h, 2 μM). The quantification of the % of stained G_1 cells is shown. pKAP-1=KAP-1-S824, pATM=ATM-S1981.

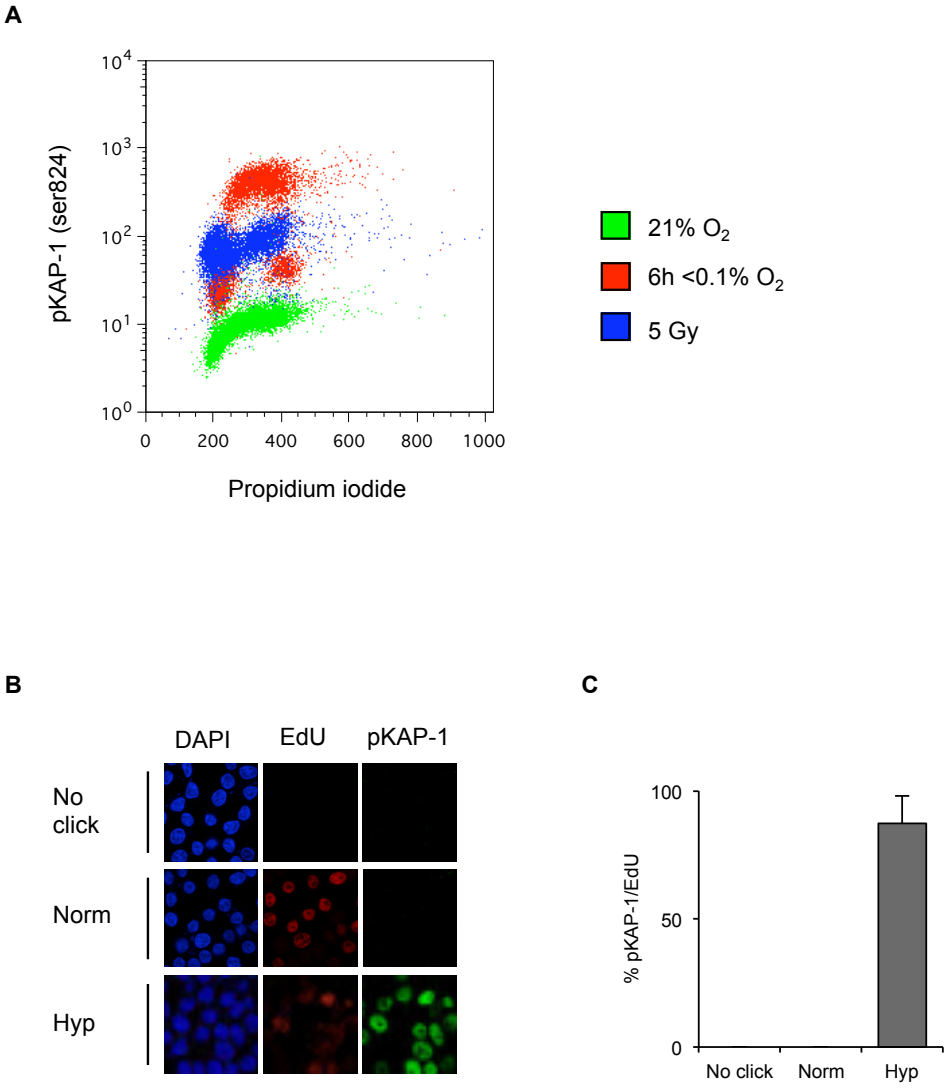


Figure 3.7. Hypoxia-induced ATM activity is restricted to S-phase
(A) RKO cells were exposed to Norm (21% O_2), Hyp (6 h, <0.1% O_2) or IR (5 Gy, cells fixed immediately post-IR). Cells were then stained for KAP-1-S824 and for DNA content using PI and analysed using FACS. Data generated with assistance from Dr Joana Senra. **(B)** RKO cells were labelled with EdU (10 µM) for 0.5 h in Norm and No click, or 6 h in Hyp and co-stained with KAP-1-S824. Hyp (6 h, <0.1% O_2). No click represents a sample where the click reaction was carried out without fluorophore. A representative image of co-localisation of KAP-1-S824 and EdU staining is shown. **(C)** Quantification of the % pKAP-1/EdU co-localisation observed in (B) is shown. pKAP-1=KAP-1-S824.

To confirm that KAP-1 phosphorylation was occurring in S-phase we carried out FACS analysis and stained for KAP-1-S824 as well as for DNA content using propidium iodide (PI). FACS demonstrated that the phosphorylated KAP-1 population was enriched in S-phase in response to hypoxia, while it was abundant throughout all cell-cycle phases in response to IR (Figure 3.7A). This was further confirmed by labelling S-phase cells with EdU in hypoxia (<0.1% O_2), which showed that EdU labelled cells accumulated KAP-1-S824 in hypoxia (Figure 3.7B/C).

It is also worth noting that when hypoxia-induced KAP-1-S824 was studied by immunofluorescence this phosphorylation had a pan-nuclear appearance with no distinct foci being observed. This is in contrast to the more discrete nuclear KAP-1-S824 foci that can be observed in response to IR (Figure 3.8). Interestingly, the pan-nuclear hypoxia-induced KAP-1-S824 pattern was similar to the previously reported ATM and γH2AX staining observed in response to hypoxia (Figure 3.3A) (Bencokova et al., 2009).

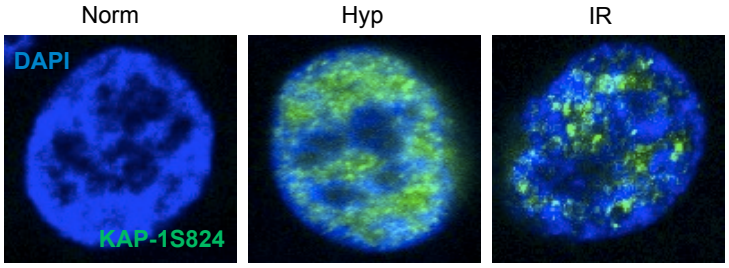


Figure 3.8. Phosphorylated KAP-1-S824 does not form distinct foci in hypoxia RKO cells were fixed and immunostained for KAP-1-S824 (green) and DAPI (blue). Norm (21% O_2), Hyp (6 h, <0.1% O_2), IR (5 Gy, cells fixed 30 minutes post-IR). Representative images are shown.

These observations are supportive of our model, where severe hypoxia does not induce DNA damage and therefore KAP-1 does not need to relocate to discrete nuclear foci. These data suggest that KAP-1 phosphorylation responds to the hypoxia-induced replication stress.

Next, we decided to compare the response to replication stress induced by either Hu or hypoxia (<0.1% O_2) in greater detail. RKO cells were exposed to Hu or hypoxia for either 6 or 24 hours. Irradiation was used as a DNA damaging control and heat (42^{o}C) as a non-DNA damaging control (Figure 3.9A) (Hunt et al., 2007). The short exposure (6 h) to both Hu and hypoxia led to phosphorylation of RPA32 confirming replication stress (Figures 3.9A). However, only the exposure to hypoxia led to a marked induction of KAP-1-S824. After a longer exposure to Hu (24 h), when DNA damage was also evident by comet assay (Figure 3.9B), Hu also induced high levels of KAP-1-S824 (Figure 3.9A). As mentioned, Hu- as well as hypoxia-induced replication stress have been previously characterised in detail and found to be remarkably similar mechanistically and kinetically (Hammond et al., 2003b). It is, therefore, remarkable that two types of replication stress that apparently seem to act by similar mechanisms have such disparate effects on ATM.

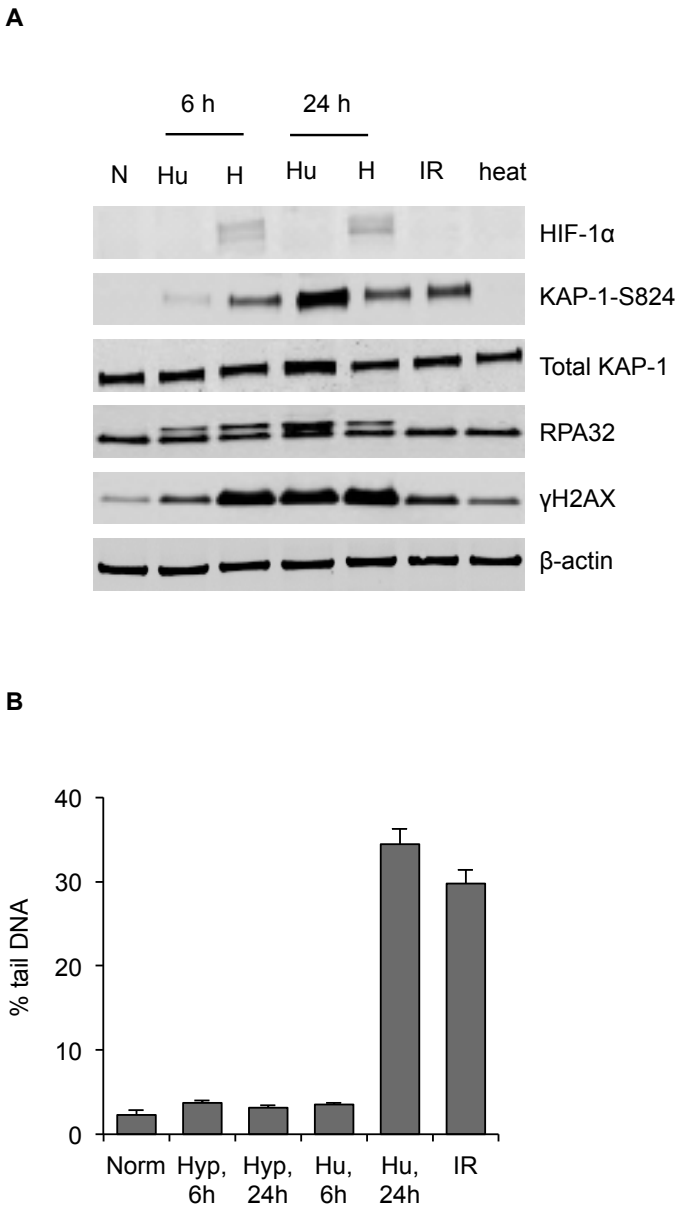
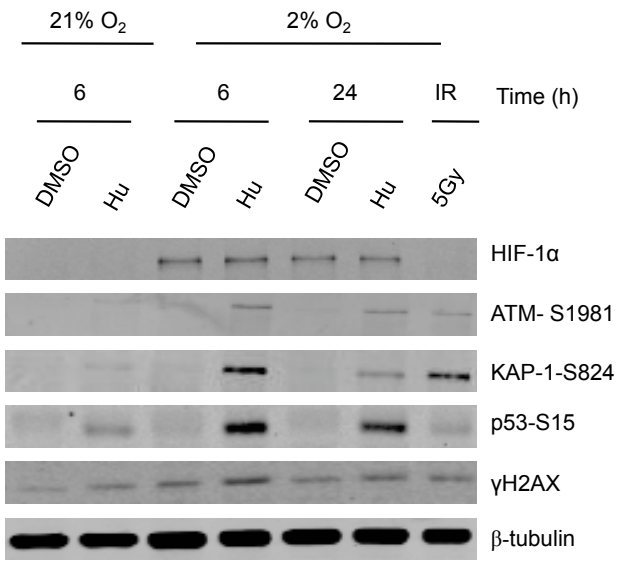


Figure 3.9. Hypoxia-induces replication stress and ATM activity
(A) RKO cells were exposed to N (21% O_2), Hu (6 or 24 h, 1 mM), H (6 or 24 h, <0.1% O_2), IR (5 Gy, cells harvested 30 minutes post IR) or heat (42.5^{o}C-1 h). Western blotting was carried out with the antibodies indicated; β-actin was used as the loading control. **(B)** RKO cells were treated as shown and an alkaline comet assay carried out. Norm (21% O_2), Hyp (6 or 24 h, <0.1% O_2), Hu (6 or 24 h, 1 mM), IR (5 Gy, cells lysed immediately after IR). Shown is the % tail DNA for each condition, n=3. Comet analysis carried out by Selvakumar Anbalagan.

The previous data, led us to hypothesize that in order to activate ATM in response to replication stress an additional signal, present in hypoxia, was required. We speculated that this additional hypoxia-induced signal may also be present in mild hypoxic conditions, not associated with replication stress (for example 2% O_2). To investigate this hypothesis we used Hu to induce replication stress in RKO cells in both normoxic and mildly hypoxic (2% O_2) conditions (Figure 3.10). As previously, neither 2% O_2 nor a short exposure to Hu in normoxia induced ATM-S1981 or KAP-1-S824. In contrast, a notable induction in KAP-1-S824 was seen when the Hu treated cells were incubated at 2% O_2. As expected, exposure to Hu induced replication stress in both normoxia and mild hypoxia (2% O_2) as shown by increased numbers of RPA32 foci (Figures 3.11A/B). Importantly, we verified that the combination of Hu and 2% O_2 had not led to the accumulation of DSBs, by carrying out an alkaline comet assay (Figures 3.11C). A table summarising the observed effects of mild (2% O_2) severe hypoxia (<0.1% O_2), Hu and the combination of Hu and mild hypoxia with respect to replication stress, DNA damage and ATM activation is shown in Figure 3.10B. Next, we asked whether other types of replication stress could also lead to DDR activation in hypoxia. Specifically, we asked if oncogene-induced replication stress could lead to enhanced ATM phosphorylation in hypoxic conditions in the absence of damage. In order to do so we overexpressed mutant K-RAS in $p53^{-/-}$ primary MEFs. The $p53^{-/-}$ background was chosen to avoid the entry of cells into senescence upon overexpression of the oncogene. Cells overexpressing mutant K-RAS or GFP (as a control) were exposed to normoxia or hypoxia (2% O_2) for 6 hours. Consistent with our hypothesis we only observed a significant ATM phosphorylation when mutant K-RAS was overexpressed in primary MEFs in hypoxic (2% O_2)

conditions (Figure 3.12A). Evidence of increased K-RAS expression is shown in Figure 3.12B/C.

A



B

	Replication stress	DNA damage	ATM activity
Hyp 2% O_2	×	×	×
Hyp <0.1% O_2	✓	×	✓
Hu	✓	×	×
Hu + 2% O_2	✓	×	✓

Figure 3.10. Hu leads to ATM activation in hypoxic conditions
(A) RKO cells were treated as indicated; Hu (6 h, 1 mM) was used in either normoxia (21% O_2) or hypoxia (2% O_2). Western blotting was carried out with the antibodies indicated; β-tubulin was used as a loading control. **(B)** Table summarising the effects of different treatments with respect to the induction of replication stress, DNA damage and ATM activity. Hu (6 h in 21% O_2, 1 mM), Hyp 2% O_2 (6 h), Hyp <0.1% O_2 (6 h), Hu + 2% O_2 (6 h in 2% O_2, 1mM).

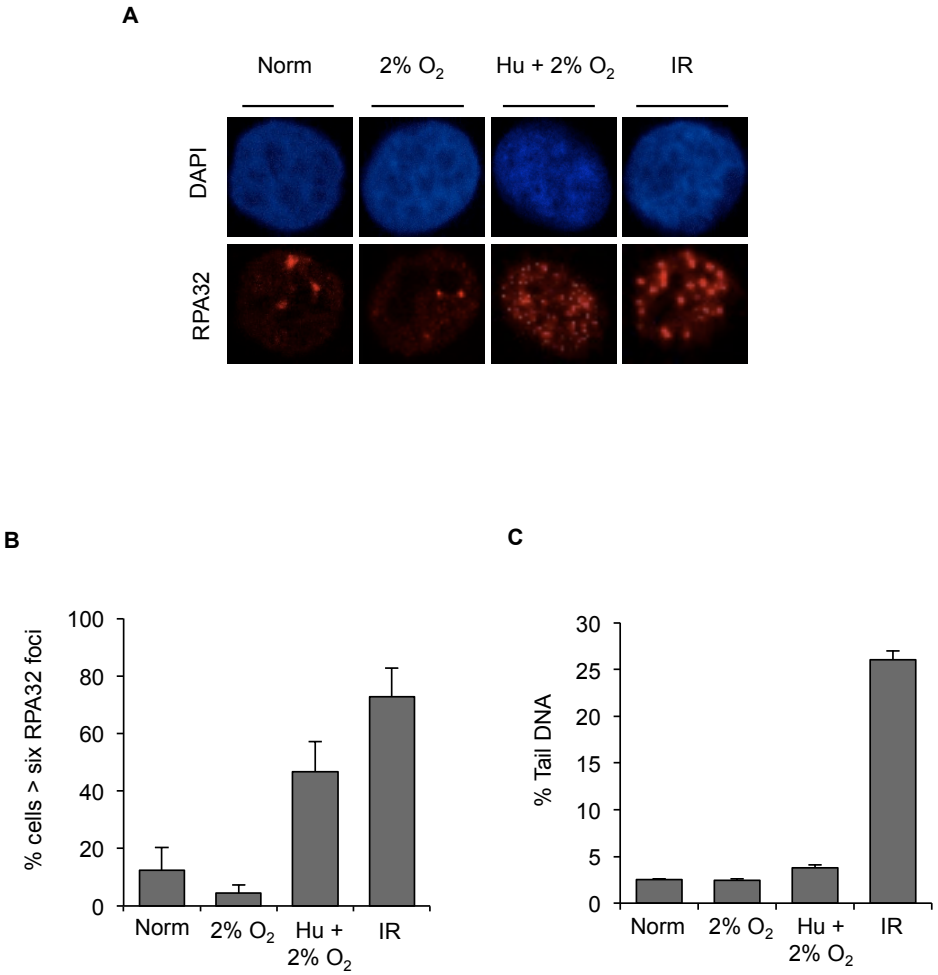


Figure 3.11. Hu treatment in hypoxia leads to replication stress but no DNA damage

(A) RKO cells were treated as indicated. Norm (21% O_2), 2% O_2 (6 h), Hu + 2% O_2 (6 h in 2% O_2, 1mM) and IR (5 Gy, cells harvested 30 minutes post IR). Cells were then stained as indicated. A representative image is shown. **(B)** Quantification of RPA32 foci shown in (A), n=3. (**C**) RKO cells were exposed to the oxygen concentrations indicated for a period of 6 h. Hu (1 mM) was added where indicated for 6 h. Cells exposed to IR (5 Gy) were lysed immediately after IR. Shown is the % tail DNA for each condition, n=2. Alkaline comet assay performed by Selvakumar Anbalagan.

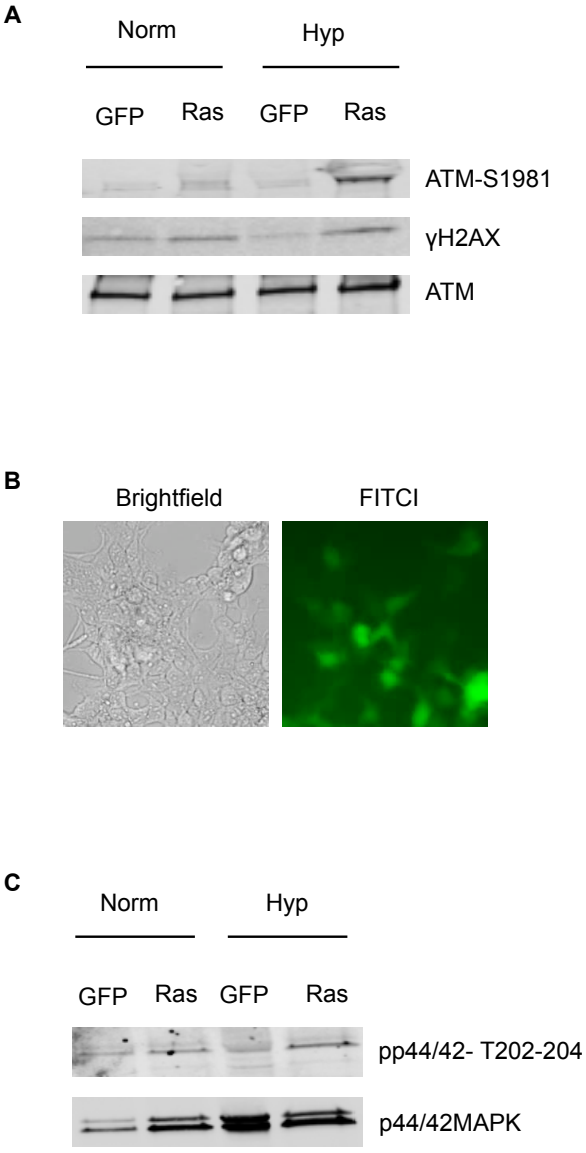


Figure 3.12. Oncogene-induced replication stress leads to ATM activation in hypoxic conditions
(**A**) Mutant K-RAS or GFP were overexpressed in $p53^{-/-}$ MEFs. These cells were then exposed to Norm (21% O_2) or Hyp (6 h, 2% O_2). Western blotting was carried out with the antibodies indicated. **(B)** As a transfection control, expression of GFP was assessed by microscopy. A representative image is shown. **(C)** Mutant K-RAS or GFP was overexpressed in $p53^{-/-}$ MEFs. These cells were then exposed to Norm (21% O_2) or Hyp (6 h, 2% O_2). The levels of p44/p42-T202-Y204 MAPK and total p44/p42 MAPK were assessed by western blotting.

3.3 DISCUSSION

We have demonstrated that hypoxia (<0.1% O_2) leads to ATM phosphorylation and activation in the absence of DNA damage (Figures 3.1-3). Furthermore, we propose that KAP-1 phosphorylation at S824 occurs in an ATM dependent but ATR independent manner in response to hypoxia (Figures 3.4/5). KAP-1 phosphorylation is restricted to the S-phase of the cell-cycle, suggesting that this signalling occurs in response to hypoxia-induced replication stress (Figures 3.6/7). However, we show that not all types of replication stress induce an ATM response, as for example a short Hu treatment cannot activate ATM in the absence of DNA damage (Figure 3.9). These results are in agreement with those of Goodarzi and colleagues, who suggested that DNA damage was required to induce KAP-1 phosphorylation at S824 (Goodarzi et al., 2009). If, however, replication stress is induced concomitantly with hypoxia (2% O_2), we show that ATM activity can then be induced despite the absence of associated DNA breaks (Figures 3.10-12). Collectively, the data shown support a model whereby replication stress induces ATM activity in the absence of damage only in the presence of an additional signal provided by the hypoxic context (Figure 3.13).

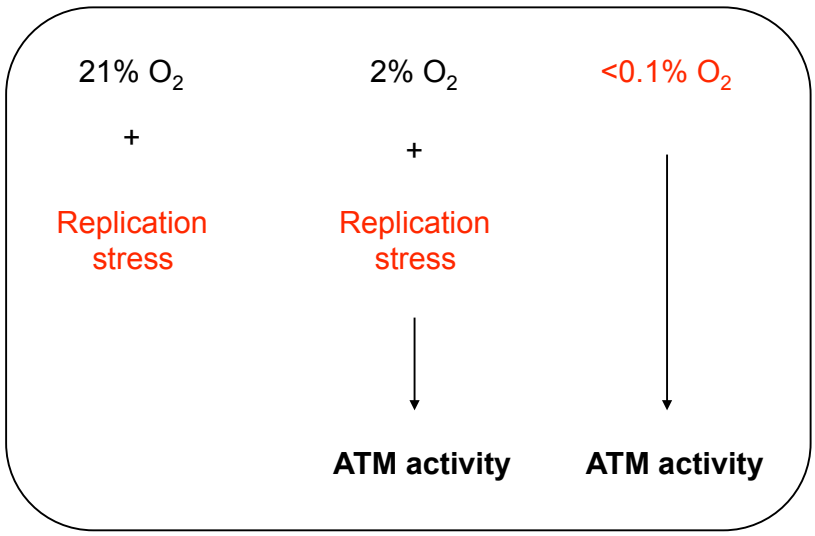


Figure 3.13. Proposed model for ATM activation in response to replication stress
Replication stress in the absence of DNA damage leads to ATM activation and downstream signalling only when occurring within a hypoxic context.

It is worth noting that reduced nucleotide pool supplies were, at least in part, a consequence of all means of replication stress-induction used in this study. Upon Hu- or oncogene-induced replication stress normal DNA replication will be perturbed in response to the limited dNTP supply and this will eventually result in decreased replication fork progression rate and ultimately replication fork collapse (Anglana et al., 2003; Bester et al., 2011). Hypoxia-induced replication stress while leading to similar drops in nucleotide supply and replication fork rate, does not lead to fork breakage (Pires et al., 2010b). This points to a critical difference between hypoxia and other types of replication stress and might help to explain the reasons for ATM activation in this context. In addition, the induction of such signalling when oncogene overexpression or Hu treatment are carried out under mild hypoxic conditions

suggests that low oxygen levels in general (and not just severe hypoxia) are able to cause a significant change in the signal required to deal with perturbed DNA replication. These findings may have important consequences since they imply that ATM signalling can be activated in response to replication stress as long as this occurs under permissive oxygen conditions.

Importantly, the activation of a DDR has previously been reported to occur *in vivo* and been proposed to act as a barrier to tumourigenesis (Bartkova et al., 2005; Gorgoulis et al., 2005). The hypoxia-induced DDR is likely to play a similar role despite being activated in the absence of detectable damage. This might occur in the early stages of tumourigenesis where rapidly proliferating cells might be subjected to oncogenic stress in a context of insufficient oxygen supply. DNA strand breaks might not be present in this context of early oncogenic stress. ATM, however, could be activated in these situations due to the coordinated action of the oncogene-induced replication stress and a permissive hypoxic context. It would also be interesting to know whether any kind of replication block leading to replication stress could be sufficient to induce ATM activation under hypoxic conditions, or whether replication stress specifically occurring due to nucleotide pool depletion is a requirement for such signalling to occur in response to hypoxia and in the absence of DNA damage.

CHAPTER 4

MECHANISM OF ATM ACTIVATION IN HYPOXIA

4.1 INTRODUCTION

As described in Chapter 1, ATM activation in response to DNA damage has been widely studied (Bakkenist and Kastan, 2003). Optimal ATM activation may depend on a variety of factors including phosphatases. These are important for the regulation of ATM activity during and after DNA damage. Several phosphatases, including members of the phosphoprotein phosphatase (PPP) family of serine/threonine protein phosphatases, PP5 and PP2A, as well as wild-type p53-induced phosphatase 1 (WIP1), have been shown to regulate ATM signalling in response to DSBs (Ali et al., 2004; Goodarzi et al., 2004; Shreeram et al., 2006). PP2A works as a holoenzyme complex, where the core enzyme is composed of the catalytic subunit (PP2A-C) and the scaffolding component (PP2A-A). Different B regulatory subunits may bind to the core enzyme to give heterotrimeric PP2A complexes with different specificities (Eichhorn et al., 2009). Mechanistically, ATM interacts with the scaffolding (PP2A-A) and catalytic (PP2A-C) subunits of PP2A in cells and this interaction is disrupted following IR, thereby regulating the autophosphorylation of ATM in response to IR (Goodarzi et al., 2004).

Furthermore, it is becoming increasingly evident that histone post-translational modifications as well as chromatin remodelling play important roles in facilitating

DDR signalling and repair, including ATM activation. Again, this has been particularly well studied in response to DSBs (reviewed in (Papamichos-Chronakis and Peterson, 2013; Sulli et al., 2012)). As described previously, in heterochromatic regions, binding of the acetyltransferase TIP60 to H3K9me3 is required for ATM acetylation by the acetyltransferase. This acetylation then facilitates ATM phosphorylation and activation (Sun et al., 2005). It is only more recently, however, that the significance of chromatin modifications occurring at the replication fork or in response to replication stress has begun to be elucidated (Jasencakova et al., 2010; Sirbu et al., 2011).

Hypoxia has not only been shown to induce a DDR, but is also known to induce a number of chromatin changes (described in detail in Chapter 1) (Johnson and Barton, 2007). These have been described at a number of different oxygen concentrations, but mainly under conditions associated with unperturbed replication (Melvin and Rocha, 2012). Whether these chromatin changes can occur at any level of hypoxia and whether some are particularly associated with the hypoxia-induced DDR has not been studied in detail to date.

Histone modifications alter the global chromatin landscape in such a manner that they can affect gene expression as well as other DNA-based processes, including replication progression (Alabert and Groth, 2012; Barski et al., 2007). Following from the results described in Chapter 3, we hypothesized that certain hypoxia-induced chromatin modifications could serve to facilitate DDR signalling, and in particular ATM activation in response to replication stress in hypoxia. In order to test this hypothesis we firstly decided to characterise hypoxia-induced chromatin changes in detail before focusing specifically on H3K9me3 and its role in facilitating ATM activation in response to hypoxia.

4.2 RESULTS

4.2.1 Characterisation of hypoxia-induced chromatin changes

We investigated the induction of a number of histone marks in a range of oxygen concentrations in RKO cells (Figures 4.1A-D). As expected, hypoxic conditions that induce replication stress (<0.1% O_2) led to the induction of γH2AX, while milder hypoxic conditions (2% O_2), where DNA replication is unaffected (Figure 3.2), did not. In agreement with published reports, we saw a mild increase in H3K9me2 (Chen et al., 2006) and H3K9me3 (Johnson and Barton, 2007) under mild hypoxic conditions (2% O_2). In contrast, we did not observe any significant changes in H3K27me3, H3K36me3 or H3K79me3 in response to hypoxia. Interestingly, the increase in H3K9me3 was especially notable in response to severe hypoxia (<0.1% O_2). Furthermore, both in response to 2% as well as <0.1% O_2, H3K9me3 levels seemed to return to near normoxic levels of expression after reoxygenation, reflecting a certain oxygen dependence in the regulation of this histone mark (Figure 4.1C and D). H3K9me3 is thought of as enriched in "chromocenters" corresponding to centrometic and pericentric heterochromatin (densely stained with DAPI in NIH 3T3 cells) (Guenatri et al., 2004). In order to assess if the increases in H3K9me3 were associated exclusively with chromocenters in response to hypoxia (<0.1% O_2) we decided to investigate the expression and localisation of H3K9me3 in NIH3T3 cells. Interestingly, H3K9me3 enrichment seemed to be ubiquitous throughout the cell nuclei in NIH 3T3 cells and its hypoxic induction seemed associated with both regions of heterochromatin and euchromatin (Figure 4.1E).

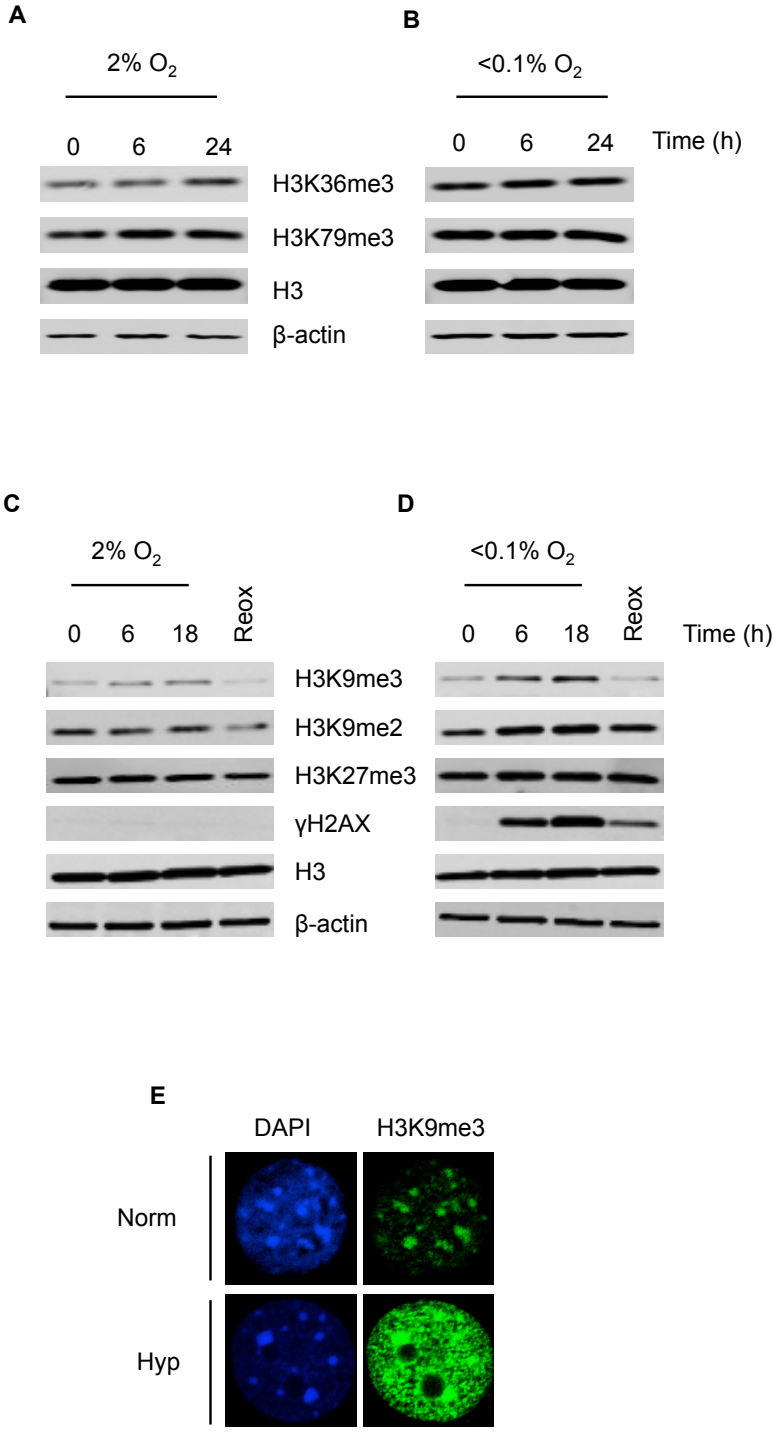


Figure 4.1. Hypoxia-induces a number of chromatin changes
(A) RKO cells were treated with either 2% or **(B)** <0.1% O_2 for the times indicated. (**C**) Treatment of RKO cells with either 2% or **(D)** <0.1% O_2 was carried out for the times indicated. Reox=6 h, <0.1% O_2 followed by 2 h of 21% O_2. The chromatin modifications investigated are shown between the western blots. **(E)** NIH 3T3 cells were fixed and immunostained for H3K9me3 following exposure to Norm (21% O_2) or Hyp (20 h, <0.1% O_2). DAPI was used to stain nuclear DNA.

Furthermore, FACS analysis of the distribution of H3K9me3 suggested that there was no cell-cycle dependence on the presence of this mark in hypoxia since H3K9me3 was induced in hypoxia throughout the cell cycle (Figure 4.2).

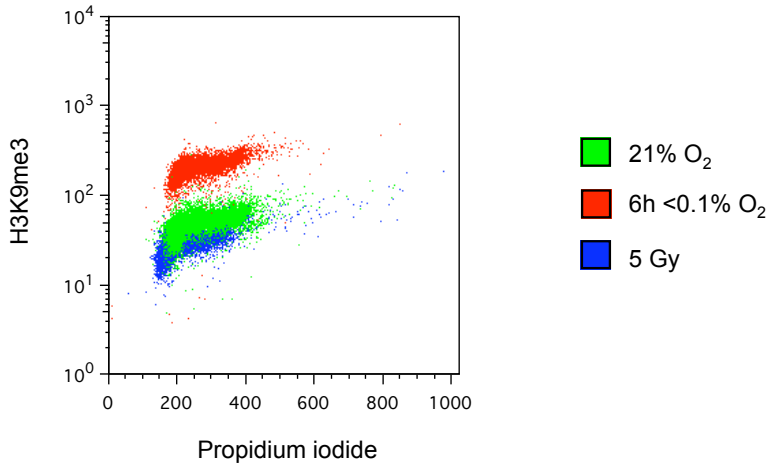


Figure 4.2. Hypoxia-induced H3K9me3 is cell-cycle independent
RKO cells were exposed to normoxia (21% O_2), hypoxia (6 h, <0.1% O_2) or irradiated with 5 Gy and fixed immediately post-IR. Cells were then stained for H3K9me3 and PI and analysed using FACS. Data generated with assistance from Dr Joana Senra.

H3K9me3 can act as a binding site for chromodomain-containing proteins such as HP1β allowing the regulation of gene repression and heterochromatin formation (Bannister et al., 2001; Lachner et al., 2001; Nielsen et al., 2002). HP1β-H3K9me3 binding allows methylation of H3K9 on neighbouring nucleosomes through the recruitment of Suv39h1 and other methyltransferases (Aagaard et al., 1999; Loyola et al., 2009). We assessed the expression of HP1β in hypoxia and observed a transient increase in chromatin bound HP1β following exposure to hypoxia. Interestingly HP1β levels also returned to baseline normoxic levels following reoxygenation, reflecting the dynamic oxygen dependent changes also observed for H3K9me3 (Figure 4.3A and

B). Increases in H3K9me3 usually lead to a decrease in histone 3 serine 10 phosphorylation (pH3S10) since these two modifications on histone 3 are thought to be mutually exclusive (Duan et al., 2008). The levels of pH3S10 in response to severe hypoxia (<0.1% O_2) were found to be markedly decreased coinciding with the increase in H3K9me3. Interestingly, pH3S10 levels remained unchanged in 2% O_2 despite the moderate increase in H3K9me3 observed under these conditions (Figure 4.3A).

We next chose to investigate the possible oxygen dependent regulation of some of the main H3K9me3 methyltransferases. Two of the methyltransferases responsible for H3K9 trimethylation, SETDB1 and Suv39h2, were found to be mildly induced at the protein level in response to hypoxia (<0.1% O_2) (Figure 4.4A, fold induction with respect to normoxic expression shown in the legend). Furthermore, the protein level of SETDB1 was decreased in response to reoxygenation, possibly reflecting the drop in H3K9me3 observed under these conditions. Levels of Suv39h2 were particularly increased in response to both reoxygenation and IR, suggesting that protein levels of this methyltransferase are also DNA damage responsive. Analysis of the mRNA expression of these three methyltransferases in response to both 2% and <0.1% O_2 suggested that these enzymes are not regulated at the transcriptional level in hypoxia. A trend towards a decrease in expression of the methyltransferases in response to <0.1% O_2 was observed, probably reflecting a general decrease in transcription under these conditions rather than a significant and specific regulation of the three methyltransferases under study.

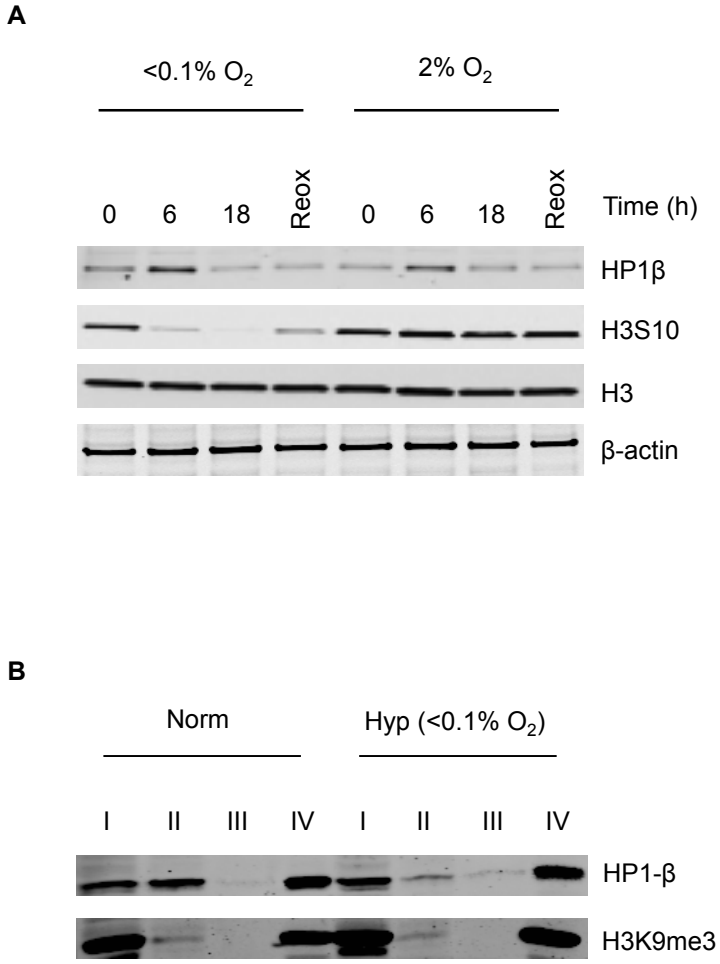


Figure 4.3. Hypoxia leads to the induction of HP1β levels
(**A**) RKO cells were treated as in 4.1(C) and (D). Western blotting was carried out with the antibodies indicated. **(B)** Chromatin fractionation experiments were carried out with RKO cells exposed to Norm (21% O_2) or Hyp (6 h, <0.1% O_2). Fraction I corresponds to the whole cell extract and IV corresponds to the most stringent nuclear fraction, n=1. Shown is a western blot of the chromatin fractions with H3K9me3 used as a nuclear fraction control.

The lack of significant changes at the mRNA level suggested that the mechanism of regulation of these three enzymes was probably not mediated directly by HIF-1α (Figure 4.4B/C). Consistent with this, the hypoxic regulation of these three methyltransferases, as well as of H3K9me3, appeared to be mainly HIF-1α independent since no significant decreases in the expression of H3K9me3, SETDB1 or Suv39h2 were observed at the protein level between the HIF-1$\alpha^{+/+}$ and HIF-1$\alpha^{-/-}$ matched RKO cells both in response to 2% and <0.1% O_2 (Figure 4.5A). A slight decrease in Suv39h1 protein levels was observed in HIF-1$\alpha^{-/-}$ cells in response to <0.1% O_2. However this did not correlate with decreased *Suv39h1* mRNA expression in this cell line. Similarly, no substantial differences in mRNA levels were observed for *Suv39h2* or *SETDB1* between the HIF-1$\alpha^{+/+}$ and HIF-1$\alpha^{-/-}$ matched RKO cells in response to <0.1% O_2, (Figure 4.5B). Furthermore, no significant reductions in the mRNA level of the methyltransferases were observed following siRNA mediated depletion of the HIF-1β subunit in normoxia or hypoxia (Figure 4.5C). Although somewhat preliminary, together these data suggest that the strong induction of H3K9me3 observed in response to hypoxia is not dependent on direct HIF-1 dependent transcriptional regulation of *Suv39h1*, *Suv39h2* or *SETDB1*.

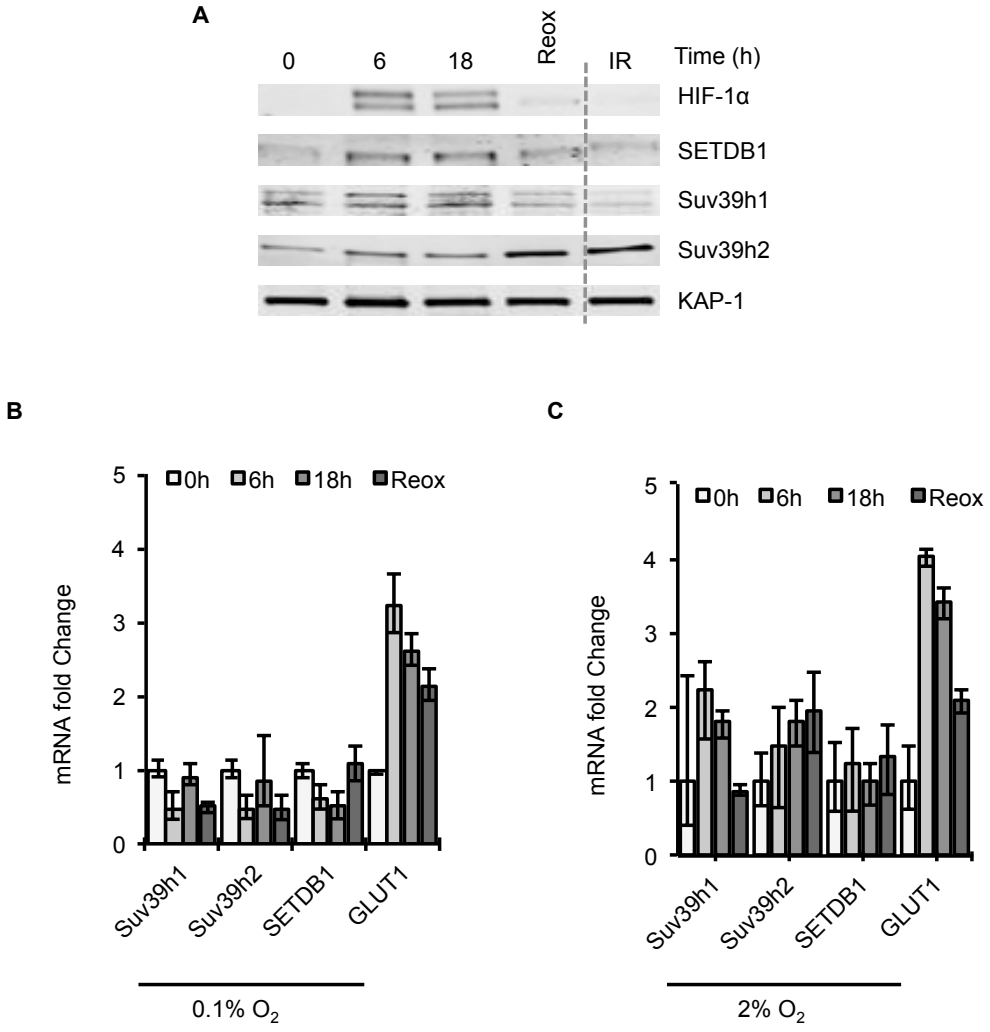


Figure 4.4 Histone methyltransferases are induced at the protein but not mRNA level by hypoxia

(A) RKO cells were exposed to 0, 6, 18 hours of <0.1% O_2, Reox (6 h, <0.1% O_2 followed by 1 h of 21% O_2); or IR (5 Gy, cells harvested 30 minutes post-IR). Western blotting was carried out with the indicated antibodies. KAP-1 was used as the loading control. Dotted grey line indicates that the lane between Reox and IR was cropped. Quantification of bands relative to 0 h: SETDB1 fold induction: 6 h=6.46, 18 h=4.57, Reox=0.87; Suv39h2 fold induction: 6 h=1.39, 18 h=1.75, Reox=1.96, IR=1.81; Suv39h1 fold induction: 6 h=0.78, 18h=1.16, Reox=0.81, IR=0.36. **(B)** The mRNA levels of *Suv39h1*, *Suv39h2*, *SETDB1* and as control *GLUT1* were measured by qPCR in RKO cells exposed to either <0.1% O_2 or **(C)** 2% O_2. The Reox sample was exposed to the relevant oxygen concentration for 6 hours and then 21% O_2 for a further 2 hours. All mRNA levels were normalised to *18S* and expressed as fold change. Error bars indicate error between technical replicates for one experiment.

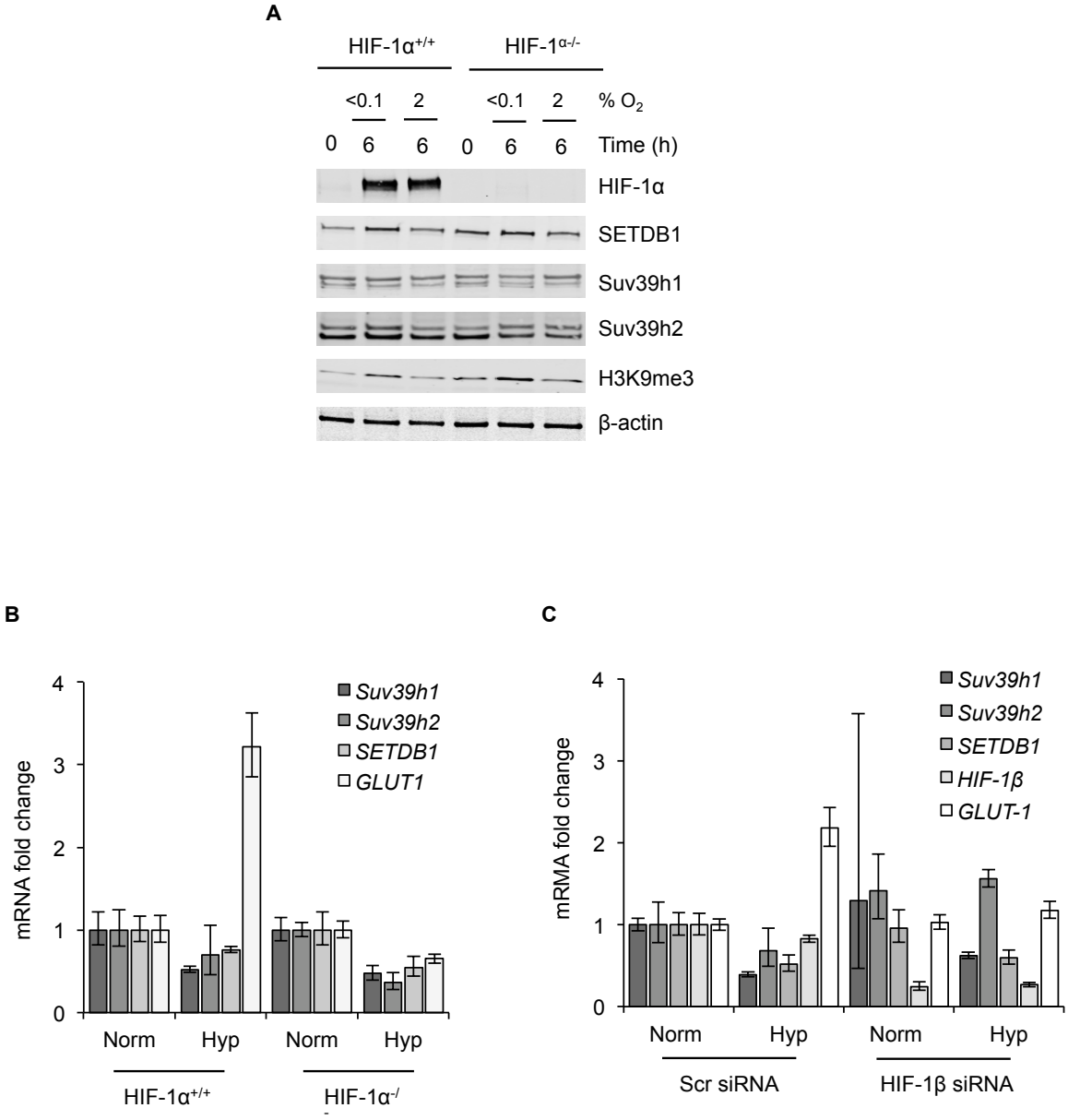


Figure 4.5. Hypoxic regulation of histone methyltransferases is HIF-1 independent

(A) RKO HIF-1α$^{+/+}$ or HIF-1α$^{-/-}$ cells were treated with <0.1% or 2% O_2 for the times indicated. Shown is a western blot for the proteins indicated. **(B)** The mRNA levels of *Suv39h1*, *Suv39h2, SETDB1* and as control *GLUT1* were measured by qPCR in RKO HIF-1α$^{+/+}$ or HIF-1α$^{-/-}$ cells exposed to <0.1% O_2 for the indicated times, n=3. **(C)** The mRNA levels of *Suv39h1*, *Suv39h2*, *SETDB1* and as control *HIF-1β* and *GLUT1* were measured by qPCR in RKO HIF-1α$^{+/+}$ or HIF-1α$^{-/-}$ cells exposed to <0.1% O_2 for the indicated times, n=2. All mRNA levels were normalised to *18S* and expressed as fold change. Error bars indicate error between technical replicates. (B) and (C) were carried out with the assistance of Dr Katarzyna Leszczynska.

4.2.2 H3K9me3 is required for ATM activation in hypoxia

Having furthered our understanding of the regulation of H3K9me3 in hypoxia, and given that this histone mark has previously been associated with ATM activation, we decided to investigate if high H3K9me3 levels were actually required for ATM-signalling in hypoxia (Kaidi and Jackson, 2013; Sun et al., 2009). KAP-1 is a transcriptional co-repressor involved in trimethylation of H3K9 through recruitment of factors such as SETDB1 and Suv39h1/2 (Groner et al., 2010; Schultz et al., 2002). RKO cells were treated with siRNA to KAP-1 and the levels of H3K9me3 and phosphorylated ATM were assessed. Upon treatment with KAP-1 siRNA a modest reduction in H3K9me3 was observed in both normoxia and hypoxia. Interestingly this correlated with a moderate reduction in phosphorylated ATM in response to hypoxia (Figure 4.6A). The quantification of the changes observed in the protein levels of H3K9me3 and ATM-S1981 are shown in Figure 4.6B. Next, we used Suv39h1/2$^{+/+}$ and Suv39h1/2$^{-/-}$ MEFs to investigate the direct role of these two principal methyltransferases in hypoxia-induced ATM (Peters et al., 2001). As a positive control for the experiment we tested whether ATM phosphorylation was impaired in the Suv39h1/2$^{-/-}$ MEFs exposed to IR. Indeed, in accordance with published findings we observed reduced ATM phosphorylation in response to IR in the knockout cell line (Figure 4.7A) (Sun et al., 2009). As expected, the Suv39h1/2$^{-/-}$ MEFs showed a decreased level of H3K9me3 in normoxia, hypoxia and IR. Most importantly, the phosphorylation of ATM was also significantly reduced in this cell line following exposure to severe hypoxia (<0.1% O_2) (Figure 4.7B). Validation of ATM phosphorylation in MEFs using an antibody against ATM-S1987 (equivalent to 1981 in humans) is shown in Appendix B, Figure B.1. In addition, we carried out lentiviral knockdown of Suv39h1 and Suv39h2 in RKO cells. During validation of this cell line

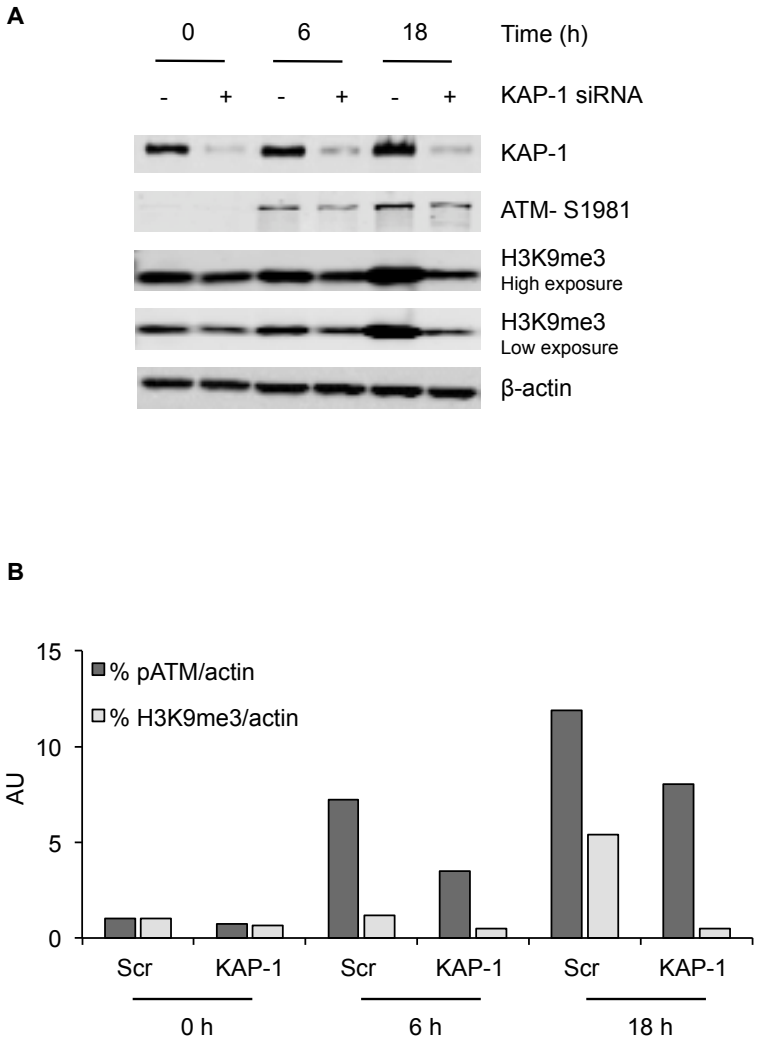


Figure 4.6. KAP-1 siRNA mediated knockdown leads to a moderate reduction in H3K9me3 and ATM phosphorylation in hypoxia
(A) RKO cells were treated with KAP-1 or scramble siRNA and exposed to 0, 6, 18 h of <0.1% O_2. Western blotting was carried out for the proteins and protein modifications indicated. β-actin was used as a loading control. The low and high exposure of H3K9me3 bands is also shown. (**B**) Quantification of the pATM/actin and H3K9me3/actin ratio for the represented experiment is shown, pATM=ATM-S1981.

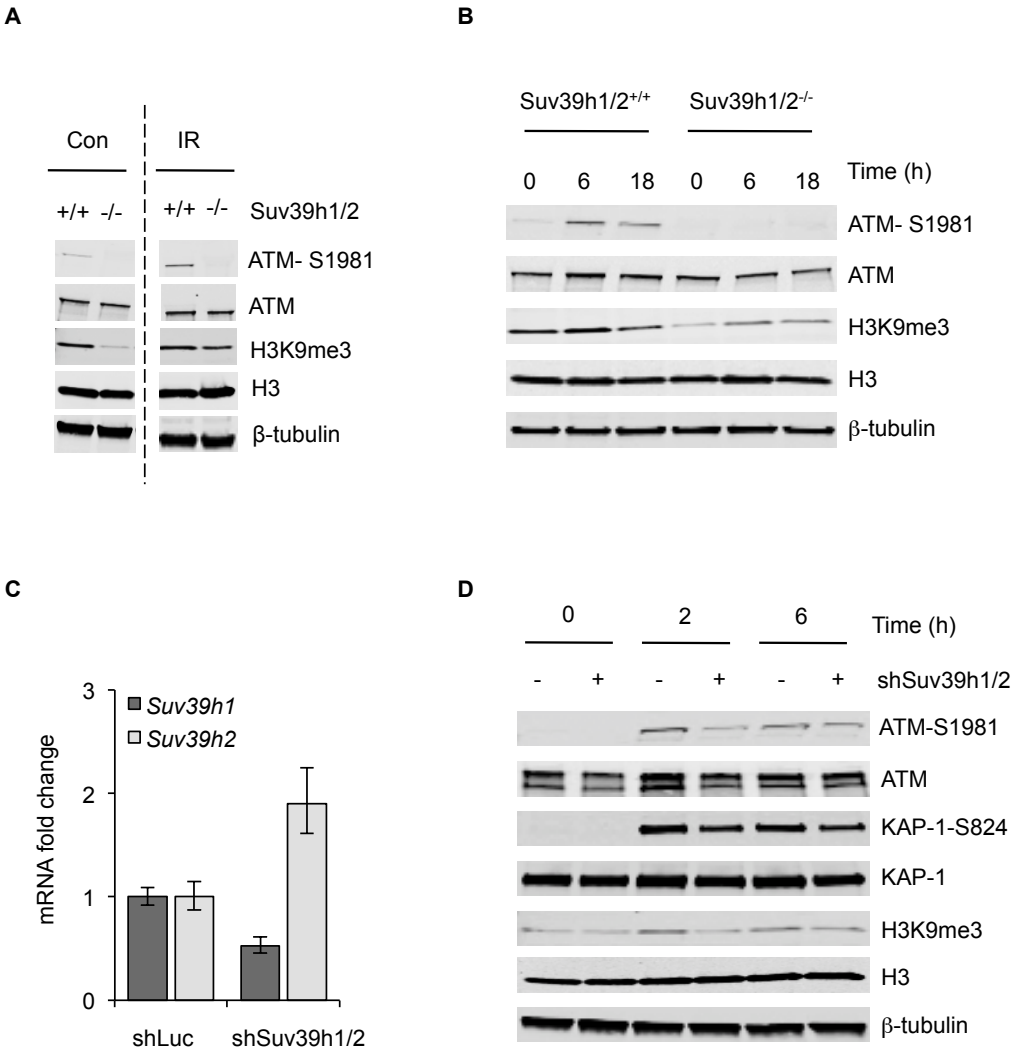


Figure 4.7. Loss of Suv39h1/2 abrogates hypoxia-induced ATM-S1981
(A) Suv39h1/2$^{+/+}$ and Suv39h1/2$^{-/-}$ MEFs were treated as indicated. Western blotting was carried out using the antibodies indicated. IR=5 Gy, cells harvested immediately post IR. β-tubulin was used as a loading control. **(B)** Suv39h1/2$^{+/+}$ and Suv39h1/2$^{-/-}$ MEFs were exposed to 0, 6, 18 h of <0.1% O_2. Western blotting was carried out using the antibodies indicated. β-tubulin was used as a loading control. **(C)** RKO cells were treated with sh against Luc or Suv39h1/2. mRNA levels of Suv39h1 and Suv39h2 were determined by qPCR, n=3. mRNA levels were normalised to *18S* and expressed as fold change. Error bars indicate error between technical replicates. **(D)** RKO cells were treated with or without shSuv39h1/2 and exposed to 0, 2 or 6 hours of <0.1% O_2. Western blotting was carried out for the proteins indicated. β-tubulin was used as a loading control.

we noticed that whereas Suv39h1 mRNA levels were repressed, mRNA expression of Suv39h2 was upregulated, implying that either the shSuv39h2 construct had not been fully integrated by these cells and/or that upon cell culture in a situation where Suv39h1 levels are reduced, a mechanism is triggered that upregulates Suv39h2 (Figure 4.7C). Despite this, levels of H3K9me3 were reduced in this shSuv39h1/2 cell line (Figure 4.7D). We decided to proceed with our studies and refer to this stable line as shSuv39h1/2 given that originally infection had been carried out with both shSuv39h1 and shSuv39h2. Most importantly, we found that ATM phosphorylation was attenuated upon reduction in H3K9me3 levels following Suv39h1/2 knockdown (Figure 4.7D).

H3K9me3 is a histone modification typically associated with gene repression. Therefore, we hypothesized that the mechanism by which H3K9me3 could be mediating ATM phosphorylation in hypoxic conditions was through the repression of a factor that normally serves to de-phosphorylate ATM, such as an ATM-specific phosphatase. We reasoned that H3K9me3-mediated repression of two well-characterised ATM-specific phosphatases, WIP1 or PP2A, could facilitate ATM activation (Freeman and Monteiro, 2010). Of note, the catalytic subunit of PP2A is encoded by 2 genes, *PPP2CA* and *PPP2CB* (sharing 97% sequence identity). The *PPP2CB* promoter is weaker resulting in a 10-fold lower expression of this gene. We, therefore decided to test the repression of PP2A-C by studying *PPP2CA* (which will be referred to as *PP2A-C* in subsequent sections) (Eichhorn et al., 2009). The expression levels of *PP2A-C,* as well as of *WIP1,* were assessed in the Suv39h1/2$^{+/+}$ and Suv39h1/2$^{-/-}$ MEFs by qPCR. What was most apparent was that the Suv39h1/2$^{-/-}$ cells had much higher levels of expression of both *WIP1* and *PP2A-C* mRNA compared to the Suv39h1/2$^{+/+}$ cells (Figure 4.8; note the difference in the scales of the

y-axis). Given that *PP2A-C* showed the greatest Suv39h1/2 dependent expression we focused on this phosphatase for further studies.

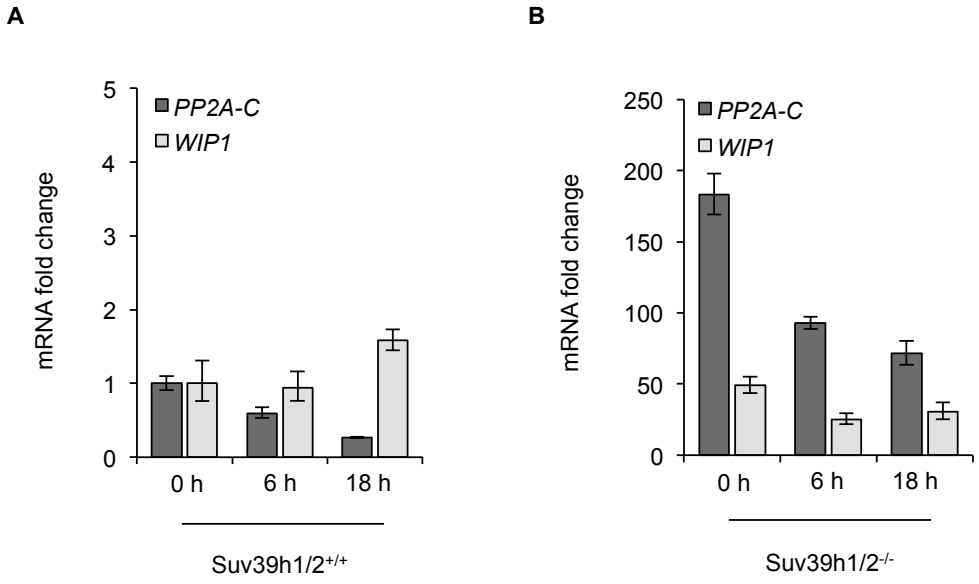


Figure 4.8. Suv39h1/2 regulate the mRNA level of certain ATM phosphatases
(A) The mRNA levels of *WIP1* and *PP2A-C* were assessed by qPCR in Suv39h1/2$^{+/+}$ and (**B**) Suv39h1/2$^{-/-}$ MEFs following exposure to hypoxia (<0.1% O_2) for the time periods indicated. All mRNA levels were normalised to *18S*. The fold change shown is relative to the level of expression in Suv39h1/2$^{+/+}$ cells. Error bars indicate error between technical replicates for the represented experiment.

We hypothesized that Suv39h1/2 could be mediating *PP2A-C* repression by accumulating H3K9me3 along this gene in response to hypoxia. Therefore, we decided to investigate the enrichment of H3K9me3 at the *PP2A-C* locus by ChIP-qPCR. We identified a candidate region based on a moderate H3K9me3 enrichment in previous ChIP-seq studies (using the UCSC genome browser) (O'Geen et al., 2011). We then performed ChIP with antibodies against H3K9me3 and H3 followed by qPCR using primers to that region. A moderate but significant increase in H3K9me3

fold enrichment relative to total H3 was observed in response to hypoxia (Figure 4.9A). A control non-enriched site was also assessed and as expected was found to have minimal fold enrichment in H3K9me3/H3 (Figure 4.9B). Importantly, the specific enrichment of H3K9me3 on the locus in *PP2A-C* correlated with a decrease in the mRNA levels of *PP2A-C* in hypoxia (<0.1% O_2) (Figure 4.10).

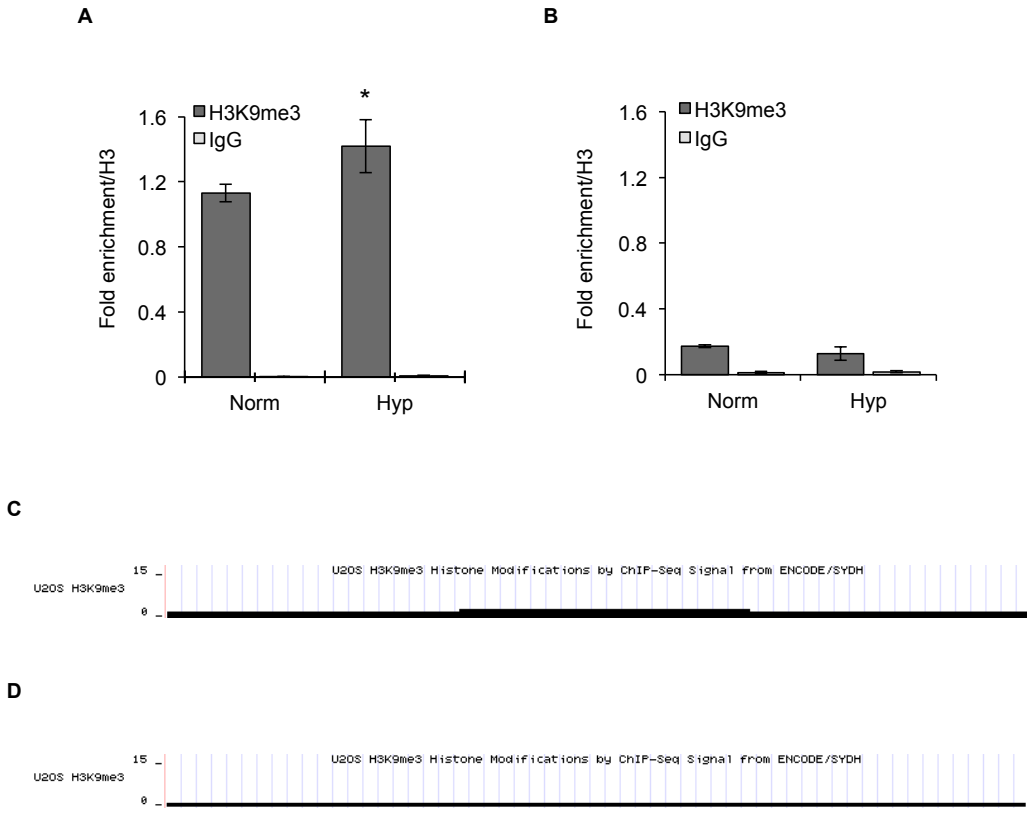


Figure 4.9. Hypoxia-induced enrichment of H3K9me3 on *PP2A-C*
(A) RKO cells were exposed to either Norm (21% O_2) or Hyp (6 h, < 0.1% O_2). The fold enrichment of H3K9me3 at the loci on *PP2A-C* was assessed by ChIP-qPCR. * denotes p value between Norm and Hyp=<0.05, n=3. **(B)** RKO cells were exposed to either Norm (21% O_2) or Hyp (6 h, <0.1% O_2). The enrichment of H3K9me3 on *PP2A-C* was assessed by ChIP-qPCR. Primers were designed to target a region where minimal H3K9me3 enrichment was predicted from the UCSC genome browser H3K9me3 profile (Assembly used: GRCh37/hg19). Error bars represent the standard error between technical replicates for the represented experiment. **(C)** ChIP-seq track for the region of predicted moderate H3K9me3 enrichment and control region **(D)** as displayed in the UCSC genome browser is shown.

Moreover, we assessed the activity of the catalytic subunit of PP2A by specific pull-down of PP2A-C followed by *in vitro* measurement of phosphatase activity; and found a significant reduction of such activity in severe hypoxic conditions. The phosphatase inhibitor Okadaic acid was used as a positive control in the experiment (Figure 4.11). Incubation of the samples with a GAPDH antibody was used as a negative control for the specificity of the pull-down. Collectively, these data suggest that a mechanism by which H3K9me3 facilitates ATM activation in response to severe hypoxia (<0.1% O_2) is through repression of ATM-specific phosphatases, for example PP2A.

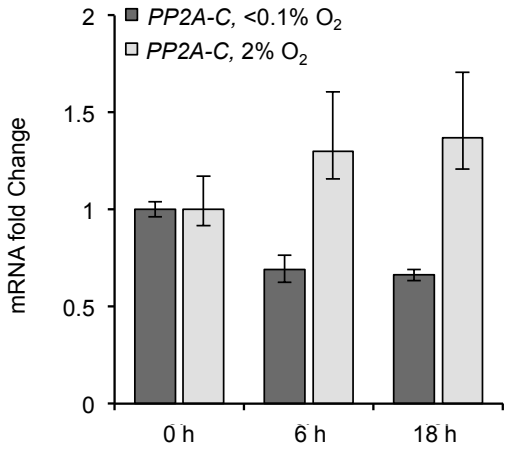


Figure 4.10. mRNA level of *PP2A-C* is downregulated in response to <0.1% O_2 but not 2% O_2
mRNA levels of *PP2A-C* were assessed by qPCR following exposure of RKO cells to either 0, 6, 18 h of hypoxia (<0.1 or 2% O_2), n=2. All mRNA levels were normalised to *18S* and expressed as fold change. Error bars represent the error between technical replicates.

Finally, we decided to verify whether H3K9me3 levels actually change in the hypoxic areas of tumours and correlate with ATM activation *in vivo*. In order to do so, subcutaneous Calu-6 xenograft tumours were grown and sections were stained for both H3K9me3, the hypoxia marker CAIX and ATM-S1981. Importantly, in CAIX positive regions of the tumour there was a clear association with both high expression of H3K9me3 and ATM-S1981 (Figure 4.12). These studies were performed in collaboration with Dr Anderson Ryan resulting in the need to use Calu-6 non-small cell lung cancer cells instead of the colorectal cancer cell line that had been used for most of the previous studies. We therefore decided to also validate the hypoxia-induced DDR response and its correlation with increased H3K9me3 levels in Calu-6 cells *in vitro* (Figure 4.12B).

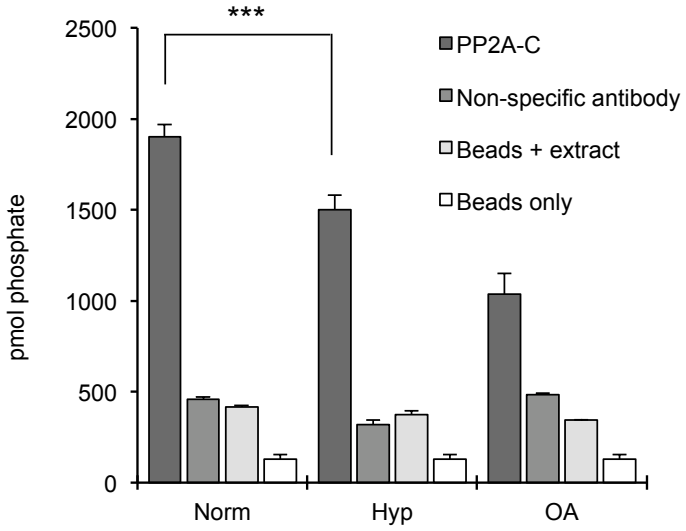
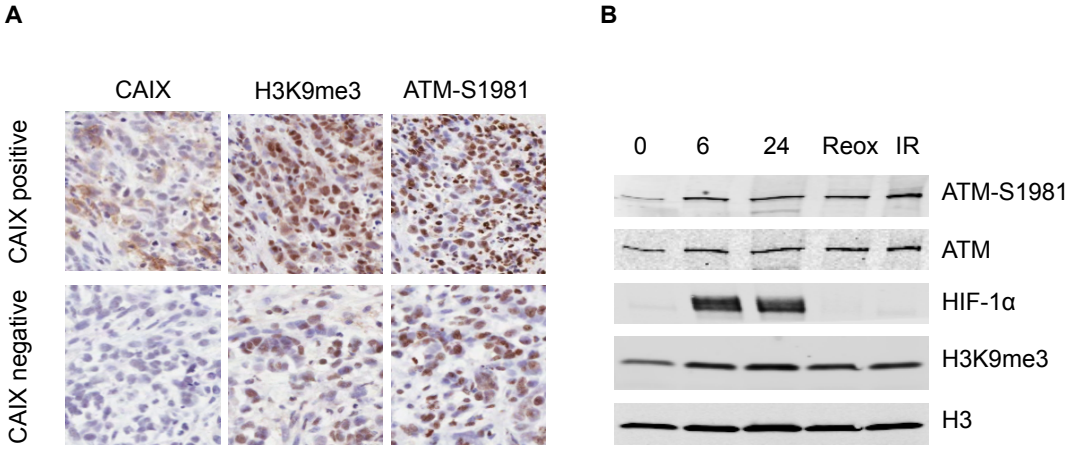


Figure 4.11. Phosphatase activity of PP2A-C is reduced in hypoxia
Phosphatase activity of PP2A-C was determined following treatment of RKO cells with either Norm (21% O_2), Hyp (6 h, <0.1% O_2) or Okadaic acid (OA) (2 h, 0.5 μM). The levels of PP2A-C specific phosphatase activity are shown in dark grey. GAPDH (non-specific antibody), beads plus extract and beads only were used as controls. Error bars indicate the standard error between technical replicates for the represented experiment. *** indicates $p<0.001$, n=3.



C

	CAIX positive					CAIX negative				
	1	2	3	4	5	6	7	8	9	10
H3K9me3	High	High	High	High	High	Low	Low	Low	Low	High
ATM-S1981	High	High	High	High	High	Low	Low	Low	High	Low

Figure 4.12 Hypoxia-induced H3K9me3 correlates with ATM activity *in vitro* and *in vivo*

(A) Serial sections from Calu-6 xenografts were stained with H3K9me3, CAIX or ATM-S1981 antibodies. Shown are representative images of regions positive or negative for CAIX staining and the corresponding H3K9me3 and ATM-S1981 staining in brown. Xenografts were grown by Dr Yanyan Jiang. **(B)** Calu-6 cells were exposed to 0, 6, 24 hours of <0.1% O_2, Reox (6 h, <0.1% O_2 followed by 1 h of 21% O_2); IR (5 Gy, cells fixed 30 minutes post IR). Western blotting was carried out with the indicated antibodies. **(C)** Five CAIX positive and negative regions were scored for both H3K9me3 and ATM-S1981. An intensity score of 2 or above represents high H3K9me3 or ATM-S1981 staining. Intensity scores of 1 or above represent CAIX positive regions. All of the CAIX positive sections were found to also have high levels of H3K9me3 and ATM-S1981. In the CAIX negative regions 4 out of 5 sections had low levels of H3K9me3 or ATM-S1981.

4.3 DISCUSSION

We have observed a number of chromatin changes occurring in response to hypoxia. Most notably, we have seen a global increase in H3K9me3 occurring in response to both 2% as well as <0.1% O_2 (Figure 4.1). This increase was more prominent in response to the lower oxygen conditions, occurred cell-cycle independently and coincided with increased protein levels of some of the principal H3K9 methyltransferases, as well as of HP1β (Figure 4.1-4). Notably, the observed increase in H3K9me3 correlated well with ATM phosphorylation both *in vitro* and *in vivo* (Figure 4.12). Reducing hypoxia-induced H3K9me3 accumulation, either through loss of KAP-1 or Suv39h1/2, subsequently decreased ATM phosphorylation under hypoxic conditions (Figure 4.6/7).

Interestingly, the induction of H3K9me3 in response to <0.1% O_2 occurred despite the lack of transcriptional upregulation of the three methyltransferases studied (Figure 4.4). Future studies could be undertaken to fully validate the lack of HIF-1 dependent regulation of the methyltransferases suggested here. It is tempting to speculate that the hypoxic induction in H3K9me3 occurs at least in part as a result of the increase in protein stability and activity of the methyltransferases. MDM2 has been shown to post-translationally down regulate methyltransferases such as Suv39h1 (Mungamuri et al., 2012). It is possible that the previously described decreased MDM2 expression in hypoxia contributes to the stabilisation of some of the histone methyltransferases under these conditions (Alarcon et al., 1999). However, from the three H3K9me3 methyltransferases considered here, Suv39h1 appeared to be the one least susceptible to hypoxic induction since no significant increases in protein or mRNA expression of this methyltransferase was observed. Furthermore, the decreased activity of the 2-oxoglutarate dependent family of histone demethylases

under hypoxic conditions undoubtedly contributes to the hypoxia-induced H3K9me3 although this was not investigated in this study (Couture et al., 2007; Sanchez-Fernandez et al., 2013).

We observed that hypoxia-induced H3K9me3 was enriched at the loci on *PP2A-C* (Figure 4.9). The enrichment of this typically repressive histone modification correlated with decreased mRNA levels and reduced phosphatase activity of PP2A-C specifically under the more severely hypoxic conditions (Figure 4.10/11). It would be interesting to investigate whether the nucleotide pool drop and/or the replication stress in hypoxia are part of the signal leading to PP2A-C repression specifically under severe hypoxic conditions. The enhanced induction of H3K9me3 in response to severe hypoxia may also explain why PP2A-C is repressed in severe hypoxia and not at 2% O_2. Overall, these data indicate that H3K9me3 could serve to negatively regulate PP2A-C following hypoxia-induced replication stress, thereby contributing to ATM phosphorylation and activation. It should be noted that although loss of Suv39h1/2 had a dramatic effect on PP2A-C mRNA expression in both normoxia and hypoxia, repression of PP2A-C in hypoxia could still be observed in the absence of Suv39h1/2 suggesting that alternative mechanisms of PP2A-C repression are also in place. Furthermore, it is likely that H3K9me3 may also facilitate ATM activation by other mechanisms besides PP2A-C repression. As mentioned above, recent reports have demonstrated a role for TIP60 in binding to H3K9me3 in regions of heterochromatin, subsequently facilitating ATM activation in these areas in response to IR (Kaidi and Jackson, 2013; Sun et al., 2005; Sun et al., 2009). However, Price and colleagues showed a dependency on the MRN complex to recruit the ATM-TIP60 complex to sites of irradiation-induced DSBs and to stimulate the acetyltransferase activity of TIP60, as well as a requirement for HP1β to be released from H3K9me3

following DNA damage (Sun et al., 2009). Given the absence of DSBs and lack of requirement for the MRN complex for ATM activation in hypoxia, it seems unlikely that this mechanism is involved in hypoxia-induced ATM activation (Bencokova et al., 2009; Cam et al., 2010). Interestingly, ATR has been reported to phosphorylate ATM in response to UV and Hu, independently of MRE11 or the NBS1-ATM interaction domain on NBS1 (Stiff et al., 2006). It is possible that ATR activation following hypoxia-induced replication stress may contribute to ATM activation. However, this is technically challenging to study given the induction of DNA damage upon ATR inhibition in hypoxia (Pires et al., 2012).

In Chapter 3 we speculated that an additional signal present in hypoxia was required in order to activate ATM in response to replication stress in the absence of DNA damage. We now propose that the additional signal may indeed be the hypoxia-induced chromatin changes, including H3K9me3. We suggest that increases in H3K9me3 (amongst other chromatin changes) and replication stress work in tandem to mediate ATM phosphorylation and activation in the absence of DNA damage (Figure 4.13).

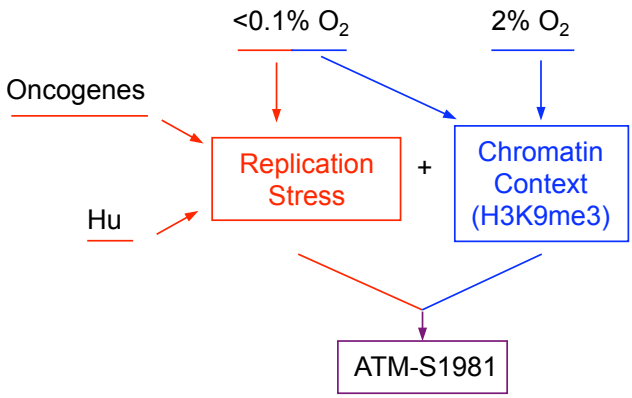


Figure 4.13. Schematic representation of the proposed model for ATM activation in hypoxia
Our model suggests two signals: replication stress (in red) and the chromatin context (in blue) lead to ATM activation in the absence of damage (in purple)

CHAPTER 5

THE ROLE OF HYPOXIA-INDUCED ATM

5.1 INTRODUCTION

Having worked towards establishing a mechanism for ATM activation in hypoxia we investigated the role of the ATM kinase under conditions of hypoxia-induced replication stress. Given that hypoxia-induced chromatin changes, including H3K9me3, appeared to be particularly important for ATM activation under these conditions, we reasoned that perhaps the chromatin context could suggest a role for ATM in hypoxia. As mentioned in Chapter 4, the activation of ATM in response to chromatin changes has been previously studied, however, this has mainly been in the context of DSB repair (Shiloh and Ziv, 2013; Sun et al., 2009). This is not surprising since ATM has a well-characterised role in responding and facilitating the repair of DNA breaks following insults such as IR (Canman et al., 1998; Jackson and Bartek, 2009). The reasons for requiring ATM activity in the absence of DNA damage, however, are far less well understood. We hypothesized that the chromatin changes induced in hypoxia, including increased H3K9me3, together with replication stress could not only serve as the signal facilitating ATM activation but could also be the reason for requiring ATM activity in these situations. We therefore asked whether

ATM could have a role in facilitating replication in situations where replication stress occurs in a "heterochromatin-like" background.

5.2 RESULTS

5.2.1 H3K9me3 is enriched at the replication fork following hypoxia-induced replication stress

The dependence on H3K9me3 for ATM activation in response to replication stress in hypoxia led us to hypothesize that ATM could be involved in facilitating replication through H3K9me3-rich regions. To address this possibility we first investigated the specific localisation of H3K9me3 using the recently described iPOND technique (diagram describing the technique is shown in Chapter 2, Figure 2.1). This technique allows the analysis of proteins and protein modification specifically occurring at or around replication forks following pull down of EdU labelled forks (Sirbu et al., 2012; Sirbu et al., 2011). Previous immunofluorescence analysis of the localisation of H3K9me3 in hypoxia suggested that this chromatin mark had a widespread nuclear appearance (Figure 4.1E). We reasoned that establishing the iPOND assay in hypoxia would allow us to determine whether the hypoxia-induced increase in H3K9me3 was also associated with or around replication forks (Sirbu et al., 2011). The exposure to EdU was optimised to ensure equal amounts of EdU labelled DNA were pulled down in each condition (Figure 5.1). This was an important control since major differences in EdU incorporation would lead to different amounts of total protein being pulled down between conditions, potentially introducing a bias in the experiment. iPOND analysis demonstrated that there was an increase in H3K9me3 at or in the vicinity of the replication fork in hypoxia (<0.1% O_2). PCNA was used as replication fork associated control (Figure 5.2).

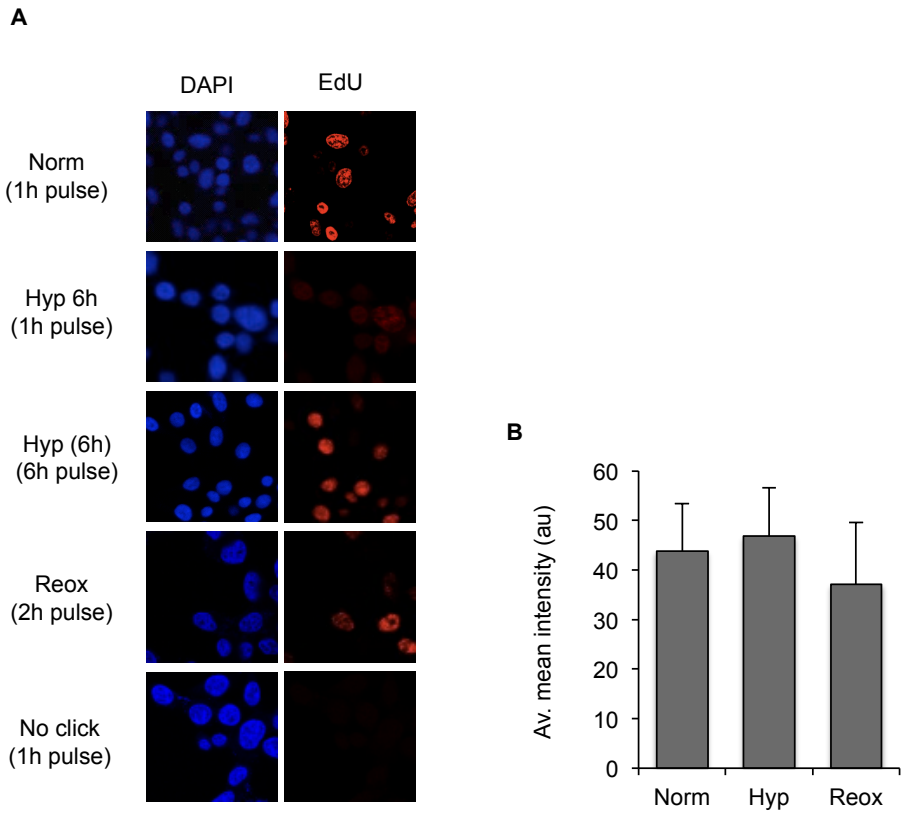


Figure 5.1. Optimisation of EdU exposure for iPOND experiments
(A) EdU labelling times were optimised to ensure approximately equal amounts of EdU were incorporated in each condition. Shown are representative images for the EdU labelling times chosen. For hypoxic treatments 1 hour of EdU incorporation results in minimal EdU incorporation due to the hypoxia-induced replication stress. 6 hours of EdU incorporation in hypoxia results in a comparable level of incorporation as seen following 1 hour of EdU labelling under normoxic conditions. Following reoxygenation from hypoxia-induced replication stress, 2 hours of EdU labelling results in a comparable level of EdU incorporation to 1 hour labelling in normoxic conditions. Norm (21% O_2), Hyp (6 h, <0.1% O_2), Reox (6 h, <0.1% O_2 followed by 2 h of 21% O_2). The No click condition is used as a negative control and represents a sample where the click reaction was carried out without fluorophore, n=3. **(B)** Cells were exposed to Norm (1h EdU incorporation), Hyp (6h EdU incorporation) or Reox (2h EdU incorporation at reoxygenation) as in (A). Quantification of EdU incorporation (expressed as the average (av.) mean intensity of all stained cells analysed) for the representative experiment is shown. Error bars indicate the standard error between the mean intensities measured for the represented experiment. Validation of comparable EdU incorporation was carried out for each iPOND experiment.

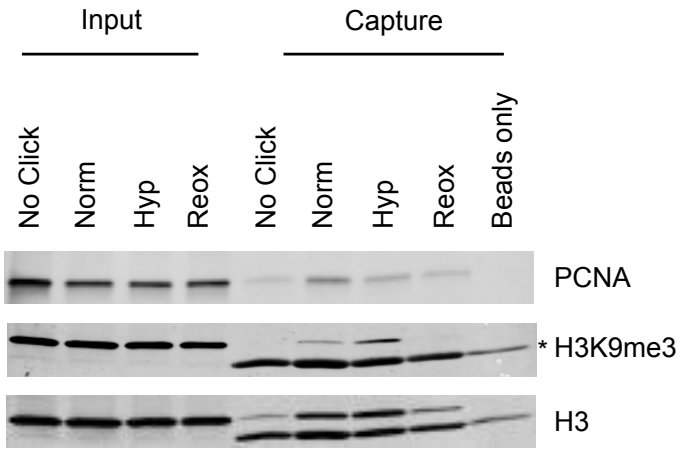


Figure 5.2. H3K9me3 is associated with replication forks in hypoxia
iPOND was carried out following exposure of RKO cells to either Norm (21% O_2), Hyp (6 h, <0.1% O_2) or Reox (6 h, <0.1% O_2 followed by 2 h of 21% O_2). EdU labelling times: Norm (1 h), Hyp (6 h), Reox (2 h, during reoxygenation period). * denotes a non-specific band observed in all lanes at the end of the gel. No click control represents a sample where the click reaction was carried out without biotin-azide.

Thymidine chase experiments (where EdU was removed and replaced by thymidine before harvesting) were also carried out following exposure to normoxia, hypoxia and reoxygenation. Chasing EdU with thymidine was used to test whether H3K9me3 was specifically enriched in areas immediately associated with the replication fork in hypoxia as opposed to just being a chromatin bound histone mark travelling along the fork (schematic representation of the thymidine chase experiment shown in Figure 5.3A). Given that minimal amounts of H3K9me3 were observed during iPOND analysis following thymidine chase experiments, it seems likely that H3K9me3 is specifically enriched at and around the replication fork specifically following hypoxia-induced replication stress (Figure 5.3B).

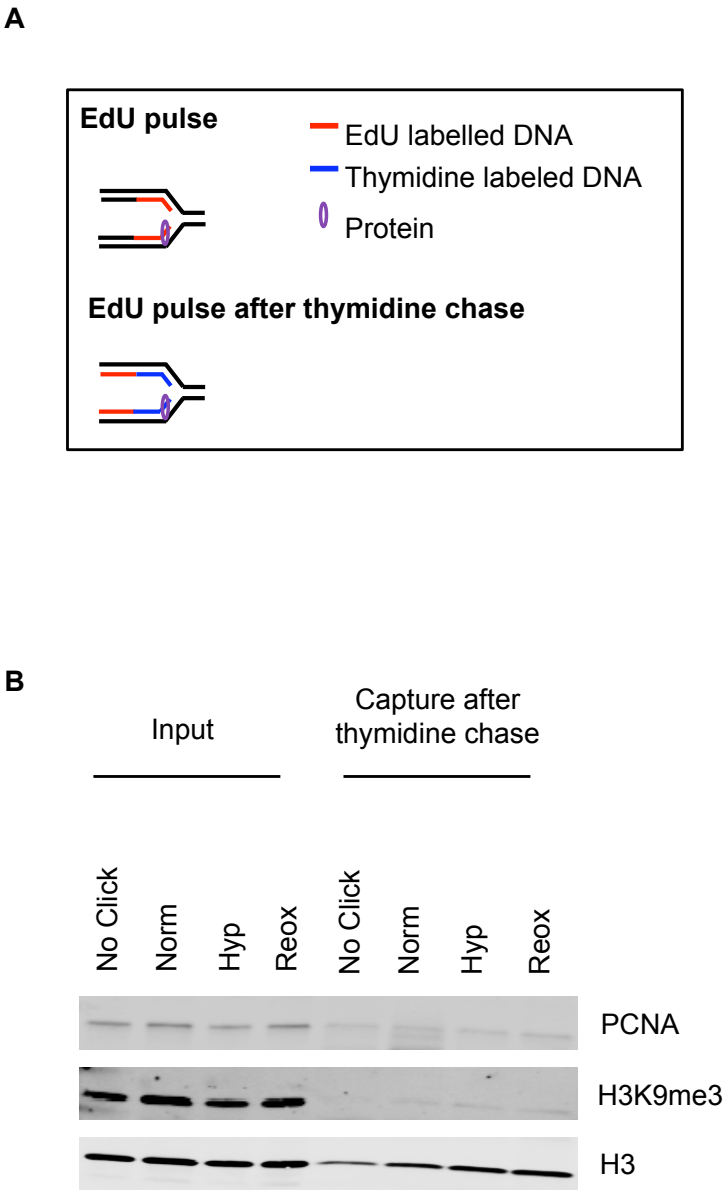


Figure 5.3. H3K9me3 is not detected at the replication fork following thymidine chase experiment

(A) Schematic representation of the thymidine chase experiment used to distinguish proteins specifically associated with the replication fork from non-specific chromatin binding factors. The thymidine chase displaces nascent EdU labelled DNA away from the replication fork. Adapted from (Sirbu et al., 2012) **(B)** iPOND was carried out following exposure of RKO cells to either Norm (21% O_2), Hyp (6 h, <0.1% O_2) or Reox (6 h, <0.1% O_2 followed by 2 h of 21% O_2). EdU labelling times: Norm (0.5 h), Hyp (3 h), Reox (1.5 h, during reoxygenation period). The chase into thymidine containing medium was performed for the last 30 minutes of each condition in Norm and Reox or for the last 3 h in Hyp. No click control represents a sample where the click reaction was carried out without biotin-azide.

As described in Chapter 3, treatment of RKO cells with Hu for 6 hours in normoxic conditions did not induce significant ATM or KAP-1 phosphorylation (Figures 3.9). If increased H3K9me3 levels together with replication stress are indeed a requirement for ATM activation in the absence of DNA damage, a short exposure to Hu would be predicted to not increase H3K9me3 levels. We tested this possibility by exposing RKO cells to 6 or 24 hours of Hu and carrying out western blotting for H3K9me3. Hu-induced replication stress did not induce a significant increase in H3K9me3 unless DSBs were also present, nicely supporting our hypothesis (Figure 5.4A). We decided to take this one step further and carried out iPOND analysis to verify that Hu treatment for 6 hours did not induce H3K9me3 levels at or around the replication fork in RKO cells. As can be seen in Figure 5.4B, no significant induction in H3K9me3 was observed around the replication fork following Hu treatment. The lack of increase in global, as well as replication fork associated H3K9me3, in response Hu-induced replication stress, highlights how unique severe hypoxia is amongst replication stresses. These results are once again supportive of a model where increased H3K9me3 is important for ATM activation following replication stress in the absence of detectable DNA damage.

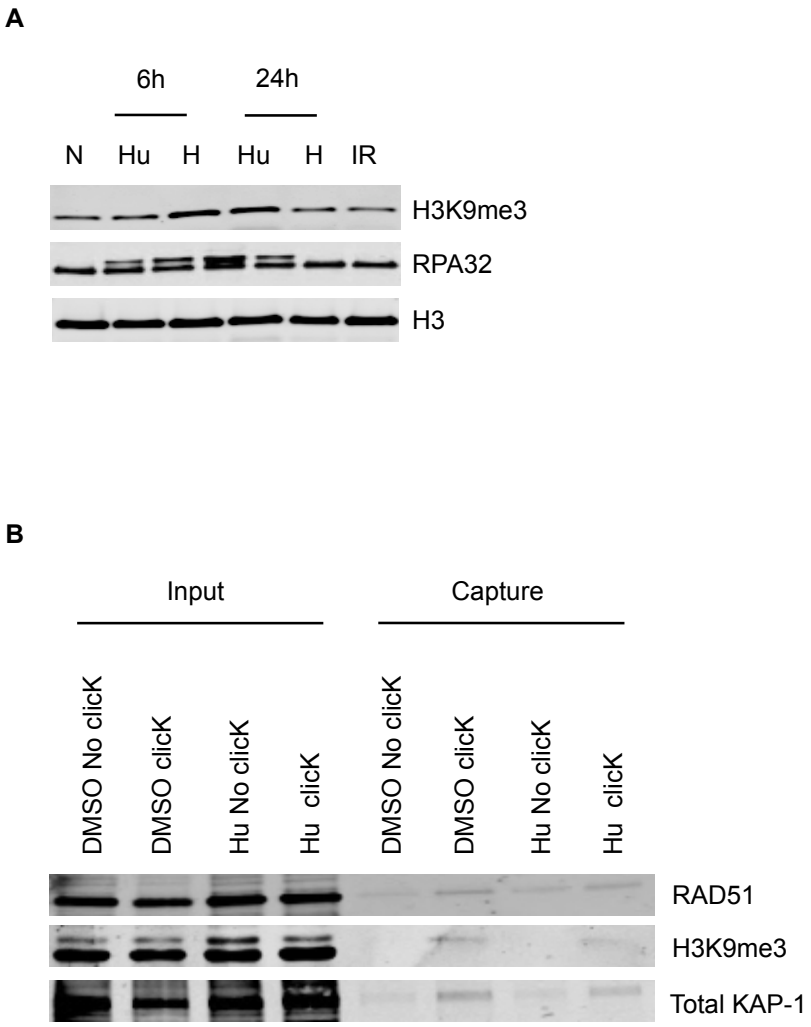


Figure 5.4. Short Hu treatment does not affect the levels of H3K9me3 either globally or at the replication fork

(A) RKO cells were exposed to N (21% O_2), Hu (6 or 24 h, 1 mM), H (6 or 24 h, <0.1% O_2), IR (5 Gy, cells harvested 30 minutes post IR). Western blotting was carried out with the antibodies indicated. Experiment shown here is part of the same experiment shown in Figure 3.9. **(B)** iPOND was carried out following exposure of cells to either DMSO or Hu (6 h, 1 mM). EdU labeling times=30 minutes for all conditions. No click control represents a sample where the click reaction was carried out without biotin-azide.

5.2.2 Loss of ATM activity leads to accumulation of DNA damage in hypoxia

The presence of H3K9me3 around the replication fork specifically in hypoxia could contribute to hypoxia-induced replication stress and potentially lead to a requirement for ATM activity under these conditions. In this scenario, hypoxia-induced ATM could be envisioned to have a role in maintaining replication in a situation where there is replication stress associated with increased H3K9me3. Loss of ATM activity would be predicted to result in failure to maintain the integrity of the replication fork leading to the generation of DNA damage in hypoxia. To test this, RKO cells were exposed to hypoxia in the presence of the ATM inhibitor KU-55933, and 53BP1 foci formation was used as a measure of DNA damage. Since most cancer cells have some background level of 53BP1 foci formation even in the absence of stress, a threshold of more than six 53BP1 foci was set. Only cells with more than six 53BP1 foci were counted as damaged. No significant increase in damage was seen in KU-55933 treated cells in normoxia (21% O_2) (Figure 5.5A). However, ATM inhibition led to an accumulation of DNA damage in hypoxic conditions. Similar results were obtained upon siRNA-mediated depletion of ATM (Figure 5.5B).

Furthermore, ATM inhibition or knockdown following exposure to 2% O_2 (where no replication stress occurs), did not lead to a significant increase in DNA damage, suggesting that the role of ATM in preventing DNA damage formation in hypoxia is restricted to conditions in which a replicating stress is observed (Figure 5.6).

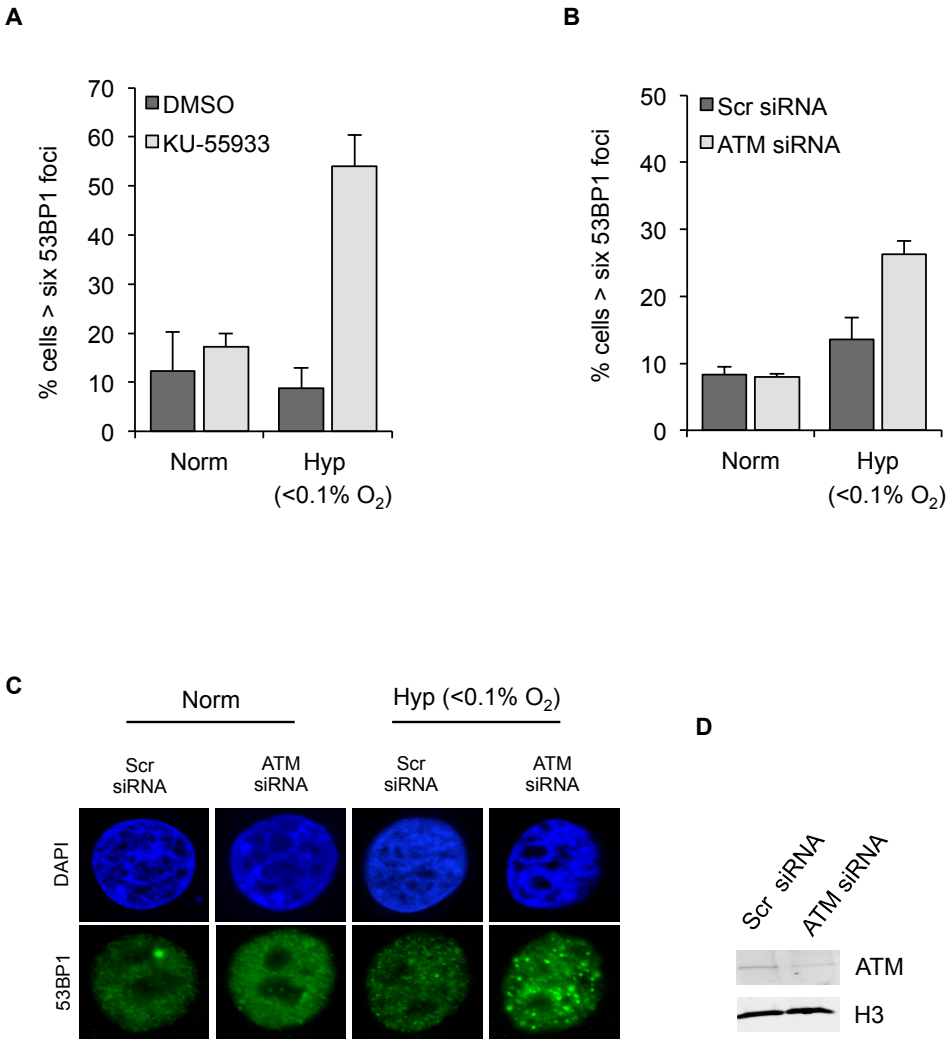


Figure 5.5. Loss of ATM activity leads to DNA damage accumulation in hypoxia

(A) RKO cells were treated with DMSO or 10 μM KU-55933 and exposed to Norm (21% O_2), Hyp (6 h, < 0.1% O_2) or Reox (6 h, <0.1% O_2 followed by 1 h of 21% O_2). The quantification of 53BP1 foci counted is shown, n=3. **(B)** RKO cells were treated with scramble (Scr) or ATM siRNA and exposed to Norm (21% O_2) or Hyp (6 h, <0.1% O_2). The quantification of 53BP1 foci counted is shown, p value between Norm Scr and Hyp Scr=>0.05, n=3. **(C)** Representative images of cells stained for 53BP1 (green) and DAPI to stain DNA (blue) are shown. **(D)** Western blotting was carried out to validate the ATM siRNA-mediated knockdown. H3 was used as the loading control.

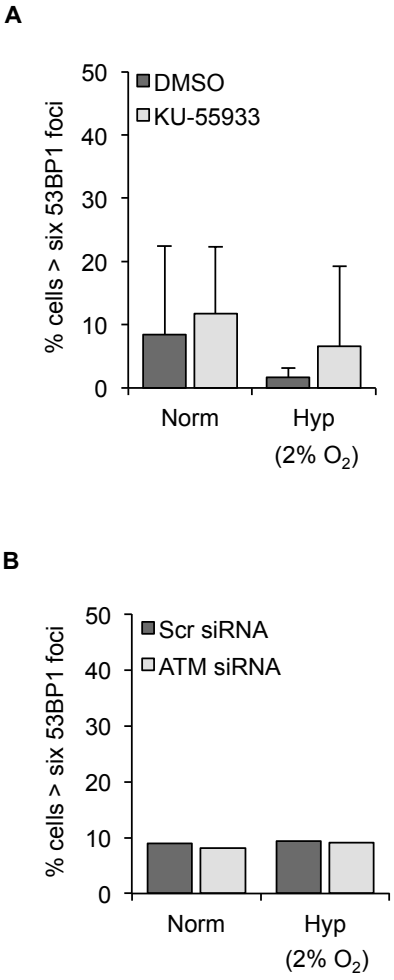


Figure 5.6. ATM inhibition or loss does not result in DNA damage accumulation in mild hypoxia (2% O_2)
(A) RKO cells were treated with DMSO or 10 μM KU-55933 and exposed to Norm (21% O_2) or Hyp (6 h, 2% O_2). The quantification of 53BP1 foci counted in two independent experiments is shown, n=3. **(B)** RKO cells were treated as above but in the presence of scramble (Scr) or ATM siRNA. The quantification of 53BP1 foci counted in one experiment is shown.

Moreover, the increase in 53BP1 foci formation was only observed in 50% of hypoxic cells treated with KU-55933, suggesting that in hypoxic conditions (<0.1% O_2) ATM prevents the accumulation of DNA damage in S-phase (Figure 5.5). To investigate this further, RKO cells were labelled with EdU and exposed to hypoxia in the presence or absence of the ATM inhibitor, KU-55933. Importantly, most of the DNA damage observed following ATM inhibition in hypoxia occurred in the EdU labelled S-phase population. Interestingly, the 53BP1 foci seemed to mainly co-localise with areas where the EdU labelling could represent areas of replicating heterochromatin in mid/late S-phase (Figure 5.7B) (Nakayasu and Berezney, 1989). In an attempt to validate the specific cell-cycle phase in which DNA damage was induced upon ATM inhibition in hypoxia we used Fucci labelled H1299 cells, in which the G_1, S and G_2/M phases can be distinguished by microscopy (Kaida and Miura, 2012). H1299 cells have no p53 and show increased levels of genomic instability; therefore, a threshold of ten 53BP1 foci was set when assessing DNA damage induction by 53BP1 foci formation in this cell line (Lai et al., 2000). Notably, in this experiment the majority of the 53BP1 foci observed in hypoxia (<0.1% O_2) following treatment with the ATM inhibitor were present in the S-phase population (Figure 5.7A). These data support the notion that loss of ATM activity leads to the accumulation of DNA damage in hypoxic conditions associated with replication stress and high H3K9me3 levels.

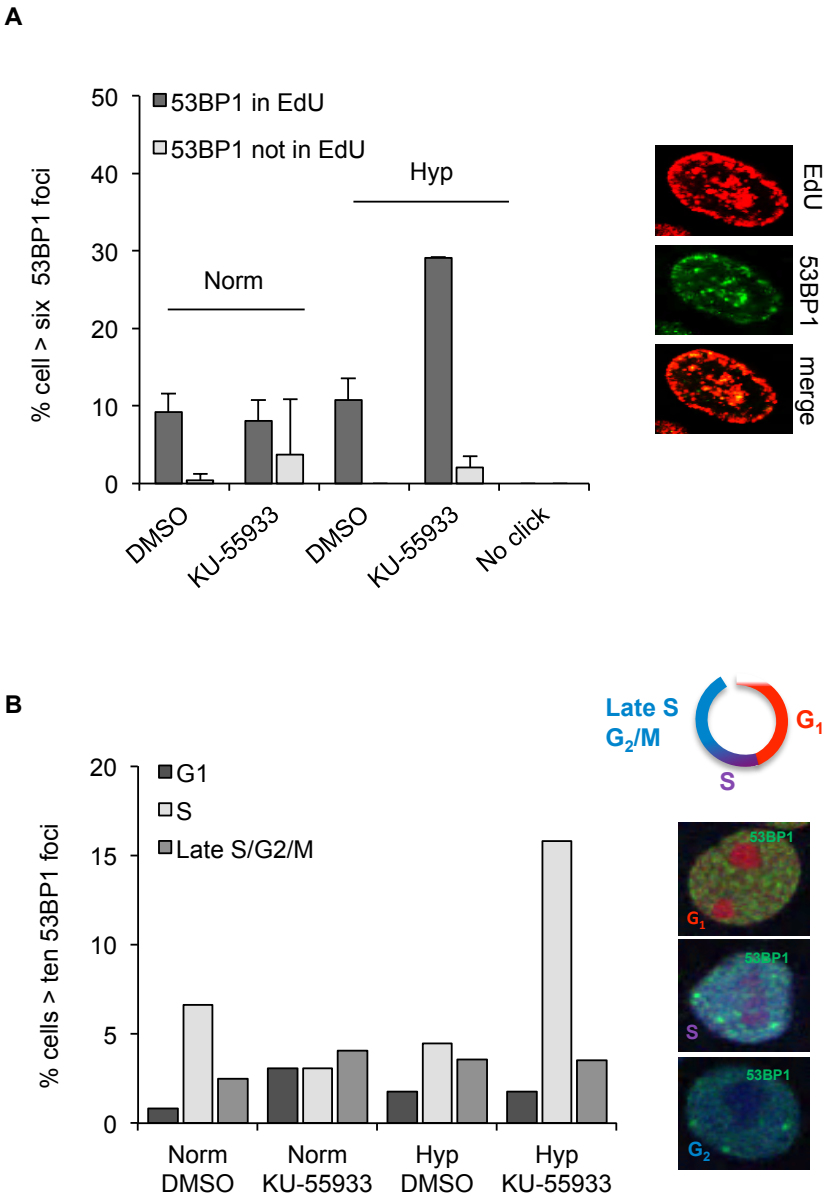


Figure 5.7. 53BP1 foci following ATM inhibition accumulate in S-phase

(A) RKO cells were labelled with EdU (10 μM) and treated with DMSO or 10 μM KU-55933 and exposed to Norm (21% O_2) or Hyp (3 h, <0.1% O_2). EdU labelling times =1 h for Norm and 3h for Hyp conditions. **(B)** H1299 cells (labelled with Fucci plasmids) were exposed to Norm (21% O_2) or Hyp (6 h, <0.1% O_2) in the presence of DMSO or 10 μM KU-55933. The quantification of 53BP1 foci counted in each cell-cycle phase in one experiment is shown together with a representative image of cells in each phase. A schematic representation of Fucci cell-cycle labelling is also shown above the image of the cells. G_1=red, S=purple, late S/G_2/M=blue, 53BP1=green.

To investigate this protective mechanism in greater detail we asked if ATM-mediated signalling to KAP-1 also prevented the accumulation of damage in hypoxia. RKO cells were exposed to either normoxia or hypoxia after siRNA-mediated knockdown of KAP-1 and the level of DNA damage under these conditions was quantified. In each of the three independent experiments carried out, KAP-1 knockdown under hypoxic conditions resulted in a trend towards an increase in the number of cells harbouring DNA damage (as assessed by 53BP1 foci formation) (Figures 5.8). However, this trend did not reach significance probably due to the great variation in 53BP1 foci observed between experiments. A potential decrease in 53BP1 foci was also observed in normoxia following KAP-1 siRNA mediated knockdown, although again this did not reach statistical significance. Taken together these data suggest that while ATM-mediated signalling has a role in preventing the accumulation of DNA damage in hypoxia, a role for KAP-1 in contributing to this signalling could not be demonstrated.

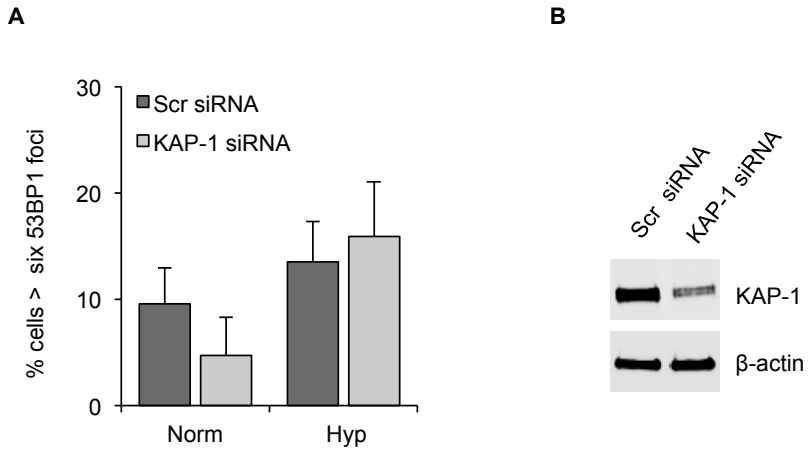


Figure 5.8. KAP-1 knockdown does not lead to DNA damage accumulation in hypoxia
(A) RKO cells were treated with scramble (Scr) or KAP-1 siRNA and exposed to Norm (21% O_2) or Hyp (6 h, <0.1% O_2). Cells were then stained for 53BP1. The quantification of 53BP1 foci counted is shown, n=3. **(B)** A western blot was carried out with the indicated antibodies to verify KAP-1 siRNA-mediated knockdown.

5.2.3 Increased H3K9me3 correlates with a requirement for ATM activity to resolve replication stress

It is important to note that the iPOND analysis showed a reduction in H3K9me3 in response to reoxygenation, indicating a dynamic oxygen dependent regulation of this chromatin modification around the replication fork (Figure 5.2). If increased amounts of H3K9me3 are part of the requirement for ATM signalling in response to replication stress, we would predict that loss of ATM activity during reoxygenation-induced replication-restart would have no effect on DNA damage levels. In support of this, we saw no ATM dependent increase in reoxygenation-induced DNA damage, as assessed by counting 53BP1 foci following ATM inhibition in cells exposed to hypoxia (<0.1% O_2) followed by reoxygenation (at 21% O_2) (Figure 5.9).

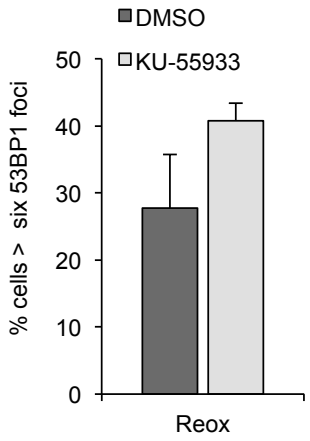


Figure 5.9 Loss of ATM activity does not lead to DNA damage accumulation in response to reoxygenation
RKO cells were treated with DMSO or 10 μM KU-55933 and exposed to Reox (6 h, <0.1% O_2 followed by 1 h of 21% O_2). Quantification of 53BP1 foci is shown, n=3.

Together these data suggest a novel role for ATM in preventing the accumulation of damage during hypoxia-induced replication stress and that this is associated with regions rich in "heterochromatin-like factors". This conclusion would predict that replication should be unaffected by ATM loss when H3K9me3 is reduced, for example, during reoxygenation-induced replication restart. In agreement with this, DNA fiber analysis showed that in conditions of reoxygenation, replication restart was unaffected by ATM inhibition (schematic representation of the DNA fiber assay is shown in Chapter 2, Figure 2.2). Surprisingly, however, following reoxygenation the number of new origins increased in the presence of the ATM inhibitor (Figure 5.10A). Inhibition of ATM under normoxic conditions had a non-significant effect on origin firing, pointing to a novel and stress-specific role for ATM in regulating appropriate origin firing following replication restart (Figure 5.10B).

The data so far indicated a possible role for ATM in facilitating replication through H3K9me3-enriched regions. Consequently, loss of ATM activity would be expected to affect the rate of DNA replication in hypoxia (<0.1% O_2). To address this, we measured replication rates in cells in either normoxia or during hypoxia by again using the DNA fiber assay (<0.1% O_2) (Figure 5.11). Inhibition of ATM did not have a significant effect on replication rates in normoxia. In contrast, replication rates were significantly slower in hypoxic cells treated with the ATM inhibitor KU-55933, compared to the hypoxic controls (Figure 5.11A). Similar results were obtained when DNA fiber analysis was carried out following siRNA-mediated depletion of ATM under normoxic or hypoxic conditions respectively (Figure 5.11B). These data demonstrate a stress-specific novel role for ATM in DNA replication.

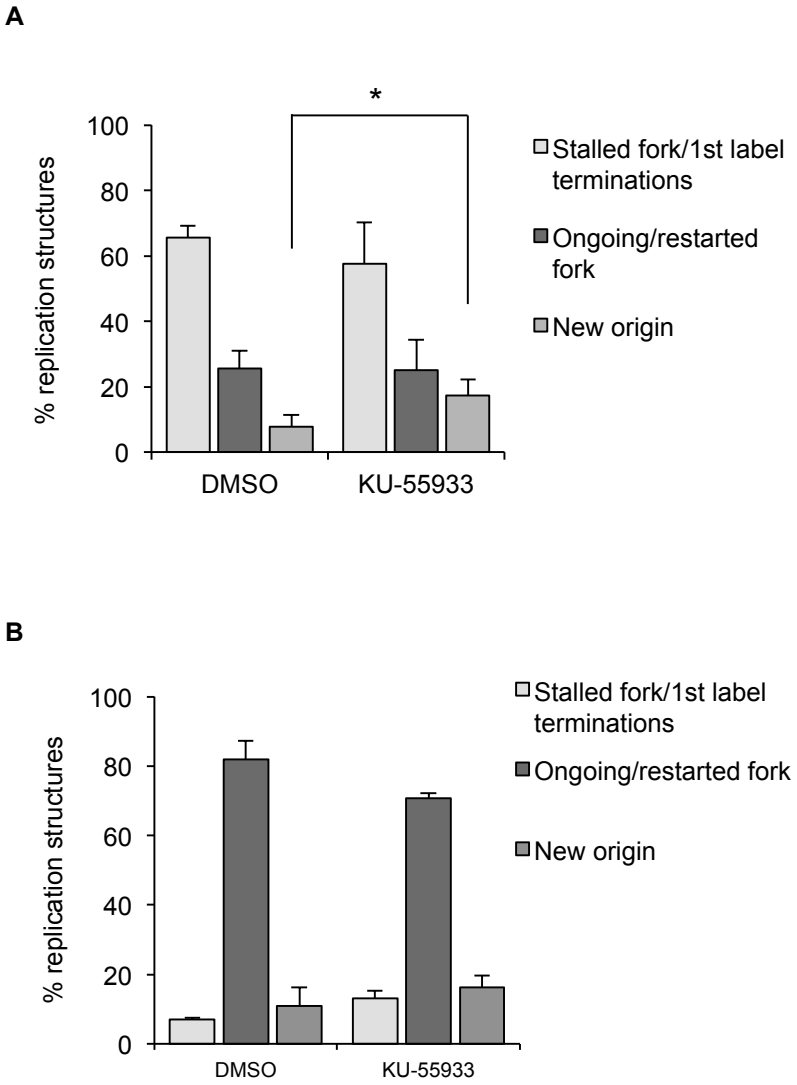


Figure 5.10. ATM inhibition has no effect on replication restart but leads to an increase in origin firing following reoxygenation-induced replication restart

(A) RKO cells were treated with DMSO or 10 μM KU-55933 and exposed to hypoxia (5 h, <0.1% O_2) followed by 1 h of reoxygenation (21% O_2). DNA fibers were spread, stained and scored, n=3. (**B**) RKO cells were treated as above but in normoxic conditions (21% O_2). DNA fibers were spread, stained and scored. Graphs represent the average % replication structures counted, n=3.

A

	Norm (IdU kb/min)	**Hyp** (IdU kb/min)
DMSO	0.42 ±0.08	0.09 ±0.05
KU-55933	0.34 ±0.12	0.02 ±0.01
	ns	p<0.05

B

	Norm (IdU kb/min)	**Hyp** (IdU kb/min)
Scr siRNA	0.22 ± 0.08	0.13 ± 0.03
ATM siRNA	0.20 ± 0.4	0.05 ± 0.01
	ns	p<0.05

C

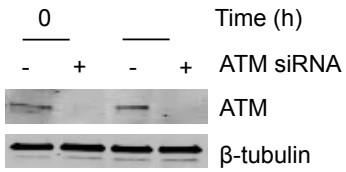


Figure 5.11 ATM controls replication speed in hypoxia
(A) The replication rates of cells treated with DMSO or 10 μM KU-55933 and exposed to Norm (21% O_2) or Hyp (6 h, <0.1% O_2) were scored. An average of the average IdU-incorporation rates for each of three independent experiments are shown, ns=non significance. **(B)** The replication rates of cells treated with scramble (Scr) or ATM siRNA and exposed to Norm (21% O_2) or Hyp (6 h, <0.1% O_2) were scored. An average of the average IdU-incorporation rates for each of three independent experiments are shown for each condition, ns=non significance. **(C)** Surplus cells collected following DNA fiber spreading were lysed and western blotting with the indicated antibodies was carried out to validate the level of ATM knockdown. β-tubulin was used as the loading control.

5.3 DISCUSSION

We have shown that ATM is active in response to replication stress when it occurs under hypoxic conditions that provide a specific chromatin context. The induction of ATM in these specific situations pointed to a potential role for ATM in resolving replication stress occurring in a "heterochromatin-like" context. In the absence of ATM activity, hypoxic cells accumulated significant levels of DNA damage. This could suggest a novel role for ATM in protecting replication structures in areas rich in factors associated with heterochromatin.

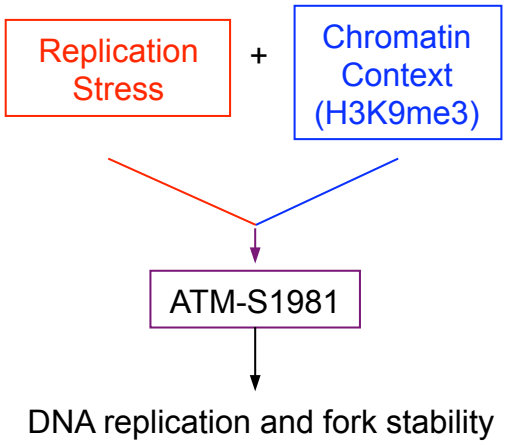


Figure 5.12. Schematic representation of our model for the activation and role of ATM in hypoxia
Replication stress in the absence of DNA damage together with the appropriate chromatin context (including elevated H3K9me3) leads to ATM activation and downstream signalling. Once active, ATM is involved in preventing the accumulation of DNA damage and maintaining DNA replication.

The results obtained using KU-55933, a specific inhibitor of ATM-kinase activity, suggest that the phenotype observed is dependent on ATM-kinase activity and not just on the presence or absence of ATM. A possible way in which ATM could facilitate replication under these conditions could be through hypoxia-induced ATM dependent phosphorylation of KAP-1, which we have shown here (Figure 3.4), and has a characterised role in chromatin relaxation (Goodarzi et al., 2011; Goodarzi et al., 2008; Ziv et al., 2006). Our data suggest that KAP-1 probably plays a limited role here. However, it is difficult to completely rule out a potential contribution of ATM-signalling to KAP-1 in this context for a number of reasons. Firstly, KAP-1 is thought to exist in two forms, a phosphorylated form and a sumoylated form. The latter is thought to be involved in heterochromatin formation, while the former has been shown to facilitate chromatin relaxation (as described in Chapter 1, Figure 1.10). By performing KAP-1 siRNA-mediated knockdown we are, therefore, potentially reducing the amount of heterochromatin being formed in a SUMO-KAP-1 dependent manner, but we are also attenuating any remaining heterochromatin relaxation (since we have reduced the possibility to phosphorylate KAP-1-S824 in an ATM dependent manner). It thus becomes difficult to fully interpret the role of ATM dependent KAP-1 phosphorylation in fork integrity. Furthermore, KAP-1 is a very abundant protein. The incomplete level of KAP-1 knockdown achieved in these experiments might not have been enough to be able to appreciate the full phenotype. Repeating these experiments following transfection of phosphomimetic (KAP-1-S824A) or phosphomutant (KAP-1-S824D) KAP-1 in cells where KAP-1 has been fully depleted (using siRNA sequence not targeting the mutants) would be very informative.

Alternatively, ATM-mediated signalling to additional targets may also be relevant, for example CHK1-TLK or CHK2 (Groth et al., 2003; Pires et al., 2010a;

Pires et al., 2010b). Importantly, under conditions of replication stress, ASF1 a downstream TLK1 target, buffers evicted H3K9me3 suggesting that the previously reported loss of ASF1 during hypoxia-induced replication stress could contribute to the increased H3K9me3 levels observed around replication forks (Jasencakova et al., 2010).

Furthermore, we unexpectedly have identified a stress-responsive novel role for ATM in replication restart. Inhibition of ATM increased origin firing during reoxygenation-induced replication restart while having no effect on normal replication. Given that no new origins are licensed once cells have entered S-phase, the increase in origin firing following ATM inhibition likely reflects an increase in the firing of dormant origins (Ge and Blow, 2010; Kawabata et al., 2011; Wohlschlegel et al., 2000). This would suggest a new role for ATM in regulating dormant origin firing in response to replication restart following replication stress in the absence of DNA damage.

Most interestingly, we have determined that inhibition or loss of ATM activity in hypoxic conditions leads to decreased DNA replication rates. Together these data demonstrate a novel stress-specific role for ATM in facilitating DNA replication during replication stress.

CHAPTER 6

FURTHER BIOLOGICAL CONSEQUENCES OF HYPOXIA-INDUCED H3K9Me3

6.1 INTRODUCTION

As described in Chapter 1, numerous studies have demonstrated the widespread repression of DNA repair genes in hypoxia and have highlighted the importance of this phenomenon in contributing to genomic instability. The detailed mechanism of this repression, however, has only been studied for a number of genes (Bindra et al., 2005b; Bristow and Hill, 2008). Moreover, most of the studies investigating DNA repair gene repression have been performed at levels of mild or moderate hypoxia (1-2% O_2), rather than levels of hypoxia associated with radioresistance (<0.1% O_2) (Begg et al., 2011; Gray et al., 1953). Very little is known about the mechanisms of repression that occur under severe hypoxia (<0.1% O_2) where the DDR will be induced and may act as a barrier to tumourigenesis to limit genomic instability (Bristow and Hill, 2008). Moreover, the mechanism of repression of genes associated specifically with the DDR rather than DNA repair has not been studied in detail.

We have found that Suv39h1/2-mediated transcriptional regulation of PP2A-C, though moderate H3K9me3 enrichment, could contribute to ATM phosphorylation and activation (Chapter 4). We decided to investigate other consequences of hypoxia-induced H3K9me3 with respect to its role in transcriptional repression and always

within the framework of the DDR. We took a candidate approach by selecting a number of different genes that we hypothesized could be repressed by this histone modification in hypoxia (the criteria for candidate gene choice will be described in detail below). Following this approach we decided to investigate *APAK* (ATM and p53 KZNF associated protein, or *ZNF420*). The KZNF (KRAB-type zinc-finger) proteins constitute the largest single-family of transcriptional regulators in mammals. *APAK* encodes a KZNF protein that binds to p53 through its KRAB in unstressed cells. APAK binding attenuates acetylation of p53 by recruiting KAP-1-HDAC1 complexes. Upon DNA damage ATM dependent phosphorylation of p53, KAP-1 and APAK results in dissociation of the APAK-p53 complex, favouring the transcriptional activity of pro-apoptotic genes by p53 (Tian et al., 2009; Yuan et al., 2012). In addition, APAK can prevent p53 from binding to pro-apoptotic gene *p53AIP1* by binding to a consensus sequence (TCTTN2−30TTGT) overlapping the p53 binding site.

Activation of p53 in response to hypoxia is arguably one of the principal consequences of the hypoxia-induced DDR. This activation is oxygen dependent, with p53 phosphorylation on serine 15 occurring only following the replication stress observed in severe levels of hypoxia (<0.1% O_2). Phosphorylation of p53 in hypoxia appears to be mainly ATR rather than ATM dependent, although ATM may contribute to p53 phosphorylation via its downstream target CHK2 (Gibson et al., 2005; Hammond et al., 2002). Loss of p53 results in significantly diminished apoptosis in hypoxia suggesting that appropriate regulation of p53 is critical for full execution of apoptosis under these conditions (Hammond and Giaccia, 2005).

In this chapter we explore the link between H3 methylation and the hypoxia-induced DDR in further detail. Having picked *APAK* from our list of candidates we

proceeded to validate the transcriptional regulation of APAK via hypoxia-induced H3K9me3. Finally, we investigated whether H3K9me3 through its role in transcriptional repression could also facilitate p53 dependent apoptosis in hypoxia.

6.2 RESULTS

6.2.1 Choice of candidate genes

We hypothesized that the repressive histone mark H3K9me3 could be involved in mediating transcriptional downregulation of certain DNA repair/DNA damage associated genes in severe hypoxia. To test this hypothesis six candidate genes were selected according to two criteria described below:

1) SETDB1, KAP1 and/or H3K9me3 enrichment as described in previously published ChIP-ChIP or ChIP-seq studies (Ceol et al., 2011; O'Geen et al., 2007).
2) Possible transcriptional downregulation in hypoxia reported in previously published microarray data (Hammond et al., 2006).

In brief, O'Geen and colleagues carried out ChIP-ChIP studies of the H3K9me3 mark through 5 kb of 26000 human promoters in Ntera2 testicular carcinoma cells as well as in three different primary human fibroblast cell lines. In the same study the authors undertook genome-wide KAP-1 ChIP-ChIP studies to gain further insight into whether some of the binding found in their H3K9me3 ChIP-ChIP study could be mediated by KAP-1-recruited complexes (O'Geen et al., 2007). More recently, Ceol and colleagues carried out ChIP-seq studies for H3K9me3 and SETDB1 in WM262

and WM451Lu melanoma cells with high or low SETDB1 expression respectively (Ceol et al., 2011). Data from a microarray carried out in *MYC/RAS* transformed MEFs exposed to <0.1% O_2 for 8 hours was used as a guideline for previously reported gene repression in hypoxia (Hammond et al., 2006).

Based on these two overarching criteria, a set of genes was selected based on whether previous significant H3K9me3 binding had been observed in the ChIP-seq studies carried out by Ceol and colleagues. This set was then compared with the datasets for KAP-1 and SETDB1 binding. A second refined set of candidates with H3K9me3 and/or SETDB1/KAP-1 binding was then compiled. This list was ranked, with genes showing both H3K9me3 and SETDB1/KAP-1 binding appearing at the top of the ranking. Where no overlap between H3K9me3/SETDB1/KAP-1 binding was observed between studies, those genes with H3K9me3 binding alone were ranked more highly than those with just SETDB1/KAP-1 binding. Highly ranked genes with a previously reported hypoxia-mediated repression were preferentially chosen for the final list. Of note, no previous evidence of hypoxia-mediated repression could be found for *APAK*. However, the strong H3K9me3 binding together with the KAP-1 binding reported for this gene warranted its inclusion in the screen. *PP1P5K1* was selected as the gene to be used as a control for minimal H3K9me3 enrichment. The final list of candidate genes is shown in Table 6.1.

Preliminary Chip-qPCR analysis was then performed to identify which of these candidate genes would display significant H3K9me3 enrichment in response to normoxia or hypoxia (<0.1% O_2) (Figure 6.1). ChIP analysis was performed with antibodies against H3K9me3 and H3 and was followed by qPCR using primers designed against regions where some degree of H3K9me3 enrichment had been

observed on the UCSC genome browser (assembly: GRCh37/hg19) (Primers and regions targeted shown in Appendix B).

In our study, *ATM* showed levels of H3K9me3 binding comparable to the control gene (*PP1P5K1*) suggesting that with the antibodies and conditions used in the cell line tested here, *ATM* does not show marked baseline H3K9me3 binding. A decrease in H3K9me3 binding was observed for *HP1α* in response to hypoxia; however, this decrease did not reach significance. *EXO1*, *53BP1* and *APAK* displayed highly significant hypoxia-induced increases in H3K9me3 in this preliminary screen (p values=0.005, 0.009, 0.003 respectively). The gene that showed the greatest H3K9me3 enrichment in both normoxia as well as hypoxia was *APAK*, with an almost two fold increased enrichment of this histone mark with respect to the next most highly enriched gene, *EXO1*. In order to ascertain that hypoxic treatment had resulted in an increase in global levels of H3K9me3, samples exposed to hypoxia (at the same time as the samples to be used for ChIP analysis) were processed for western blotting. As shown in Figure 6.1B, hypoxia resulted in the expected increase in H3K9me3 in these experiments.

Table 6.1. Table of candidate genes to be tested for hypoxia-induced H3K9me3 enrichment by ChIP-qPCR
The reasons for the choice of each candidate as well as the proposed function of each candidate (as described in their Uniprot entry. http://www.uniprot.org) are shown.

Gene	Reasons for choice	Proposed function
ATM	H3K9me3 binding (Ceol et al., 2011) Repressed in <0.1% O_2 (Hammond et al., 2006)	Serine/threonine protein kinase. Cell cycle checkpoint activator upon DSB formation Essential for efficient DDR signalling
EXO1	H3K9me3 binding (Ceol et al., 2011) Repressed in <0.1% O_2 (Hammond et al., 2006)	5' to 3' double stranded DNA exonuclease Important for MMR and HR
HP1α	H3K9me3 binding (Ceol et al., 2011) Repressed in <0.1% O_2 (Hammond et al., 2006)	Protein enriched in heterochromatin Recognises and binds H3K9me3 leading to epigenetic repression. Involved in HR
53BP1	SETDB1 binding (Ceol et al., 2011) Repressed in <0.1% O_2 (Hammond et al., 2006)	Important for efficient DDR signalling Recruited to sites of DNA damage where it is phosphorylated in an ATR/ATM manner. p53 binding protein
APAK	H3K9me3 binding (Ceol et al., 2011) KAP-1 bound (O'Geen et al., 2007)	ATM and p53-associated KZNF protein. Negative regulator of p53 dependent apoptosis
PPIP5K1	Minimal H3K9me3 binding No known SETDB1/KAP-1 binding or hypoxia-mediated repression	-

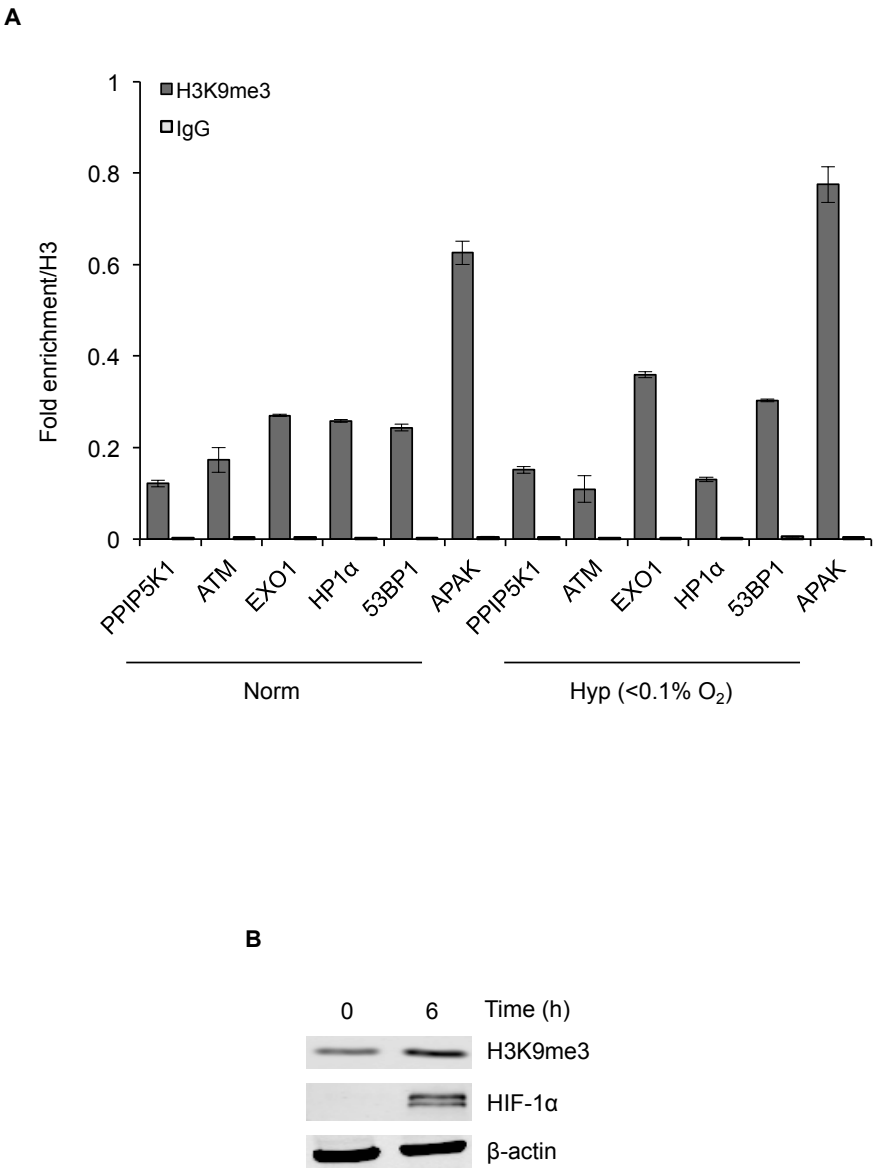


Figure 6.1. ChIP-qPCR analysis for possible enrichment of H3K9me3 binding on DDR/DNA repair genes in hypoxia

(A) RKO cells were exposed to either Norm (21% O_2), or Hyp (6 h, <0.1% O_2). The fold enrichment of H3K9me3 on the indicated genes was assessed by ChIP followed by qPCR. *PP1P5K1* was chosen as a control gene with minimal H3K9me3-binding. Error bars indicate error between technical replicates, n=2. (B) RKO cells were exposed to the same conditions as in (A) during the same experiment. Western blotting was carried out for the indicated proteins. β-actin was used as the loading control.

6.2.2 APAK is repressed in an oxygen dependent manner

We decided to focus on validating *APAK* as a gene potentially repressed in an H3K9me3 dependent manner in hypoxia. This gene not only displayed a high baseline level of H3K9me3 but the enrichment of this histone mark was significantly upregulated upon exposure to hypoxia (Figure 6.1A). Hypoxia-induced H3K9me3 binding was verified using the same sets of primers as we had done initially, as well as using an additional set of primers targeting another region also associated with high H3K9me3 binding on the UCSC browser (Figure 6.2A/B). Importantly, these new ChIP-qPCR analyses validated the enrichment of this histone modification specifically in hypoxia. Notably, this enrichment was decreased following reoxygenation mirroring the oxygen dependent global changes in this histone mark previously assessed by western blotting (Figure 4.1). As expected, ChIP-qPCR analysis of a negative control region displaying minimal H3K9me3 binding on the UCSC browser profile, showed minimal H3K9me3 enrichment in normoxia, hypoxia and reoxygenation, suggesting the previously observed H3K9me3 enrichment was specific (Figure 6.2C). Remarkably data on the UCSC genome browser not only showed H3K9me3 binding along the *APAK* gene but also displayed a proportion of the gene correlating with regions associated with heterochromatin, as shown in light grey and underlined in dark red on the right hand side of the image (Figure 6.3A). Note, that this is only a representative image of chromatin state segmentation as assessed by computationally integrating ChIP-seq data using a Hidden Markov Model (HMM) as described in (Ernst and Kellis, 2010). While we cannot assume that the profile for the RKO cell line in hypoxia would show similar chromatin states, this predicted chromatin state segmentation is supportive of this gene being

transcriptionally silenced by heterochromatin associated chromatin marks such as H3K9me3 (Figure 6.3A).

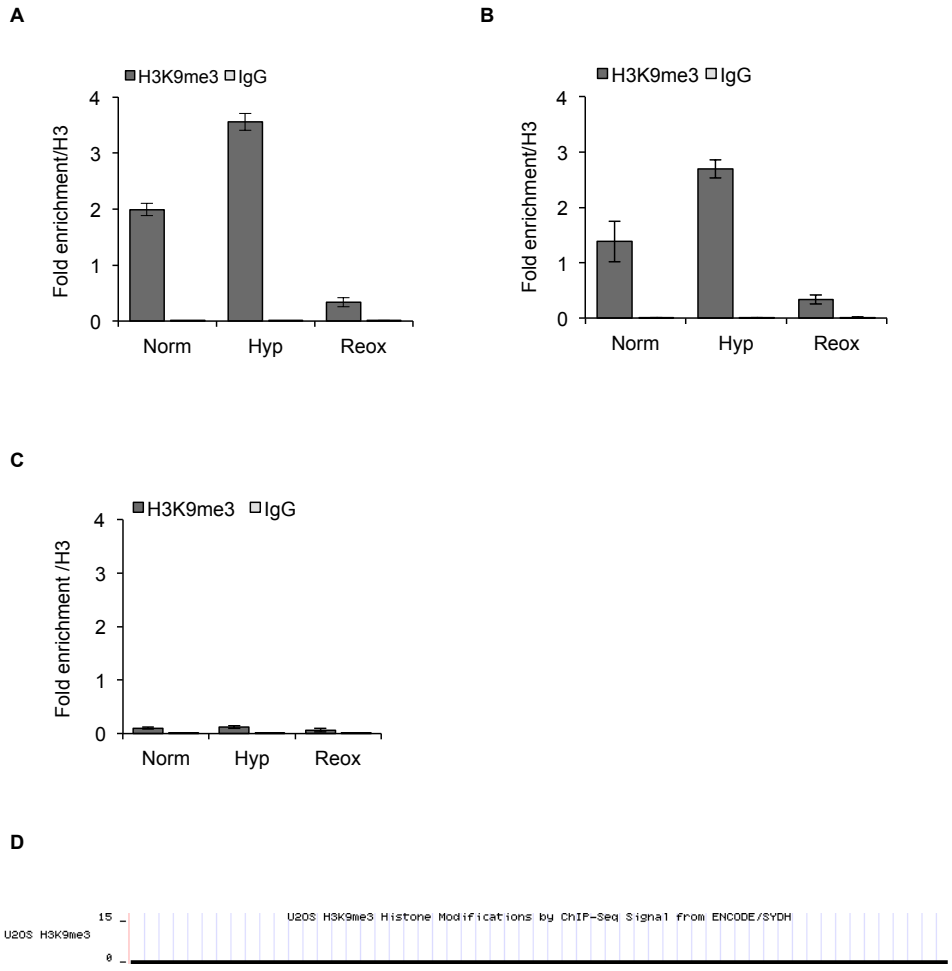


Figure 6.2. Specific H3K9me3 enrichment on *APAK* in response to hypoxia

(A) RKO cells were exposed to either Norm (21% O_2), Hyp (6 h, <0.1% O_2) or Reox (6 h, <0.1% O_2 followed by 1 h of 21% O_2). H3K9me3 fold enrichment at the *APAK* loci was assessed by ChIP followed by qPCR for each sample. (**B**) RKO cells were exposed to the same conditions as in (A) and ChIP analysis was carried out to assess the level of H3K9me3 fold enrichment as before but with a new set of primers, n=3. (**C**) RKO cells were exposed to the same conditions as in (A). The fold enrichment of H3K9me3 on a region along the *APAK* gene where minimal binding was expected was assessed by ChIP as above (assembly used: GRCh37/hg19). In each case a representative graph is shown with error bars indicating the standard error between technical replicates. **(D)** ChIP-seq track for the control region chosen as displayed in the UCSC genome browser is shown.

We next considered whether the observed H3K9me3 enrichment on *APAK* correlated with a decrease in mRNA levels of this gene in an oxygen dependent manner. To test this hypothesis we exposed RKO cells to 21%, 2% or <0.1% O_2 as well as subsequent reoxygenation (from <0.1% O_2). *APAK* mRNA levels were found to be significantly repressed at <0.1% O_2 but not in milder hypoxic condition (2% O_2) (Figure 6.3B). Furthermore, in line with the oxygen dependent regulation of H3K9me3 (Figure 4.1), *APAK* mRNA levels were not repressed following reoxygenation (Figure 6.3B). Interestingly, APAK protein levels were reduced after prolonged exposure to <0.1% O_2 (Figure 6.3C). Assessment of *APAK* mRNA levels in the matched RKO HIF-1$\alpha^{+/+}$ HIF-1$\alpha^{-/-}$ cell line pair suggested that the hypoxia-induced decrease in *APAK* expression was HIF-1α independent (Figure 6.4A). Further analysis, albeit preliminary, suggested that HIF-2α was unlikely to play a role in hypoxia-mediated *APAK* repression since HIF-1β siRNA-mediated knockdown did not affect *APAK* repression (Figure 6.4B). The specific and seemingly HIF-1α independent transcriptional regulation of *APAK* in response to <0.1% O_2 was consistent with the oxygen dependent regulation of H3K9me3, supporting the hypothesis that this chromatin mark may be involved in repressing this gene in response to severe hypoxia.

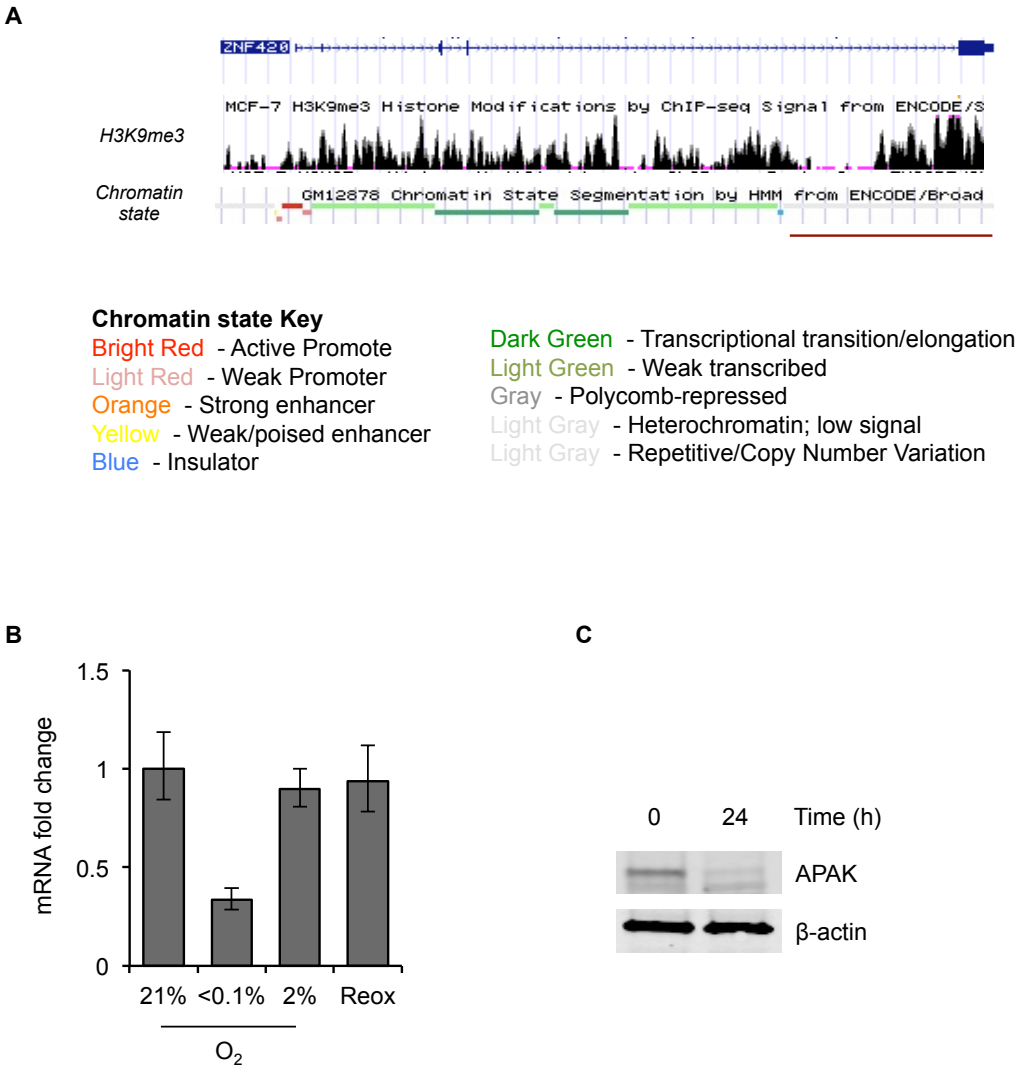


Figure 6.3. *APAK* is repressed in an oxygen dependent manner
(A) Track showing H3K9me3 binding along *APAK* in MCF cells as displayed on UCSC genome browser. A representative schematic of a possible set of chromatin state segmentation along the *APAK* gene is also shown (assembly used: GRCh37/hg19) **(B)** The mRNA levels of *APAK* were measured by qPCR in RKO cells exposed to either 21%, <0.1% or 2% O_2 (for 6 hours) or Reox (6 h, <0.1% O_2 followed by 2 h of 21% O_2), n=3 All mRNA levels were normalised to *18S* and expressed as fold change. Error bars indicate error between technical replicates. **(C)** RKO cells were exposed to hypoxia (<0.1 % O_2) for the times indicated. Western blotting was carried out for APAK. β-actin was used as the loading control.

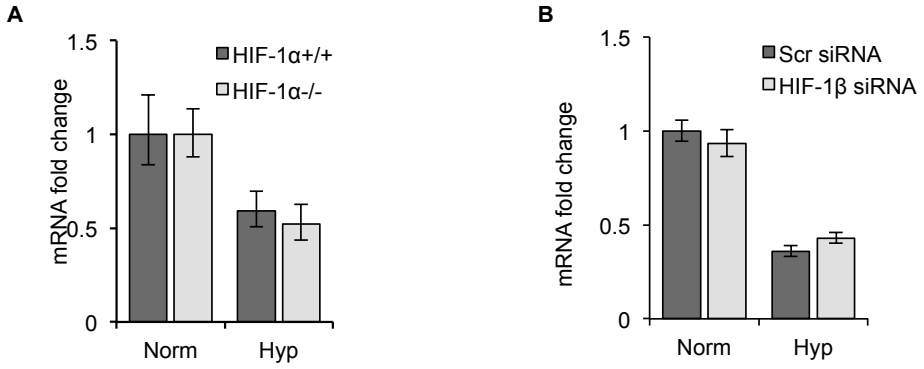


Figure 6.4. *APAK* is repressed in HIF-1 independent manner
(B) *APAK* mRNA levels were measured by qPCR in RKO HIF-1 $\alpha^{+/+}$ and HIF1 $\alpha^{-/-}$ cells exposed to Norm (21% O_2) or Hyp (16 h, <0.1% O_2), n=3. Data generated with assistance from Nur Firdaus Isa. **(B)** RKO cells treated with scramble (Scr) or HIF-1β siRNA and exposed to Norm (21% O_2) or Hyp (16 h, <0.1% O_2). *APAK* mRNA levels were assessed by qPCR, n=2. All mRNA levels were normalised to *18S* and expressed as fold change. Evidence of HIF-1α loss and HIF-1β knockdown is shown in Figure 4.4. Error bars indicate error between technical replicates.

6.2.3 SETDB1 is involved in mediating *APAK* repression in hypoxia

When designing *APAK* primers to be used for the initial ChIP analysis we noticed that the chosen region of H3K9me3 binding also showed binding of the methyltransferase SETDB1. To test the involvement of this methyltransferase in mediating *APAK* repression in hypoxia we treated RKO cells with siRNA to SETDB1. Knockdown of SETDB1 resulted in partial re-expression of *APAK* mRNA levels in hypoxia, while having no effect on *APAK* expression in normoxia or reoxygenation (Figure 6.5A/B).

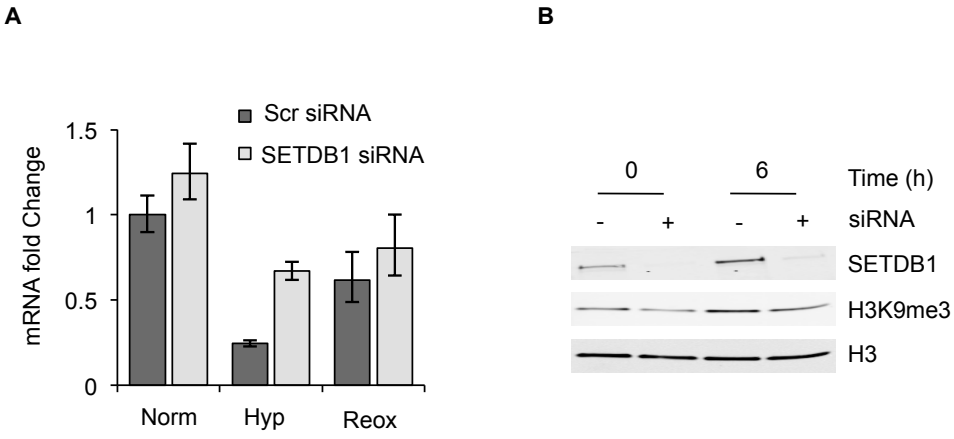


Figure 6.5. *APAK* is repressed in a SETDB1 dependent manner
(A) RKO cells were treated with scramble (Scr) or SETDB1 siRNA and exposed to Norm (21% O_2), Hyp (6 h, <0.1% O_2) or Reox (6 h, <0.1% O_2 followed by 2 h of 21% O_2). *APAK* mRNA levels were assessed by qPCR, n=3. All mRNA levels were normalised to *18S* and expressed as fold change. Error bars indicate error between technical replicates for the represented experiment. **(B)** Western blotting was carried out in RKO cells treated with SETDB1 siRNA as in (A) with the indicated antibodies to validate SETDB1 siRNA-mediated knockdown.

Next, we investigated if other methyltransferases besides SETDB1 could mediate hypoxia dependent *APAK* repression. G9a can mediate both H3K9 mono- and dimethylation, which can serve to facilitate subsequent H3K9me3 spreading (Jenuwein et al., 1998; Tachibana et al., 2001; Tachibana et al., 2002). siRNA-mediated depletion of G9a did not have a significant effect on *APAK* repression, although interestingly G9a protein levels appeared to be slightly increased in hypoxic conditions (Figure 6.6A/B). The same results were obtained by using a specific G9a inhibitor, UNC0642, despite the decrease in H3K9me2 and H3K9me3 observed following treatment with increasing concentrations of the inhibitor (Figure 6.6C/D).

Importantly, this inhibitor has been shown to have more than 20000-fold selectivity for G9a over 13 other tested methyltransferases including SETDB1 (Liu et al., 2013).

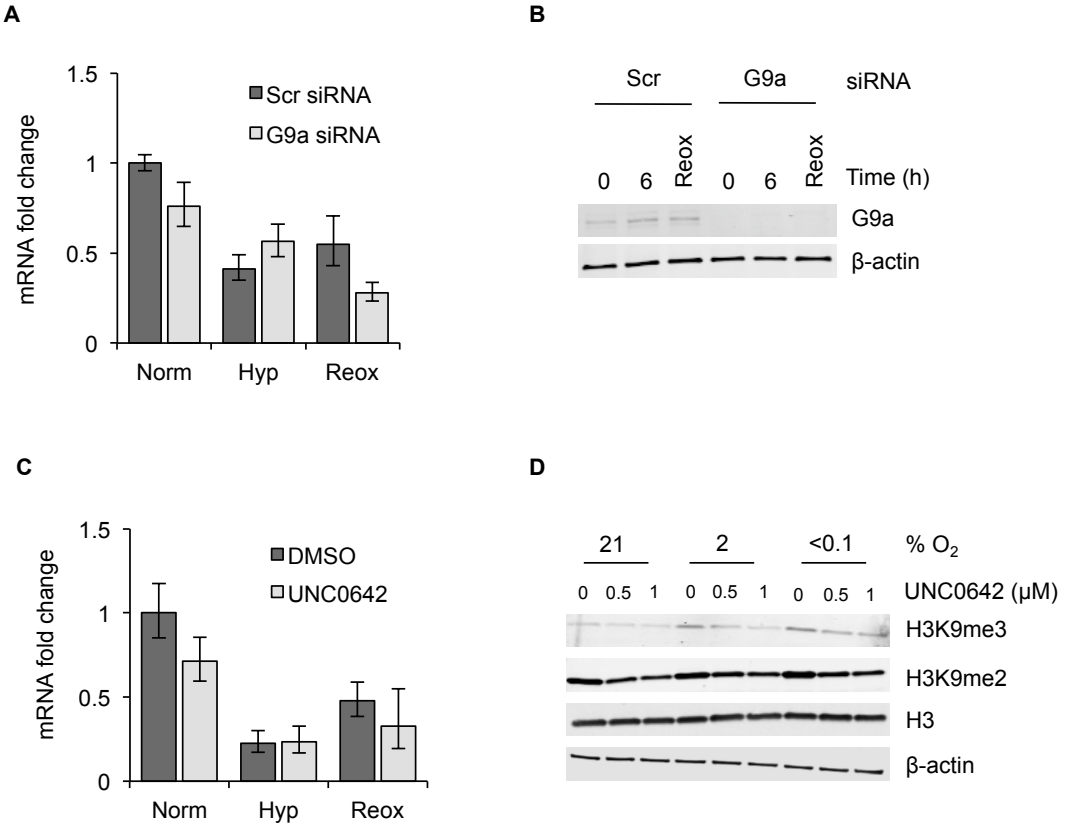


Figure 6.6. *APAK* is repressed in G9a independent manner
(A) RKO cells were treated with G9a or scramble (Scr) siRNA and exposed to Norm (21% O_2), Hyp (6 h, <0.1% O_2) or Reox (6 h, <0.1% O_2 followed by 2 h of 21% O_2). *APAK* mRNA levels were assessed by qPCR, n=2. **(B)** Western blotting was carried out following treatment of RKO cells with either G9a or scramble siRNA. G9a protein levels were used to assess G9a siRNA efficiency; β-actin was used as loading control. **(C)** RKO cells were treated with G9a inhibitor, UNC0642 (1 μM) and exposed to the same hypoxia/reoxygenation treatments as in (A). *APAK* mRNA levels were assessed by qPCR, n=3. In both (A) and (C) mRNA levels were normalised to *18S* and expressed as fold change. Error bars indicate error between technical replicates for the represented experiment. **(D)** RKO cells were treated with UNC0642 at the indicated range of concentrations and exposed to 21%, 2%, or <0.1% O_2. Western blotting was carried out as indicated. β-actin was used as the loading control. Data generated with assistance from Dr Joana Senra.

Finally, we tested the possible involvement of the Suv39h1 methyltransferase on hypoxia-mediated *APAK* repression. To do so we used the shSuv39h1/2 stable RKO cell line described in Chapter 4 (Figure 4.7). In these cells we noticed that Suv39h1 loss did not lead to a significant effect on *APAK* repression (Figure 6.7). Suv39h2 could contribute to *APAK* repression; however, this could not be investigated here due to the technical difficulties described previously. Taken together, these data suggest that SETDB1 is likely the principal methyltransferase involved in mediating *APAK* repression in hypoxia.

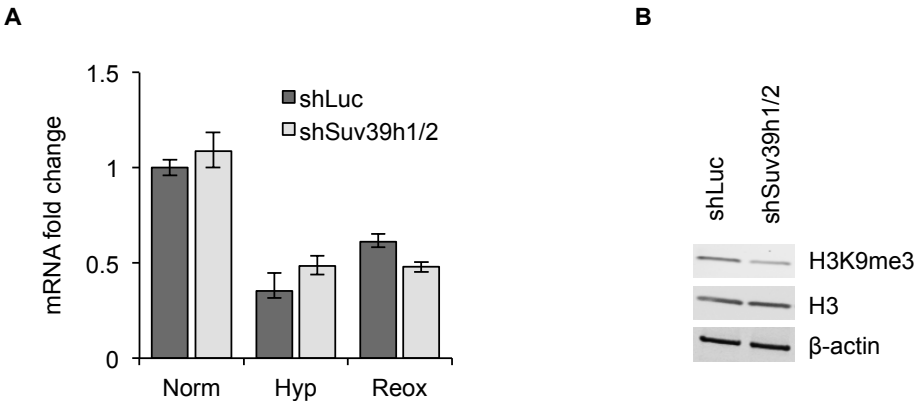


Figure 6.7. *APAK* is repressed in a Suv39h1 independent manner
(A) *APAK* mRNA levels were measured by qPCR in RKO cells treated either with shLuc or shSuv39h1/2 and exposed to Norm (21% O_2), Hyp (6 h, <0.1% O_2) or Reox (6 h, <0.1% O_2 followed by 2 h of 21% O_2), n=3. mRNA levels were normalised to *18S* and expressed as fold change. Error bars indicate error between technical replicates for the represented experiment. **(B)** Western blotting was carried out with RKO cells treated with either shRNA against Luc or Suv39h1/2 with the indicated antibodies. Levels of H3K9me3 were assessed as readout of Suv39h1/2 knockdown. β-actin was used as the loading control.

6.2.4 APAK and p53-mediated apoptosis

APAK repression specifically in response to severe hypoxia was consistent with a requirement for APAK regulation only under conditions where p53 is active, and is known to have a role in mediating apoptosis. If APAK could also serve as a negative regulator of p53 dependent apoptosis in hypoxia, we would predict that APAK overexpression would lead to a decrease in hypoxia-induced apoptosis. In support of this hypothesis, transfection of a MYC-tagged APAK construct resulted in a decrease in the number of RKO cells undergoing apoptosis when exposed to severe hypoxia, as assessed by PARP cleavage and nuclear morphology (Figure 6.8). The increase in apoptotic markers within the timeframe of H3K9me3 induction shown here to negatively correlate with APAK expression, support our hypothesis that H3K9me3 dependent regulation of APAK may be important for optimal apoptosis induction in a wild-type p53 background in hypoxia.

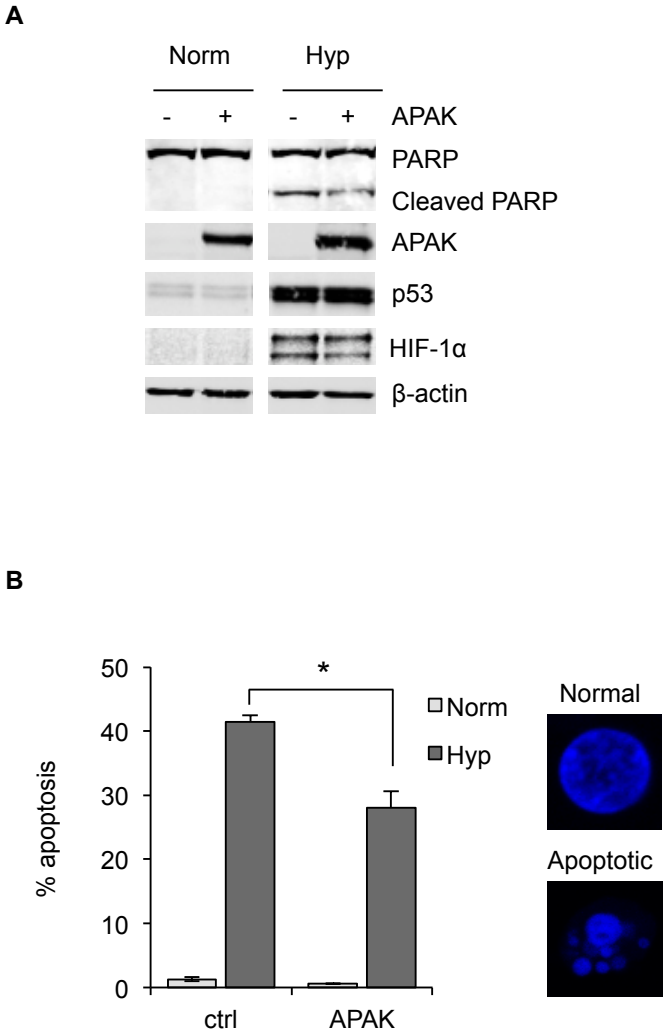


Figure 6.8. *APAK* overexpression leads to reduced apoptosis in hypoxia
(A) RKO cells were transfected with MYC-tagged APAK (+) or MYC-empty (-) plasmids and were exposed to Norm (21% O_2) or Hyp (18 h, <0.1% O_2). Western blotting was carried out with the indicated antibodies. β-actin was used as loading control. **(B)** RKO cells were treated as in (A) and apoptotic cells were counted. The graph represents the number of apoptotic/non-apoptotic cells expressed as a % of the whole population, n=3. A representative image of normal and apoptotic cells is also shown. Error bars indicate standard error between the 10 fields of view counted for the representative experiment shown. Data generated with the assistance of Dr Katarzyna Leszczynska

6.3 DISCUSSION

Having taken a candidate approach to identify DNA repair/DDR genes that may be regulated in hypoxia in an H3K9me3 dependent manner, we identified three potential candidates: *53BP1*, *EXO1* and *APAK*. Despite the fact that the ChIP-qPCR analysis carried out was preliminary, the significant H3K9me3 enrichment on *53BP1* and *EXO1* observed could be interesting to validate in future studies (Figure 6.1). Failure to detect significant H3K9me3 enrichment (above the baseline set by the control gene, *PP1P5K1*) for genes that had previously been shown to have H3K9me3 binding probably reflects differences in H3K9me3 binding between different cell lines and within the different experimental conditions used.

Following this initial analysis we chose to investigate the gene showing the highest levels of H3K9me3 enrichment in hypoxia. Here, we provide evidence to demonstrate that one of the consequences of hypoxia-induced H3K9me3 is the repression of *APAK* mRNA levels (Figures 6.2/3). Interestingly, SETDB1 appears to be the principal methyltransferase involved in regulating the expression of this gene since loss of Suv39h1 or G9a did not affect *APAK* expression in hypoxia (Figures 6.5-6.7). Suv39h2 could also play a role and this could not be investigated in this study for technical reasons. H3K9me3-mediated repression of *APAK* may have an important role in appropriate regulation of apoptosis in hypoxia, since APAK overexpression under these conditions resulted in significant decrease in apoptotic markers (Figure 6.8).

Hypoxia has been proposed to compromise genomic stability in tumours, in part by causing the repression of a variety of DNA repair genes and pathways (Bristow and Hill, 2008). In conditions of severe hypoxia, however, the activation of the DDR

may work to mount a barrier to tumourigenesis (Pires et al., 2010b; Squatrito et al., 2010). The activation of p53 as part of this DDR will contribute to such barrier by leading to p53 dependent apoptosis and, therefore, elimination of cells that if allowed to survive would likely contribute to the worsening of genomic instability and progression to a more malignant phenotype (Graeber et al., 1996). At least in this respect, the mechanism of *APAK* repression, as well as the function described here, are consistent with the function of p53 in this context. Future studies could be designed to investigate if the mechanism by which APAK overexpression leads to a decrease in apoptosis is indeed due to negative regulation of p53 or whether APAK regulates apoptosis via other mechanisms in hypoxia.

Furthermore, it could be envisioned that exploiting alternative approaches of mediating APAK downregulation may result in increased apoptosis in p53-proficient cells under a range of hypoxic conditions. The use of inhibitors to H3K9me3 demethylases, for example, would be predicted to result in an increase in H3K9me3 levels, and potentially a reduction in APAK. It would be interesting to test if the use of these inhibitors could result in APAK repression under conditions where this gene is not normally downregulated (such as mild hypoxia). The use of specific demethylase inhibitors in combination with DNA damaging agents (that would induce p53) would then be predicted to result in an increase in p53 dependent apoptosis potentially increasing sensitivity to these DNA damaging agents.

ATM dependent APAK phosphorylation and dissociation from p53 has been previously involved in facilitating p53 dependent transcriptional activity following methyl methanesulfonate, etoposide, camptothecin, cisplatin and dox treatment (Wang et al., 2010). Since severe hypoxia also results in ATM phosphorylation and activation, it is possible that phosphorylation of any remaining APAK protein under

these conditions further contributes to facilitating p53 dependent apoptosis, a possibility that could be tested in future studies.

Interestingly, *APAK* is located within a cluster of zinc-finger genes on chromosome 19. This cluster has been proposed to have evolved to facilitate HERV (human endogenous retroviral) silencing through KAP-1/SETDB1 dependent H3K9me3 spreading (Lukic et al., 2013). In this recent study, the authors propose that tethering of KAP-1 by interaction between its KRAB-binding domain and the KRAB domain in KRAB-ZNF genes such as *APAK*, could lead to the appropriate silencing of new HERV incorporating in the germ line. This study proposed that *APAK* itself would probably be involved in the silencing of HERV17-int (Lukic et al., 2013). This would provide an alternative role for APAK besides its function as a negative regulator of p53 dependent apoptosis, again maintaining genomic stability by preventing the aberrant re-expression of HERVs. Importantly, many of the features adopted to allow survival under hypoxic conditions by cancer cells are remnants of developmental adaptations (Papandreou et al., 2005). It would be interesting to determine whether the same mechanisms evolved to keep HERV sequences at bay during embryonic development are also in place in the hypoxic cancer cell. If this were to be the case, the hypoxia and SETDB1-mediated repression of *APAK* shown here could lead to a compromise in such repression in hypoxic cancer cells, leading to potential re-expression of endogenous retroviruses such as HERV17-int. If other ZNF genes on the cluster in chromosome 19 are also epigenetically regulated in hypoxia via H3K9me3, it is possible that this could be a widespread mechanism of retroviral re-expression in hypoxia. Such re-expression could enhance genomic instability highlighting how hypoxia-mediated epigenetic mechanisms can act as a double-edged sword in either preventing or worsening genomic instability in tumours. It is possible

that the differential effects exerted on genomic stability maintenance by hypoxia-induced H3K9me3 repression of genes such as *APAK*, may depend on the genetic background of the cancer cells under study, as well as the stage in tumourigenesis being considered.

CHAPTER 7

GENERAL DISCUSSION

We have shown that replication stress results in ATM activation in the absence of detectable DNA damage only when cells are also exposed to hypoxia, which provides a specific chromatin context. We have used severe hypoxia (<0.1% O_2), Hu and oncogene overexpression as sources of replication stress in this study (Figure 7.1). We demonstrate that one of the key components of this chromatin context is H3K9me3. In particular, we propose that when replication stress occurs in a chromatin context with "heterochromatin-like" features, such as increased H3K9me3; ATM is required to maintain appropriate DNA replication and prevent the accumulation of DNA damage. Our data, therefore, supports the hypothesis that the chromatin context in which replication stress occurs can strongly influence the DDR activated as a consequence of such stress. We propose that chromatin changes, including H3K9me3, can both facilitate ATM activation and lead to a requirement for the activity of this kinase following replication stress. Furthermore, we demonstrate that H3K9me3 may play a role in facilitating p53 dependent apoptosis in hypoxia through repression of the negative regulator of p53, APAK. The impact of this chromatin mark in contributing to the signalling of important DDR players, such as ATM or p53, underpins the importance of the study of the chromatin context when considering DDR signalling. While we have focused on H3K9me3, it is evident that other chromatin marks will

likely play a role in facilitating ATM activation and DDR signalling in general in response to hypoxia.

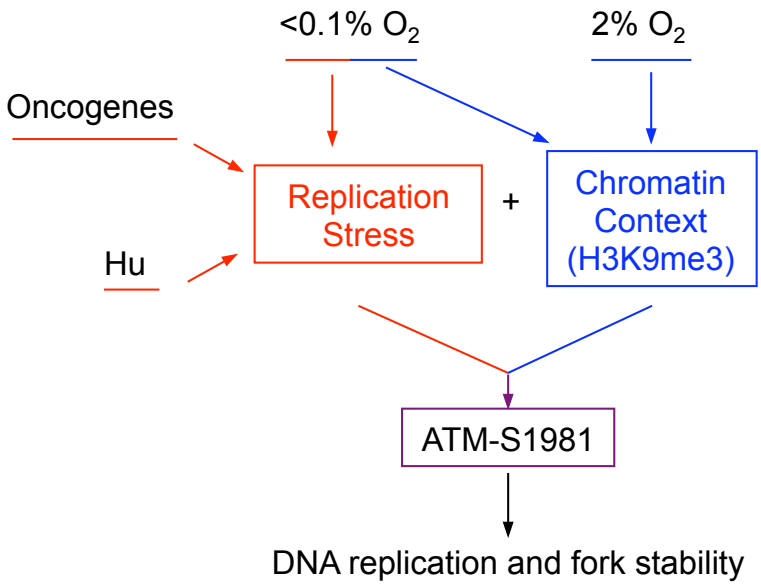


Figure 7.1. Schematic representation of our model of ATM activation and function in hypoxia
Replication stress in the absence of DNA damage induced by either: hypoxia (<0.1% O_2), oncogene expression or Hu treatment, leads to ATM activation and downstream signalling only in the hypoxia-induced chromatin context. As demonstrated, one of the critical components of this chromatin context is H3K9me3. Once active, ATM is involved in preventing the accumulation of DNA damage and maintaining DNA replication.

7.1 ATM and its role in replication in an H3K9me3-rich context

Interestingly, ATR and ATM have been previously reported to regulate origin firing during unperturbed replication with transient ATM activity being detected during ongoing replication in the absence of replication stress in *Xenopus laevis*. The authors of this study proposed that regulation of CDK2 or CDC7 by ATR and ATM could regulate origin firing during replication (Shechter et al., 2004). In contrast, here, we provide a stress-specific role for ATM in maintaining DNA replication rates in response to hypoxia-induced replication stress in RKO colorectal cancer cells. Furthermore, following reoxygenation-induced replication restart, we demonstrate that ATM inhibition results in increased origin firing. We did not observe any significant effects on origin firing or replication rates following ATM inhibition/loss in the absence of stress. Differences between *Xenopus laevis* and human cancer cells could provide a possible explanation for the difference in requirement for baseline ATM activity during replication. Of note, Gautier and colleagues have previously reported that in *Xenopus laevis* egg extracts DSB may be generated during normal DNA replication. Furthermore, MRE11 phosphorylation following DSB generation during DNA replication has been proposed to be important for the repair of the DSB generated during normal DNA replication in *Xenopus laevis* (Costanzo et al., 2001). The generation of DSB breaks in *Xenopus* egg extracts could explain the requirement for ATM activation during normal replication in this system.

Importantly, the unscheduled origin firing reported here to occur in response to reoxygenation, may lead to increased DNA damage in a context where significant ROS-induced damage will already be present, and where the DNA repair capabilities of the cell may be reduced (Bristow and Hill, 2008). Loss of ATM in this context may, therefore, lead to an increase in genomic instability. Interestingly, in response to

hypoxia, ATM inhibition/loss resulted in a decrease in DNA replication rates with no changes in origin firing (data not shown). These observations suggest that ATM is probably not directly regulating the classical S-phase checkpoint under these conditions, again underscoring the differences between hypoxia-induced ATM activity and ATM activation following DSB. However, it is possible that ATM might be signalling to checkpoint proteins such as CHK1 or CHK2, which may have functions different from their "classical" checkpoint regulation activities in this context.

Elegant studies point to the importance of maintaining appropriate histone deposition and recycling in response to replication stress. Furthermore, recovery of stalled replication forks and appropriate replication restart involves the co-ordinated action of multiple factors and it has been proposed that a specific set of chromatin changes might also be required for these processes (Jasencakova et al., 2010; Sirbu et al., 2011). Little is known about what chromatin reassembly or histone deposition events take place during and/or following hypoxia-induced replication stress. The appropriate replication of the complex set of hypoxia-induced histone modifications will be important for inheritance of epigenetic information. We have shown that H3K9me3 is enriched at or around replication forks in response to replication stress during hypoxia, and that it is reduced upon reoxygenation-induced replication restart. One possible role for ATM in resolving hypoxia-induced replication stress may be in the co-ordination of appropriate histone deposition during the slow replication that occurs in hypoxia (Figure 7.2). The SWI/SNF chromatin remodeller SMARCAD1 has been shown to mediate appropriate chromatin maturation by forming a complex with KAP-1/HDAC1/2 and G9a, allowing H3K9me3 deposition and histone deacetylation following replication (Rowbotham et al., 2011).

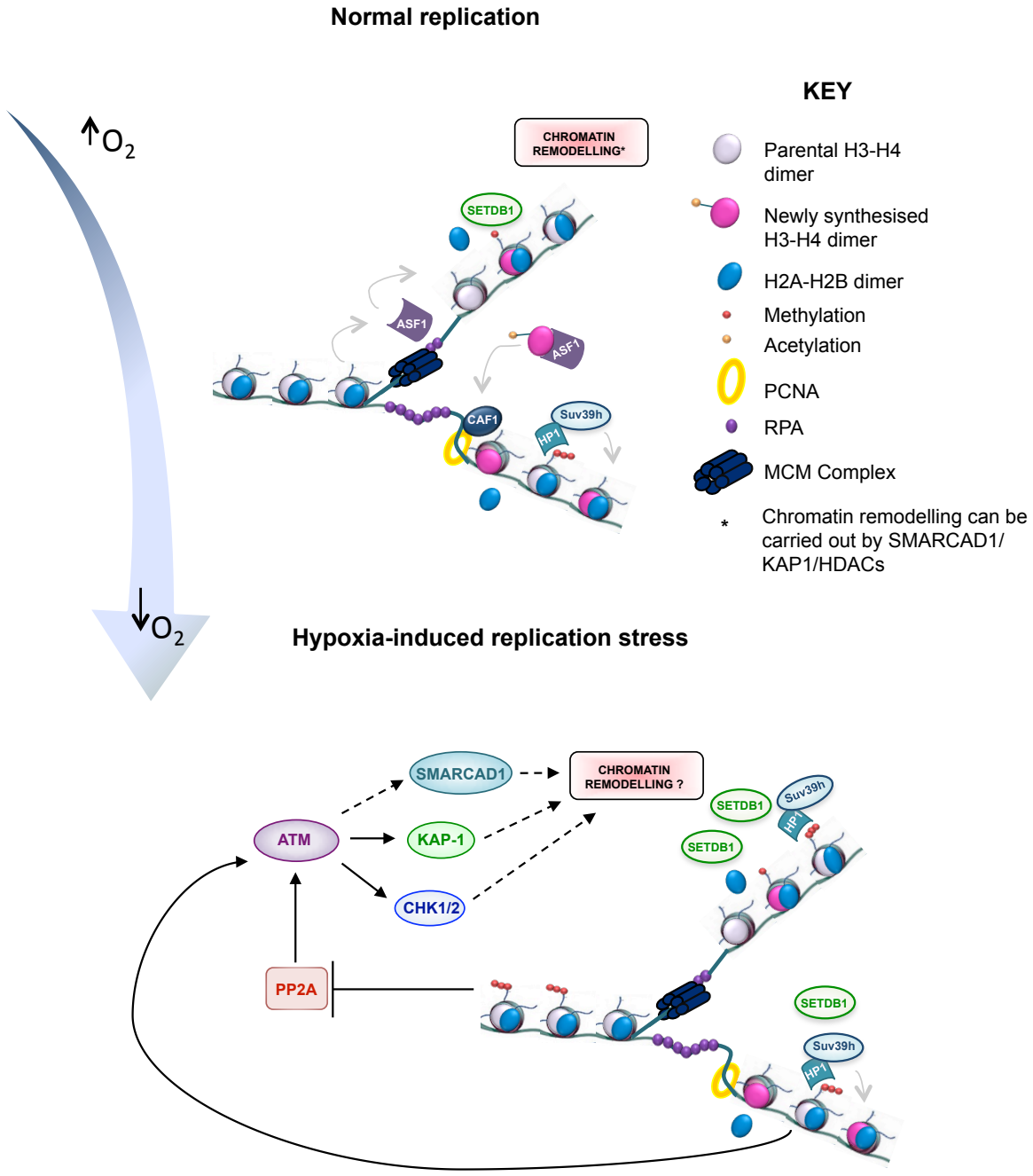


Figure 7.2. Chromatin maturation regulation during replication in response to normoxia and hypoxia
Schematic representation of the proposed differences between chromatin remodelling occurring during normal replication, as well as under hypoxia-induced replication stress. One of the consequences of global increases in H3K9me3 may be the repression of PP2A, which could contribute to ATM-mediated signalling in severe hypoxia (0.1% O_2). Adapted from (Alabert and Groth, 2012).

Importantly, SMARCAD1 has a predicted S/T-Q phosphorylation site (Matsuoka et al., 2007). Studies aimed at deciphering whether phosphorylation at this site could affect the activity of this chromatin remodeller could be undertaken. ATM dependent SMARCAD1 phosphorylation in response to replication stress could facilitate appropriate propagation of H3K9me3 following replication stress in hypoxia (Figure 7.3). Furthermore, ASF1, a chaperone with known roles in maintaining histone deposition and recycling during replication stress is repressed under hypoxic conditions (Groth et al., 2005; Pires et al., 2010a). The limited amounts of this H3K9me3 chaperone in hypoxia may contribute to the abundance of this histone mark in areas around the replication fork despite the presence of replication stress. Failure to chaperone this chromatin mark in hypoxia, could exacerbate replication stress and could contribute to the necessity to activate ATM to resolve such stress. In response to UV or IR, ATM-CHK1 signalling can lead to the phosphorylation of TLK1 at S695, an event that may serve to regulate ASF1 function during S-phase (Groth et al., 2003). Appropriate co-ordination of whatever ASF1 protein may be present in hypoxia may be particularly critical and this could occur through ATM (or indeed ATR) signalling to CHK1 (Pires et al., 2010a) (Figure 7.2).

Irrespective of its downstream effector target, the evidence provided here points to a non-expected role for ATM in maintaining appropriate replication in hypoxia. The study of a role for ATM in facilitating DNA replication in response to replication stress in other contexts would be extremely interesting. The requirement for ATM/ATR for efficient replication of some DNA tumour viruses such as human papillomavirus or Kaposi's sarcoma-associated herpesvirus (amongst others) has been described (Koopal et al., 2007; Moody and Laimins, 2009; Singh et al., 2013). In this context replication stress occurs as a consequence of the increased proliferation of

host cells following viral infection and results in the interaction of the viruses with host DDR components such as ATM (Nikitin and Luftig, 2011; Turnell and Grand, 2012). Targeting ATM in this context, specifically if the increased replication stress is also occurring in a hypoxic context, may prevent viral replication and may be an effective strategy to target these cancer types.

7.2 Hypoxia-induced chromatin changes and the absence of detectable DNA damage

The absence of DNA damage in hypoxia despite the presence of robust replication stress is intriguing and still not completely understood. Compacted chromatin has long been known to pose a barrier to DNA damage generation and DDR signalling, at least in response to IR (Costes et al., 2010; Elia and Bradley, 1992; Goodarzi et al., 2008). It would be interesting to investigate if the hypoxia-induced "heterochromatin-like" context poses a barrier to DNA damage generation, detection or both. It is possible that small amounts of DNA damage do occur in hypoxia but the enrichment of heterochromatin associated factors such as H3K9me3 masks the damage making it difficult to detect. Furthermore, signalling of any potential damage may be hindered by these chromatin changes, again preventing the detection of any damage by 53BP1 foci formation or other similar assays. The substantial H2AX phosphorylation observed in hypoxia, albeit not present in discrete foci could be used to argue that signalling may not be hampered under these conditions. Alternatively, the increased chromatin compaction that would be predicted to result from an increase in factors such as H3K9me3 or HP1β may actually protect the cells from the generation of DNA damage. This would suggest that hypoxia, with its increase in chromatin changes associated with heterochromatin, is somewhat refractory to DNA damage generation.

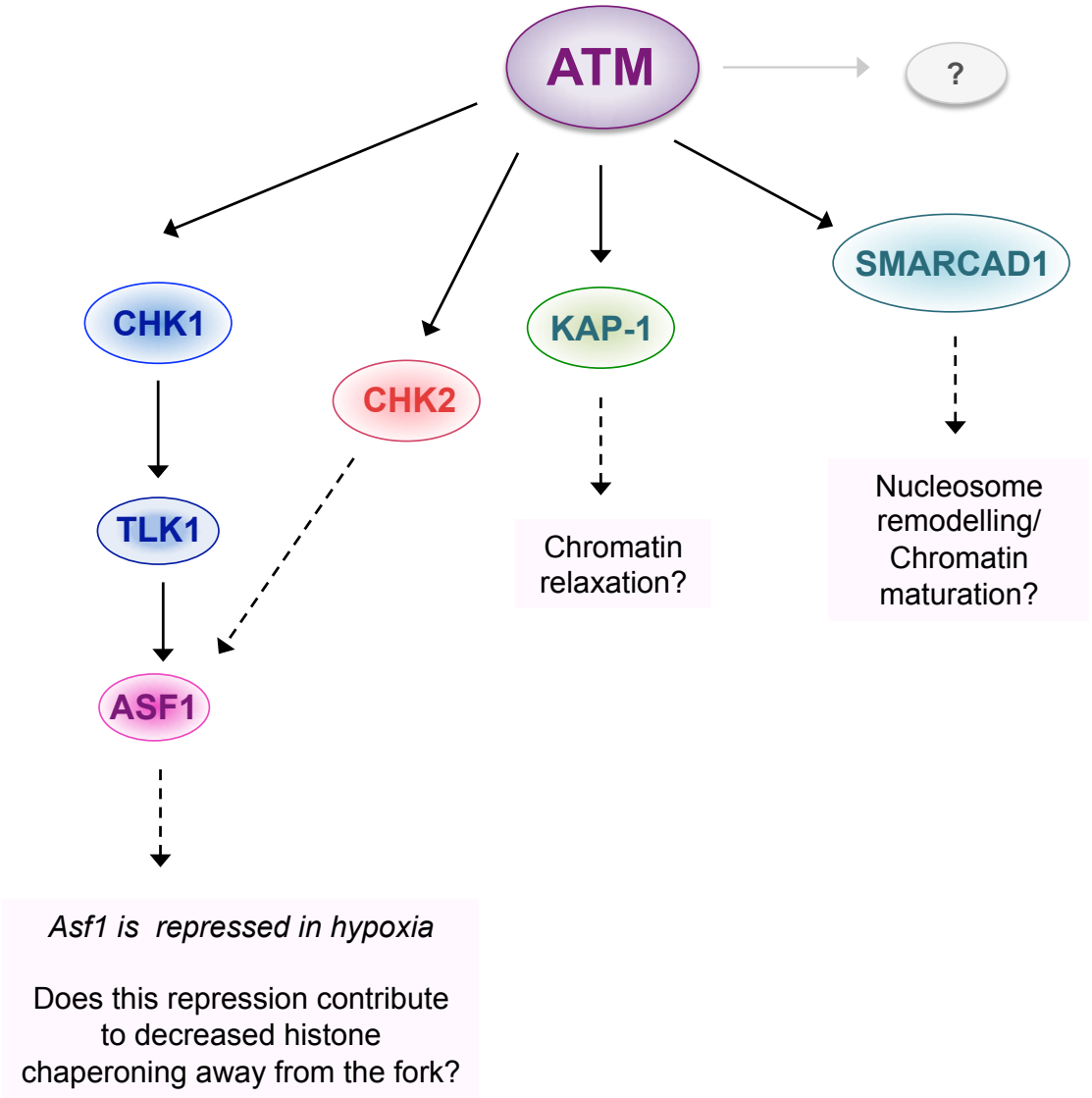


Figure 7.3. Summary of possible downstream ATM targets to be investigated in future studies
Schematic representation of the possible downstream targets of ATM that could mediate or contribute to its role in maintaining DNA replication in hypoxia.

Perhaps more importantly, it is possible that the slow but maintained replication observed in response to hypoxia prevents the collapse or breakage of replication forks even in a context where replication fork stalling and areas of ssDNA are clearly visible. Interestingly, RPA32 foci formation decreases over time in hypoxia, suggesting that regions of ssDNA may be decreased as replication progresses (Pires et al., 2010b). Endonucleases have been reported to process vulnerable or aberrant replication structures that may be formed after replication stress into DSBs (Zeman and Cimprich, 2013). We have shown preliminarily here, that H3K9me3 binding is enriched on *EXO1* in hypoxia. It is tempting to speculate that, if hypoxia-induced H3K9me3 results in EXO1 endonuclease repression, this might result in a decreased number of nucleolytic cleavage events and subsequently less probability of DSB induction despite prolonged replication stress.

7.3 Targeting the hypoxia-induced DDR and chromatin changes

The radiation resistance of hypoxic tumour cells is a major barrier to effective radiotherapy (Begg et al., 2011). Some of the chromatin changes reported here could potentially contribute to the need for increased IR doses to result in the same amount of cell kill in hypoxic conditions. The oxygen dependency in the increase in H3K9me3 shown here correlates well with the increased radioresistance observed with decreasing oxygen concentrations. Pharmacological inhibition of H3K9me3 could potentially lead to decreases in chromatin compaction that may result in an increase in the amount of DNA damage observed in hypoxia. Furthermore, we have shown that reducing H3K9me3 levels in hypoxia results in a reduction in ATM activation and, therefore, may lead to increased sensitisation of hypoxic cells to DNA-damaging therapies such as radiotherapy. Given that we have demonstrated that loss

of Suv39h1/2 leads to a decrease in ATM activation in hypoxic conditions, it is reasonable to suppose that inhibition or loss of these methyltransferases would lead to a sensitisation of hypoxic cells to radiotherapy (Ayrapetov et al., 2011; Kaidi and Jackson, 2013; Sun et al., 2005). In support of this, the use of HDAC inhibitors has recently been shown to radiosensitise tumour cells by a number of mechanisms including a hampering of ATM signalling (Sharma et al., 2013; Thurn et al., 2013). Attenuation of ATM-mediated signalling following the chromatin remodelling changes that may occur following HDAC inhibition in hypoxic conditions, may present an opportunity to radiosensitise cells under these conditions. Furthermore, targeting of Suv39h1/2 could potentially also be undertaken in combination with other agents targeting the DDR, such as ATR inhibitors, in order to further sensitise a variety of tumour types to hypoxia/reoxygenation.

7.4 Hypoxia-induced chromatin changes and ATM-mediated signalling – Break or accelerator of tumourigenesis?

Any therapeutic approach aimed at either directly targeting ATM activation or indirectly modulating the chromatin changes that are required for ATM signalling, should take into account the fact that ATM activation in the early stages of tumourigenesis may have a protective role. Inhibition of ATM function in these cases may accelerate the development of secondary or incipient malignancies. A role for Suv39h1 in preventing RAS-induced lymphoma development *in vivo* has been demonstrated, supporting the concept that Suv39h1/2-mediated regulation of ATM activity in a hypoxic context could halt tumourigenesis in response to oncogenic stress (Braig et al., 2005). We propose that the hypoxia-induced chromatin context could have a role to play in facilitating the activation of the DDR in response to replication

stress before DNA damage accumulates. Therefore, cells undergoing hyperproliferation due to oncogenic activation in a hypoxic environment would activate ATM, independently of the levels of DNA damage. This implies that the barrier to tumourigenesis induced by the DDR in hypoxic pre- or early neoplastic lesions could occur earlier than predicted and, most importantly, before the accumulation of damage in response to oncogene activation (Bartkova et al., 2005; Gorgoulis et al., 2005). Furthermore, the proposed role for H3K9me3 in facilitating hypoxia-induced p53 dependent apoptosis could contribute to such barrier.

However, the hypoxia dependent induction of the DDR early in tumourigenesis may significantly contribute to the selective pressure to lose/mutate genes such as ATM or p53 and therefore drive development of therapy resistant disease (Graeber et al., 1996; Squatrito et al., 2010). It is possible that once DDR components such as ATM or p53 have been lost or mutated, hypoxia-induced chromatin changes (and perhaps in particular H3K9me3) may then act as a double-edged sword as tumourigenesis progresses. Interestingly, chromatin changes characteristic of heterochromatin are frequently found in tumours, and we have demonstrated here that H3K9me3 correlates with hypoxic regions of the tumour *in vitro* and *in vivo*. Furthermore, Mutant K-RAS overexpression, leads to increased CDC6 induction, and CDC6 expression correlates with heterochromatic markers such as increased H3K9me3 in colon and lung cancer (Di Micco et al., 2011). The induction of H3K9me3 upon oncogene overexpression has been proposed to maintain viability of the oncogene expressing cell via protection of the genome by chromatin compaction (Sulli et al., 2012). Perhaps some of the chromatin changes observed in response to hypoxia also originally evolved in an attempt to protect genome integrity. However, a cancer cell with the potential to survive under <0.1% O_2 or under persistent oncogene

induced replication stress will probably do so since it has already acquired a markedly aggressive phenotype (Sulli et al., 2012; Vaupel, 2010). The protection of such cells by inducing a "heterochromatin-like" environment in this case may promote tumourigenesis rather than halt it. Interestingly, chromatin modifying enzymes associated with heterochromatin are not frequently lost/mutated in cancer and in fact many have been shown to be overexpressed in a variety of tumour types, as is the case of SETDB1 (Ceol et al., 2011; Rodriguez-Paredes et al., 2013). Taken together, these facts could suggest that certain chromatin changes may favour tumour development, perhaps in the later stages of tumour development and progression. It is tempting to speculate that, while hypoxia-induced chromatin changes may at the very early stages of neoplasia facilitate the barrier to tumourigenesis by facilitating DDR activation, they may in later stages become part of the response adopted by the tumour to survive. At later stages in tumourigenesis, increases in H3K9me3 may thus become one more of the weapons hijacked by the tumour to survive and thrive under hypoxic conditions. Future therapeutic strategies aimed at targeting chromatin changes or ATM signalling should take these considerations into account.

APPENDICES

APPENDIX A

Published papers

1) Reprinted from Molecular Cell, 52, 5, **Olcina, M.M.,** Foskolou, I.P., Anbalagan, S., Senra, J.M., Pires, I.M., Jiang, Y., Ryan, A.J and Hammond, E.M., Replication Stress and Chromatin Context Link ATM activation to a Role in DNA replication, 758,766, Copyright 2013, with permission from Elsevier.†
2) Reprinted with permission from ACS chemical biology, 8,7, Cazares-Korner C., Pires, I.M., Swallow, I.D., Grayer, S., O'Connor, L., **Olcina, M.M**., Christlieb, M., Conway, S.J. and Hammond, E.M., CH-01 is a hypoxia-activated prodrug that sensitizes cells to hypoxia/reoxygenation through inhibition of Chk1 and Aurora A, 1451,1459. Copyright 2013 American Chemical Society.
3) Reprinted with permission from, Journal of Medicinal Chemistry, 56, 8, Hewings, D.S., Fedorov, O., Filippakopoulos, P., Martin, S., Picaud, S., Tumber, A., Wells, C., **Olcina, M.M.,** Freeman, K., Gill, A., Ritchie, A.J., Sheppard, D.W., Russell, A.J., Hammond, E.M., Knapp, S., Brennan, P.E. and Conway, S.J., Optimization of 3,5-dimethylisoxazole derivatives as potent BET bromodomain ligands, 3217-3227. Copyright 2013 American Chemical Society.
4) Reprinted by permission from Macmillan Publishers Ltd: Cell Death and Disease, 3, Fokas, E., Prevo, R., Pollard, J.R., Reaper, P.M., Charlton, P.A., Cornelissen, B., Vallis, K.A., Hammond, E.M., **Olcina, M.M**., McKenna, W.G., Muschel, R.J. and Brunner, T. B., Targeting ATR in vivo using the novel inhibitor VE-822 results in selective sensitization of pancreatic tumors to radiation, e441, Copyright 2012.
5) Reprinted by permission from Macmillan Publishers Ltd: British Journal of Cancer, 107, Pires, I.M., **Olcina, M.M.**, Anbalagan, S., Pollard, J.R., Reaper, P.M., Charlton, P.A., McKenna W.G. and Hammond, E.M., Targeting radiation resistant hypoxic tumour cells through ATR inhibition. 291-299, Copyright 2012.
6) Reprinted with permission from Clinical Cancer Research, 16, **Olcina M.,** Lecane, P.S., and Hammond, E.M., Targeting hypoxic cells through the DNA damage response. 5624-5629. Copyright 2010

† Most of the data included in Chapters 3, 4 and 5 are part of this publication.

APPENDIX B

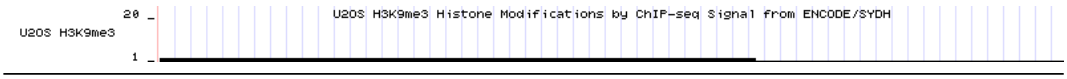
B.1. Validation of ATM phosphorylation in MEFs



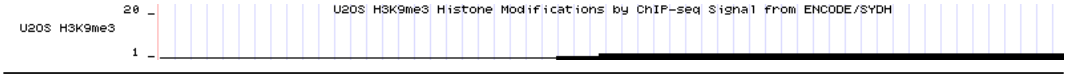
Figure B.1. Validation of ATM phosphorylation in MEFs using a monoclonal antibody with reactivity towards mouse ATM
Suv39h1/2$^{+/+}$ and Suv39h1/2$^{-/-}$ MEFs were treated as indicated. Western blotting was carried out using the indicated antibodies. The ATM-S1987 antibody was produced from a synthetic peptide corresponding to amino acids 1974-1988. β-tublin was used as a loading control.

B.2. Details of primers used in Chapter 6 (Figure 6.1)

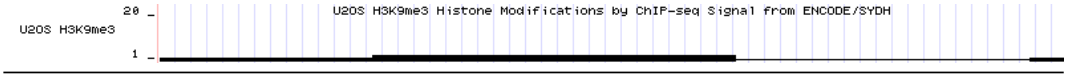
Gene	Length	Product size	Tm	% GC	5'-3'	Position
ATM	20	82	59.99	50	L: GCTGTCTTTCTGCCATGTGA	chr11:108,109,923-108,110,004
	20		59.82	50	R: ATTGTGGGTTTCTGGTGAGG	



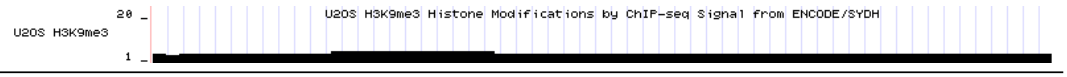
Gene	Length	Product size	Tm	% GC	5'-3'	Position
EXO1	20	64	59.90	50	L: GGAGAAACCCTGATTGGACA	chr1:242,017,982-242,018,045
	20		60.34	50	R: CCAAGAACCCACCAATTCTG	



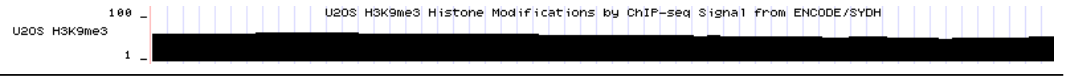
Gene	Length	Product size	Tm	% GC	5'-3'	Position
HP1α/CBX5	21	77	59.69	47.62	L:GAGGGCATCTTCTGATTGTTG	chr12:54,650,094-54,650,170
	20		60.78	45	R: CATGCATTGCAGGATGCTTA	



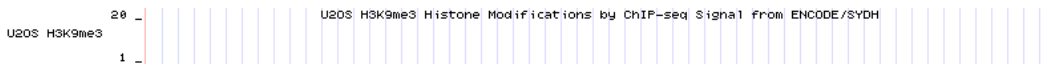
Gene	Length	Product size	Tm	% GC	5'-3'	Position
53BP1	20	71	60.13	45	L: TTGCAACGCTCTTCTGAATG	chr15:43,744,420- 43,744,490
	20		59.17	50	R:TGCTCAGCCGAGAACAATAG	



Gene	Length	Product size	Tm	% GC	5'-3'	Position
APAK/ ZNF420	20	70	59.74	55	L: GTGTGGCAAGGCCTTTAGTC	chr19:37,619,666-37,619,735
	20		60.07	55	R: GGGCTTCTCACCAGTATGGA	



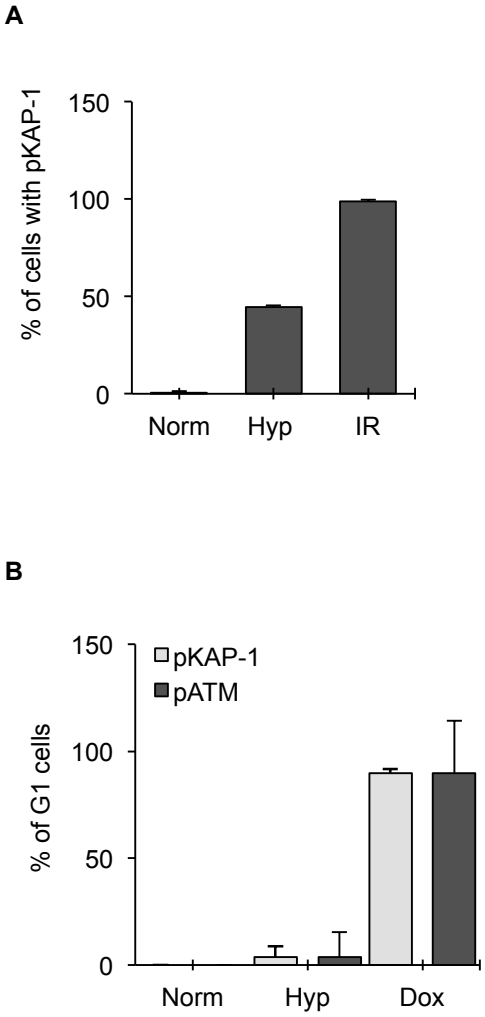
Gene	Length	Product size	Tm	% GC	5'-3'	Position
PP1P5K1	20	73	60.21	50	L: CATGGAACACCCTTCAAACC	chr15:43,851,111-43,851,183
	20		59.91	55	R: TGGGGTATATCTGGCAGGAG	



APPENDIX C

Statement of previous acceptance or concurrent submission of thesis for degree

Part of the figure shown below was used as part of figures 3.6, 3.7 and 3.8 in my MSc thesis "The role of KAP-1 in hypoxia". The Msc thesis stated above was submitted as part of the taught MSc course in Radiation Biology at The University of Oxford, on 25th August 2010. This is allowable under Examination Regulations 16.7.5.i.



REFERENCES

Aagaard, L., Laible, G., Selenko, P., Schmid, M., Dorn, R., Schotta, G., Kuhfittig, S., Wolf, A., Lebersorger, A., Singh, P.B., Reuter, G., and Jenuwein, T. (1999). Functional mammalian homologues of the Drosophila PEV-modifier Su(var)3-9 encode centromere-associated proteins which complex with the heterochromatin component M31. Embo J *18*, 1923-1938.

Ahmad, K., and Henikoff, S. (2002). The histone variant H3.3 marks active chromatin by replication-independent nucleosome assembly. Mol Cell *9*, 1191-1200.

Alabert, C., and Groth, A. (2012). Chromatin replication and epigenome maintenance. Nat Rev Mol Cell Biol *13*, 153-167.

Alarcon, R., Koumenis, C., Geyer, R.K., Maki, C.G., and Giaccia, A.J. (1999). Hypoxia induces p53 accumulation through MDM2 down-regulation and inhibition of E6-mediated degradation. Cancer Res *59*, 6046-6051.

Ali, A., Zhang, J., Bao, S., Liu, I., Otterness, D., Dean, N.M., Abraham, R.T., and Wang, X.F. (2004). Requirement of protein phosphatase 5 in DNA-damage-induced ATM activation. Genes Dev *18*, 249-254.

Alvarez, F., Munoz, F., Schilcher, P., Imhof, A., Almouzni, G., and Loyola, A. (2011). Sequential establishment of marks on soluble histones H3 and H4. J Biol Chem *286*, 17714-17721.

Ambrose, M., Goldstine, J.V., and Gatti, R.A. (2007). Intrinsic mitochondrial dysfunction in ATM-deficient lymphoblastoid cells. Hum Mol Genet *16*, 2154-2164.

Andegeko, Y., Moyal, L., Mittelman, L., Tsarfaty, I., Shiloh, Y., and Rotman, G. (2001). Nuclear retention of atm at sites of dna double strand breaks. J Biol Chem *276*, 38224-38230.

Anglana, M., Apiou, F., Bensimon, A., and Debatisse, M. (2003). Dynamics of DNA replication in mammalian somatic cells: nucleotide pool modulates origin choice and interorigin spacing. Cell *114*, 385-394.

Annunziato, A.T. (2012). Assembling chromatin: The long and winding road. Biochim Biophys Acta *1819*, 196-210.

Annunziato, A.T., and Seale, R.L. (1983). Histone deacetylation is required for the maturation of newly replicated chromatin. J Biol Chem *258*, 12675-12684.

Avvakumov, G.V., Walker, J.R., Xue, S., Li, Y., Duan, S., Bronner, C., Arrowsmith, C.H., and Dhe-Paganon, S. (2008). Structural basis for recognition of hemi-methylated DNA by the SRA domain of human UHRF1. Nature *455*, 822-825.

Ayrapetov, M.K., Xu, C., Sun, Y., Zhu, K., Parmar, K., D'Andrea, A.D., and Price, B.D. (2011). Activation of Hif1alpha by the prolylhydroxylase inhibitor dimethyoxalyglycine decreases radiosensitivity. PLoS One *6*, e26064.

Bakkenist, C.J., and Kastan, M.B. (2003). DNA damage activates ATM through intermolecular autophosphorylation and dimer dissociation. Nature *421*, 499-506.

Baldeyron, C., Soria, G., Roche, D., Cook, A.J., and Almouzni, G. (2011). HP1alpha recruitment to DNA damage by p150CAF-1 promotes homologous recombination repair. J Cell Biol *193*, 81-95.

Bannister, A.J., Zegerman, P., Partridge, J.F., Miska, E.A., Thomas, J.O., Allshire, R.C., and Kouzarides, T. (2001). Selective recognition of methylated lysine 9 on histone H3 by the HP1 chromo domain. Nature *410*, 120-124.

Barlow, J.H., Faryabi, R.B., Callen, E., Wong, N., Malhowski, A., Chen, H.T., Gutierrez-Cruz, G., Sun, H.W., McKinnon, P., Wright, G., Casellas, R., Robbiani, D.F., Staudt, L., Fernandez-Capetillo, O., and Nussenzweig, A. (2013). Identification of early replicating fragile sites that contribute to genome instability. Cell *152*, 620-632.

Barski, A., Cuddapah, S., Cui, K., Roh, T.Y., Schones, D.E., Wang, Z., Wei, G., Chepelev, I., and Zhao, K. (2007). High-resolution profiling of histone methylations in the human genome. Cell *129*, 823-837.

Bartkova, J., Horejsi, Z., Koed, K., Kramer, A., Tort, F., Zieger, K., Guldberg, P., Sehested, M., Nesland, J.M., Lukas, C., Orntoft, T., Lukas, J., and Bartek, J. (2005). DNA damage response as a candidate anti-cancer barrier in early human tumorigenesis. Nature *434*, 864-870.

Bartkova, J., Rezaei, N., Liontos, M., Karakaidos, P., Kletsas, D., Issaeva, N., Vassiliou, L.V., Kolettas, E., Niforou, K., Zoumpourlis, V.C., Takaoka, M., Nakagawa, H., Tort, F., Fugger, K., Johansson, F., Sehested, M., Andersen, C.L.,

Dyrskjot, L., Orntoft, T., Lukas, J., Kittas, C., Helleday, T., Halazonetis, T.D., Bartek, J., and Gorgoulis, V.G. (2006). Oncogene-induced senescence is part of the tumorigenesis barrier imposed by DNA damage checkpoints. Nature *444*, 633-637.

Beattie, T.R., and Bell, S.D. (2011). The role of the DNA sliding clamp in Okazaki fragment maturation in archaea and eukaryotes. Biochem Soc Trans *39*, 70-76.

Begg, A.C., Stewart, F.A., and Vens, C. (2011). Strategies to improve radiotherapy with targeted drugs. Nat Rev Cancer *11*, 239-253.

Bencokova, Z., Kaufmann, M.R., Pires, I.M., Lecane, P.S., Giaccia, A.J., and Hammond, E.M. (2009). ATM activation and signaling under hypoxic conditions. Mol Cell Biol *29*, 526-537.

Benkovic, S.J., Valentine, A.M., and Salinas, F. (2001). Replisome-mediated DNA replication. Annual review of biochemistry *70*, 181-208.

Benlhabib, H., and Mendelson, C.R. (2011). Epigenetic regulation of surfactant protein A gene (SP-A) expression in fetal lung reveals a critical role for Suv39h methyltransferases during development and hypoxia. Mol Cell Biol *31*, 1949-1958.

Bester, A.C., Roniger, M., Oren, Y.S., Im, M.M., Sarni, D., Chaoat, M., Bensimon, A., Zamir, G., Shewach, D.S., and Kerem, B. (2011). Nucleotide deficiency promotes genomic instability in early stages of cancer development. Cell *145*, 435-446.

Bhaskara, S., Knutson, S.K., Jiang, G., Chandrasekharan, M.B., Wilson, A.J., Zheng, S., Yenamandra, A., Locke, K., Yuan, J.L., Bonine-Summers, A.R., Wells, C.E., Kaiser, J.F., Washington, M.K., Zhao, Z., Wagner, F.F., Sun, Z.W., Xia, F., Holson, E.B., Khabele, D., and Hiebert, S.W. (2010). Hdac3 is essential for the maintenance of chromatin structure and genome stability. Cancer Cell *18*, 436-447.

Bindra, R.S., Crosby, M.E., and Glazer, P.M. (2007). Regulation of DNA repair in hypoxic cancer cells. Cancer Metastasis Rev *26*, 249-260.

Bindra, R.S., Gibson, S.L., Meng, A., Westermark, U., Jasin, M., Pierce, A.J., Bristow, R.G., Classon, M.K., and Glazer, P.M. (2005a). Hypoxia-induced down-regulation of BRCA1 expression by E2Fs. Cancer Res *65*, 11597-11604.

Bindra, R.S., and Glazer, P.M. (2005). Genetic instability and the tumor microenvironment: towards the concept of microenvironment-induced mutagenesis. Mutat Res *569*, 75-85.

Bindra, R.S., and Glazer, P.M. (2007). Co-repression of mismatch repair gene expression by hypoxia in cancer cells: role of the Myc/Max network. Cancer Lett *252*, 93-103.

Bindra, R.S., Schaffer, P.J., Meng, A., Woo, J., Maseide, K., Roth, M.E., Lizardi, P., Hedley, D.W., Bristow, R.G., and Glazer, P.M. (2005b). Alterations in DNA repair gene expression under hypoxia: elucidating the mechanisms of hypoxia-induced genetic instability. Ann N Y Acad Sci *1059*, 184-195.

Black, J.C., Van Rechem, C., and Whetstine, J.R. (2012). Histone lysine methylation dynamics: establishment, regulation, and biological impact. Mol Cell *48*, 491-507.

Blasius, M., Forment, J.V., Thakkar, N., Wagner, S.A., Choudhary, C., and Jackson, S.P. (2011). A phospho-proteomic screen identifies substrates of the checkpoint kinase Chk1. Genome Biol *12*, R78.

Bochman, M.L., and Schwacha, A. (2009). The Mcm complex: unwinding the mechanism of a replicative helicase. Microbiology and molecular biology reviews : MMBR *73*, 652-683.

Bonner, W.M., Redon, C.E., Dickey, J.S., Nakamura, A.J., Sedelnikova, O.A., Solier, S., and Pommier, Y. (2008). GammaH2AX and cancer. Nat Rev Cancer *8*, 957-967.

Bottini, A., Berruti, A., Bersiga, A., Brizzi, M.P., Brunelli, A., Gorzegno, G., DiMarco, B., Aguggini, S., Bolsi, G., Cirillo, F., Filippini, L., Betri, E., Bertoli, G., Alquati, P., and Dogliotti, L. (2000). p53 but not bcl-2 immunostaining is predictive of poor clinical complete response to primary chemotherapy in breast cancer patients. Clin Cancer Res *6*, 2751-2758.

Botuyan, M.V., Lee, J., Ward, I.M., Kim, J.E., Thompson, J.R., Chen, J., and Mer, G. (2006). Structural basis for the methylation state-specific recognition of histone H4-K20 by 53BP1 and Crb2 in DNA repair. Cell *127*, 1361-1373.

Bouquet, F., Ousset, M., Biard, D., Fallone, F., Dauvillier, S., Frit, P., Salles, B., and Muller, C. (2011). A DNA-dependent stress response involving DNA-PK occurs in hypoxic cells and contributes to cellular adaptation to hypoxia. J Cell Sci *124*, 1943-1951.

Brahimi-Horn, M.C., and Pouyssegur, J. (2009). HIF at a glance. J Cell Sci *122*, 1055-1057.

Braig, M., Lee, S., Loddenkemper, C., Rudolph, C., Peters, A.H.F.M., Schlegelberger, B., Stein, H., Dorken, B., Jenuwein, T., and Schmitt, C.A. (2005). Oncogene-induced senescence as an initial barrier in lymphoma development. Nature *436*, 660-665.

Brewer, B.J., and Fangman, W.L. (1988). A replication fork barrier at the 3' end of yeast ribosomal RNA genes. Cell *55*, 637-643.

Bristow, R.G., and Hill, R.P. (2008). Hypoxia and metabolism. Hypoxia, DNA repair and genetic instability. Nat Rev Cancer *8*, 180-192.

Brown, J.M., and Giaccia, A.J. (1998). The unique physiology of solid tumors: opportunities (and problems) for cancer therapy. Cancer Res *58*, 1408-1416.

Brown, J.M., and Wilson, W.R. (2004). Exploiting tumour hypoxia in cancer treatment. Nat Rev Cancer *4*, 437-447.

Brown, K.D., Rathi, A., Kamath, R., Beardsley, D.I., Zhan, Q., Mannino, J.L., and Baskaran, R. (2003). The mismatch repair system is required for S-phase checkpoint activation. Nat Genet *33*, 80-84.

Bruick, R.K., and McKnight, S.L. (2001). A conserved family of prolyl-4-hydroxylases that modify HIF. Science *294*, 1337-1340.

Bryant, H.E., Schultz, N., Thomas, H.D., Parker, K.M., Flower, D., Lopez, E., Kyle, S., Meuth, M., Curtin, N.J., and Helleday, T. (2005). Specific killing of BRCA2-deficient tumours with inhibitors of poly(ADP-ribose) polymerase. Nature *434*, 913-917.

Cam, H., Easton, J.B., High, A., and Houghton, P.J. (2010). mTORC1 signaling under hypoxic conditions is controlled by ATM-dependent phosphorylation of HIF-1alpha. Mol Cell *40*, 509-520.

Campos, E.I., Fillingham, J., Li, G., Zheng, H., Voigt, P., Kuo, W.H., Seepany, H., Gao, Z., Day, L.A., Greenblatt, J.F., and Reinberg, D. (2010). The program for processing newly synthesized histones H3.1 and H4. Nat Struct Mol Biol *17*, 1343-1351.

Canman, C.E., Lim, D.S., Cimprich, K.A., Taya, Y., Tamai, K., Sakaguchi, K., Appella, E., Kastan, M.B., and Siliciano, J.D. (1998). Activation of the ATM kinase by ionizing radiation and phosphorylation of p53. Science *281*, 1677-1679.

Cann, K.L., and Dellaire, G. (2011). Heterochromatin and the DNA damage response: the need to relax. Biochem Cell Biol *89*, 45-60.

Carney, J.P., Maser, R.S., Olivares, H., Davis, E.M., Le Beau, M., Yates, J.R., 3rd, Hays, L., Morgan, W.F., and Petrini, J.H. (1998). The hMre11/hRad50 protein complex and Nijmegen breakage syndrome: linkage of double-strand break repair to the cellular DNA damage response. Cell *93*, 477-486.

Cazares-Korner, C., Pires, I.M., Swallow, I.D., Grayer, S.C., O'Connor, L.J., Olcina, M.M., Christlieb, M., Conway, S.J., and Hammond, E.M. (2013). CH-01 is a Hypoxia-Activated Prodrug That Sensitizes Cells to Hypoxia/Reoxygenation Through Inhibition of Chk1 and Aurora A. ACS Chem Biol *8*, 1451-1459.

Celeste, A., Petersen, S., Romanienko, P.J., Fernandez-Capetillo, O., Chen, H.T., Sedelnikova, O.A., Reina-San-Martin, B., Coppola, V., Meffre, E., Difilippantonio, M.J., Redon, C., Pilch, D.R., Olaru, A., Eckhaus, M., Camerini-Otero, R.D., Tessarollo, L., Livak, F., Manova, K., Bonner, W.M., Nussenzweig, M.C., and Nussenzweig, A. (2002). Genomic instability in mice lacking histone H2AX. Science *296*, 922-927.

Ceol, C.J., Houvras, Y., Jane-Valbuena, J., Bilodeau, S., Orlando, D.A., Battisti, V., Fritsch, L., Lin, W.M., Hollmann, T.J., Ferre, F., Bourque, C., Burke, C.J., Turner, L., Uong, A., Johnson, L.A., Beroukhim, R., Mermel, C.H., Loda, M., Ait-Si-Ali, S., Garraway, L.A., Young, R.A., and Zon, L.I. (2011). The histone methyltransferase SETDB1 is recurrently amplified in melanoma and accelerates its onset. Nature *471*, 513-517.

Cha, R.S., and Kleckner, N. (2002). ATR homolog Mec1 promotes fork progression, thus averting breaks in replication slow zones. Science *297*, 602-606.

Chan, N., Koritzinsky, M., Zhao, H., Bindra, R., Glazer, P.M., Powell, S., Belmaaza, A., Wouters, B., and Bristow, R.G. (2008). Chronic hypoxia decreases synthesis of homologous recombination proteins to offset chemoresistance and radioresistance. Cancer Res *68*, 605-614.

Chan, N., Pires, I.M., Bencokova, Z., Coackley, C., Luoto, K.R., Bhogal, N., Lakshman, M., Gottipati, P., Oliver, F.J., Helleday, T., Hammond, E.M., and Bristow, R.G. (2010). Contextual synthetic lethality of cancer cell kill based on the tumor microenvironment. Cancer Res *70*, 8045-8054.

Charrier, J.D., Durrant, S.J., Golec, J.M., Kay, D.P., Knegtel, R.M., MacCormick, S., Mortimore, M., O'Donnell, M.E., Pinder, J.L., Reaper, P.M., Rutherford, A.P., Wang, P.S., Young, S.C., and Pollard, J.R. (2011). Discovery of potent and selective

inhibitors of ataxia telangiectasia mutated and Rad3 related (ATR) protein kinase as potential anticancer agents. J Med Chem *54*, 2320-2330.

Chen, H., Lisby, M., and Symington, L.S. (2013). RPA coordinates DNA end resection and prevents formation of DNA hairpins. Mol Cell *50*, 589-600.

Chen, H., Yan, Y., Davidson, T.L., Shinkai, Y., and Costa, M. (2006). Hypoxic stress induces dimethylated histone H3 lysine 9 through histone methyltransferase G9a in mammalian cells. Cancer Res *66*, 9009-9016.

Chen, L., Nievera, C.J., Lee, A.Y., and Wu, X. (2008). Cell cycle-dependent complex formation of BRCA1.CtIP.MRN is important for DNA double-strand break repair. J Biol Chem *283*, 7713-7720.

Chou, D.M., Adamson, B., Dephoure, N.E., Tan, X., Nottke, A.C., Hurov, K.E., Gygi, S.P., Colaiacovo, M.P., and Elledge, S.J. (2010). A chromatin localization screen reveals poly (ADP ribose)-regulated recruitment of the repressive polycomb and NuRD complexes to sites of DNA damage. Proc Natl Acad Sci U S A *107*, 18475-18480.

Chuang, L.S., Ian, H.I., Koh, T.W., Ng, H.H., Xu, G., and Li, B.F. (1997). Human DNA-(cytosine-5) methyltransferase-PCNA complex as a target for p21WAF1. Science *277*, 1996-2000.

Ciccia, A., and Elledge, S.J. (2010). The DNA damage response: making it safe to play with knives. Mol Cell *40*, 179-204.

Cimprich, K.A., and Cortez, D. (2008). ATR: an essential regulator of genome integrity. Nat Rev Mol Cell Biol *9*, 616-627.

Clapier, C.R., and Cairns, B.R. (2009). The biology of chromatin remodeling complexes. Annual review of biochemistry *78*, 273-304.

Cliby, W.A., Roberts, C.J., Cimprich, K.A., Stringer, C.M., Lamb, J.R., Schreiber, S.L., and Friend, S.H. (1998). Overexpression of a kinase-inactive ATR protein causes sensitivity to DNA-damaging agents and defects in cell cycle checkpoints. Embo J *17*, 159-169.

Cockman, M.E., Masson, N., Mole, D.R., Jaakkola, P., Chang, G.W., Clifford, S.C., Maher, E.R., Pugh, C.W., Ratcliffe, P.J., and Maxwell, P.H. (2000). Hypoxia inducible factor-alpha binding and ubiquitylation by the von Hippel-Lindau tumor suppressor protein. J Biol Chem *275*, 25733-25741.

Collis, S.J., DeWeese, T.L., Jeggo, P.A., and Parker, A.R. (2005). The life and death of DNA-PK. Oncogene *24*, 949-961.

Conti, C., Leo, E., Eichler, G.S., Sordet, O., Martin, M.M., Fan, A., Aladjem, M.I., and Pommier, Y. (2010). Inhibition of histone deacetylase in cancer cells slows down replication forks, activates dormant origins, and induces DNA damage. Cancer Res *70*, 4470-4480.

Cook, P.J., Ju, B.G., Telese, F., Wang, X., Glass, C.K., and Rosenfeld, M.G. (2009). Tyrosine dephosphorylation of H2AX modulates apoptosis and survival decisions. Nature *458*, 591-596.

Cortez, D., Guntuku, S., Qin, J., and Elledge, S.J. (2001). ATR and ATRIP: partners in checkpoint signaling. Science *294*, 1713-1716.

Costa, A., Ilves, I., Tamberg, N., Petojevic, T., Nogales, E., Botchan, M.R., and Berger, J.M. (2011). The structural basis for MCM2-7 helicase activation by GINS and Cdc45. Nat Struct Mol Biol *18*, 471-477.

Costanzo, V., Robertson, K., Bibikova, M., Kim, E., Grieco, D., Gottesman, M., Carroll, D., and Gautier, J. (2001). Mre11 protein complex prevents double-strand break accumulation during chromosomal DNA replication. Mol Cell *8*, 137-147.

Costanzo, V., Robertson, K., Ying, C.Y., Kim, E., Avvedimento, E., Gottesman, M., Grieco, D., and Gautier, J. (2000). Reconstitution of an ATM-dependent checkpoint that inhibits chromosomal DNA replication following DNA damage. Mol Cell *6*, 649-659.

Costes, S.V., Chiolo, I., Pluth, J.M., Barcellos-Hoff, M.H., and Jakob, B. (2010). Spatiotemporal characterization of ionizing radiation induced DNA damage foci and their relation to chromatin organization. Mutat Res *704*, 78-87.

Costes, S.V., Ponomarev, A., Chen, J.L., Nguyen, D., Cucinotta, F.A., and Barcellos-Hoff, M.H. (2007). Image-based modeling reveals dynamic redistribution of DNA damage into nuclear sub-domains. PLoS computational biology *3*, e155.

Couture, J.F., Collazo, E., Ortiz-Tello, P.A., Brunzelle, J.S., and Trievel, R.C. (2007). Specificity and mechanism of JMJD2A, a trimethyllysine-specific histone demethylase. Nat Struct Mol Biol *14*, 689-695.

Crosby, M.E., Kulshreshtha, R., Ivan, M., and Glazer, P.M. (2009). MicroRNA regulation of DNA repair gene expression in hypoxic stress. Cancer Res *69*, 1221-1229.

Dai, Y., and Grant, S. (2010). New insights into checkpoint kinase 1 in the DNA damage response signaling network. Clin Cancer Res *16*, 376-383.

Das, C., Lucia, M.S., Hansen, K.C., and Tyler, J.K. (2009). CBP/p300-mediated acetylation of histone H3 on lysine 56. Nature *459*, 113-117.

de Laat, W.L., Jaspers, N.G., and Hoeijmakers, J.H. (1999). Molecular mechanism of nucleotide excision repair. Genes Dev *13*, 768-785.

Denko, N.C. (2008). Hypoxia, HIF1 and glucose metabolism in the solid tumour. Nat Rev Cancer *8*, 705-713.

Dewhirst, M.W., Cao, Y., and Moeller, B. (2008). Cycling hypoxia and free radicals regulate angiogenesis and radiotherapy response. Nat Rev Cancer *8*, 425-437.

Di Micco, R., Fumagalli, M., Cicalese, A., Piccinin, S., Gasparini, P., Luise, C., Schurra, C., Garre, M., Nuciforo, P.G., Bensimon, A., Maestro, R., Pelicci, P.G., and d'Adda di Fagagna, F. (2006). Oncogene-induced senescence is a DNA damage response triggered by DNA hyper-replication. Nature *444*, 638-642.

Di Micco, R., Sulli, G., Dobreva, M., Liontos, M., Botrugno, O.A., Gargiulo, G., dal Zuffo, R., Matti, V., d'Ario, G., Montani, E., Mercurio, C., Hahn, W.C., Gorgoulis, V., Minucci, S., and d'Adda di Fagagna, F. (2011). Interplay between oncogene-induced DNA damage response and heterochromatin in senescence and cancer. Nat Cell Biol *13*, 292-302.

Dillon, S.C., Zhang, X., Trievel, R.C., and Cheng, X. (2005). The SET-domain protein superfamily: protein lysine methyltransferases. Genome Biol *6*, 227.

Dings, J., Meixensberger, J., Jager, A., and Roosen, K. (1998). Clinical experience with 118 brain tissue oxygen partial pressure catheter probes. Neurosurgery *43*, 1082-1095.

Duan, Q., Chen, H., Costa, M., and Dai, W. (2008). Phosphorylation of H3S10 blocks the access of H3K9 by specific antibodies and histone methyltransferase. Implication in regulating chromatin dynamics and epigenetic inheritance during mitosis. J Biol Chem *283*, 33585-33590.

Economopoulou, M., Langer, H.F., Celeste, A., Orlova, V.V., Choi, E.Y., Ma, M., Vassilopoulos, A., Callen, E., Deng, C., Bassing, C.H., Boehm, M., Nussenzweig, A., and Chavakis, T. (2009). Histone H2AX is integral to hypoxia-driven neovascularization. Nat Med *15*, 553-558.

Eichhorn, P.J., Creyghton, M.P., and Bernards, R. (2009). Protein phosphatase 2A regulatory subunits and cancer. Biochim Biophys Acta *1795*, 1-15.

Elia, M.C., and Bradley, M.O. (1992). Influence of chromatin structure on the induction of DNA double strand breaks by ionizing radiation. Cancer Res *52*, 1580-1586.

Elser, M., Borsig, L., Hassa, P.O., Erener, S., Messner, S., Valovka, T., Keller, S., Gassmann, M., and Hottiger, M.O. (2008). Poly(ADP-ribose) polymerase 1 promotes tumor cell survival by coactivating hypoxia-inducible factor-1-dependent gene expression. Mol Cancer Res *6*, 282-290.

Elvidge, G.P., Glenny, L., Appelhoff, R.J., Ratcliffe, P.J., Ragoussis, J., and Gleadle, J.M. (2006). Concordant regulation of gene expression by hypoxia and 2-oxoglutarate-dependent dioxygenase inhibition: the role of HIF-1alpha, HIF-2alpha, and other pathways. J Biol Chem *281*, 15215-15226.

English, C.M., Adkins, M.W., Carson, J.J., Churchill, M.E., and Tyler, J.K. (2006). Structural basis for the histone chaperone activity of Asf1. Cell *127*, 495-508.

Ernst, J., and Kellis, M. (2010). Discovery and characterization of chromatin states for systematic annotation of the human genome. Nature biotechnology *28*, 817-825.

Errico, A., and Costanzo, V. (2010). Differences in the DNA replication of unicellular eukaryotes and metazoans: known unknowns. EMBO Rep *11*, 270-278.

Falck, J., Coates, J., and Jackson, S.P. (2005). Conserved modes of recruitment of ATM, ATR and DNA-PKcs to sites of DNA damage. Nature *434*, 605-611.

Falck, J., Petrini, J.H., Williams, B.R., Lukas, J., and Bartek, J. (2002). The DNA damage-dependent intra-S phase checkpoint is regulated by parallel pathways. Nat Genet *30*, 290-294.

Fallone, F., Britton, S., Nieto, L., Salles, B., and Muller, C. (2012). ATR controls cellular adaptation to hypoxia through positive regulation of hypoxia-inducible factor 1 (HIF-1) expression. Oncogene.

Fanning, E., Klimovich, V., and Nager, A.R. (2006). A dynamic model for replication protein A (RPA) function in DNA processing pathways. Nucleic Acids Res *34*, 4126-4137.

Farmer, H., McCabe, N., Lord, C.J., Tutt, A.N., Johnson, D.A., Richardson, T.B., Santarosa, M., Dillon, K.J., Hickson, I., Knights, C., Martin, N.M., Jackson, S.P., Smith, G.C., and Ashworth, A. (2005). Targeting the DNA repair defect in BRCA mutant cells as a therapeutic strategy. Nature *434*, 917-921.

Feng, Q., Wang, H., Ng, H.H., Erdjument-Bromage, H., Tempst, P., Struhl, K., and Zhang, Y. (2002). Methylation of H3-lysine 79 is mediated by a new family of HMTases without a SET domain. Curr Biol *12*, 1052-1058.

Fine, L.G., and Norman, J.T. (2002). The breathing kidney. J Am Soc Nephrol *13*, 1974-1976.

Floyd, S.R., Pacold, M.E., Huang, Q., Clarke, S.M., Lam, F.C., Cannell, I.G., Bryson, B.D., Rameseder, J., Lee, M.J., Blake, E.J., Fydrych, A., Ho, R., Greenberger, B.A., Chen, G.C., Maffa, A., Del Rosario, A.M., Root, D.E., Carpenter, A.E., Hahn, W.C., Sabatini, D.M., Chen, C.C., White, F.M., Bradner, J.E., and Yaffe, M.B. (2013). The bromodomain protein Brd4 insulates chromatin from DNA damage signalling. Nature *498*, 246-250.

Fokas, E., Prevo, R., Pollard, J.R., Reaper, P.M., Charlton, P.A., Cornelissen, B., Vallis, K.A., Hammond, E.M., Olcina, M.M., Gillies McKenna, W., Muschel, R.J., and Brunner, T.B. (2012). Targeting ATR in vivo using the novel inhibitor VE-822 results in selective sensitization of pancreatic tumors to radiation. Cell Death Dis *3*, e441.

Freeman, A.K., and Monteiro, A.N. (2010). Phosphatases in the cellular response to DNA damage. Cell Commun Signal *8*, 27.

Freiberg, R.A., Hammond, E.M., Dorie, M.J., Welford, S.M., and Giaccia, A.J. (2006a). DNA damage during reoxygenation elicits a Chk2-dependent checkpoint response. Mol Cell Biol *26*, 1598-1609.

Freiberg, R.A., Krieg, A.J., Giaccia, A.J., and Hammond, E.M. (2006b). Checking in on hypoxia/reoxygenation. Cell Cycle *5*, 1304-1307.

Gambus, A., Jones, R.C., Sanchez-Diaz, A., Kanemaki, M., van Deursen, F., Edmondson, R.D., and Labib, K. (2006). GINS maintains association of Cdc45 with MCM in replisome progression complexes at eukaryotic DNA replication forks. Nat Cell Biol *8*, 358-366.

Gatei, M., Jakob, B., Chen, P., Kijas, A.W., Becherel, O.J., Gueven, N., Birrell, G., Lee, J.H., Paull, T.T., Lerenthal, Y., Fazry, S., Taucher-Scholz, G., Kalb, R., Schindler, D., Waltes, R., Dork, T., and Lavin, M.F. (2011). ATM protein-dependent

phosphorylation of Rad50 protein regulates DNA repair and cell cycle control. J Biol Chem *286*, 31542-31556.

Gatei, M., Young, D., Cerosaletti, K.M., Desai-Mehta, A., Spring, K., Kozlov, S., Lavin, M.F., Gatti, R.A., Concannon, P., and Khanna, K. (2000). ATM-dependent phosphorylation of nibrin in response to radiation exposure. Nat Genet *25*, 115-119.

Ge, X.Q., and Blow, J.J. (2010). Chk1 inhibits replication factory activation but allows dormant origin firing in existing factories. J Cell Biol *191*, 1285-1297.

Ghosal, G., and Chen, J. (2013). DNA damage tolerance: a double-edged sword guarding the genome. Translational cancer research *2*, 107-129.

Giaccia, A., Siim, B.G., and Johnson, R.S. (2003). HIF-1 as a target for drug development. Nat Rev Drug Discov *2*, 803-811.

Gibson, S.L., Bindra, R.S., and Glazer, P.M. (2005). Hypoxia-induced phosphorylation of Chk2 in an ataxia telangiectasia mutated-dependent manner. Cancer Res *65*, 10734-10741.

Gibson, S.L., Bindra, R.S., and Glazer, P.M. (2006). CHK2-dependent phosphorylation of BRCA1 in hypoxia. Radiat Res *166*, 646-651.

Gilad, O., Nabet, B.Y., Ragland, R.L., Schoppy, D.W., Smith, K.D., Durham, A.C., and Brown, E.J. (2010). Combining ATR suppression with oncogenic Ras synergistically increases genomic instability, causing synthetic lethality or tumorigenesis in a dosage-dependent manner. Cancer Res *70*, 9693-9702.

Goldberg, M., Stucki, M., Falck, J., D'Amours, D., Rahman, D., Pappin, D., Bartek, J., and Jackson, S.P. (2003). MDC1 is required for the intra-S-phase DNA damage checkpoint. Nature *421*, 952-956.

Goodarzi, A.A., Jeggo, P., and Lobrich, M. (2010). The influence of heterochromatin on DNA double strand break repair: Getting the strong, silent type to relax. DNA Repair (Amst) *9*, 1273-1282.

Goodarzi, A.A., Jonnalagadda, J.C., Douglas, P., Young, D., Ye, R., Moorhead, G.B., Lees-Miller, S.P., and Khanna, K.K. (2004). Autophosphorylation of ataxia-telangiectasia mutated is regulated by protein phosphatase 2A. Embo J *23*, 4451-4461.

Goodarzi, A.A., Kurka, T., and Jeggo, P.A. (2011). KAP-1 phosphorylation regulates CHD3 nucleosome remodeling during the DNA double-strand break response. Nat Struct Mol Biol *18*, 831-839.

Goodarzi, A.A., Noon, A.T., Deckbar, D., Ziv, Y., Shiloh, Y., Lobrich, M., and Jeggo, P.A. (2008). ATM signaling facilitates repair of DNA double-strand breaks associated with heterochromatin. Mol Cell *31*, 167-177.

Goodarzi, A.A., Noon, A.T., and Jeggo, P.A. (2009). The impact of heterochromatin on DSB repair. Biochem Soc Trans *37*, 569-576.

Gordan, J.D., Bertout, J.A., Hu, C.J., Diehl, J.A., and Simon, M.C. (2007). HIF-2alpha promotes hypoxic cell proliferation by enhancing c-myc transcriptional activity. Cancer Cell *11*, 335-347.

Gorgoulis, V.G., Vassiliou, L.V., Karakaidos, P., Zacharatos, P., Kotsinas, A., Liloglou, T., Venere, M., Ditullio, R.A., Jr., Kastrinakis, N.G., Levy, B., Kletsas, D., Yoneta, A., Herlyn, M., Kittas, C., and Halazonetis, T.D. (2005). Activation of the DNA damage checkpoint and genomic instability in human precancerous lesions. Nature *434*, 907-913.

Gorrini, C., Squatrito, M., Luise, C., Syed, N., Perna, D., Wark, L., Martinato, F., Sardella, D., Verrecchia, A., Bennett, S., Confalonieri, S., Cesaroni, M., Marchesi, F., Gasco, M., Scanziani, E., Capra, M., Mai, S., Nuciforo, P., Crook, T., Lough, J., and Amati, B. (2007). Tip60 is a haplo-insufficient tumour suppressor required for an oncogene-induced DNA damage response. Nature *448*, 1063-1067.

Graeber, T.G., Osmanian, C., Jacks, T., Housman, D.E., Koch, C.J., Lowe, S.W., and Giaccia, A.J. (1996). Hypoxia-mediated selection of cells with diminished apoptotic potential in solid tumours. Nature *379*, 88-91.

Graeber, T.G., Peterson, J.F., Tsai, M., Monica, K., Fornace, A.J., Jr., and Giaccia, A.J. (1994). Hypoxia induces accumulation of p53 protein, but activation of a G1-phase checkpoint by low-oxygen conditions is independent of p53 status. Mol Cell Biol *14*, 6264-6277.

Gray, L.H., Conger, A.D., Ebert, M., Hornsey, S., and Scott, O.C. (1953). The concentration of oxygen dissolved in tissues at the time of irradiation as a factor in radiotherapy. Br J Radiol *26*, 638-648.

Green, D.R., and Kroemer, G. (2009). Cytoplasmic functions of the tumour suppressor p53. Nature *458*, 1127-1130.

Greer, E.L., and Shi, Y. (2012). Histone methylation: a dynamic mark in health, disease and inheritance. Nature reviews Genetics *13*, 343-357.

Groner, A.C., Meylan, S., Ciuffi, A., Zangger, N., Ambrosini, G., Denervaud, N., Bucher, P., and Trono, D. (2010). KRAB-zinc finger proteins and KAP1 can mediate long-range transcriptional repression through heterochromatin spreading. PLoS Genet *6*, e1000869.

Groth, A. (2009). Replicating chromatin: a tale of histones. Biochem Cell Biol *87*, 51-63.

Groth, A., Corpet, A., Cook, A.J., Roche, D., Bartek, J., Lukas, J., and Almouzni, G. (2007). Regulation of replication fork progression through histone supply and demand. Science *318*, 1928-1931.

Groth, A., Lukas, J., Nigg, E.A., Sillje, H.H., Wernstedt, C., Bartek, J., and Hansen, K. (2003). Human Tousled like kinases are targeted by an ATM- and Chk1-dependent DNA damage checkpoint. Embo J *22*, 1676-1687.

Groth, A., Ray-Gallet, D., Quivy, J.P., Lukas, J., Bartek, J., and Almouzni, G. (2005). Human Asf1 regulates the flow of S phase histones during replicational stress. Mol Cell *17*, 301-311.

Guenatri, M., Bailly, D., Maison, C., and Almouzni, G. (2004). Mouse centric and pericentric satellite repeats form distinct functional heterochromatin. The Journal of cell biology *166*, 493-505.

Guo, Z., Kozlov, S., Lavin, M.F., Person, M.D., and Paull, T.T. (2010). ATM activation by oxidative stress. Science *330*, 517-521.

Gupta, A., Sharma, G.G., Young, C.S., Agarwal, M., Smith, E.R., Paull, T.T., Lucchesi, J.C., Khanna, K.K., Ludwig, T., and Pandita, T.K. (2005). Involvement of human MOF in ATM function. Mol Cell Biol *25*, 5292-5305.

Halazonetis, T.D., Gorgoulis, V.G., and Bartek, J. (2008). An oncogene-induced DNA damage model for cancer development. Science *319*, 1352-1355.

Hammond, E.M., Denko, N.C., Dorie, M.J., Abraham, R.T., and Giaccia, A.J. (2002). Hypoxia links ATR and p53 through replication arrest. Mol Cell Biol *22*, 1834-1843.

Hammond, E.M., Dorie, M.J., and Giaccia, A.J. (2003a). ATR/ATM targets are phosphorylated by ATR in response to hypoxia and ATM in response to reoxygenation. J Biol Chem *278*, 12207-12213.

Hammond, E.M., Dorie, M.J., and Giaccia, A.J. (2004). Inhibition of ATR leads to increased sensitivity to hypoxia/reoxygenation. Cancer Res *64*, 6556-6562.

Hammond, E.M., and Giaccia, A.J. (2004). The role of ATM and ATR in the cellular response to hypoxia and re-oxygenation. DNA Repair (Amst) *3*, 1117-1122.

Hammond, E.M., and Giaccia, A.J. (2005). The role of p53 in hypoxia-induced apoptosis. Biochem Biophys Res Commun *331*, 718-725.

Hammond, E.M., Green, S.L., and Giaccia, A.J. (2003b). Comparison of hypoxia-induced replication arrest with hydroxyurea and aphidicolin-induced arrest. Mutat Res *532*, 205-213.

Hammond, E.M., Kaufmann, M.R., and Giaccia, A.J. (2007). Oxygen sensing and the DNA-damage response. Curr Opin Cell Biol *19*, 680-684.

Hammond, E.M., Mandell, D.J., Salim, A., Krieg, A.J., Johnson, T.M., Shirazi, H.A., Attardi, L.D., and Giaccia, A.J. (2006). Genome-wide analysis of p53 under hypoxic conditions. Mol Cell Biol *26*, 3492-3504.

Hanahan, D., and Weinberg, R.A. (2000). The hallmarks of cancer. Cell *100*, 57-70.

Hanahan, D., and Weinberg, R.A. (2011). Hallmarks of cancer: the next generation. Cell *144*, 646-674.

Harper, J.W., and Elledge, S.J. (2007). The DNA damage response: ten years after. Mol Cell *28*, 739-745.

Hickman, J.A., Potten, C.S., Merritt, A.J., and Fisher, T.C. (1994). Apoptosis and cancer chemotherapy. Philos Trans R Soc Lond B Biol Sci *345*, 319-325.

Hockel, M., Schlenger, K., Aral, B., Mitze, M., Schaffer, U., and Vaupel, P. (1996a). Association between tumor hypoxia and malignant progression in advanced cancer of the uterine cervix. Cancer Res *56*, 4509-4515.

Hockel, M., Schlenger, K., Mitze, M., Schaffer, U., and Vaupel, P. (1996b). Hypoxia and Radiation Response in Human Tumors. Semin Radiat Oncol *6*, 3-9.

Hockel, M., and Vaupel, P. (2001). Tumor hypoxia: definitions and current clinical, biologic, and molecular aspects. J Natl Cancer Inst *93*, 266-276.

Horsman, M.R., Mortensen, L.S., Petersen, J.B., Busk, M., and Overgaard, J. (2012). Imaging hypoxia to improve radiotherapy outcome. Nature reviews Clinical oncology *9*, 674-687.

Hu, C.J., Wang, L.Y., Chodosh, L.A., Keith, B., and Simon, M.C. (2003). Differential roles of hypoxia-inducible factor 1alpha (HIF-1alpha) and HIF-2alpha in hypoxic gene regulation. Mol Cell Biol *23*, 9361-9374.

Huang, J., Dorsey, J., Chuikov, S., Perez-Burgos, L., Zhang, X., Jenuwein, T., Reinberg, D., and Berger, S.L. (2010). G9a and Glp methylate lysine 373 in the tumor suppressor p53. J Biol Chem *285*, 9636-9641.

Huang, J., Sengupta, R., Espejo, A.B., Lee, M.G., Dorsey, J.A., Richter, M., Opravil, S., Shiekhattar, R., Bedford, M.T., Jenuwein, T., and Berger, S.L. (2007). p53 is regulated by the lysine demethylase LSD1. Nature *449*, 105-108.

Hubbi, M.E., Kshitiz, Gilkes, D.M., Rey, S., Wong, C.C., Luo, W., Kim, D.H., Dang, C.V., Levchenko, A., and Semenza, G.L. (2013). A nontranscriptional role for HIF-1alpha as a direct inhibitor of DNA replication. Sci Signal *6*, ra10.

Hubbi, M.E., Luo, W., Baek, J.H., and Semenza, G.L. (2011). MCM proteins are negative regulators of hypoxia-inducible factor 1. Mol Cell *42*, 700-712.

Huen, M.S., Grant, R., Manke, I., Minn, K., Yu, X., Yaffe, M.B., and Chen, J. (2007). RNF8 transduces the DNA-damage signal via histone ubiquitylation and checkpoint protein assembly. Cell *131*, 901-914.

Hunt, C.R., Pandita, R.K., Laszlo, A., Higashikubo, R., Agarwal, M., Kitamura, T., Gupta, A., Rief, N., Horikoshi, N., Baskaran, R., Lee, J.H., Lobrich, M., Paull, T.T., Roti Roti, J.L., and Pandita, T.K. (2007). Hyperthermia activates a subset of ataxia-telangiectasia mutated effectors independent of DNA strand breaks and heat shock protein 70 status. Cancer Res *67*, 3010-3017.

Hurley, P.J., Wilsker, D., and Bunz, F. (2007). Human cancer cells require ATR for cell cycle progression following exposure to ionizing radiation. Oncogene *26*, 2535-2542.

Huyen, Y., Zgheib, O., Ditullio, R.A., Jr., Gorgoulis, V.G., Zacharatos, P., Petty, T.J., Sheston, E.A., Mellert, H.S., Stavridi, E.S., and Halazonetis, T.D. (2004). Methylated

lysine 79 of histone H3 targets 53BP1 to DNA double-strand breaks. Nature *432*, 406-411.

Ivanov, A.V., Peng, H., Yurchenko, V., Yap, K.L., Negorev, D.G., Schultz, D.C., Psulkowski, E., Fredericks, W.J., White, D.E., Maul, G.G., Sadofsky, M.J., Zhou, M.M., and Rauscher, F.J., 3rd (2007). PHD domain-mediated E3 ligase activity directs intramolecular sumoylation of an adjacent bromodomain required for gene silencing. Mol Cell *28*, 823-837.

Jackson, S.P., and Bartek, J. (2009). The DNA-damage response in human biology and disease. Nature *461*, 1071-1078.

Jackson, V., and Chalkley, R. (1981a). A new method for the isolation of replicative chromatin: selective deposition of histone on both new and old DNA. Cell *23*, 121-134.

Jackson, V., and Chalkley, R. (1981b). A reevaluation of new histone deposition on replicating chromatin. J Biol Chem *256*, 5095-5103.

Jasencakova, Z., Scharf, A.N., Ask, K., Corpet, A., Imhof, A., Almouzni, G., and Groth, A. (2010). Replication stress interferes with histone recycling and predeposition marking of new histones. Mol Cell *37*, 736-743.

Jeggo, P.A., Carr, A.M., and Lehmann, A.R. (1998). Splitting the ATM: distinct repair and checkpoint defects in ataxia-telangiectasia. Trends in genetics : TIG *14*, 312-316.

Jeggo, P.A., and Lobrich, M. (2007). DNA double-strand breaks: their cellular and clinical impact? Oncogene *26*, 7717-7719.

Jenuwein, T., Laible, G., Dorn, R., and Reuter, G. (1998). SET domain proteins modulate chromatin domains in eu- and heterochromatin. Cellular and molecular life sciences : CMLS *54*, 80-93.

Johnson, A., and O'Donnell, M. (2005). Cellular DNA replicases: components and dynamics at the replication fork. Annual review of biochemistry *74*, 283-315.

Johnson, A.B., and Barton, M.C. (2007). Hypoxia-induced and stress-specific changes in chromatin structure and function. Mutat Res *618*, 149-162.

Johnson, A.B., Denko, N., and Barton, M.C. (2008). Hypoxia induces a novel signature of chromatin modifications and global repression of transcription. Mutat Res *640*, 174-179.

Kaelin, W.G., Jr. (2005). The concept of synthetic lethality in the context of anticancer therapy. Nat Rev Cancer *5*, 689-698.

Kaelin, W.G., Jr., and Ratcliffe, P.J. (2008). Oxygen sensing by metazoans: the central role of the HIF hydroxylase pathway. Mol Cell *30*, 393-402.

Kaida, A., and Miura, M. (2012). Visualizing the effect of hypoxia on fluorescence kinetics in living HeLa cells using the fluorescent ubiquitination-based cell cycle indicator (Fucci). Exp Cell Res *318*, 288-297.

Kaidi, A., and Jackson, S.P. (2013). KAT5 tyrosine phosphorylation couples chromatin sensing to ATM signalling. Nature *498*, 70-74.

Karytinos, A., Forneris, F., Profumo, A., Ciossani, G., Battaglioli, E., Binda, C., and Mattevi, A. (2009). A novel mammalian flavin-dependent histone demethylase. J Biol Chem *284*, 17775-17782.

Kastan, M.B. (2004). ATM-the first step in helping cells deal with DNA damage. Biomed Pharmacother *58*, 72-73.

Kastan, M.B., and Bartek, J. (2004). Cell-cycle checkpoints and cancer. Nature *432*, 316-323.

Kawabata, T., Luebben, S.W., Yamaguchi, S., Ilves, I., Matise, I., Buske, T., Botchan, M.R., and Shima, N. (2011). Stalled fork rescue via dormant replication origins in unchallenged S phase promotes proper chromosome segregation and tumor suppression. Mol Cell *41*, 543-553.

Kenneth, N.S., Mudie, S., van Uden, P., and Rocha, S. (2009). SWI/SNF regulates the cellular response to hypoxia. J Biol Chem *284*, 4123-4131.

Kenneth, N.S., and Rocha, S. (2008). Regulation of gene expression by hypoxia. Biochem J *414*, 19-29.

Kim, Y.C., Gerlitz, G., Furusawa, T., Catez, F., Nussenzweig, A., Oh, K.S., Kraemer, K.H., Shiloh, Y., and Bustin, M. (2009). Activation of ATM depends on chromatin interactions occurring before induction of DNA damage. Nat Cell Biol *11*, 92-96.

Klein, T.J., and Glazer, P.M. (2010). The tumor microenvironment and DNA repair. Semin Radiat Oncol *20*, 282-287.

Klose, R.J., Kallin, E.M., and Zhang, Y. (2006). JmjC-domain-containing proteins and histone demethylation. Nature reviews Genetics *7*, 715-727.

Kolas, N.K., Chapman, J.R., Nakada, S., Ylanko, J., Chahwan, R., Sweeney, F.D., Panier, S., Mendez, M., Wildenhain, J., Thomson, T.M., Pelletier, L., Jackson, S.P., and Durocher, D. (2007). Orchestration of the DNA-damage response by the RNF8 ubiquitin ligase. Science *318*, 1637-1640.

Koopal, S., Furuhjelm, J.H., Jarviluoma, A., Jaamaa, S., Pyakurel, P., Pussinen, C., Wirzenius, M., Biberfeld, P., Alitalo, K., Laiho, M., and Ojala, P.M. (2007). Viral oncogene-induced DNA damage response is activated in Kaposi sarcoma tumorigenesis. PLoS pathogens *3*, 1348-1360.

Koshiji, M., To, K.K., Hammer, S., Kumamoto, K., Harris, A.L., Modrich, P., and Huang, L.E. (2005). HIF-1alpha induces genetic instability by transcriptionally downregulating MutSalpha expression. Mol Cell *17*, 793-803.

Kouzarides, T. (2007). Chromatin modifications and their function. Cell *128*, 693-705.

Kozlov, S.V., Graham, M.E., Jakob, B., Tobias, F., Kijas, A.W., Tanuji, M., Chen, P., Robinson, P.J., Taucher-Scholz, G., Suzuki, K., So, S., Chen, D., and Lavin, M.F. (2011). Autophosphorylation and ATM activation: additional sites add to the complexity. J Biol Chem *286*, 9107-9119.

Kozlov, S.V., Graham, M.E., Peng, C., Chen, P., Robinson, P.J., and Lavin, M.F. (2006). Involvement of novel autophosphorylation sites in ATM activation. Embo J *25*, 3504-3514.

Kumareswaran, R., Ludkovski, O., Meng, A., Sykes, J., Pintilie, M., and Bristow, R.G. (2012). Chronic hypoxia compromises repair of DNA double-strand breaks to drive genetic instability. J Cell Sci *125*, 189-199.

Kuzminov, A. (1995). Collapse and repair of replication forks in Escherichia coli. Molecular microbiology *16*, 373-384.

Lachner, M., O'Carroll, D., Rea, S., Mechtler, K., and Jenuwein, T. (2001). Methylation of histone H3 lysine 9 creates a binding site for HP1 proteins. Nature *410*, 116-120.

Lai, S.L., Perng, R.P., and Hwang, J. (2000). p53 gene status modulates the chemosensitivity of non-small cell lung cancer cells. Journal of biomedical science *7*, 64-70.

Lando, D., Peet, D.J., Whelan, D.A., Gorman, J.J., and Whitelaw, M.L. (2002). Asparagine hydroxylation of the HIF transactivation domain a hypoxic switch. Science *295*, 858-861.

Larsen, D.H., Poinsignon, C., Gudjonsson, T., Dinant, C., Payne, M.R., Hari, F.J., Rendtlew Danielsen, J.M., Menard, P., Sand, J.C., Stucki, M., Lukas, C., Bartek, J., Andersen, J.S., and Lukas, J. (2010). The chromatin-remodeling factor CHD4 coordinates signaling and repair after DNA damage. J Cell Biol *190*, 731-740.

Le, Q.T., Chen, E., Salim, A., Cao, H., Kong, C.S., Whyte, R., Donington, J., Cannon, W., Wakelee, H., Tibshirani, R., Mitchell, J.D., Richardson, D., O'Byrne, K.J., Koong, A.C., and Giaccia, A.J. (2006). An evaluation of tumor oxygenation and gene expression in patients with early stage non-small cell lung cancers. Clin Cancer Res *12*, 1507-1514.

Lee, D.H., Goodarzi, A.A., Adelmant, G.O., Pan, Y., Jeggo, P.A., Marto, J.A., and Chowdhury, D. (2012). Phosphoproteomic analysis reveals that PP4 dephosphorylates KAP-1 impacting the DNA damage response. Embo J *31*, 2403-2415.

Lee, J.H., Goodarzi, A.A., Jeggo, P.A., and Paull, T.T. (2010a). 53BP1 promotes ATM activity through direct interactions with the MRN complex. Embo J *29*, 574-585.

Lee, J.S., Kim, Y., Bhin, J., Shin, H.J., Nam, H.J., Lee, S.H., Yoon, J.B., Binda, O., Gozani, O., Hwang, D., and Baek, S.H. (2011). Hypoxia-induced methylation of a pontin chromatin remodeling factor. Proc Natl Acad Sci U S A *108*, 13510-13515.

Lee, J.S., Kim, Y., Kim, I.S., Kim, B., Choi, H.J., Lee, J.M., Shin, H.J., Kim, J.H., Kim, J.Y., Seo, S.B., Lee, H., Binda, O., Gozani, O., Semenza, G.L., Kim, M., Kim, K.I., Hwang, D., and Baek, S.H. (2010b). Negative regulation of hypoxic responses via induced Reptin methylation. Mol Cell *39*, 71-85.

Li, B., Carey, M., and Workman, J.L. (2007). The role of chromatin during transcription. Cell *128*, 707-719.

Li, G.M. (2008). Mechanisms and functions of DNA mismatch repair. Cell research *18*, 85-98.

Lim, D.S., Kim, S.T., Xu, B., Maser, R.S., Lin, J., Petrini, J.H., and Kastan, M.B. (2000). ATM phosphorylates p95/nbs1 in an S-phase checkpoint pathway. Nature *404*, 613-617.

Lindahl, T., and Barnes, D.E. (2000). Repair of endogenous DNA damage. Cold Spring Harb Symp Quant Biol *65*, 127-133.

Lindahl, T., and Nyberg, B. (1972). Rate of depurination of native deoxyribonucleic acid. Biochemistry *11*, 3610-3618.

Lisztwan, J., Imbert, G., Wirbelauer, C., Gstaiger, M., and Krek, W. (1999). The von Hippel-Lindau tumor suppressor protein is a component of an E3 ubiquitin-protein ligase activity. Genes Dev *13*, 1822-1833.

Liu, F., Barsyte-Lovejoy, D., Li, F., Xiong, Y., Korboukh, V., Huang, X.P., Allali-Hassani, A., Janzen, W.P., Roth, B.L., Frye, S.V., Arrowsmith, C.H., Brown, P.J., Vedadi, M., and Jin, J. (2013). Discovery of an in Vivo Chemical Probe of the Lysine Methyltransferases G9a and GLP. J Med Chem *56*, 8931-8942.

Liu, Q., Guntuku, S., Cui, X.S., Matsuoka, S., Cortez, D., Tamai, K., Luo, G., Carattini-Rivera, S., DeMayo, F., Bradley, A., Donehower, L.A., and Elledge, S.J. (2000). Chk1 is an essential kinase that is regulated by Atr and required for the G(2)/M DNA damage checkpoint. Genes Dev *14*, 1448-1459.

Liu, S.K., Coackley, C., Krause, M., Jalali, F., Chan, N., and Bristow, R.G. (2008). A novel poly(ADP-ribose) polymerase inhibitor, ABT-888, radiosensitizes malignant human cell lines under hypoxia. Radiother Oncol *88*, 258-268.

Lou, Z., Minter-Dykhouse, K., Franco, S., Gostissa, M., Rivera, M.A., Celeste, A., Manis, J.P., van Deursen, J., Nussenzweig, A., Paull, T.T., Alt, F.W., and Chen, J. (2006). MDC1 maintains genomic stability by participating in the amplification of ATM-dependent DNA damage signals. Mol Cell *21*, 187-200.

Loyola, A., Tagami, H., Bonaldi, T., Roche, D., Quivy, J.P., Imhof, A., Nakatani, Y., Dent, S.Y., and Almouzni, G. (2009). The HP1alpha-CAF1-SetDB1-containing complex provides H3K9me1 for Suv39-mediated K9me3 in pericentric heterochromatin. EMBO Rep *10*, 769-775.

Lu, Y., Chu, A., Turker, M.S., and Glazer, P.M. (2011). Hypoxia-induced epigenetic regulation and silencing of the BRCA1 promoter. Mol Cell Biol *31*, 3339-3350.

Luger, K., Mader, A.W., Richmond, R.K., Sargent, D.F., and Richmond, T.J. (1997). Crystal structure of the nucleosome core particle at 2.8 A resolution. Nature *389*, 251-260.

Lukas, C., Melander, F., Stucki, M., Falck, J., Bekker-Jensen, S., Goldberg, M., Lerenthal, Y., Jackson, S.P., Bartek, J., and Lukas, J. (2004). Mdc1 couples DNA double-strand break recognition by Nbs1 with its H2AX-dependent chromatin retention. Embo J *23*, 2674-2683.

Lukic, S., Nicolas, J.C., and Levine, A.J. (2013). The diversity of zinc-finger genes on human chromosome 19 provides an evolutionary mechanism for defense against inherited endogenous retroviruses. Cell Death Differ.

Luo, J., Su, F., Chen, D., Shiloh, A., and Gu, W. (2000). Deacetylation of p53 modulates its effect on cell growth and apoptosis. Nature *408*, 377-381.

Mailand, N., Bekker-Jensen, S., Faustrup, H., Melander, F., Bartek, J., Lukas, C., and Lukas, J. (2007). RNF8 ubiquitylates histones at DNA double-strand breaks and promotes assembly of repair proteins. Cell *131*, 887-900.

Makino, Y., Uenishi, R., Okamoto, K., Isoe, T., Hosono, O., Tanaka, H., Kanopka, A., Poellinger, L., Haneda, M., and Morimoto, C. (2007). Transcriptional up-regulation of inhibitory PAS domain protein gene expression by hypoxia-inducible factor 1 (HIF-1): a negative feedback regulatory circuit in HIF-1-mediated signaling in hypoxic cells. J Biol Chem *282*, 14073-14082.

Martin-Oliva, D., Aguilar-Quesada, R., O'Valle, F., Munoz-Gamez, J.A., Martinez-Romero, R., Garcia Del Moral, R., Ruiz de Almodovar, J.M., Villuendas, R., Piris, M.A., and Oliver, F.J. (2006). Inhibition of poly(ADP-ribose) polymerase modulates tumor-related gene expression, including hypoxia-inducible factor-1 activation, during skin carcinogenesis. Cancer Res *66*, 5744-5756.

Marzluff, W.F., Wagner, E.J., and Duronio, R.J. (2008). Metabolism and regulation of canonical histone mRNAs: life without a poly(A) tail. Nature reviews Genetics *9*, 843-854.

Matsuoka, S., Ballif, B.A., Smogorzewska, A., McDonald, E.R., 3rd, Hurov, K.E., Luo, J., Bakalarski, C.E., Zhao, Z., Solimini, N., Lerenthal, Y., Shiloh, Y., Gygi, S.P., and Elledge, S.J. (2007). ATM and ATR substrate analysis reveals extensive protein networks responsive to DNA damage. Science *316*, 1160-1166.

Maxwell, P.H. (2005). The HIF pathway in cancer. Semin Cell Dev Biol *16*, 523-530.

Maxwell, P.H., Wiesener, M.S., Chang, G.W., Clifford, S.C., Vaux, E.C., Cockman, M.E., Wykoff, C.C., Pugh, C.W., Maher, E.R., and Ratcliffe, P.J. (1999). The tumour suppressor protein VHL targets hypoxia-inducible factors for oxygen-dependent proteolysis. Nature *399*, 271-275.

McIntosh, D., and Blow, J.J. (2012). Dormant origins, the licensing checkpoint, and the response to replicative stresses. Cold Spring Harbor perspectives in biology *4*.

Mello, J.A., Sillje, H.H., Roche, D.M., Kirschner, D.B., Nigg, E.A., and Almouzni, G. (2002). Human Asf1 and CAF-1 interact and synergize in a repair-coupled nucleosome assembly pathway. EMBO Rep *3*, 329-334.

Melvin, A., and Rocha, S. (2012). Chromatin as an oxygen sensor and active player in the hypoxia response. Cell Signal *24*, 35-43.

Mihaylova, V.T., Bindra, R.S., Yuan, J., Campisi, D., Narayanan, L., Jensen, R., Giordano, F., Johnson, R.S., Rockwell, S., and Glazer, P.M. (2003). Decreased expression of the DNA mismatch repair gene Mlh1 under hypoxic stress in mammalian cells. Mol Cell Biol *23*, 3265-3273.

Miller, K.M., Tjeertes, J.V., Coates, J., Legube, G., Polo, S.E., Britton, S., and Jackson, S.P. (2010). Human HDAC1 and HDAC2 function in the DNA-damage response to promote DNA nonhomologous end-joining. Nat Struct Mol Biol *17*, 1144-1151.

Mimura, I., Nangaku, M., Kanki, Y., Tsutsumi, S., Inoue, T., Kohro, T., Yamamoto, S., Fujita, T., Shimamura, T., Suehiro, J., Taguchi, A., Kobayashi, M., Tanimura, K., Inagaki, T., Tanaka, T., Hamakubo, T., Sakai, J., Aburatani, H., Kodama, T., and Wada, Y. (2012). Dynamic change of chromatin conformation in response to hypoxia enhances the expression of GLUT3 (SLC2A3) by cooperative interaction of hypoxia-inducible factor 1 and KDM3A. Mol Cell Biol *32*, 3018-3032.

Mole, D.R., Blancher, C., Copley, R.R., Pollard, P.J., Gleadle, J.M., Ragoussis, J., and Ratcliffe, P.J. (2009). Genome-wide association of hypoxia-inducible factor (HIF)-1alpha and HIF-2alpha DNA binding with expression profiling of hypoxia-inducible transcripts. J Biol Chem *284*, 16767-16775.

Moody, C.A., and Laimins, L.A. (2009). Human papillomaviruses activate the ATM DNA damage pathway for viral genome amplification upon differentiation. PLoS pathogens *5*, e1000605.

Moon, H.E., Cheon, H., Chun, K.H., Lee, S.K., Kim, Y.S., Jung, B.K., Park, J.A., Kim, S.H., Jeong, J.W., and Lee, M.S. (2006). Metastasis-associated protein 1 enhances angiogenesis by stabilization of HIF-1alpha. Oncol Rep *16*, 929-935.

Moreno-Herrero, F., de Jager, M., Dekker, N.H., Kanaar, R., Wyman, C., and Dekker, C. (2005). Mesoscale conformational changes in the DNA-repair complex Rad50/Mre11/Nbs1 upon binding DNA. Nature *437*, 440-443.

Moyal, L., Lerenthal, Y., Gana-Weisz, M., Mass, G., So, S., Wang, S.Y., Eppink, B., Chung, Y.M., Shalev, G., Shema, E., Shkedy, D., Smorodinsky, N.I., van Vliet, N., Kuster, B., Mann, M., Ciechanover, A., Dahm-Daphi, J., Kanaar, R., Hu, M.C., Chen, D.J., Oren, M., and Shiloh, Y. (2011). Requirement of ATM-dependent monoubiquitylation of histone H2B for timely repair of DNA double-strand breaks. Mol Cell *41*, 529-542.

Mungamuri, S.K., Benson, E.K., Wang, S., Gu, W., Lee, S.W., and Aaronson, S.A. (2012). p53-mediated heterochromatin reorganization regulates its cell fate decisions. Nat Struct Mol Biol *19*, 478-484, S471.

Nakamura, H., Tanimoto, K., Hiyama, K., Yunokawa, M., Kawamoto, T., Kato, Y., Yoshiga, K., Poellinger, L., Hiyama, E., and Nishiyama, M. (2008). Human mismatch repair gene, MLH1, is transcriptionally repressed by the hypoxia-inducible transcription factors, DEC1 and DEC2. Oncogene *27*, 4200-4209.

Nakayasu, H., and Berezney, R. (1989). Mapping replicational sites in the eucaryotic cell nucleus. J Cell Biol *108*, 1-11.

Natsume, R., Eitoku, M., Akai, Y., Sano, N., Horikoshi, M., and Senda, T. (2007). Structure and function of the histone chaperone CIA/ASF1 complexed with histones H3 and H4. Nature *446*, 338-341.

Negrini, S., Gorgoulis, V.G., and Halazonetis, T.D. (2010). Genomic instability--an evolving hallmark of cancer. Nat Rev Mol Cell Biol *11*, 220-228.

Nielsen, P.R., Nietlispach, D., Mott, H.R., Callaghan, J., Bannister, A., Kouzarides, T., Murzin, A.G., Murzina, N.V., and Laue, E.D. (2002). Structure of the HP1 chromodomain bound to histone H3 methylated at lysine 9. Nature *416*, 103-107.

Nikitin, P.A., and Luftig, M.A. (2011). At a crossroads: human DNA tumor viruses and the host DNA damage response. Future virology *6*, 813-830.

Noon, A.T., Shibata, A., Rief, N., Lobrich, M., Stewart, G.S., Jeggo, P.A., and Goodarzi, A.A. (2010). 53BP1-dependent robust localized KAP-1 phosphorylation is

essential for heterochromatic DNA double-strand break repair. Nat Cell Biol *12*, 177-184.

Nuciforo, P.G., Luise, C., Capra, M., Pelosi, G., and d'Adda di Fagagna, F. (2007). Complex engagement of DNA damage response pathways in human cancer and in lung tumor progression. Carcinogenesis *28*, 2082-2088.

O'Geen, H., Echipare, L., and Farnham, P.J. (2011). Using ChIP-seq technology to generate high-resolution profiles of histone modifications. Methods Mol Biol *791*, 265-286.

O'Geen, H., Squazzo, S.L., Iyengar, S., Blahnik, K., Rinn, J.L., Chang, H.Y., Green, R., and Farnham, P.J. (2007). Genome-wide analysis of KAP1 binding suggests autoregulation of KRAB-ZNFs. PLoS Genet *3*, e89.

Oda, H., Hubner, M.R., Beck, D.B., Vermeulen, M., Hurwitz, J., Spector, D.L., and Reinberg, D. (2010). Regulation of the histone H4 monomethylase PR-Set7 by CRL4(Cdt2)-mediated PCNA-dependent degradation during DNA damage. Mol Cell *40*, 364-376.

Okuno, Y., Nakamura-Ishizu, A., Otsu, K., Suda, T., and Kubota, Y. (2012). Pathological neoangiogenesis depends on oxidative stress regulation by ATM. Nat Med *18*, 1208-1216.

Olcina, M., Lecane, P.S., and Hammond, E.M. (2010). Targeting hypoxic cells through the DNA damage response. Clin Cancer Res *16*, 5624-5629.

Olcina, M.M., Foskolou, I.P., Anbalagan, S., Senra, J.M., Pires, I.M., Jiang, Y., Ryan, A.J., and Hammond, E.M. (2013). Replication stress and chromatin context link ATM activation to a role in DNA replication. Mol Cell *52*, 758-766.

Olcina, M.M., and Hammond, E.M. (2014). Hypoxia and the DNA Damage Response. In Hypoxia and Cancer: Biological Implications and Therapeutic Opportunities, G. Melillo, ed. (Springer New York), pp. 21-41.

Onder, T.T., Kara, N., Cherry, A., Sinha, A.U., Zhu, N., Bernt, K.M., Cahan, P., Marcarci, B.O., Unternaehrer, J., Gupta, P.B., Lander, E.S., Armstrong, S.A., and Daley, G.Q. (2012). Chromatin-modifying enzymes as modulators of reprogramming. Nature *483*, 598-602.

Palmero, I., and Serrano, M. (2001). Induction of senescence by oncogenic Ras. Methods Enzymol *333*, 247-256.

Papamichos-Chronakis, M., and Peterson, C.L. (2013). Chromatin and the genome integrity network. Nature reviews Genetics *14*, 62-75.

Papandreou, I., Powell, A., Lim, A.L., and Denko, N. (2005). Cellular reaction to hypoxia: sensing and responding to an adverse environment. Mutat Res *569*, 87-100.

Parsons, J.L., Khoronenkova, S.V., Dianova, II, Ternette, N., Kessler, B.M., Datta, P.K., and Dianov, G.L. (2012). Phosphorylation of PNKP by ATM prevents its proteasomal degradation and enhances resistance to oxidative stress. Nucleic Acids Res *40*, 11404-11415.

Peasland, A., Wang, L.Z., Rowling, E., Kyle, S., Chen, T., Hopkins, A., Cliby, W.A., Sarkaria, J., Beale, G., Edmondson, R.J., and Curtin, N.J. (2011). Identification and evaluation of a potent novel ATR inhibitor, NU6027, in breast and ovarian cancer cell lines. Br J Cancer *105*, 372-381.

Pei, H., Zhang, L., Luo, K., Qin, Y., Chesi, M., Fei, F., Bergsagel, P.L., Wang, L., You, Z., and Lou, Z. (2011). MMSET regulates histone H4K20 methylation and 53BP1 accumulation at DNA damage sites. Nature *470*, 124-128.

Perry, C.A., and Annunziato, A.T. (1989). Influence of histone acetylation on the solubility, H1 content and DNase I sensitivity of newly assembled chromatin. Nucleic Acids Res *17*, 4275-4291.

Peters, A.H., O'Carroll, D., Scherthan, H., Mechtler, K., Sauer, S., Schofer, C., Weipoltshammer, K., Pagani, M., Lachner, M., Kohlmaier, A., Opravil, S., Doyle, M., Sibilia, M., and Jenuwein, T. (2001). Loss of the Suv39h histone methyltransferases impairs mammalian heterochromatin and genome stability. Cell *107*, 323-337.

Pinheiro, I., Margueron, R., Shukeir, N., Eisold, M., Fritzsch, C., Richter, F.M., Mittler, G., Genoud, C., Goyama, S., Kurokawa, M., Son, J., Reinberg, D., Lachner, M., and Jenuwein, T. (2012). Prdm3 and Prdm16 are H3K9me1 methyltransferases required for mammalian heterochromatin integrity. Cell *150*, 948-960.

Pires, I.M., Bencokova, Z., McGurk, C., and Hammond, E.M. (2010a). Exposure to acute hypoxia induces a transient DNA damage response which includes Chk1 and TLK1. Cell Cycle *9*, 2502-2507.

Pires, I.M., Bencokova, Z., Milani, M., Folkes, L.K., Li, J.L., Stratford, M.R., Harris, A.L., and Hammond, E.M. (2010b). Effects of acute versus chronic hypoxia on DNA damage responses and genomic instability. Cancer Res *70*, 925-935.

Pires, I.M., Olcina, M.M., Anbalagan, S., Pollard, J.R., Reaper, P.M., Charlton, P.A., McKenna, W.G., and Hammond, E.M. (2012). Targeting radiation-resistant hypoxic tumour cells through ATR inhibition. Br J Cancer *107*, 291-299.

Pollard, P.J., Loenarz, C., Mole, D.R., McDonough, M.A., Gleadle, J.M., Schofield, C.J., and Ratcliffe, P.J. (2008). Regulation of Jumonji-domain-containing histone demethylases by hypoxia-inducible factor (HIF)-1alpha. Biochem J *416*, 387-394.

Poot, R.A., Bozhenok, L., van den Berg, D.L., Steffensen, S., Ferreira, F., Grimaldi, M., Gilbert, N., Ferreira, J., and Varga-Weisz, P.D. (2004). The Williams syndrome transcription factor interacts with PCNA to target chromatin remodelling by ISWI to replication foci. Nat Cell Biol *6*, 1236-1244.

Portela, A., and Esteller, M. (2010). Epigenetic modifications and human disease. Nature biotechnology *28*, 1057-1068.

Prevo, R., Fokas, E., Reaper, P.M., Charlton, P.A., Pollard, J.R., McKenna, W.G., Muschel, R.J., and Brunner, T.B. (2012). The novel ATR inhibitor VE-821 increases sensitivity of pancreatic cancer cells to radiation and chemotherapy. Cancer Biol Ther *13*.

Probst, H., Schiffer, H., Gekeler, V., and Scheffler, K. (1989). Oxygen dependent regulation of mammalian ribonucleotide reductase in vivo and possible significance for replicon initiation. Biochem Biophys Res Commun *163*, 334-340.

Puddu, F., Piergiovanni, G., Plevani, P., and Muzi-Falconi, M. (2011). Sensing of replication stress and Mec1 activation act through two independent pathways involving the 9-1-1 complex and DNA polymerase epsilon. PLoS Genet *7*, e1002022.

Radman-Livaja, M., Verzijlbergen, K.F., Weiner, A., van Welsem, T., Friedman, N., Rando, O.J., and van Leeuwen, F. (2011). Patterns and mechanisms of ancestral histone protein inheritance in budding yeast. PLoS Biol *9*, e1001075.

Rankin, E.B., Giaccia, A.J., and Hammond, E.M. (2009). Bringing H2AX into the angiogenesis family. Cancer Cell *15*, 459-461.

Ray-Gallet, D., Woolfe, A., Vassias, I., Pellentz, C., Lacoste, N., Puri, A., Schultz, D.C., Pchelintsev, N.A., Adams, P.D., Jansen, L.E., and Almouzni, G. (2011). Dynamics of histone H3 deposition in vivo reveal a nucleosome gap-filling mechanism for H3.3 to maintain chromatin integrity. Mol Cell *44*, 928-941.

Reaper, P.M., Griffiths, M.R., Long, J.M., Charrier, J.D., Maccormick, S., Charlton, P.A., Golec, J.M., and Pollard, J.R. (2011a). Selective killing of ATM- or p53-deficient cancer cells through inhibition of ATR. Nat Chem Biol.

Reaper, P.M., Griffiths, M.R., Long, J.M., Charrier, J.D., Maccormick, S., Charlton, P.A., Golec, J.M., and Pollard, J.R. (2011b). Selective killing of ATM- or p53-deficient cancer cells through inhibition of ATR. Nat Chem Biol *7*, 428-430.

Reichard, P., and Ehrenberg, A. (1983). Ribonucleotide reductase--a radical enzyme. Science *221*, 514-519.

Remus, D., and Diffley, J.F. (2009). Eukaryotic DNA replication control: lock and load, then fire. Curr Opin Cell Biol *21*, 771-777.

Riballo, E., Kuhne, M., Rief, N., Doherty, A., Smith, G.C., Recio, M.J., Reis, C., Dahm, K., Fricke, A., Krempler, A., Parker, A.R., Jackson, S.P., Gennery, A., Jeggo, P.A., and Lobrich, M. (2004). A pathway of double-strand break rejoining dependent upon ATM, Artemis, and proteins locating to gamma-H2AX foci. Mol Cell *16*, 715-724.

Rice, G.C., Hoy, C., and Schimke, R.T. (1986). Transient hypoxia enhances the frequency of dihydrofolate reductase gene amplification in Chinese hamster ovary cells. Proc Natl Acad Sci U S A *83*, 5978-5982.

Riley, T., Sontag, E., Chen, P., and Levine, A. (2008). Transcriptional control of human p53-regulated genes. Nat Rev Mol Cell Biol *9*, 402-412.

Rodriguez-Paredes, M., Martinez de Paz, A., Simo-Riudalbas, L., Sayols, S., Moutinho, C., Moran, S., Villanueva, A., Vazquez-Cedeira, M., Lazo, P.A., Carneiro, F., Moura, C.S., Vieira, J., Teixeira, M.R., and Esteller, M. (2013). Gene amplification of the histone methyltransferase SETDB1 contributes to human lung tumorigenesis. Oncogene.

Rogakou, E.P., Pilch, D.R., Orr, A.H., Ivanova, V.S., and Bonner, W.M. (1998). DNA double-stranded breaks induce histone H2AX phosphorylation on serine 139. J Biol Chem *273*, 5858-5868.

Rouschop, K.M., van den Beucken, T., Dubois, L., Niessen, H., Bussink, J., Savelkouls, K., Keulers, T., Mujcic, H., Landuyt, W., Voncken, J.W., Lambin, P., van der Kogel, A.J., Koritzinsky, M., and Wouters, B.G. (2010). The unfolded protein response protects human tumor cells during hypoxia through regulation of the autophagy genes MAP1LC3B and ATG5. J Clin Invest *120*, 127-141.

Rouse, J., and Jackson, S.P. (2002). Interfaces between the detection, signaling, and repair of DNA damage. Science *297*, 547-551.

Rowbotham, S.P., Barki, L., Neves-Costa, A., Santos, F., Dean, W., Hawkes, N., Choudhary, P., Will, W.R., Webster, J., Oxley, D., Green, C.M., Varga-Weisz, P., and Mermoud, J.E. (2011). Maintenance of silent chromatin through replication requires SWI/SNF-like chromatin remodeler SMARCAD1. Mol Cell *42*, 285-296.

Sakaue-Sawano, A., Kurokawa, H., Morimura, T., Hanyu, A., Hama, H., Osawa, H., Kashiwagi, S., Fukami, K., Miyata, T., Miyoshi, H., Imamura, T., Ogawa, M., Masai, H., and Miyawaki, A. (2008). Visualizing spatiotemporal dynamics of multicellular cell-cycle progression. Cell *132*, 487-498.

Sambrook, J., and Russell, D.W. (2001). Molecular Cloning - a laboratory manual, Vol 1 (New York: Cold Spring Harbor Laboratory Press).

Sancar, A., Lindsey-Boltz, L.A., Unsal-Kacmaz, K., and Linn, S. (2004). Molecular mechanisms of mammalian DNA repair and the DNA damage checkpoints. Annu Rev Biochem *73*, 39-85.

Sanchez-Fernandez, E.M., Tarhonskaya, H., Al-Qahtani, K., Hopkinson, R.J., McCullagh, J.S., Schofield, C.J., and Flashman, E. (2013). Investigations on the oxygen dependence of a 2-oxoglutarate histone demethylase. Biochem J *449*, 491-496.

Sanchez, Y., Wong, C., Thoma, R.S., Richman, R., Wu, Z., Piwnica-Worms, H., and Elledge, S.J. (1997). Conservation of the Chk1 checkpoint pathway in mammals: linkage of DNA damage to Cdk regulation through Cdc25. Science *277*, 1497-1501.

Savitsky, K., Bar-Shira, A., Gilad, S., Rotman, G., Ziv, Y., Vanagaite, L., Tagle, D.A., Smith, S., Uziel, T., Sfez, S., Ashkenazi, M., Pecker, I., Frydman, M., Harnik, R., Patanjali, S.R., Simmons, A., Clines, G.A., Sartiel, A., Gatti, R.A., Chessa, L., Sanal, O., Lavin, M.F., Jaspers, N.G., Taylor, A.M., Arlett, C.F., Miki, T., Weissman, S.M., Lovett, M., Collins, F.S., and Shiloh, Y. (1995). A single ataxia telangiectasia gene with a product similar to PI-3 kinase. Science *268*, 1749-1753.

Schodel, J., Bardella, C., Sciesielski, L.K., Brown, J.M., Pugh, C.W., Buckle, V., Tomlinson, I.P., Ratcliffe, P.J., and Mole, D.R. (2012). Common genetic variants at the 11q13.3 renal cancer susceptibility locus influence binding of HIF to an enhancer of cyclin D1 expression. Nat Genet *44*, 420-425, S421-422.

Schodel, J., Oikonomopoulos, S., Ragoussis, J., Pugh, C.W., Ratcliffe, P.J., and Mole, D.R. (2011). High-resolution genome-wide mapping of HIF-binding sites by ChIP-seq. Blood *117*, e207-217.

Schofield, C.J., and Ratcliffe, P.J. (2004). Oxygen sensing by HIF hydroxylases. Nat Rev Mol Cell Biol *5*, 343-354.

Schoppy, D.W., Ragland, R.L., Gilad, O., Shastri, N., Peters, A.A., Murga, M., Fernandez-Capetillo, O., Diehl, J.A., and Brown, E.J. (2012). Oncogenic stress sensitizes murine cancers to hypomorphic suppression of ATR. J Clin Invest *122*, 241-252.

Schorl, C., and Sedivy, J.M. (2007). Analysis of cell cycle phases and progression in cultured mammalian cells. Methods *41*, 143-150.

Schultz, D.C., Ayyanathan, K., Negorev, D., Maul, G.G., and Rauscher, F.J., 3rd (2002). SETDB1: a novel KAP-1-associated histone H3, lysine 9-specific methyltransferase that contributes to HP1-mediated silencing of euchromatic genes by KRAB zinc-finger proteins. Genes Dev *16*, 919-932.

Semenza, G.L. (2010). Defining the role of hypoxia-inducible factor 1 in cancer biology and therapeutics. Oncogene *29*, 625-634.

Sena, J.A., Wang, L., and Hu, C.J. (2013). BRG1 and BRM chromatin-remodeling complexes regulate the hypoxia response by acting as coactivators for a subset of hypoxia-inducible transcription factor target genes. Mol Cell Biol *33*, 3849-3863.

Sharif, J., Muto, M., Takebayashi, S., Suetake, I., Iwamatsu, A., Endo, T.A., Shinga, J., Mizutani-Koseki, Y., Toyoda, T., Okamura, K., Tajima, S., Mitsuya, K., Okano, M., and Koseki, H. (2007). The SRA protein Np95 mediates epigenetic inheritance by recruiting Dnmt1 to methylated DNA. Nature *450*, 908-912.

Sharma, N.L., Groselj, B., Hamdy, F.C., and Kiltie, A.E. (2013). The emerging role of histone deacetylase (HDAC) inhibitors in urological cancers. BJU Int *111*, 537-542.

Shechter, D., Costanzo, V., and Gautier, J. (2004). ATR and ATM regulate the timing of DNA replication origin firing. Nat Cell Biol *6*, 648-655.

Shi, Y., Lan, F., Matson, C., Mulligan, P., Whetstine, J.R., Cole, P.A., and Casero, R.A. (2004). Histone demethylation mediated by the nuclear amine oxidase homolog LSD1. Cell *119*, 941-953.

Shiloh, Y. (2003). ATM and related protein kinases: safeguarding genome integrity. Nat Rev Cancer *3*, 155-168.

Shiloh, Y., and Ziv, Y. (2013). The ATM protein kinase: regulating the cellular response to genotoxic stress, and more. Nat Rev Mol Cell Biol *14*, 197-210.

Shreeram, S., Demidov, O.N., Hee, W.K., Yamaguchi, H., Onishi, N., Kek, C., Timofeev, O.N., Dudgeon, C., Fornace, A.J., Anderson, C.W., Minami, Y., Appella, E., and Bulavin, D.V. (2006). Wip1 phosphatase modulates ATM-dependent signaling pathways. Mol Cell *23*, 757-764.

Singh, V.V., Dutta, D., Ansari, M.A., Dutta, S., and Chandran, B. (2013). Kaposi's Sarcoma-Associated Herpesvirus Induces ATM and H2AX DNA Damage Response Early During de novo Infection of Primary Endothelial Cells Which Play Roles In Latency Establishment. J Virol.

Sirbu, B.M., Couch, F.B., and Cortez, D. (2012). Monitoring the spatiotemporal dynamics of proteins at replication forks and in assembled chromatin using isolation of proteins on nascent DNA. Nat Protoc *7*, 594-605.

Sirbu, B.M., Couch, F.B., Feigerle, J.T., Bhaskara, S., Hiebert, S.W., and Cortez, D. (2011). Analysis of protein dynamics at active, stalled, and collapsed replication forks. Genes & development *25*, 1320-1327.

So, S., Davis, A.J., and Chen, D.J. (2009). Autophosphorylation at serine 1981 stabilizes ATM at DNA damage sites. J Cell Biol *187*, 977-990.

Sobel, R.E., Cook, R.G., Perry, C.A., Annunziato, A.T., and Allis, C.D. (1995). Conservation of deposition-related acetylation sites in newly synthesized histones H3 and H4. Proc Natl Acad Sci U S A *92*, 1237-1241.

Sogo, J.M., Lopes, M., and Foiani, M. (2002). Fork reversal and ssDNA accumulation at stalled replication forks owing to checkpoint defects. Science *297*, 599-602.

Sorensen, C.S., Syljuasen, R.G., Falck, J., Schroeder, T., Ronnstrand, L., Khanna, K.K., Zhou, B.B., Bartek, J., and Lukas, J. (2003). Chk1 regulates the S phase checkpoint by coupling the physiological turnover and ionizing radiation-induced accelerated proteolysis of Cdc25A. Cancer Cell *3*, 247-258.

Soria, G., Polo, S.E., and Almouzni, G. (2012). Prime, repair, restore: the active role of chromatin in the DNA damage response. Mol Cell *46*, 722-734.

Squatrito, M., Brennan, C.W., Helmy, K., Huse, J.T., Petrini, J.H., and Holland, E.C. (2010). Loss of ATM/Chk2/p53 pathway components accelerates tumor development and contributes to radiation resistance in gliomas. Cancer Cell *18*, 619-629.

Stanley, F.K., Moore, S., and Goodarzi, A.A. (2013). CHD chromatin remodelling enzymes and the DNA damage response. Mutat Res *750*, 31-44.

Stewart, G.S., Maser, R.S., Stankovic, T., Bressan, D.A., Kaplan, M.I., Jaspers, N.G., Raams, A., Byrd, P.J., Petrini, J.H., and Taylor, A.M. (1999). The DNA double-strand break repair gene hMRE11 is mutated in individuals with an ataxia-telangiectasia-like disorder. Cell *99*, 577-587.

Stewart, G.S., Panier, S., Townsend, K., Al-Hakim, A.K., Kolas, N.K., Miller, E.S., Nakada, S., Ylanko, J., Olivarius, S., Mendez, M., Oldreive, C., Wildenhain, J., Tagliaferro, A., Pelletier, L., Taubenheim, N., Durandy, A., Byrd, P.J., Stankovic, T., Taylor, A.M., and Durocher, D. (2009). The RIDDLE syndrome protein mediates a ubiquitin-dependent signaling cascade at sites of DNA damage. Cell *136*, 420-434.

Stewart, G.S., Wang, B., Bignell, C.R., Taylor, A.M., and Elledge, S.J. (2003). MDC1 is a mediator of the mammalian DNA damage checkpoint. Nature *421*, 961-966.

Stiff, T., Walker, S.A., Cerosaletti, K., Goodarzi, A.A., Petermann, E., Concannon, P., O'Driscoll, M., and Jeggo, P.A. (2006). ATR-dependent phosphorylation and activation of ATM in response to UV treatment or replication fork stalling. Embo J *25*, 5775-5782.

Stracker, T.H., Roig, I., Knobel, P.A., and Marjanovic, M. (2013). The ATM signaling network in development and disease. Frontiers in genetics *4*, 37.

Strahl, B.D., and Allis, C.D. (2000). The language of covalent histone modifications. Nature *403*, 41-45.

Stucki, M. (2009). Histone H2A.X Tyr142 phosphorylation: a novel sWItCH for apoptosis? DNA Repair (Amst) *8*, 873-876.

Stucki, M., Clapperton, J.A., Mohammad, D., Yaffe, M.B., Smerdon, S.J., and Jackson, S.P. (2005). MDC1 directly binds phosphorylated histone H2AX to regulate cellular responses to DNA double-strand breaks. Cell *123*, 1213-1226.

Stucki, M., and Jackson, S.P. (2006). gammaH2AX and MDC1: anchoring the DNA-damage-response machinery to broken chromosomes. DNA Repair (Amst) *5*, 534-543.

Sulli, G., Di Micco, R., and d'Adda di Fagagna, F. (2012). Crosstalk between chromatin state and DNA damage response in cellular senescence and cancer. Nat Rev Cancer *12*, 709-720.

Sun, Y., Jiang, X., Chen, S., Fernandes, N., and Price, B.D. (2005). A role for the Tip60 histone acetyltransferase in the acetylation and activation of ATM. Proc Natl Acad Sci U S A *102*, 13182-13187.

Sun, Y., Jiang, X., Xu, Y., Ayrapetov, M.K., Moreau, L.A., Whetstine, J.R., and Price, B.D. (2009). Histone H3 methylation links DNA damage detection to activation of the tumour suppressor Tip60. Nat Cell Biol *11*, 1376-1382.

Tachibana, M., Sugimoto, K., Fukushima, T., and Shinkai, Y. (2001). Set domain-containing protein, G9a, is a novel lysine-preferring mammalian histone methyltransferase with hyperactivity and specific selectivity to lysines 9 and 27 of histone H3. J Biol Chem *276*, 25309-25317.

Tachibana, M., Sugimoto, K., Nozaki, M., Ueda, J., Ohta, T., Ohki, M., Fukuda, M., Takeda, N., Niida, H., Kato, H., and Shinkai, Y. (2002). G9a histone methyltransferase plays a dominant role in euchromatic histone H3 lysine 9 methylation and is essential for early embryogenesis. Genes Dev *16*, 1779-1791.

Tanaka, M., Lai, J.S., and Herr, W. (1992). Promoter-selective activation domains in Oct-1 and Oct-2 direct differential activation of an snRNA and mRNA promoter. Cell *68*, 755-767.

Taverna, S.D., Li, H., Ruthenburg, A.J., Allis, C.D., and Patel, D.J. (2007). How chromatin-binding modules interpret histone modifications: lessons from professional pocket pickers. Nat Struct Mol Biol *14*, 1025-1040.

Thurn, K.T., Thomas, S., Raha, P., Qureshi, I., and Munster, P.N. (2013). Histone deacetylase regulation of ATM-mediated DNA damage signaling. Mol Cancer Ther *12*, 2078-2087.

Tian, C., Xing, G., Xie, P., Lu, K., Nie, J., Wang, J., Li, L., Gao, M., Zhang, L., and He, F. (2009). KRAB-type zinc-finger protein Apak specifically regulates p53-dependent apoptosis. Nat Cell Biol *11*, 580-591.

Toledo, L.I., Altmeyer, M., Rask, M.B., Lukas, C., Larsen, D.H., Povlsen, L.K., Bekker-Jensen, S., Mailand, N., Bartek, J., and Lukas, J. (2013). ATR prohibits replication catastrophe by preventing global exhaustion of RPA. Cell *155*, 1088-1103.

Toledo, L.I., Murga, M., Zur, R., Soria, R., Rodriguez, A., Martinez, S., Oyarzabal, J., Pastor, J., Bischoff, J.R., and Fernandez-Capetillo, O. (2011). A cell-based screen identifies ATR inhibitors with synthetic lethal properties for cancer-associated mutations. Nat Struct Mol Biol *18*, 721-727.

Toustrup, K., Sorensen, B.S., Alsner, J., and Overgaard, J. (2012). Hypoxia gene expression signatures as prognostic and predictive markers in head and neck radiotherapy. Semin Radiat Oncol *22*, 119-127.

Towbin, B.D., Gonzalez-Aguilera, C., Sack, R., Gaidatzis, D., Kalck, V., Meister, P., Askjaer, P., and Gasser, S.M. (2012). Step-wise methylation of histone H3K9 positions heterochromatin at the nuclear periphery. Cell *150*, 934-947.

Tsukada, Y., Fang, J., Erdjument-Bromage, H., Warren, M.E., Borchers, C.H., Tempst, P., and Zhang, Y. (2006). Histone demethylation by a family of JmjC domain-containing proteins. Nature *439*, 811-816.

Turnell, A.S., and Grand, R.J. (2012). DNA viruses and the cellular DNA-damage response. J Gen Virol *93*, 2076-2097.

Urquhart, A.J., Gatei, M., Richard, D.J., and Khanna, K.K. (2011). ATM mediated phosphorylation of CHD4 contributes to genome maintenance. Genome integrity *2*, 1.

Vaupel, P. (2010). Metabolic microenvironment of tumor cells: a key factor in malignant progression. Exp Oncol *32*, 125-127.

Vaupel, P., and Harrison, L. (2004). Tumor hypoxia: causative factors, compensatory mechanisms, and cellular response. Oncologist *9 Suppl 5*, 4-9.

Vaupel, P., and Hockel, M. (2001). Hypoxia in cervical cancer: pathogenesis, characterization, and biological/clinical consequences. Zentralblatt fur Gynakologie *123*, 192-197.

Vaupel, P., Kallinowski, F., and Okunieff, P. (1989). Blood flow, oxygen and nutrient supply, and metabolic microenvironment of human tumors: a review. Cancer Res *49*, 6449-6465.

Vedadi, M., Barsyte-Lovejoy, D., Liu, F., Rival-Gervier, S., Allali-Hassani, A., Labrie, V., Wigle, T.J., Dimaggio, P.A., Wasney, G.A., Siarheyeva, A., Dong, A., Tempel, W., Wang, S.C., Chen, X., Chau, I., Mangano, T.J., Huang, X.P., Simpson, C.D., Pattenden, S.G., Norris, J.L., Kireev, D.B., Tripathy, A., Edwards, A., Roth, B.L., Janzen, W.P., Garcia, B.A., Petronis, A., Ellis, J., Brown, P.J., Frye, S.V.,

Arrowsmith, C.H., and Jin, J. (2011). A chemical probe selectively inhibits G9a and GLP methyltransferase activity in cells. Nat Chem Biol *7*, 566-574.

Vempati, R.K., Jayani, R.S., Notani, D., Sengupta, A., Galande, S., and Haldar, D. (2010). p300-mediated acetylation of histone H3 lysine 56 functions in DNA damage response in mammals. J Biol Chem *285*, 28553-28564.

Vidali, G., Boffa, L.C., Bradbury, E.M., and Allfrey, V.G. (1978). Butyrate suppression of histone deacetylation leads to accumulation of multiacetylated forms of histones H3 and H4 and increased DNase I sensitivity of the associated DNA sequences. Proc Natl Acad Sci U S A *75*, 2239-2243.

Voigt, P., LeRoy, G., Drury, W.J., 3rd, Zee, B.M., Son, J., Beck, D.B., Young, N.L., Garcia, B.A., and Reinberg, D. (2012). Asymmetrically modified nucleosomes. Cell *151*, 181-193.

Vousden, K.H., and Lane, D.P. (2007). p53 in health and disease. Nat Rev Mol Cell Biol *8*, 275-283.

Wang, B., and Elledge, S.J. (2007). Ubc13/Rnf8 ubiquitin ligases control foci formation of the Rap80/Abraxas/Brca1/Brcc36 complex in response to DNA damage. Proc Natl Acad Sci U S A *104*, 20759-20763.

Wang, F., Zhang, R., Beischlag, T.V., Muchardt, C., Yaniv, M., and Hankinson, O. (2004). Roles of Brahma and Brahma/SWI2-related gene 1 in hypoxic induction of the erythropoietin gene. J Biol Chem *279*, 46733-46741.

Wang, S., Tian, C., Xiao, T., Xing, G., He, F., Zhang, L., and Chen, H. (2010). Differential regulation of Apak by various DNA damage signals. Mol Cell Biochem *333*, 181-187.

Wang, W., Winlove, C.P., and Michel, C.C. (2003). Oxygen partial pressure in outer layers of skin of human finger nail folds. J Physiol *549*, 855-863.

Wang, Y., Cortez, D., Yazdi, P., Neff, N., Elledge, S.J., and Qin, J. (2000). BASC, a super complex of BRCA1-associated proteins involved in the recognition and repair of aberrant DNA structures. Genes Dev *14*, 927-939.

Watters, D., Khanna, K.K., Beamish, H., Birrell, G., Spring, K., Kedar, P., Gatei, M., Stenzel, D., Hobson, K., Kozlov, S., Zhang, N., Farrell, A., Ramsay, J., Gatti, R., and Lavin, M. (1997). Cellular localisation of the ataxia-telangiectasia (ATM) gene product and discrimination between mutated and normal forms. Oncogene *14*, 1911-1921.

White, D.E., Negorev, D., Peng, H., Ivanov, A.V., Maul, G.G., and Rauscher, F.J., 3rd (2006). KAP1, a novel substrate for PIKK family members, colocalizes with numerous damage response factors at DNA lesions. Cancer Res *66*, 11594-11599.

Wohlschlegel, J.A., Dwyer, B.T., Dhar, S.K., Cvetic, C., Walter, J.C., and Dutta, A. (2000). Inhibition of eukaryotic DNA replication by geminin binding to Cdt1. Science *290*, 2309-2312.

Wong, R.R., Chan, L.K., Tsang, T.P., Lee, C.W., Cheung, T.H., Yim, S.F., Siu, N.S., Lee, S.N., Yu, M.Y., Chim, S.S., Wong, Y.F., and Chung, T.K. (2011). CHD5 Downregulation Associated with Poor Prognosis in Epithelial Ovarian Cancer. Gynecologic and obstetric investigation *72*, 203-207.

Workman, P., Aboagye, E.O., Balkwill, F., Balmain, A., Bruder, G., Chaplin, D.J., Double, J.A., Everitt, J., Farningham, D.A., Glennie, M.J., Kelland, L.R., Robinson, V., Stratford, I.J., Tozer, G.M., Watson, S., Wedge, S.R., and Eccles, S.A. (2010). Guidelines for the welfare and use of animals in cancer research. Br J Cancer *102*, 1555-1577.

Wu, J., Chen, Y., Lu, L.Y., Wu, Y., Paulsen, M.T., Ljungman, M., Ferguson, D.O., and Yu, X. (2011). Chfr and RNF8 synergistically regulate ATM activation. Nat Struct Mol Biol *18*, 761-768.

Wu, J., Zhang, X., Zhang, L., Wu, C.Y., Rezaeian, A.H., Chan, C.H., Li, J.M., Wang, J., Gao, Y., Han, F., Jeong, Y.S., Yuan, X., Khanna, K.K., Jin, J., Zeng, Y.X., and Lin, H.K. (2012a). Skp2 E3 ligase integrates ATM activation and homologous recombination repair by ubiquitinating NBS1. Mol Cell *46*, 351-361.

Wu, X., Ranganathan, V., Weisman, D.S., Heine, W.F., Ciccone, D.N., O'Neill, T.B., Crick, K.E., Pierce, K.A., Lane, W.S., Rathbun, G., Livingston, D.M., and Weaver, D.T. (2000). ATM phosphorylation of Nijmegen breakage syndrome protein is required in a DNA damage response. Nature *405*, 477-482.

Wu, X., Zhu, Z., Li, W., Fu, X., Su, D., Fu, L., Zhang, Z., Luo, A., Sun, X., and Dong, J.T. (2012b). Chromodomain helicase DNA binding protein 5 plays a tumor suppressor role in human breast cancer. Breast Cancer Res *14*, R73.

Xia, X., Lemieux, M.E., Li, W., Carroll, J.S., Brown, M., Liu, X.S., and Kung, A.L. (2009). Integrative analysis of HIF binding and transactivation reveals its role in maintaining histone methylation homeostasis. Proc Natl Acad Sci U S A *106*, 4260-4265.

Xiao, A., Li, H., Shechter, D., Ahn, S.H., Fabrizio, L.A., Erdjument-Bromage, H., Ishibe-Murakami, S., Wang, B., Tempst, P., Hofmann, K., Patel, D.J., Elledge, S.J., and Allis, C.D. (2009). WSTF regulates the H2A.X DNA damage response via a novel tyrosine kinase activity. Nature *457*, 57-62.

Yang, J., Ledaki, I., Turley, H., Gatter, K.C., Montero, J.C., Li, J.L., and Harris, A.L. (2009). Role of hypoxia-inducible factors in epigenetic regulation via histone demethylases. Ann N Y Acad Sci *1177*, 185-197.

Yazdi, P.T., Wang, Y., Zhao, S., Patel, N., Lee, E.Y., and Qin, J. (2002). SMC1 is a downstream effector in the ATM/NBS1 branch of the human S-phase checkpoint. Genes Dev *16*, 571-582.

Yee, K.S., and Vousden, K.H. (2005). Complicating the complexity of p53. Carcinogenesis *26*, 1317-1322.

Yoo, Y.G., Kong, G., and Lee, M.O. (2006). Metastasis-associated protein 1 enhances stability of hypoxia-inducible factor-1alpha protein by recruiting histone deacetylase 1. Embo J *25*, 1231-1241.

Young, L.C., McDonald, D.W., and Hendzel, M.J. (2013). Kdm4b histone demethylase is a DNA damage response protein and confers a survival advantage following gamma-irradiation. J Biol Chem *288*, 21376-21388.

Young, S.D., Marshall, R.S., and Hill, R.P. (1988). Hypoxia induces DNA overreplication and enhances metastatic potential of murine tumor cells. Proc Natl Acad Sci U S A *85*, 9533-9537.

Yuan, J., Narayanan, L., Rockwell, S., and Glazer, P.M. (2000). Diminished DNA repair and elevated mutagenesis in mammalian cells exposed to hypoxia and low pH. Cancer Res *60*, 4372-4376.

Yuan, L., Tian, C., Wang, H., Song, S., Li, D., Xing, G., Yin, Y., He, F., and Zhang, L. (2012). Apak competes with p53 for direct binding to intron 1 of p53AIP1 to regulate apoptosis. EMBO Rep *13*, 363-370.

Zeman, M.K., and Cimprich, K.A. (2013). Causes and consequences of replication stress. Nat Cell Biol *16*, 2-9.

Zeng, L., Yap, K.L., Ivanov, A.V., Wang, X., Mujtaba, S., Plotnikova, O., Rauscher, F.J., 3rd, and Zhou, M.M. (2008). Structural insights into human KAP1 PHD finger-bromodomain and its role in gene silencing. Nat Struct Mol Biol *15*, 626-633.

Ziv, Y., Bielopolski, D., Galanty, Y., Lukas, C., Taya, Y., Schultz, D.C., Lukas, J., Bekker-Jensen, S., Bartek, J., and Shiloh, Y. (2006). Chromatin relaxation in response to DNA double-strand breaks is modulated by a novel ATM- and KAP-1 dependent pathway. Nat Cell Biol *8*, 870-876.

Zou, L., and Elledge, S.J. (2003). Sensing DNA damage through ATRIP recognition of RPA-ssDNA complexes. Science *300*, 1542-1548.